Investigations in Time and of Space Using the FIRST Survey:
Radio Source Variability and the Evolution of FR II Quasars

Nithyanandan Thyagarajan

Submitted in partial fulfillment of the
requirements for the degree
of Doctor of Philosophy
in the Graduate School of Arts and Sciences.

COLUMBIA UNIVERSITY

2011

Abstract

Investigations in Time and of Space Using the FIRST Survey:

Radio Source Variability and the Evolution of FR II Quasars

Nithyanandan Thyagarajan

The *FIRST* survey covered $\sim$ 10,000 deg^2 of the sky over a decade, providing unprecedented levels of flux density sensitivity ($\sim$ 1 mJy) at 1.4 GHz, uniformity to within 15% (at $\sim$ 0.15 mJy rms), 5$''$4 angular resolution, astrometric accuracy to better than 1$''$ and has cataloged $\gtrsim$ 800,000 sources. It has made enormous contributions to diverse scientific ends including such subjects as radio source populations, quasars, large-scale structure and clustering of radio sources, gravitational lensing, cosmology, etc. I present the motivation, analysis and results of two projects also intended to demonstrate the power and expand the scope of the *FIRST* survey's scientific reach.

A comprehensive search for variable and transient radio sources has been conducted using the $\sim$ 55,000 snapshot images of the *FIRST* survey. An analysis leading to the discovery of 1,651 variable and transient objects down to mJy levels over a wide range of timescales (few minutes to years) is presented. The multi-wavelength matching for counterparts reveals the diverse classes of objects exhibiting variability. Interestingly, $\sim$ 60% of the objects in the sample have either no classified counterparts or no corresponding sources at any other wavelength and require multi-wavelength follow-up observations. I discuss these classes of variables and speculate on the identity of objects that lack multi-wavelength counterparts. Thus, the *FIRST* survey has yielded the largest sample by far of radio variables and transients to date to unprecedented levels of sensitivity and sky coverage and demonstrates the promise of future radio instruments which have transient-detection as one of their key science projects.

For decades, radio astronomers have attempted to use double-lobed radio sources to constrain the angular size-redshift $(\theta - z)$ relation and to derive cosmological parameters therefrom. Most of the early attempts have, embarrassingly, shown general consistency with a static Euclidean universe rather than with Friedmann models. These earlier results can be attributed to a combination of selection effects, sample definition problems, and inconsistencies in analysis. However, some recent and more successful analyses have still failed to distinguish among different Friedmann models. A catalog of ~ 680 FR II quasars was constructed from the *FIRST* sources with redshifts taken from the SDSS spectroscopic QSO catalog and a similar sized sample from the SDSS photometric QSO catalog which are the largest quasar compilations to date. Using statistical analyses, no evidence for intrinsic evolution of sizes with redshift is found. A static Euclidean model for the universe is clearly ruled out. However, new degeneracies between parameters in the multi-dimensional χ^2-surface are found which can only be resolved with additional, independent information. Notable differences are found between the spectroscopic and photometric samples raising questions about the nature and origin of these populations.

Contents

List of Tables

List of Figures

Acknowledgments

First and foremost, I wish to acknowledge the unconditional support, love and affection I have enjoyed from my family who have made enormous personal sacrifices in order that I may reach this small milestone unhindered. I admire their selfless nature and I certainly have a lot to learn from them.

Next, I would like to thank personally Prof. David Helfand and Prof. Jacqueline van Gorkom. Having been far away from home for the duration of my doctoral studies, I consider them to be my "academic parents". Their optimism, encouragement, and support during trying times are why I have been able to weather many a storm. Both were always open to my ideas and views, be it in astronomy or otherwise. David, my advisor, always stood by me in my work and has been someone I could rely upon. His approach to my mistakes was very positive, in a way that provoked more thought. He helped me keep an open mind and realize it is the key to discovering interesting science. His vast experience helped me learn to discern the important from the rest. Jacqueline has been close to me since the beginning. Her open and straightforward personality always helped keep things in the right perspective. My interactions with her have been very insightful and stimulating. Her own undiminished sincerity and dedication to her work has been truly inspiring.

I am very grateful to Prof. Rajaram Nityananda, Prof. Harishankar Ramachandran and Prof. Bala Iyer who were my undergraduate project advisors. They provided the stepping stones. I also thank all my teachers at Columbia University, IIT Madras, and elementary, middle, and high schools, without whom there would be no foundation.

I thank the rest of my thesis committee members: Prof. Richard White, Prof. Zoltan Haiman and Prof. Lam Hui for their valuable feedback on my thesis. Finally, I thank the faculty, staff, and friends in the astronomy department at Columbia University who made my stay here very pleasant and memorable.

Mother,

as the most special one who was ahead of your time, who led by example despite being slowed down by those around you, who, through unwavering love and care, taught and still continues to impart to me the wisdom to value every moment, to embrace and smile at every situation, to keep an open mind, to transcend the infinite manifestations of duality encountered in life from the mild to the extreme, to realize the ego is the greatest obstacle to true learning, to recognize only what is inside appears projected outwardly, and, to not lose the joy in the journey worrying about the destination, I, in an attempt to express the inexpressible, humbly dedicate everything to you and am forever indebted and lucky to feel your eternal presence.

Chapter 1

Introduction

The *FIRST* survey has been key to understanding a wide range of new science. It is impossible to do full justice in summarizing completely the diverse impact the *FIRST* survey has made in astronomy, especially in the radio regime. What follows in this chapter is a modest attempt to highlight the role the *FIRST* survey has played to date, beginning with a short description of the survey.

1.1 The *FIRST* Survey

Detailed information about the *FIRST* survey can be found in Becker et al. (1995) and on the web (http://sundog.stsci.edu). *FIRST* – Faint Images of the Radio Sky at Twenty-cm – is a project designed to produce the radio equivalent of the Palomar Observatory Sky Survey over 9,900 deg^2 of the North Galactic Cap. Using the NRAO Very Large Array (VLA) in its B-configuration, 3-minute snapshots were acquired covering a hexagonal grid using 2×7 3-MHz frequency channels centered at 1365 and 1435 MHz. The data are edited, self-calibrated, mapped, and CLEANed using an automated pipeline based largely on routines in the Astronomical Image Processing System (AIPS). A final atlas of maps is produced by coadding the twelve images adjacent to each pointing center. These maps have $1\farcs8$ pixels, a typical rms of 0.15 mJy, and an angular resolution of $5\farcs4$. The noise in the coadded maps varies by only 15% from the best to the worst places in the maps, except in the vicinity of bright sources (> 100 mJy) where sidelobes can lead to an increased noise level. At the 1 mJy source detection threshold, there are ~ 90 sources deg^{-2}, $\sim 35\%$ of which have resolved structure on scales from $2''$-$30''$.

A source catalog including peak and integrated flux densities and sizes derived from fitting a two-dimensional Gaussian to each source is generated from the coadded images. The astrometric reference frame of the maps is accurate to $0\overset{''}{.}05$, and individual sources have 90% confidence error circles of radius $< 0\overset{''}{.}5$ at the 3 mJy level and $1''$ at the survey threshold. Approximately 15% of the sources have optical counterparts at the limit of the POSS I plates (E~ 20.0); unambiguous optical identifications ($< 5\%$ false rates) are achievable to $m_v \sim 24$. The survey area has been chosen to coincide with that of the Sloan Digital Sky Survey (SDSS); at the $m_v \sim 23$ limit of SDSS, $\sim 30\%$ of the optical counterparts to *FIRST* sources are detected.

1.2   Radio Source Population

The *FIRST* has been an immense source of information, either directly or indirectly, in understanding the population of radio sources. White et al. (1997) made one of the first attempts to classify the radio sources in *FIRST* by comparing it to other catalogs namely, the Guide Star Catalog, the IRAS Faint Source Catalog and the *ROSAT* Catalog. Helfand et al. (1999) matched the then $\sim 50\%$ complete *FIRST* survey with catalogs of bright stars to find 26 high-confidence detections, effectively doubling the number of known stellar radio emitters at that time, which are rare. Blanton et al. (2000, 2001) have demonstrated that bent-double radio sources from *FIRST* can be used as tracers of cluster environments at moderate to high redshifts. A high-redshift ($z = 0.96$) cluster has been discovered using a wide-angled tail radio source from the *FIRST* survey (Blanton et al. 2003). The excellent positional accuracy and the angular resolution of the *FIRST* survey used in conjunction with other radio surveys such as the *WENSS, TEXAS, MRC, NVSS*, and *PMN* helped create a sample of Ultra Steep Spectra radio sources brighter than 10 mJy at 1400 MHz (De Breuck et al. 2000), which are known to be tracers of high-redshift radio galaxies (HzRGs). They

concluded that 85% of the sample might be HzRGs and that the majority of the non-HzRGs in their sample is found in clusters. Magliocchetti et al. (2000) have been able to characterize the redshift distribution of radio sources at 1 mJy obtained from the *FIRST* catalog by selecting 365 sources and carrying out multi-object spectroscopy. They find $\sim 45\%$ of the sample to be early-type galaxies at relatively high redshifts ($z \gtrsim 0.2$), $\sim 15\%$ to be late-type galaxies at intermediate redshifts ($0.02 \lesssim z \lesssim 0.2$), $\sim 6\%$ to be very local starburst galaxies ($z \lesssim 0.05$) and $\sim 9\%$ to be Seyfert 1/quasar-type galaxies, all at $z \gtrsim 0.8$.

Spectroscopy from the 2dF survey of *FIRST* radio sources with $S \geq 1$ mJy down to a magnitude limit of $b_J = 19.45$ showed 63% of the sample consisted of absorption line systems ('Classical' radio galaxies) which are likely to be FR I sources at $z \gtrsim 0.1$ with $10^{21} \lesssim P_{1.4\text{GHz}}/\text{W Hz}^{-1}\ \text{sr}^{-1} \lesssim 10^{24}$, while 32% consisted of late-type galaxies and starbursts in the very nearby universe ($z \lesssim 0.1$) and $P_{1.4GHz} \lesssim 10^{21.5}\ \text{W Hz}^{-1}\ \text{sr}^{-1}$ (Magliocchetti et al. 2002). Using the *FIRST* and *NVSS* surveys, Machalski et al. (2001) were able to identify a sample of low-luminosity giant radio sources with projected physical sizes $\sim$ Mpc and to determine their physical parameters such as redshifts, energy densities, etc. This sample could be useful in determining whether the large sizes are a consequence of age or environment. Using the *FIRST* and *GB6* surveys, Guerra et al. (2002) point out that, until data from high frequency radio surveys become available, selecting sources with inverted spectra between 1.4 GHz and 4.8 GHz is the most promising method of finding Gigahertz Peaked Spectrum (GPS) sources that peak above 4.8 GHz. Using a *FIRST*-based survey in conjunction with *VLA* and *MERLIN* observations, a sample of Compact Steep Spectrum (CSS) sources was created, out of which one of the sources might not be evolving to later stages with extended radio structures, possibly due to lack of stable fueling (Kunert-Bajraszewska et al. 2005a; Marecki et al. 2006a; Kunert-Bajraszewska et al. 2006b). This is believed to be a prototype for CSS sources with FR II morphologies that fade

away instead of becoming large-scale objects. The *FIRST* survey has also provided information on the dichotomy of FR morphologies. For instance, objects that are a hybrid of FR I and FR II morphologies could be crucial in understanding the origin of this dichotomy. By confirming a few objects from the *FIRST* survey as hybrids with two different kinds of jets from the same central object, Gawroński et al. (2006) find support for the idea that difference in environments may be a more plausible cause for the dichotomy rather than differences in the source's central engine and jet plasma composition, since it is difficult to reconcile the view that the same central engine could exhibit dual nature in each of its jets. The problem of restarting jets/recurring activity in AGN manifesting in X-shaped radio structures has also been addressed with data from the *FIRST* survey. Marecki et al. (2006b) have used such X-shaped radio sources to find some support for the argument that a rapid repositioning of the central engine, which in turn is most likely a consequence of mergers, is the cause for the X-shaped structures seen. On the other hand, Cheung (2007) has compiled a list of 100 such X-shaped or winged radio sources which could potentially offer clinching evidence in favour or against alternate theories on the origin of the wings – rapid repositioning of the central engine probably as the result of a merger, or the backflow of plasma from the currently active radio lobes into an asymmetric medium surrounding the AGN. Using stacking procedures on sub-threshold *FIRST* images for AGNs from SDSS, de Vries et al. (2007) have been able to underline the notion that the radio emission in star-forming systems can dominate the emission associated with AGN. Similar procedures on optically-selected radio-quiet galaxies have shown strong evidence that quiescent LRGs harbor AGNs, which has clear implications for galaxy-formation scenarios (Hodge et al. 2008).

1.3   Quasars

The contribution of the *FIRST* survey in this area has been immeasurable. The pilot phase of the *FIRST* Bright Quasar Survey (*FBQS*; Gregg et al. 1996) used the initial 300 deg^2 of the *FIRST* survey combined with the digitized POSS plates to select 219 quasar candidates to $E \leq 17.50$, half of which are radio-quiet. This work was further extended by White et al. (2000) using 2,682 deg^2 of the *FIRST* survey to create a sample of 636 radio-selected optically bright quasars. The survey detects both radio-loud and radio-quiet quasars out to $z > 3$ including 29 BAL QSOs, both high- and low-ionization. Becker et al. (2000) followed up on this sample to establish the existence of a substantial population of radio-loud BAL quasars and showed that their radio properties are inconsistent with simple unified models in which BAL quasars are a subset of quasars seen edge-on; instead, their results support a scenario in which BALs are an early stage in the development of new or refueled quasars. The latter scenario found more support after the discovery of a BAL quasar with a classic FR II morphology allowing estimation of its orientation (Gregg et al. 2000). The *FBQS* has helped in creating a composite spectrum using the radio-selected quasars for the different classes such as radio-quiet, radio-loud, high- and low-ionization BAL quasars (Brotherton et al. 2001). *FIRST* was instrumental in discovering two low-ionization BAL QSOs in addition to finding the first known radio-loud BAL QSO, which are a rare phenomenon, while the *FIRST* data was found to be efficient at selecting BAL QSOs in radio-quiet and radio-moderate regions owing to its flux sensitivity (Becker et al. 1997). Subsequently, a radio-loud/radio-quiet binary quasar pair was also discovered (Brotherton et al. 1999). Helfand et al. (2001) conducted a long-term (~ 45 yr) optical variability survey for a sample radio-selected quasars from the *FBQS* which is one of the largest such samples so far. They find many intriguing trends including little or no dependence of variability amplitude on radio or optical flux, radio luminosity, or redshift. Variability amplitude is higher in the blue band

than the red band. The dependence on radio loudness is mostly flat except for a slight upturn for the extremely radio-loud objects, and the decrease in variability amplitude for optically luminous quasars is confined to radio-quiet objects. But most importantly, they have demonstrated the complex interdependence of the observed variability on frequency, redshift, bolometric luminosity, radio loudness, and possibly other parameters.

The *FBQS* has shown evidence for significant correlation between radio luminosity and black hole mass and that this relationship is continuous with radio loudness, thus suggesting a scheme to unify radio-loud and radio-quiet objects (Lacy et al. 2001). Also, the different dependencies of radio and optical luminosities on black hole mass could play a role in explaining why the radio luminosity distribution of quasar surveys differs so much depending on whether or not it is based on radio-selection. Cirasuolo et al. (2003) also rule out the classical dichotomy of radio-loud and radio-quiet quasars by matching the *FIRST* survey with the 2dF Quasar Redshift Survey. A confirmation of the existence of relativistic jets in radio-intermediate quasars is provided by Wang et al. (2006) by studying variability and brightness temperatures. Results from White et al. (2007) have revealed the statistical properties of radio sources in the nano-Jansky regime even when the individual sources have flux densities orders of magnitude below the typical field rms. In addition, they find, at best, marginal evidence for bimodal distribution in radio loudness.

McGreer et al. (2006) discovered a $z = 6.12$ radio-loud BAL quasar in the NOAO Deep Wide Field Survey using spectroscopic follow-up with the Keck II telescope. One of the largest samples of 422 FR II quasars was constructed by de Vries et al. (2006) who characterized their properties and radio morphologies including creating composite optical spectra by matching *FIRST* data and SDSS DR3 quasars. As will be explained in subsequent chapters, I have created and made use of a sample of FR II quasars which is at least four times greater than theirs. FR II BAL quasars are

shown to be belonging to an extremely rare class of objects which, by their rarity, imply the coexistence of the emergence of radio jets and lobes, and the BAL phase are very short-lived ($\lesssim 10^5$ yr) and even shorter by an order of magnitude in the high-ionization cases (Gregg et al. 2006).

1.4   Gravitational Lensing

The *FBQS* offers two advantages as a source of potential gravitational lenses. First, since the quasars are bright, they are more likely to be lensed than quasars from fainter surveys. Second, radio observations can be used both to confirm the source as a lensed object and to constrain models of the lens. Kamionkowski et al. (1998) have demonstrated that the *FIRST* survey should be able to detect a statistically significant weak-lensing signal even to scales larger than $1°$, which extends beyond signals in the optical regime and thus provides the possibility of measurement in the linear regime of structure formation. Schechter et al. (1998) have reported the discovery of a new gravitational lens using data from the *FBQS*. Using the then incomplete *FIRST* survey, Lehár et al. (2001) designed an efficient search for gravitationally lensed radio lobes and found two lenses, one of which was a new discovery. They predict that the full survey should yield five to 10 lenses. Lacy et al. (2002), in searching for very red quasars, discovered a lensed low-ionization BAL quasar at $z = 2.65$ with the lensing galaxy at $z \approx 0.95$. The lensing galaxy is found to contain a small amount of dust but is otherwise a fairly typical massive elliptical galaxy. Chang et al. (2004) have detected the first 3σ measurement of a lensing signal at the $450'$ scale using radio sources. Further, they were able to constrain the power spectrum normalization, σ_8, which was found to be consistent with the *WMAP* CMB experiment, and the median redshift of the radio sample to be ≈ 2.2, consistent with existent models of radio source luminosity functions. Ryan et al. (2008) present evidence for a dark

lens (optically unidentified) galaxy which, if proven, could be a unique confirmation for the ΛCDM paradigm. However, it has been argued that instead of being a dark lens, the object is most likely a massive, heavily obscured galaxy in which the nuclear activity is currently in an early evolutionary stage (Frey et al. 2010).

1.5   Large-scale Structure of Radio Sources

FIRST made possible the first high-significance measurement of the two-point angular correlation function for a deep radio sample and showed correlation on scales between $0°.2$ and $2°$ modeled by a power-law $A\theta^{\gamma}$, where $A \approx 3 \times 10^{-3}$ and $\gamma \approx -1.1$ (Cress et al. 1996). Magliocchetti et al. (1998) have studied the variance and skewness in the distribution using the counts-in-cells method for sources in the *FIRST* survey. They estimated the angular correlation from these parameters and found a spatial correlation length $r_0 \sim 10h^{-1}$ Mpc. Their results further indicate that the large-scale clustering of radio sources is in conformity with the gravitational instability picture for the growth of perturbations from a primordial Gaussian field; their measurements do not require invoking initial non-Gaussian perturbations. Blake & Wall (2002) quantify angular clustering in wide-angle radio surveys such as the *NVSS* and *FIRST* taking into account the problem of multiple-component sources. Their results are at variance with those of Magliocchetti et al. (1998). In particular, they find a shallower slope for the angular correlation function than reported by Magliocchetti et al. (1998) and attribute the difference to the problem of multiple-component sources which could also lead to the skewness reported earlier. They also claim that the *FIRST* sample could contain a non-negligible fraction of low-redshift starburst galaxies that trace non-linear clustering and hence are a source of skewness. Magliocchetti et al. (2004) dispute the findings of Blake & Wall (2002) and conclude by matching *FIRST* to the 2dF Galaxy Redshift Survey that the amplitude and slope for the correlation

of AGN were, respectively, $\simeq 11$ Mpc and 2 while those for the optically selected galaxies were, respectively, 6.7 Mpc and 1.6. Overzier et al. (2003) have performed radio clustering analysis to conclude that clustering amplitude increases with radio flux density, implying that the most powerful FR II sources are more clustered; this is consistent with the fact that they are found in very rich environments. They also find the clustering scale to be $\sim 14h^{-1}$ Mpc similar to those found for extremely red objects, and propose that these may be the same systems seen at different evolutionary stages.

1.6   Cosmology

The *FIRST* survey has had an indisputable impact in cosmology as already described to some extent in §1.3, §1.4 and §1.5. Another notable addition to this list would be the work of Buchalter et al. (1998) who tried to constrain cosmological models using the double-lobed, edge-brightened FR II quasars and found the data, contrary to past work, to be consistent with the standard Friedmann models than with a static Euclidean universe. We explore this further in chapter 3.

1.7   Multi-Wavelength Astronomy

The *FIRST* survey represents a major contribution to multi-wavelength astronomy. Some of the results from the literature quoted in the previous sections have already made use of heavy cross-correlations between *FIRST* and various catalogs, especially at optical, infrared and X-ray wavelengths.

To add further to the list, I present a few more multi-wavelength results from the literature. A combination of the *FIRST* and *IRAS* data led van Breugel (1999) to suggest that a large fraction of ULIRGs may be powered by luminous starbursts, not by hidden, luminous AGN. Besides showing no evidence for bimodality in radio loud-

ness, Brinkmann et al. (2000) characterized the various properties and correlations between radio and X-ray observations of AGN using *FIRST* and *ROSAT*. Menou et al. (2001) have been able to go deeper than the optical magnitude limit for the *FBQS* by using 290 $\deg^2$ of the *SDSS* and find a four-fold increase in the rate of identification of BAL quasars, claiming that the full survey should yield a much more robust characterization of the properties of this population of rare objects. In conjunction with the *2MASS* data, Gregg et al. (2002) have found two very red quasars and discuss two causes for such an occurrence – reddening due to the host galaxy and reddening due to a lensing galaxy. Extending this work, Lacy et al. (2002) find some support for the latter model and estimate that this effect could prevent the detection of red quasars and in particular, the class of iron BAL quasars. The *FIRST* data has been crucial to spectroscopic quasar target selection for the *SDSS* (Richards et al. 2002). Ivezić et al. (2002) have matched the *FIRST* and *SDSS* catalogs to find many interesting results. For instance, they confirm that the AGN-to-starburst galaxy number ratio increases with radio flux and find that radio emission from AGNs is more concentrated than that from starburst galaxies. Besides identifying over 70,000 optical counterparts in the Cambridge APM scans of the POSS-I plates for radio sources from the then-incomplete *FIRST* survey data, McMahon et al. (2002) also show that *FIRST*, used as an astrometric standard, helped improve the absolute astrometry of the POSS plates by nearly an order of magnitude to 0″.15 rms. Hopkins et al. (2003) have used the *FIRST* data with the SDSS to build three reliable estimators of star formation.

Clewley & Jarvis (2004) have used the data from radio surveys and SDSS to constrain the cosmological evolution of luminosity for FR I radio sources as being consistent with a constant comoving space density with redshift, as opposed to the strong positive evolution for more powerful sources. Georgakakis et al. (2004) argue that cross-correlating the *FIRST* data with the *XMM-Newton* survey can effectively

identify all 'normal' star-forming galaxies within X-ray samples. They find a majority of objects in their sample to represent AGN activity, two sources possessing narrow emission line spectra suggesting 'normal' galaxies powered by star-formation, and one double radio source associated with X-ray cluster emission. Zakamska et al. (2004) have been able to identify a sample of type II quasars from the *SDSS* using multi-wavelength surveys ranging from radio to X-ray frequencies and conclude that the candidates in their sample are consistent with their interpretation as powerful obscured AGNs. Flesch & Hardcastle (2004) have presented an all-sky optical catalog of radio/X-ray sources using data from the *ROSAT*, *NVSS*, *FIRST*, *SUMMS* (70% completion), APM and USNO-A catalogs. For nearly 87,000 sources, they list the probabilities that the source is a QSO, galaxy, star or erroneous radio/X-ray association. Mickaelian et al. (2006) have matched the ROSAT-FSC high-galactic latitude objects with a variety of optical catalogs, *NVSS* and *FIRST*, and the *IRAS* and *2MASS* catalogs to create a sample of 2791 sources. They find the catalog to contain 65.4% extragalactic sources 86% of which are AGN (QSOs, BL Lacs, Seyferts) and 34.6% stellar objects (mostly main-sequence stars with spectral types F-G-K-M and a few WDs and CVs). Sánchez-Sutil et al. (2006) have presented a catalog of 70 ultra luminous X-ray sources (ULXs) with radio counterparts and find that 11 of them are new cases of non-nuclear ULX sources with possibly associated radio emission.

Studying the optical properties of radio-selected narrow-line Seyfert 1 galaxies, Whalen et al. (2006) have found that, aside from radio properties, there is no evidence for them being different from traditional narrow-line Seyfert 1 galaxies. They also increased the number of such objects by 16, an increase by a factor of ~ 5. By matching the maxBCG and *FIRST* catalogs, Croft et al. (2007) have determined $\sim 20\%$ of BCGs are detected in the radio, $\sim 93\%$ of which are radio-loud AGNs. The radio-loud fraction seems to have a strong dependence on stellar mass of the host and, for a given stellar mass, BCGs in rich clusters have a higher tendency to be radio-

loud than those in poor clusters or groups, suggesting that the wider environment has some influence on radio-loudness.

Combining radio observations with optical and infrared color selection, Glikman et al. (2007) have demonstrated an efficient selection algorithm ($\sim 50\%$ efficiency) to select quasars substantially redder than those found in optical surveys.

1.8 Technical Test-bed

Proctor (2006), despite limited success in looking for bent-double radio galaxies (triples), has shown how the *FIRST* data can be excellent for testing algorithms such as pattern recognition. White et al. (2007) have also helped in calibrating the VLA's snapshot bias by deriving an empirical expression, although the cause for the bias is still mysterious. Carballo et al. (2008) have used neural networks to identify high-z ($z \geq 3.6$) QSOs with improved efficiency from the *FIRST* survey using radio data and optical photometry without spectra. Chang & Refregier (2002) have tested interferometric image reconstruction using shapelets and claim faithful and accurate reconstruction, suitable for measuring small distortions induced by gravitational lensing in the shapes of background sources by intervening structures.

1.9 Motivation

The foregoing partial list of applications might suggest that the *FIRST* survey has been exhaustively mined. However, the above is only a small fraction of all the research done with *FIRST* and is intended to show the breadth of the science. The impact of *FIRST* has been impressive as evidenced by its ~ 1000 citations. However there is much more to be done with *FIRST* and it is likely to have a lasting value, first, as a continuing tool to address a wide range of science, and second, as a very rich reference point of the radio sky in the years to come when more powerful arrays

become operational. In this thesis, I address two as yet unexplored questions with *FIRST*, the variability of the radio sky and the evolution of FR II quasars. Besides addressing key scientific questions, these projects will demonstrate that the *FIRST* survey still holds much promise and will continue to have an impact even after the arrival of the next-generation radio instruments.

1.9.1 Variables and Transients in the Radio Sky

The twinkling of stars in the night sky has been a source of entertainment, fascination, and wonder to humans since prehistoric times. Over the past several centuries, the systematic study of astronomical variability has increasingly been used to understand the physical properties of unreachably remote systems, and to discover whole new classes of astronomical objects. The coming decade will see a vast expansion in our ability to monitor the variable sky, and continuing advances in understanding may be anticipated.

The variability of astronomical objects arises from both intrinsic and extrinsic causes. Atmospheric, Interplanetary (IPS), and Inter-Stellar Scattering (ISS), secular changes in a source's intrinsic luminosity, changes in the orientation and velocity of relativistic beams in the case of AGN, pulsational instabilities, gravitational collapse, changes in absorption along the line of sight, and gravitational microlensing are a few of the known causes of variability. Detailed study of these phenomena offers insight into a variety of fundamental questions including particle acceleration mechanisms, the structure of the IPM and ISM, accretion and outflow physics, stellar evolution and death, the nature of strong-field gravity, the nuclear equation of state, etc.

The first celestial radio source detected – the Sun – was discovered as a consequence of its variability (Hey 1946). Nonetheless, while variability has continued to be a source of discovery and insight in the radio regime, few dedicated searches for variables and transients have been undertaken, primarily because the observing times

required to conduct deep wide-field surveys are large and current instruments tend to have poor figures of merit for variability studies (Cordes et al. 2004).

In chapter 2, the first comprehensive search for variability in the complete *FIRST* data base is presented. The number of known radio variables is increased by at least an order of magnitude to 1651 with timescales ranging from minutes to years owing to the survey's sensitivity limit of ~ 1 mJy, wide-angle sky coverage of $\sim 9{,}000$ deg^2, and the survey design. I explain in depth why the *FIRST* data are suitable for conducting a search for radio transients and variables. A detailed description of the motivation, the background, the analysis, and the results will be provided.

1.9.2 Evolution of FR II Quasars

With the discovery of double-lobed radio quasars it was believed that a cosmological standard rod had been found. Since radio images would offer accurate measurements of sizes, immediately an interesting application turned out to be constraining the geometry of the universe since the angular size-redshift $(\theta - z)$ relation is a sensitive function of the cosmological parameters.

Although numerous studies have been conducted on these lines, with few exceptions, most have, embarrassingly, generally shown consistency with static Euclidean models rather than with Friedmann models. Most of these are believed to have been compromised by lack of homogeneity, selection effects, etc. With the data and images from the *FIRST* survey and the SDSS, the data is essentially uniform and homogeneous. With high-precision results from other cosmological experiments, such as the WMAP, there are two interesting alternatives to pursue using the $\theta - z$ relation in cosmology. First, there is the possibility to independently constrain the cosmological models. Second, assuming the models of concordant cosmology, the intrinsic size evolution of these standard rods can be estimated. The latter could eventually play a role in the decades-long discussion on the evolution of double-lobed radio sources, as

well as provide useful modeling constraints in the cosmological simulations of these sources.

By far the biggest sample of FR II quasars has been extracted from the *FIRST* survey in conjunction with the spectroscopic and photometric QSO catalogs from the SDSS. Besides ruling out static Euclidean models for the universe (unlike most of the previous studies) and reducing the size of the error bars in the estimated parameters, we find previously unknown degeneracies between them. No conclusive evidence for any significant evolution of size with redshift is found. Remarkable differences in the physical properties of the photometric and spectroscopic samples of FR II quasars are observed, thus raising questions on the nature and origin of these two apparently different populations. Chapter 3 describes in detail the background, the challenges and results of the $\theta - z$ analysis of FR II quasars.

Chapter 2

Variables and Transients in the *FIRST* Survey

2.1 Background

Several next-generation instruments spanning many octaves of the electromagnetic spectrum include the search for variability as one of their primary scientific goals. In the optical domain, a number of surveys focus on time-domain astronomy. The Supernova Legacy Survey (SNLS; Sullivan 2009) identifies SN from multiple epochs to obtain constraints on dark energy. The recently commissioned Palomar Transient Factory (PTF; Rau et al. 2009) has a $12k \times 8k$ CCD providing a 7.9 deg^2 field of view, and achieves 5σ limiting magnitudes of 21.0 and 21.6 in MOULD-R and SDSS-g bands, respectively, in a 60 s exposure. The ongoing 5-Day Cadence and Dynamic Cadence surveys are sensitive to timescales from minutes to years, sampling a range of phenomena such as SNe, Galactic variable stars, orphan gamma-ray burst afterglows, microlensing, etc. The Panoramic Survey Telescope and Rapid Response System (Pan-STARRS; Kaiser 2004) is another instrument, one of whose primary aims is to survey the sky for variables and transients. It will consist of an array of four 1.8-m telescopes each with a 1.4 billion pixel CCD camera and a 7 deg^2 field-of-view. It aims to survey about three-fourths of the sky in each of the passbands $g,\ r,\ i,\ z$ and Y; survey speeds of ~ 6000 deg^2 per night will be achieved, yielding a 5σ point-source detection threshold $m \simeq 24$ in the r-band. The Large Synoptic Survey Telescope (LSST; Ivezić et al. 2008; Tyson & Angel 2001) is designed to survey $\sim 30,000$ deg^2 of the sky, searching for optical variables on timescales of minutes to years down

to $r \sim 24.5$ or better in individual visits, and will cover the entire visible sky each week. At the high-energy end of the spectrum, a number of instruments have been dedicated to the monitoring of burst events and transients. The Fermi Observatory is currently surveying the gamma-ray sky every three hours, providing information on both steady and variable sources.

Indeed, one of the key scientific aims of the next generation of radio telescopes such as LOFAR, ASKAP, MWA and, eventually, the SKA is a study of radio variability. As discussed by Hessels et al. (2009), LOFAR will survey the sky for pulsars and fast transients at low frequencies (30-240 MHz) with an emphasis on timescales of less than a second. CVs, X-ray binaries, GRBs, SNe, AGN, flare stars, exoplanets and many more new phenomena are expected to contribute to its inventory of radio transients and variables (Fender et al. 2008). The Australian SKA Pathfinder (ASKAP; Johnston et al. 2007, 2008) is designed to achieve very high survey speeds and noise levels down to $\sim 10 - 100$ μJy in an hour in the 1 GHz band, and will shed light on GRBs, radio supernovae (RSNe), Intra-Day Variables (IDVs), etc. The Murchison Widefield Array (MWA) will operate in the 80-300 MHz range carrying out a blind search for variables and transients in addition to targeting explosive events, stellar and planetary phenomena, and compact objects over a range of timescales from nanoseconds to years (Lonsdale et al. 2009). The EVLA (Napier 2006; Rupen 2000) will offer vastly improved sensitivity along with dynamic scheduling, providing a host of new capabilities for transient and variable searches. Finally, a search for radio variables and transients also forms an important part of the scientific objectives of the Square Kilometer Array (SKA). The SKA is expected to discover a number of classes of variable radio objects such as pulsars and magnetars, GRBs that are γ-ray loud and γ-ray quiet in both afterglow and prompt emission, sub-stellar objects such as brown dwarfs and exoplanets, microquasars, and potentially new classes of astrophysical phenomena (Cordes et al. 2004; Cordes 2008; Wilkinson et al. 2004).

Most of the research on radio variability to date has focused on bright radio samples (e.g., Gregorini et al. (1986), $S > 0.4$ Jy at 408 MHz; Lister et al. (2001), $S > 0.4$ Jy at 5 GHz; Aller et al. (2003), $S > 1.3$ Jy at 5 GHz). At these flux densities, the radio source population is dominated by AGN, while at fainter flux densities ($\lesssim 1$ mJy), it is dominated by star-forming galaxies (Windhorst et al. 1999; Richards et al. 1999; Hopkins et al. 2000). Research on the variability of faint radio sources has so far yielded small samples as a consequence of the small areas searched and the longer integration times required. Carilli et al. (2003) observed the Lockman Hole region on timescales of 19 days and 17 months down to 0.1 mJy at 1.4 GHz and discovered nine variable sources, providing an upper limit to the areal density of variable radio sources, as well as constraints on the beaming angle of GRBs and confusion limits relevant to searches for GRB afterglows based on the detection rates. Archival VLA calibrator observations spanning 22 years with 944 independent epochs have been used by Bower et al. (2007) to search for radio transients over a single field with half-power beam widths $9\rlap{.}'0$ and $5\rlap{.}'4$ at 5 GHz and 8.4 GHz, respectively. The typical flux density threshold is 300 μJy. They identify eight transients in single epochs and two transients in two-month averages of the data. Two of the transients were identified as RSNe, while the absence of optical counterparts for the remainder offers a wide variety of possibilities including Orphaned GRB Afterglows (OGRBA), stellar sources, propagation effects, microlensing events, or perhaps mechanisms heretofore unknown.

In the Galaxy, single radio bursts detected from the Parkes Multibeam Pulsar Survey revealed a new population of neutron stars: Rotating Radio Anomalous Transients (RRATs; McLaughlin et al. 2006). Galactic Center Radio Transients (GCRTs; Hyman et al. 2002, 2005, 2009) have diverse light curves with outburst periods and burst durations varying from minutes to months. Lacking counterparts at other wavelengths, their hosts, and the physical mechanisms involved, remain a mystery.

Two large, sensitive, wide-field surveys exist at radio wavelengths. The NRAO VLA Sky Survey (NVSS; Condon et al. 1998) covered the entire sky north of -40° declination at 1.4 GHz with a resolution of $45''$ and an rms noise of 0.45 mJy. The Faint Images of the Radio Sky at Twenty cm survey (*FIRST*; White et al. 1997) has covered $\gtrsim 9,000$ deg^2 of the sky at 1.4 GHz with a uniform rms of 0.15 mJy and an angular resolution of $5''.4$. A number of authors have used these two surveys in their overlap region to search for radio transients. Levinson et al. (2002) tried to constrain the detection rates of orphaned radio afterglows often associated with GRBs. Gal-Yam et al. (2006) attempted to characterize the sample generated by Levinson et al. (2002). They report the detection of a radio SN in a nearby galaxy and the detection of a source with no optical counterpart, concluding the latter is unlikely to be associated with a GRB. They also place tighter constraints on the beaming factor of GRBs and a limit on total rate of nearby relativistic explosions, implying that most core collapse SNe do not eject unconfined relativistic outflows. These studies are complicated by the mismatched resolutions and flux density sensitivities of the NVSS and the *FIRST* surveys.

de Vries et al. (2004) have used ~ 120 deg^2 of the *FIRST* survey data near $\delta = 0°$ taken in 1995 and then repeated in 2002 to study the optical properties of sources that exhibit significant radio variability at 1.4 GHz over this seven-year interval. They find 123 variable objects with flux densities ranging from ~ 2 - 1000 mJy. They conclude that there is a higher fraction of quasars in the sample of variables compared to the non-varying sample.

Here, we use the data from the *FIRST* survey to create the largest, unbiased sample of variable radio sources to date down to a sensitivity level of a few mJy. In §2.2.1, we describe the attributes of the *FIRST* survey relevant to a study of radio variability. In §2.3, we present our approach to extracting a sample of variables from the more than two million individual source observations contained in the database.

We then describe (§2.4) our refinement of the list of variable candidates, the parameterization of their variability, and a summary of their properties. In §2.5, §2.6 and §2.7, we present the results of our analysis, including the cross-identification of our sample of transients and variables with existing data at optical wavelengths (and in other spectral regimes), and a discussion of the classes of variables identified, as well as the new populations which might exist among the unidentified radio variables.

2.2   The Data

The *FIRST* survey, described below, is the most sensitive large-area radio survey in existence, and provides a database that is uniform in angular resolution and flux density sensitivity. Until the next generation of radio instruments arrives, it provides an opportunity to produce the largest unbiased survey yet undertaken for radio transients and variables. The *FIRST* survey is described again below in this context.

2.2.1   The *FIRST* Survey

The *FIRST* survey covered $\sim 9{,}055$ deg^2 ($8{,}444$ deg^2 in the north Galactic cap and 611 deg^2 in the south Galactic cap) with observations conducted between 1993 and 2004 using the NRAO VLA in its B-configuration operating at a frequency of 1.4 GHz (Becker et al. 1995). Roughly 65,000 three-minute snapshot images were obtained over this period. All of the work published to date, including the *FIRST* catalog, has been based on images constructed by co-adding these snapshots with appropriate weightings (for details, see White et al. 1997); this process yielded images with a uniform noise level of ~ 0.15 mJy. The final catalog contains 816,331 sources with a source detection threshold of ~ 1 mJy, yielding a source density of ~ 90 deg^{-2}. The astrometric accuracy of the catalog is better than $1''$. The co-added maps have $1{.}''8$ pixels and an angular resolution of $5{.}''4$. The FWHM of the VLA's primary beam is

$\sim 30'$. The catalog also assigns a sidelobe probability to each source.

Becker et al. (1995) describe the survey design and objectives in full detail. Here, we provide a brief review of the aspects of the survey relevant to a variability search. In order to obtain uniform sensitivity and sky coverage in the most efficient manner possible, a hexagonal grid is optimal. The pointing centers of each snapshot were placed at the vertices of this hexagonal grid, the shape of which changes slowly with declination. The typical spacing between two neighbouring snapshots is $\lesssim 26'$. Thus all adjacent snapshots overlap. The time between overlapping observations varies: ~ 3 minutes between adjacent snapshots along the same declination strip in the east-west direction, ~ 1 to many days between adjacent snapshots that lie on two adjacent strips of declination in the north-south direction, and ~ 1 to few years between two adjacent blocks of annual allocations. Thus, while the survey was not undertaken to find variables and transients, its design is implicitly conducive for a search for radio variability on timescales of minutes to years.

In this project, we use all of the snapshots from the North Galactic Cap data which covers 8,444 $\deg^2$. Part of the South Galactic Cap coverage was repeated, and is in the process of being observed at a third epoch; preliminary variability results have already been reported by de Vries et al. (2004) and a comprehensive analysis of this data set will be undertaken separately when the current observations are completed.

In addition, we have restricted our analysis to isolated point sources. Variable sources are necessarily compact. Even though compact components of extended sources could vary, we limit our attention herein to point-like (unresolved) sources with a sidelobe probability below 0.15. Further, an additional selection criterion was imposed requiring these sources to be relatively isolated with no neighbours within $18''$; this minimizes the likelihood that differing multi-component fits between observations will produce spurious evidence of variability.

Figure 2.1 shows the flux density histograms of all sources, point-like sources, and

isolated point-like sources. Out of a total source count of 816,331, there are 692,209 sources with sidelobe probabilities less than or equal to 0.15. Of these, 577,940 are isolated sources (out to $18''$ radius) and 279,407 meet our criterion for being point-like (major axis $< 5''\!.95$). We examine the variability characteristics of these 279,407 sources which have been observed between two and seven times each.
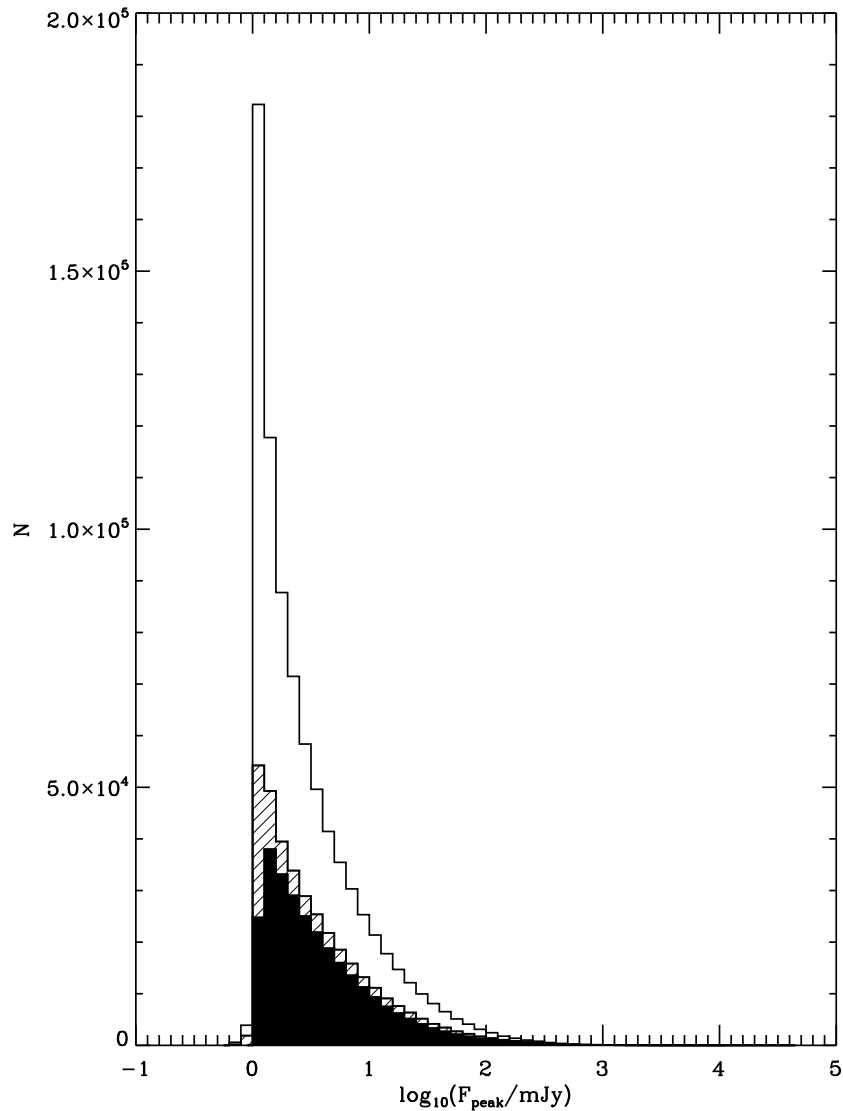
Figure 2.1: Histogram of peak flux densities for sources in the *FIRST* survey. The hatched area includes all point sources, while the black shaded histogram is for the isolated point sources used in this study.

2.2.2   VLA Data-recording Glitch

It recently became clear that the on-line VLA recording system suffers from a rare glitch that manifests itself many times in the *FIRST* snapshot database. Although the exact nature and cause for this glitch have not been completely understood, the result is that a few visibilities from one snapshot can be appended to the adjacent snapshot. The prototypical example that led to the discovery of this glitch is the source claimed to be a transient based on a comparison with the NVSS: VLA 172059.9+38522 (Gal-Yam et al. 2006; Levinson et al. 2002). The authors speculated that this could be a prototype for a new class of transients. Upon investigation, it was discovered that one of the snapshot images containing the location of this source had been affected by the VLA glitch. A thorough search of the database found that 190 snapshot images (0.29%) are apparently affected by this problem; while in many cases the problem can be fixed by deleting a few records from the *uv* data set, in other cases subtler anomalies appear. As a consequence, we have simply excluded all these snapshot images from our analysis. Additional grid images excised include those found to contain imaging artifacts and those with large calibration errors (see below).

2.3   Data Analysis

Using the positions of isolated, point-like sources from the *FIRST* catalog, we created a comprehensive inventory of each object location and the corresponding pixel locations in each of the grid images in which it appeared. Every object was found to be covered by from two to seven snapshot images as expected from the survey design described above.

2.3.1 Gaussian Fitting

In each of the snapshot images, at the location of the object, a peak flux density was estimated by fitting a Gaussian plus a flat baseline component. The position, width and position angle of the Gaussian, already available from the catalog, were held fixed. The RMS noise in each image was also measured around the object's location. In the case of a marginal (or non-) detection of the object in a snapshot image, a 3σ upper limit was assigned.

2.3.2 Identification & Removal of Striped Images

Artefacts in radio interferometric images arise for a number of reasons such as calibration errors, interference, etc. For a large-scale survey such as *FIRST*, it is difficult to ensure high data quality at all times during the observations. One not uncommon problem of snapshot images is a striped pattern corrupting an image owing to un-excised interference or other deconvolution problems.

After deriving a preliminary list of candidate variables, we plotted their positions on the sky, and found that some objects were spatially clustered. These clusters had different shapes, including linear, elliptical and irregular appearances, and their sizes spanned several degrees on the sky. Such strong clustering is highly suggestive of systematic problems with the images. We investigated the snapshot images associated with these clustered objects and found that many, especially toward the southern limit of the survey, have clearly visible striped patterns running across them. The width of these stripes is typically greater than the angular resolution of the images. Having restricted ourselves to isolated point-like sources, we were able to make use of the baseline fitting performed in §2.3.1. We flagged any image that contained one or more sources with a baseline component greater than 1.75 times the local image noise. A total of 2162 (3.96%) such snapshot images were deleted from subsequent analysis. Figure 2.2 illustrates how this step significantly eliminated the non-physical

clustering of variable and transient source candidates.

(a) Before flagging   *(b)* After flagging
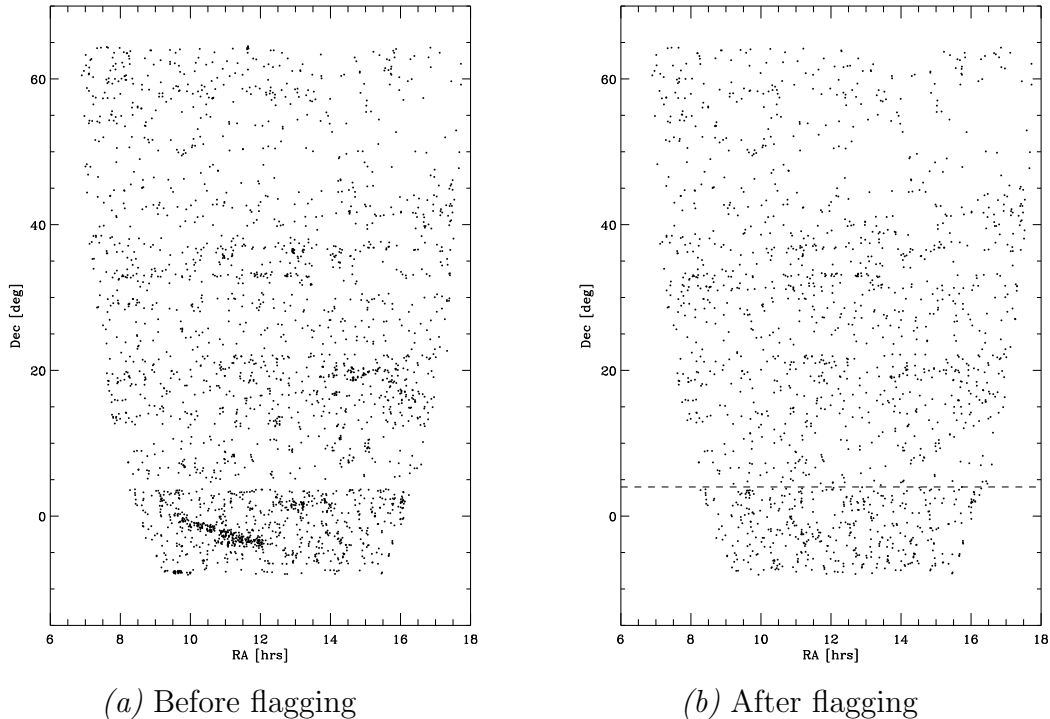
Figure 2.2: The sky positions (J2000) of outliers before (*Left*) and after (*Right*) flagging and removing the snapshot images that contain one or more sources with a significant baseline component from the gaussian fitting routine (See §2.3.2). Note the clear reduction in the source clusters. The horizontal dashed line indicates the boundary in declination below which the outlier density shows enhancement; this is a consequence of the change in the convolving beam size which reduces the number of sources eliminated from consideration by modest extent (cf. Figure 2.11).

2.3.3   Identifying Global Calibration Amplitude Errors

While amplitude and phase calibration errors are minimized in the *FIRST* imaging pipeline for individual snapshots, it is important to keep in mind that the survey is spread over very large scales in space and time. The overall calibration scale, then, could well vary over the course of the survey (see White et al. 1997). Relevant to our study is the variation of the overall calibration scale in the neighbourhood of each source since we are interested only in the snapshot images that contain the particular source under consideration.

An estimation of the calibration error was performed after a first iteration of steps in §2.3.4 but before the identification of any variables or transients. The algorithm used considers sources in each snapshot image and compares their behaviour to that in all the neighbouring snapshots in which they are also found. The null hypothesis, true for a vast majority of the sources, is that sources will exhibit a constant peak flux density across the different snapshots in which they are found. A best-fit algorithm assigns a multiplicative amplitude calibration correction factor to each snapshot image such that when it is applied, all the sources in the neighbourhood are as close to the null hypothesis behaviour as possible in a "minimum absolute deviation" sense. Thus, the amplitude calibration variations are estimated locally.

Figure 2.3 shows the histogram of the amplitude correction factors, where a value of unity indicates no correction need be applied. It can be seen that the distribution, especially the inner core comprising the large majority of snapshot images, can be reasonably fit with a gaussian profile with a standard deviation of 4.4%. However, tails can be seen on both sides of the distribution indicating some large fluctuations in the amplitude calibration for a small fraction of the images. We have accounted for the typical calibration uncertainty using a conservative value of 5% in determining the uncertainty of primary-beam-corrected flux densities of individual snapshots as described in §2.3.5.

We experimented with different thresholds for the largest allowed amplitude calibration offsets. Setting a threshold of 20%, we found the ratio of snapshots with correction factors above this threshold to the decrease in the number of candidate variables was high when compared to the scenario considering the snapshots with correction factors below this threshold. We also performed an extra iteration, computing the amplitude correction factor after removing sources that were found to be candidate variables and recomputing the calibration correction factors. We find evidence that the change in the amplitude correction factors between the two iterations
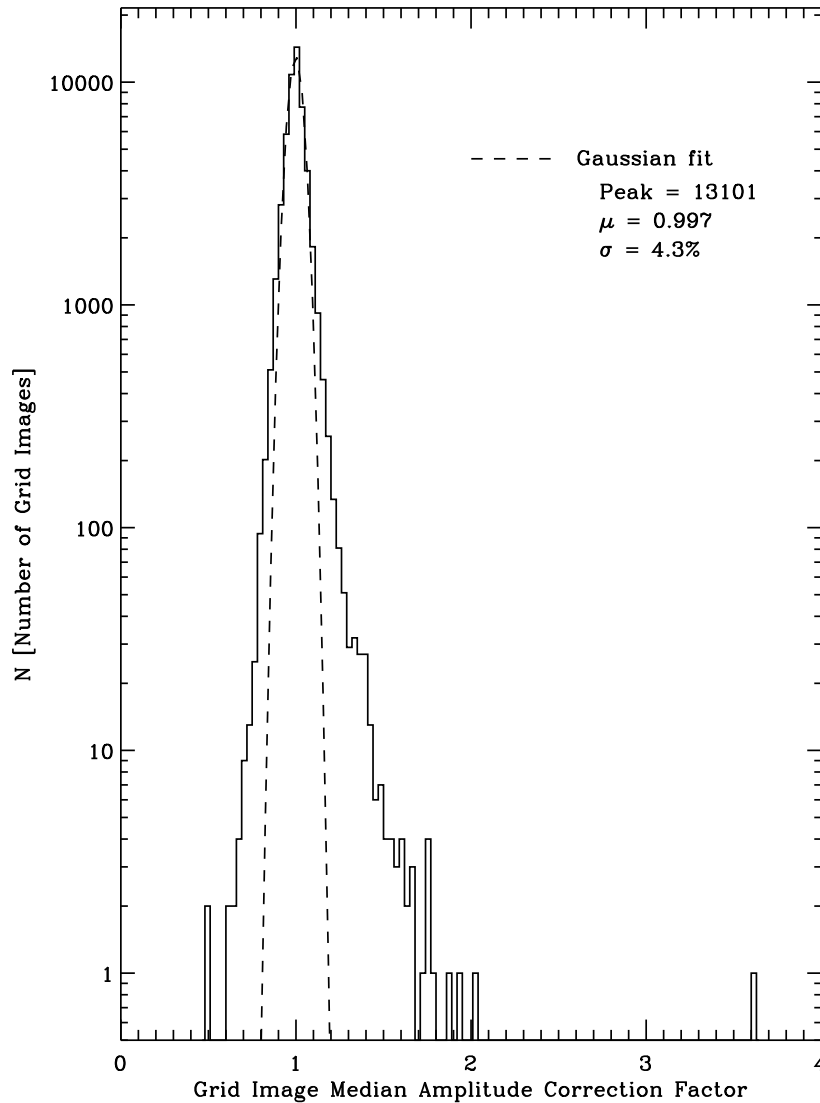
Figure 2.3: Histogram of overall amplitude correction factors for grid images. The dashed line represents the best gaussian fit to the histogram whose parameters (peak, mean (μ) and standard deviation (σ)) are displayed in the plot.

is greater for snapshots that contain putative variables than for ones that do not (figure 2.4). However, the final list of variable candidates between one such iteration and the next changes only by $\sim 2\%$. Thus, we have used only snapshot images that have an amplitude offset less than 20% after one iteration of the amplitude correction factor estimation.

For the retained set of images, on an image by image basis, we apply the overall
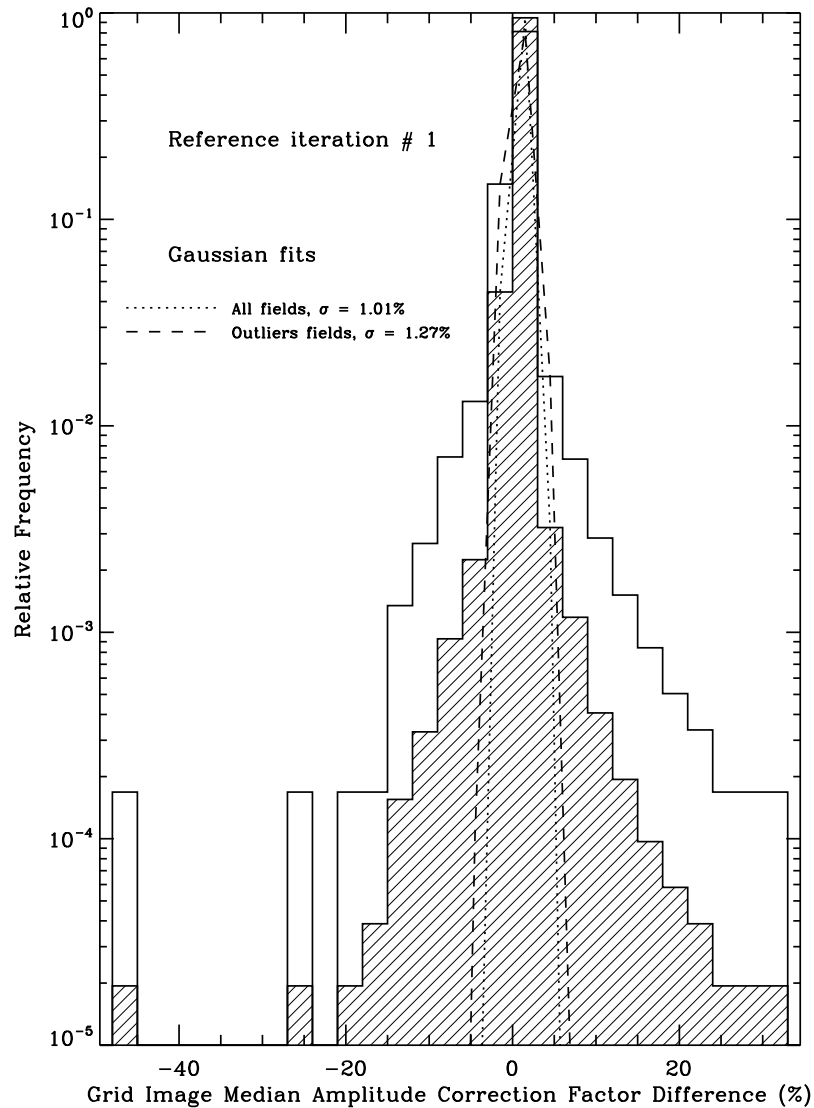
Figure 2.4: Relative frequencies of the difference in median calibration offsets (in percent) for the grid images between the first and second iterations where the second iteration has excluded the outliers (determined from the previous iteration) from the calibration calculations. The shaded portion represents all snapshot images while the unshaded portion represents snapshot images that contain one or more outliers. The unshaded distribution is clearly wider than the shaded one as indicated by the gaussian fits, implying that the amplitude calibrations of the snapshot images are affected by the inclusion of the outliers.

amplitude calibration correction factors to the peak flux densities, local image noise values, and baseline components for all the sources found in those images. From here on, these corrected values are treated as the true values.

2.3.4 Determining the Primary Beam Empirically

The data were obtained in 2×7 3-MHz channels near 1.4 GHz. While the center frequency of these bands was fixed for most of the survey observations, the interference environment was constantly changing, leading to data editing which affects the effective center frequency of the observing band(s). Thus, the frequency-dependent primary beam, normally derived from the AIPS task PBCOR, cannot be precisely determined.

Our selection algorithm makes use of the hypothesis that the non-varying source population is expected to dominate the variable one. Hence, with the off-axis angle information available for each source in each snapshot image, the primary beam can be empirically determined. Due to aforementioned reasons, it is conceivable that the primary beam could be time-dependent. However, we see from figure 2.5 that the difference between our estimate for the primary beam and the nominal VLA primary beam is of the order of only a few percent. We indeed find from figure 2.6 that the uncertainty arising out of the primary beam estimation is negligible irrespective of source flux densities.

The peak flux density of such an isolated, point-like object measured in a snapshot image (determined as described in §2.3.1) is normalized by the reported catalog flux density (after taking into account the CLEAN bias as quantified by White et al. 2007). Since the snapshot images and the fitted peak flux densities derived therefrom have not been corrected for the primary beam attenuation, adopting the null hypothesis that a source's flux density stays constant means that these normalized values yield a primary beam normalization at the off-axis angle of the measured source. When this normalization is performed for all objects, we obtain an empirical primary beam:

$$\text{empirical PB} = \frac{\text{measured map peakflux (mJy)}}{\text{catalog peakflux (mJy)} - \text{CB (mJy)}}$$

where, CB is the CLEAN bias.

The empirical primary beam values obtained from all the objects in each of their corresponding snapshot images were binned in angular offset from the center of the primary beam. A sixth-degree polynomial was fitted to determine an analytical expression for the empirical primary beam. The error in the primary beam estimate is the uncertainty in the mean estimate for the primary beam in each bin, which is the standard deviation in each bin divided by the square root of the number of offsets in that bin. Thus, a primary beam error estimate (used in §2.3.5) is assigned to each data point on each light curve depending on which bin of angular offset the data point falls into.

Figure 2.5 shows the scatter plot of normalized flux densities from all the usable snapshot images in the upper panel; in the lower panel, the bin-averaged data points from the upper panel are overplotted on the polynomial fit. Fits were obtained independently in eight separate declination zones, but no significant variations ($> 0.9\%$) with declination were seen, so a single empirical primary beam was used for the whole survey.

2.3.5 Sources of Uncertainty in the Peak Flux Density

We estimate the sources of uncertainty in the peak flux density obtained for an object detected in a snapshot image. If $F = Af/p$, where F is the reported flux density, A is the absolute amplitude calibration (ideally $A = 1$) and $p = p(\theta)$, the primary beam value at an offset (θ) from the field center, the principal uncertainties that need to be accounted for include the following:

i. local noise in the grid image in the vicinity of the source (Δf): This will further be amplified because of the primary beam effect, especially for sources far from the field center. $\Delta F = A\,\Delta f/p$.
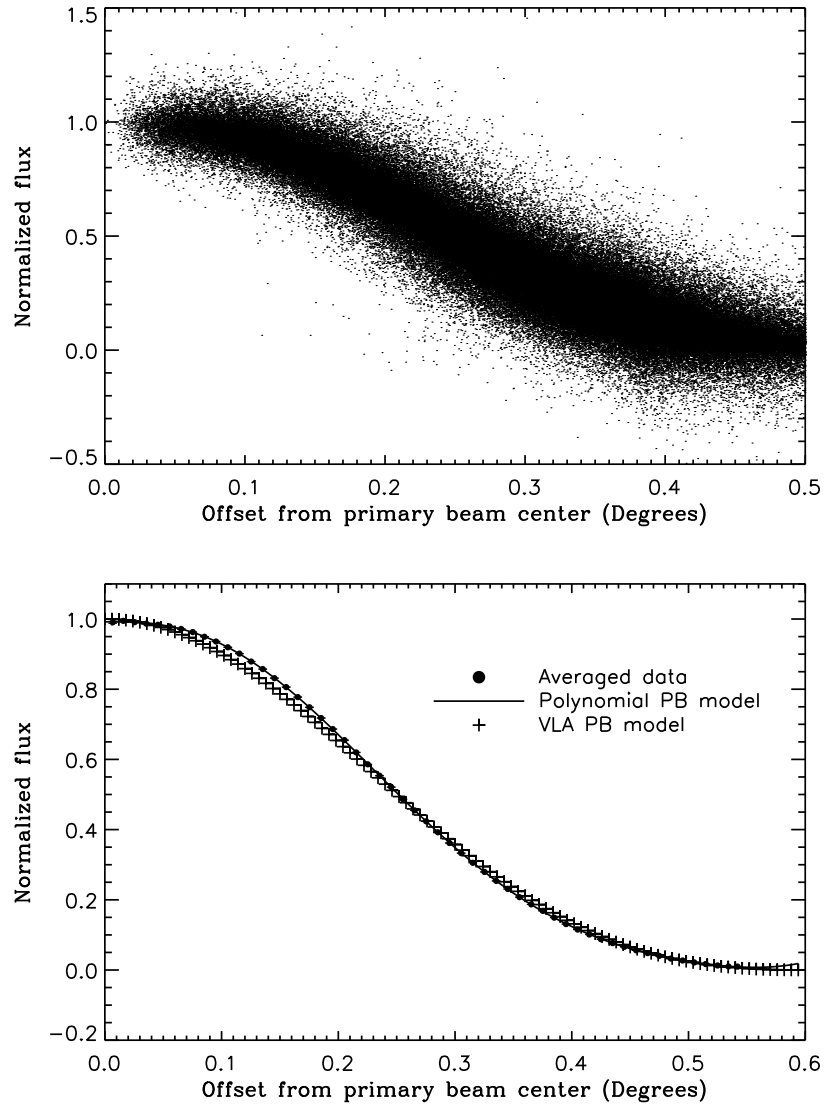
Figure 2.5: *Upper panel*: Fitted peak Gaussian flux densities of isolated point sources in the snapshot images normalized by their respective catalog flux densities. *Lower panel:* Binned average (filled circles) of the panel above over-plotted with the fitted polynomial primary beam model (solid line) and the nominal primary beam correction factor found in AIPS ('plus' symbols).

ii. uncertainties in primary beam (Δp): We have computed empirically the primary beam and its uncertainty from the data as described in §2.3.4. $\Delta F = A\, f/p^2 \,\Delta p$.

iii. uncertainties in the overall flux calibration amplitude (ΔA): This uncertainty is $\sim 5\%$ and was estimated as described in §2.3.3. $\Delta F = \Delta A\, f/p$.

iv. pointing errors of the VLA antenna ($\Delta\theta$): This is not the same as the positional accuracy of the sources in the catalog. The antennas have an rms pointing error of $\Delta\theta \sim 10''$. This translates to an error in flux density, $\Delta F = A\,f/p^2\,\frac{\mathrm{d}p}{\mathrm{d}\theta}\,\Delta\theta$.

The overall error is obtained by adding all the above errors in quadrature. The dominant contributions come from the map noise for fainter sources and the amplitude calibration errors for brighter sources.

$$\Delta F = \sqrt{(\Delta A\,f/p)^2 + (A\,\Delta f/p)^2 + (A\,f/p^2\,\Delta p)^2 + \left(A\,f/p^2\,\frac{\mathrm{d}p}{\mathrm{d}\theta}\,\Delta\theta\right)^2}$$

Figure 2.6 shows the contributions of these different sources of uncertainty as a function of angular offset from the center of the image for two sources observed (without primary beam correction) to have flux densities of 1 mJy and 10 mJy, respectively.

2.4   Selection of Variable Candidates

2.4.1   Mean Inferred Peak vs. Catalog Peak Flux Density

Owing to the reasons discussed in §2.2.2, §2.3.2 and §2.3.3, the snapshot images that form the basis of our search are a subset of those from which the *FIRST* catalog was constructed. The catalog peak flux densities were derived by a weighted average estimate of the inferred fluxes where the weights are related to the square of the primary beam pattern (White et al. 1997; Condon et al. 1998). We have recalculated the mean value for each source using only those snapshot images actually included in our search and denote it by $\overline{f}$, where $\overline{f} = \sum_i p_i^2 f_i / \sum_i p_i^2$. $\overline{f}$ and $\langle f \rangle$ will be used interchangeably hereafter.

Inferred peak flux density points that lie far from $\overline{f}$ are considered outliers. We
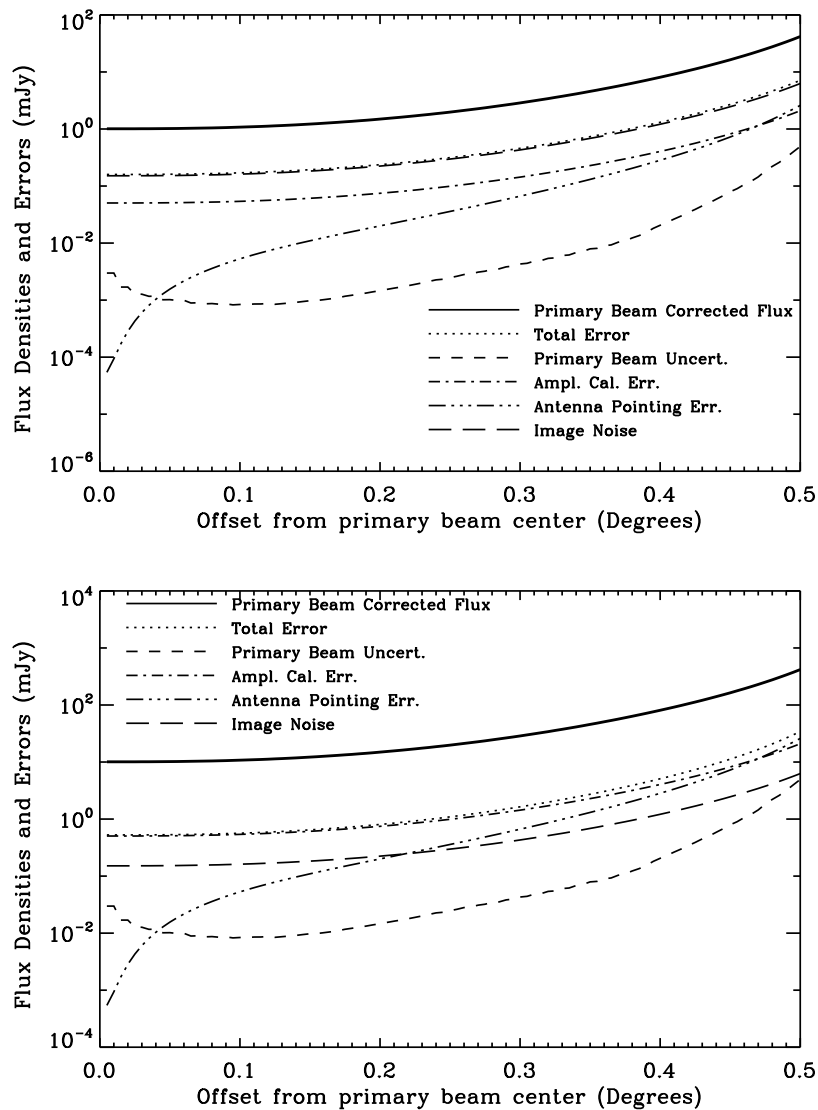
Figure 2.6: Relative contributions of errors from various causes. *Upper panel*: For a source with an observed peak flux density of 1 mJy. *Lower panel*: For a source with an observed peak flux density of 10 mJy. The solid line shows the primary beam-corrected intrinsic flux densities of sources as a function of off-axis angle.

have selected as candidate variables outliers that deviate from $\overline{f}$ by more than five times their inferred peak flux density uncertainty, defined in §2.3.5.

2.4.2 Removal of Contamination from False Positives

We have identified several additional effects other than genuine variability that can generate outliers.

- **Low-Quality Images**: Noisy images and images with interference and other deconvolution errors are significant sources of false detections. Such outliers have been largely eliminated using the technique described in §2.3.2; a few additional bad fields containing large numbers of spurious sources were also deleted.

- **Sidelobes**: There were instances in which sidelobes from nearby sources have significant flux density in one grid image but are absent or marginal in others, thus producing an apparent source that looks both genuine and variable. The *FIRST* catalog-generation algorithm does calculate a sidelobe probability for each source, and we selected only objects with a sidelobe probability less than 0.15. Nonetheless, some unlabeled sidelobes are still present. All fields containing bright sources were examined carefully to eliminate sidelobes as spurious variables. Variable and transient sources suspected of being sidelobes from strong sources with peak flux densities of > 500 mJy within a radius of $31'$ have been flagged.

- **Calibration Problems**: Defective calibration can cause sources to vary between different snapshot images even after incorporating the grid image amplitude correction factors. To identify and eliminate such sources, we used the catalog to select a few (usually between two and four) objects that were neighbours of each outlier (within a $9'$ radius) and were also point-like. These were normalized by their respective mean peak flux densities. Each was examined for any deviations from the ideal normalized value of unity. Some neighbours exhibited the same variability pattern as the outliers, thus confirming the presence of

remaining calibration problems. Some others were simply inconsistent with no variation, making the corresponding outliers suspect. We used this procedure on all outliers to select a final list that appeared to be free from calibration problems. About 30 outliers could be flagged as suspect when using 3σ for the neighbours' normalized flux density deviation from ideal mean and 17 were so flagged using 3.5σ (figure 2.7).
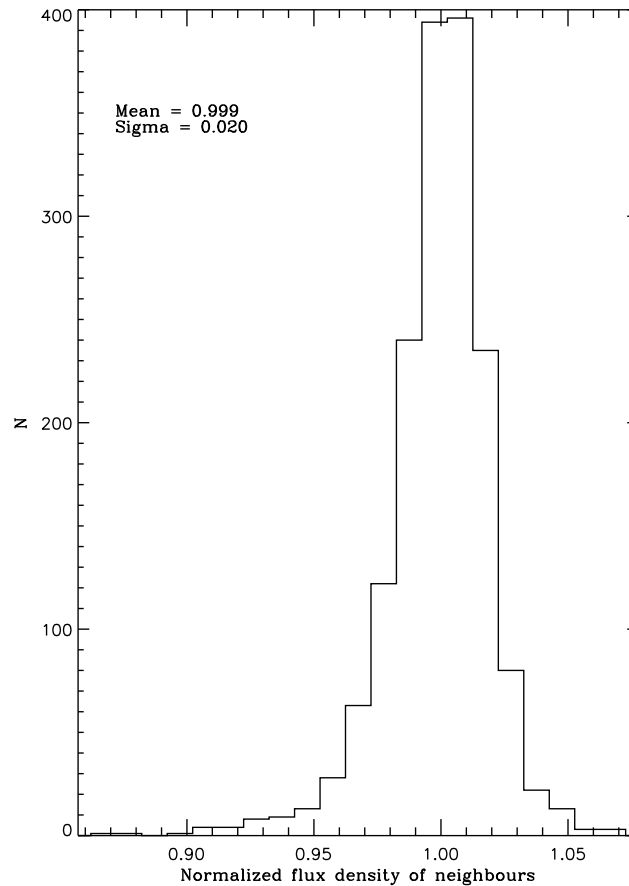
Figure 2.7: Histogram of mean normalized flux densities of neighbouring sources associated with outliers.

After removal of all identified false positives, we are left with a sample of 1651 variables and transients.

2.4.3   Indicators of Variability

We examined this sample of candidates based on their degree of variability. We used three indicators to select variable and transient candidates.

2.4.3.1 χ^2-probability

We define $\chi^2 = \sum_i \left(\frac{f_i - \overline{f}}{\sigma_i}\right)^2$ and χ^2-probability= $P(\chi^2, \nu)$ as the probability that a χ^2-statistic falls above a certain value $\chi^2 = \sum_i \left(\frac{f_i - \overline{f}}{\sigma_i}\right)^2$, with $f_i =$ inferred peak flux density of the ith data point, $\overline{f} =$ average inferred peak flux density weighted by the primary beam, $\sigma_i =$ uncertainty in f_i, $\nu = n - 1$ is the number of degrees of freedom, and n, is the number of data points in the light curve. Since there is only one constraint in the model for the null hypothesis – that the peak flux density is constant with time – it follows that $\nu = n - 1$.

The probability threshold chosen is $P(\chi^2, \nu) \leq 5.733 \times 10^{-7}$ which is equivalent to the probability that the absolute value of a normally distributed variable falls beyond five standard deviations.

2.4.3.2   Maximum Deviation from Mean Inferred Peak Flux Density

An alternate indicator of variability is the maximum deviation of any individual data point in a light curve from the null hypothesis that the flux density is constant at a value given by the mean inferred peak flux density. We denote this by σ_{max} defined as $\text{MAX}\left\{\left|\frac{f_i - \overline{f}}{\sigma_i}\right|\right\}$. We chose a threshold $\sigma_{\text{max}} \geq 5$.

2.4.3.3   Data Point Pair with Most Significant Flux Density Difference & Timescale Information

In order to preserve information about variations between any pair of data points in a light curve (and the associated timescale), we also estimate the variation of each point from all the others in a light curve. The significance of this difference is given

by the ratio obtained by dividing the difference by the uncertainties in the two flux density estimates added in quadrature,

$$\Delta_{ij} = \frac{|f_i - f_j|}{\sqrt{\sigma_i^2 + \sigma_j^2}}$$

where, Δ_{ij} = significance ratio between i^{th} and j^{th} data points, f_i = inferred peak flux density at the ith data point, f_j = inferred peak flux density at the jth data point, σ_i = uncertainty in f_i, and, σ_j = uncertainty in f_j. We select the pair that has the maximum absolute value defined as $\Delta_{\text{max}} = \text{MAX}\{\Delta_{ij}\}$. For an outlier selected with this indicator, the threshold is $\Delta_{\text{max}} \geq 6$.

$P(\chi^2, \nu)$ is an indicator of overall variability of a light curve that can arise from low but sustained variations, large, sudden variations, or both. Although $P(\chi^2, \nu)$ provides a valid statistical indicator of variability, information about timescales and the temporal localization of the variability has been ignored. Unlike the indicator $P(\chi^2, \nu)$, σ_{max} and Δ_{max} are indicators of large sudden variability and temporally localize the variability in the light curve.

A similar estimation of $P(\chi^2, \nu)$, σ_{max} and Δ_{max} are performed for the neighbours of the outliers. The respective thresholds were chosen as those beyond which the population of varying sources and their non-varying neighbours look statistically different as defined by a K-S test.

Figure 2.8 displays a scatter plot showing the relation between Δ_{max} and $\overline{f}$. Similarly, figure 2.9 shows the distribution of σ_{max} against $\overline{f}$. Note that in both the figures, a few objects have a relatively low significance on one variability indicator alone, but are still included as variable when accounted for by other indicators of variability. Figure 2.10 illustrates the distribution of outliers described by the parameter $P(\chi^2, \nu)$. The fraction of outliers to the right of the dashed line are those selected by criteria other than the $P(\chi^2, \nu)$ criterion. The number with a left arrow indicates

the number of outliers with even smaller probabilities that could not be represented in the plot.
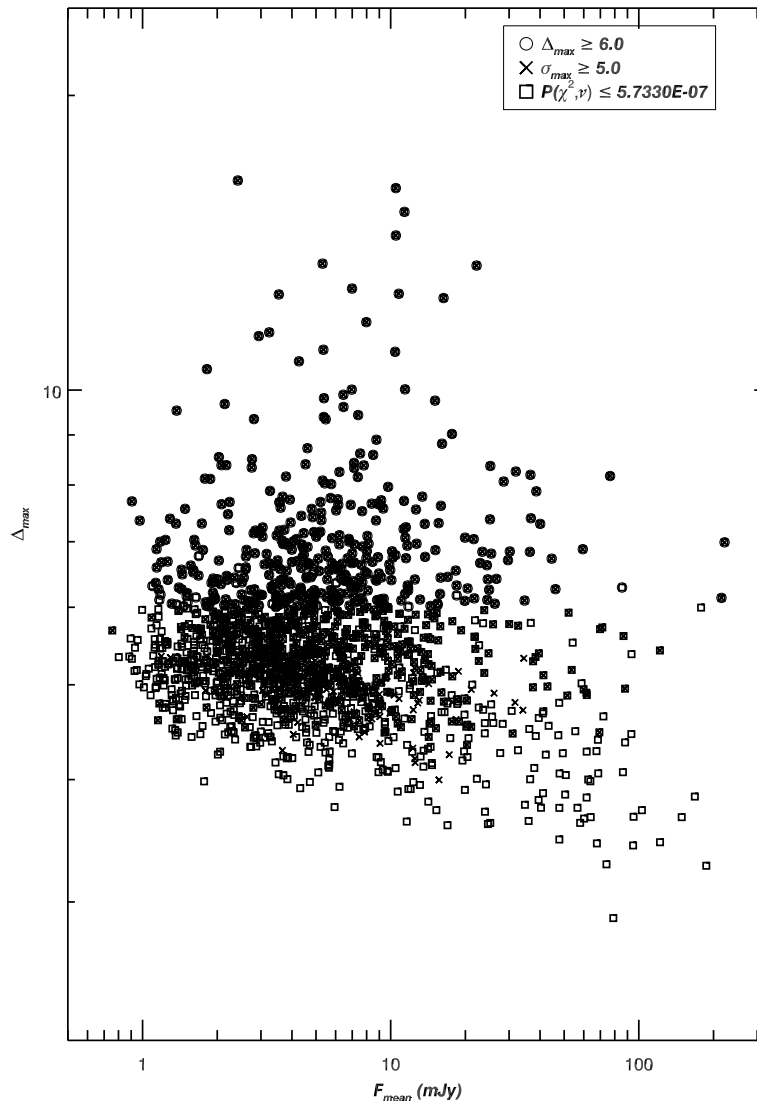
Figure 2.8: The measure of variability, namely, $\Delta_{\max}$ plotted against average peak flux density. The different symbols correspond to outliers that were selected on the basis of various measures of variability.

The sky positions of the outliers are shown in figure 2.2. One notable feature is that the density of outliers below a declination of $\approx 4°$ is enhanced. This is because the synthesized beam with which the data is convolved increases below a declination of $\approx 4°$ as is clearly illustrated in figure 2.11. Consequently, more objects meet
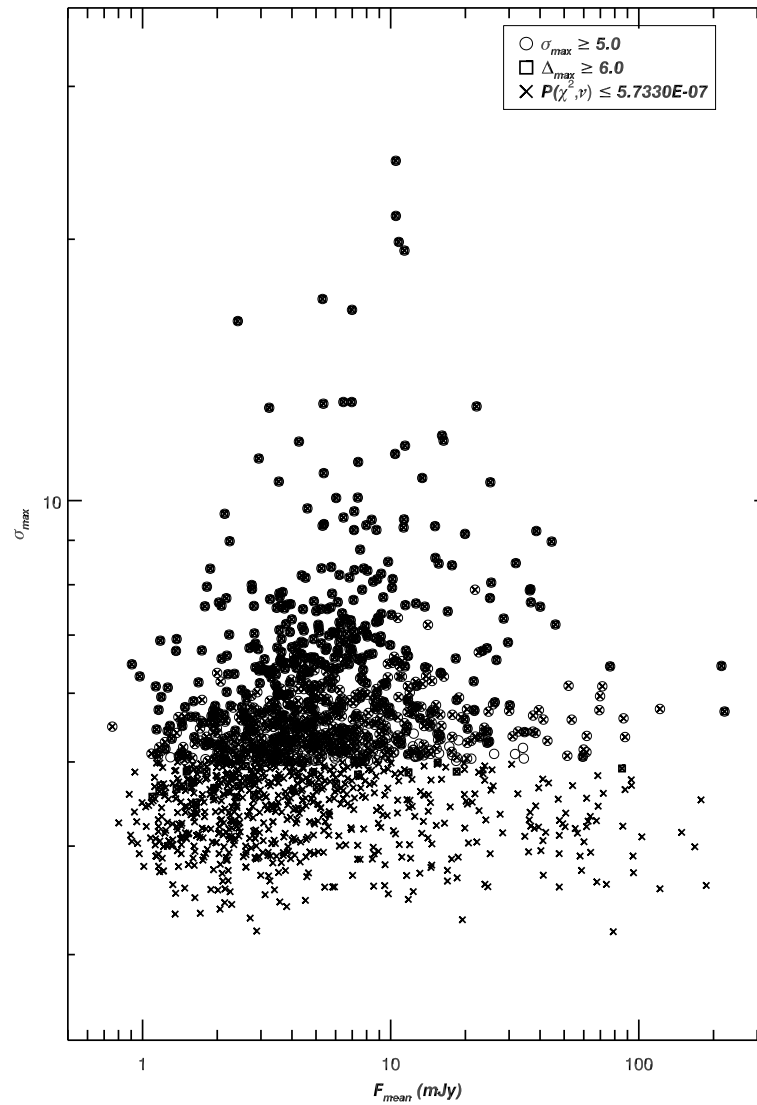
Figure 2.9: The measure of variability, namely, $\sigma_{\max}$ plotted against average peak flux density. The different symbols correspond to outliers that were selected on the basis of various measures of variability.

the criterion for a point-like source, increasing the density of both non-variable and variable objects.
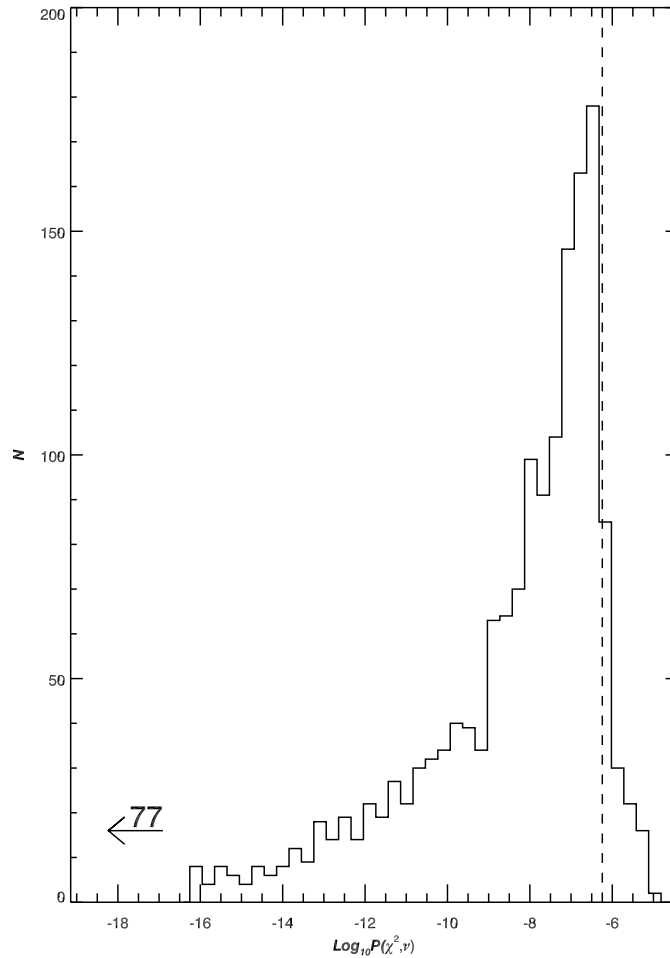
Figure 2.10: The histogram of logarithmic values of χ^2-probability, $P(\chi^2, \nu)$. The fraction of outliers to the right of the dashed line are those selected by criteria other than the $P(\chi^2, \nu)$ criterion. The number with a left arrow indicates the number of outliers with even smaller probabilities that could not be represented in the plot.

2.5 A Catalog of Highly Variable Radio Sources

Table 2.1 presents a sample page from the list of 1651 highly variable radio sources identified in our study. The complete table is available in appendix A (Table A.1). Column 1 provides the source position derived from the *FIRST* catalog. Columns 2 and 3 give, respectively, the *FIRST* catalog peak flux density and the mean peak flux density derived from the light curves. The range of flux densities for the source derived from the grid images are in column 4, while column 5 provides the NVSS
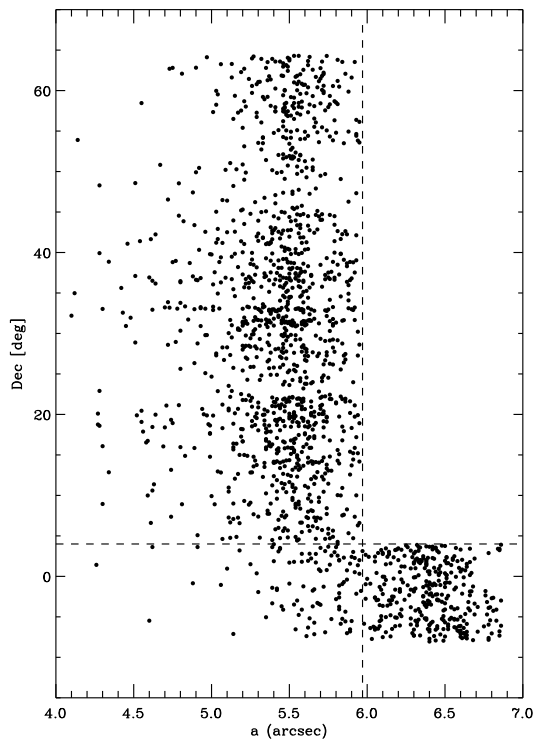
Figure 2.11: Scatter plot of the sizes of outliers vs. the declination. The horizontal dashed line shows the boundaries where the deconvolving beam size changes (cf. Figure 2.2). The vertical dashed line arises from our definition of point-like – a source with an intrinsic size $< 2\overset{''}{.}5$.

catalog peak flux density. Note that, while *FIRST* and NVSS have very different angular resolutions, our restriction of this study to isolated point sources in the higher-resolution *FIRST* survey means resolution effects should not be a factor in most cases.

These data are followed by the number of observations available (col. 6). The next three columns provide the three measures of variability: $P(\chi^2, \nu)$ for the light curve (col. 7), the maximum deviation of a single data point from the mean flux density in the light curve (col. 8), and the difference (in σ) between the most significantly different pair of data points (col. 9). The maximum-to-minimum flux density ratio is provided in column 10. The $T_{\min}$ (days) in column 11 denotes the minimum timescale at which two data points differ by at least 6σ. In cases where the maximum absolute difference of any pair of data points never reaches a value 6σ, the value denotes the

timescale at which the maximum absolute difference in column 10 is attained. In a few cases where the date of observation cannot be reliably obtained from the snapshot header, the entry is left without a numerical value. Column 12 contains a flag 'BN' if the outlier is found to be in the vicinity of a source brighter than 500 mJy within $31'$. Column 13 provides the distance of the mean normalized peak flux density of the neighbours corresponding to each outlier from the mean of the distribution of such normalized neighbour peak flux densities corresponding to all outliers and is a proxy for the quality of the field. The higher the absolute value in this column, the less ideal the quality of field surrounding the outlier and hence, the less reliable the physical variability of the outlier.

The type of light curve is denoted in column 14 by V (Variable) and T (Transient). The apparent SDSS-i band magnitudes are provided in column 15 where a SDSS match is available. Finally, column 16 gives the best ranked counterpart at other wavelengths. This ranking is explained in §2.6.

Figure 2.12 shows the distribution of the ratio of maximum to minimum flux density for our 1651 variables which ranges from 25% to a factor of > 20; overplotted is this ratio for the sample of variable sources (de Vries et al. 2004) with the same flux density distribution as ours. The areal density of their variables is $\sim 1 \deg^{-2}$ while we find it to be $\sim 0.2 \deg^{-2}$ for our sample. This difference is due to the lower threshold of detection (4σ) used by de Vries et al. (2004). The lower limits are indicated at the respective locations denoted by a number on top of the histogram bars in the plot and have been included in the corresponding bin-count. In figure 2.13, we show how this ratio differs for different classes of variable objects. The relation between maximum-to-minimum flux density ratio and mean peak flux density is shown as a scatter plot in figure 2.14.

Table 2.1. Summary of Properties of Variables & Transients

Coordinates (J2000)	f (mJy)				N	Measures			$\frac{\text{Max.}}{\text{Min.}}$	T_{min}	Flags	σ_{nbr}	Type	i	Cross-ID
	Cat.	$\overline{f}$	Range	NVSS		$P(\chi^2,\nu)$	σ_{max}	$\Delta_{max}(\sigma)$		(days)				Mag.	
11 55 54.609 -02 43 49.51	10.04	10.13	4.79 - 10.74	9.95	3	0.000	7.94	6.84	2.24	8	$\cdots$	0.30	V	$\cdots$	$\cdots$
11 56 46.553 +42 38 07.61	12.64	11.51	10.06 - 20.45	$\cdots$	3	2.220e-16	6.72	7.24	2.03	483	$\cdots$	0.50	V	16.68	SDSS-G
11 57 02.446 +21 02 28.29	5.18	4.96	<3.42 - <12.08	$\cdots$	5	8.067e-07	5.01	4.85	>1.48	1	$\cdots$	0.18	V	$\cdots$	$\cdots$
11 57 25.452 +41 51 19.55	5.75	5.84	<3.15 - 8.83	6.39	4	1.300e-10	5.79	6.56	>2.31	0	$\cdots$	0.26	V	$\cdots$	$\cdots$
11 58 46.776 +58 40 50.34	4.49	4.67	3.08 - 5.36	2.57	3	3.521e-07	3.72	4.27	>1.30	0	BN	0.38	V	$\cdots$	$\cdots$
11 58 50.768 -02 53 43.93	4.87	5.36	<4.26 - 6.67	4.95	4	7.102e-08	3.93	4.57	>1.45	0	$\cdots$	0.82	V	$\cdots$	$\cdots$
11 59 22.573 -05 52 17.18	2.38	2.29	1.09 - 2.95	$\cdots$	3	5.333e-07	4.76	4.53	2.48	2	$\cdots$	-0.01	V	$\cdots$	$\cdots$
11 59 25.118 +15 12 33.36	6.24	6.29	5.29 - 12.35	5.92	4	7.551e-08	5.33	5.90	2.33	25	$\cdots$	0.67	V	$\cdots$	$\cdots$
12 00 13.553 +43 06 42.70	1.45	1.31	<0.81 - 2.39	$\cdots$	4	4.918e-10	5.32	6.05	>2.96	2	$\cdots$	1.29	V	$\cdots$	$\cdots$
12 00 27.319 +32 58 10.69	1.93	2.03	<1.50 - 2.41	$\cdots$	4	1.237e-07	5.23	5.57	>1.61	1	$\cdots$	-0.05	V	20.56	SDSS-QSO(P)
12 01 02.933 +39 11 44.80	2.82	3.00	1.93 - <4.88	$\cdots$	4	4.344e-07	3.70	4.48	2.35	23	BN	-0.12	V	$\cdots$	$\cdots$
12 01 05.881 +20 23 10.85	5.91	5.85	2.56 - 6.19	4.28	3	1.173e-06	5.18	4.78	2.33	5	$\cdots$	0.10	V	21.24	SDSS-G
12 01 07.863 +24 53 33.32	8.78	8.96	3.04 - 9.15	8.08	3	3.141e-12	7.27	6.50	3.01	2	$\cdots$	-0.73	V	$\cdots$	$\cdots$
12 01 35.629 +33 12 33.28	4.75	4.53	<3.05 - <9.02	4.00	6	1.176e-08	5.61	5.35	>1.58	$\cdots$	$\cdots$	-1.50	V	$\cdots$	$\cdots$
12 01 49.193 +03 39 03.44	9.18	9.05	4.67 - 9.58	8.73	3	9.368e-07	5.22	4.64	1.95	1	$\cdots$	0.19	V	19.73	SDSS-G
12 02 10.433 +16 33 28.02	1.25	1.28	<1.05 - <3.75	$\cdots$	4	1.010e-07	4.06	5.25	>2.02	1	$\cdots$	0.23	V	21.28	SDSS-G
12 02 25.829 +30 37 38.12	4.44	4.46	<2.47 - <7.81	3.76	3	7.749e-11	6.39	6.17	>1.97	3	$\cdots$	0.64	V	19.39	SDSS-G
12 02 40.649 +21 56 20.99	8.40	7.14	6.76 - 11.24	9.19	3	1.356e-07	5.27	5.28	1.66	0	$\cdots$	-3.10	V	20.14	SDSS-G
12 02 49.673 +31 36 40.33	2.51	2.70	<1.67 - <15.62	$\cdots$	6	1.080e-09	5.48	5.70	>1.83	95	$\cdots$	-0.92	V	$\cdots$	$\cdots$
12 02 53.621 +34 31 29.70	4.54	4.47	1.43 - <15.83	4.61	5	1.110e-16	7.09	6.79	3.43	5	$\cdots$	0.68	V	$\cdots$	$\cdots$
12 02 55.734 +04 33 47.25	2.23	2.21	1.39 - 3.10	$\cdots$	3	2.049e-07	3.65	4.87	>2.24	388	BN	-0.25	V	$\cdots$	$\cdots$
12 03 02.267 +03 37 53.99	2.49	2.60	<1.66 - 3.29	$\cdots$	4	3.952e-11	5.99	6.56	>1.99	1	$\cdots$	-0.56	V	19.26	SDSS-QSO(P)
12 03 19.427 +04 38 15.57	3.64	3.58	2.24 - <13.88	3.39	4	2.063e-10	5.13	5.72	>1.73	388	BN	-0.11	V	$\cdots$	$\cdots$
12 03 57.217 -01 38 26.51	2.20	2.34	<1.73 - <7.93	$\cdots$	4	3.608e-08	5.28	5.61	>1.70	1	$\cdots$	1.18	V	16.02	SDSS-G
12 04 28.315 +03 52 59.25	5.38	5.42	<4.02 - 7.42	$\cdots$	4	1.167e-08	4.92	5.35	>1.53	1	BN	0.61	V	$\cdots$	$\cdots$
12 04 39.877 +50 28 20.71	2.32	2.32	1.43 - 3.59	$\cdots$	3	2.244e-09	4.80	5.94	2.50	27	$\cdots$	-0.09	V	$\cdots$	$\cdots$
12 04 50.878 +29 20 33.40	1.90	1.66	<1.40 - 2.96	$\cdots$	3	1.839e-08	4.35	5.92	>2.12	11	$\cdots$	-1.03	V	21.79	SDSS-G

Figure 2.12: Histogram of ratios of maximum to minimum peak flux densities of all of our variable objects. The shaded histogram is for objects from the sample of de Vries et al. (2004). The numbers appearing on top of the bins indicates the number of lower limits that fall inside this bin. These lower limits were derived from using 3σ upper limits for non-detections in the denominator.

2.6   Identification of Variable Radio Sources

Table 2.2 presents the results of cross-matching our catalog of variable sources with a variety of catalogs and databases. The first column lists the source type, followed by the specific catalogs used for cross identification and the matching radius adopted for each (col. 3). The rank in column 4 indicates the order in which the matches were applied; e.g., we first sought matches with bright star catalogs, then with a pulsar catalog, then with quasar catalogs, etc. This is important in interpreting the number
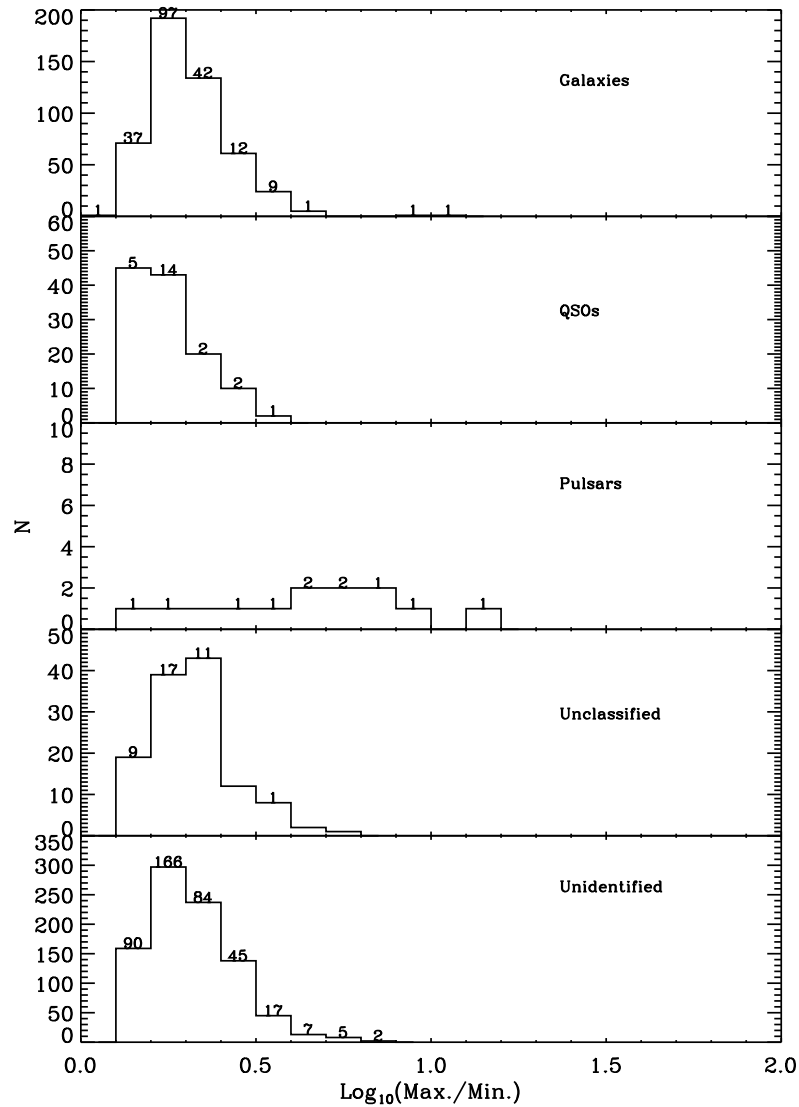
Figure 2.13: Histogram of ratios of maximum to minimum peak flux densities of different classes of variable objects. The numbers appearing on top of the bins indicates the number of lower limits that fall inside this bin. These lower limits were derived from using 3σ upper limits for non-detections in the denominator.

of matches N found in column 5 where we list both the number of unique matches to the specified catalog and, in parentheses, the number of total matches including those previously identified in a higher-ranked catalog. For example, the photometric SDSS quasar catalog has 68 total matches, but only 67 of them are real; the 68th is also matched to a pulsar (which is the true identification).
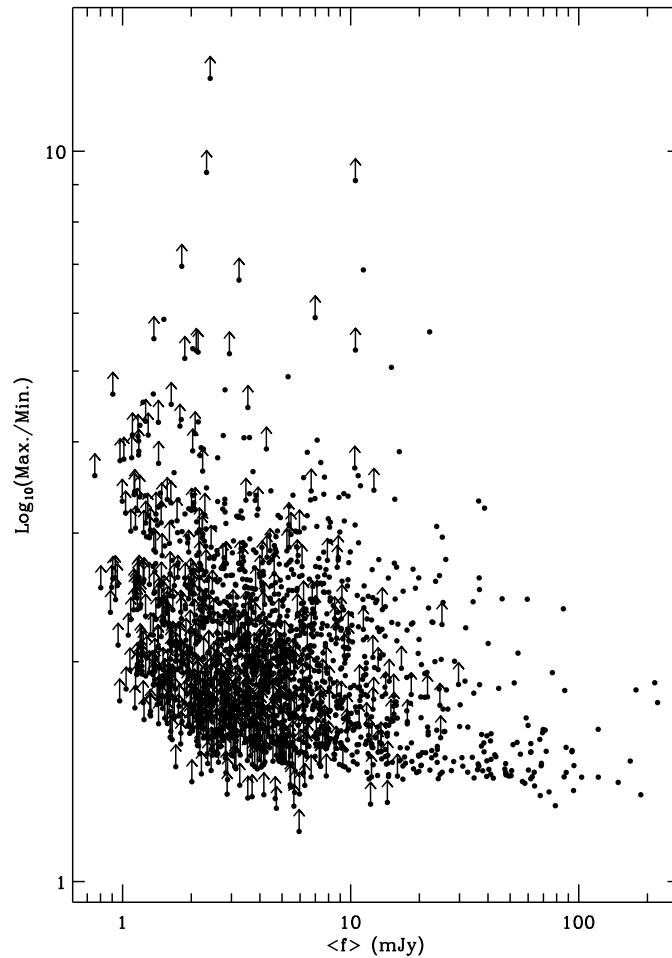
Figure 2.14: Scatter plot of the ratios of maximum to minimum peak flux densities of all objects against their average peak flux densities. The upward arrows denote that the value of the ratio is derived from a minimum peak flux density which was a non-detection whose 3σ upper limit was used, correspondingly yielding a lower limit for the ratio. The numerator-denominator pair in the ratio comes from the pair of data points in the light curve that yields the maximum absolute value of Δ_{max}.

Column 6 gives the match number as a percentage of all variable sources (e.g., a total of 7.3% of all variables are SDSS quasars). Columns 7 and 8, respectively, give the percentage of all *FIRST* sources matching each catalog that are identified as variable (e.g., 76% of all *FIRST* pulsars are variable, but only 1.2% of SDSS spectroscopically identified quasars with *FIRST* counterparts are highly variable), and the percentage of all *FIRST* isolated point sources the catalog matches represent. Parentheses are used as in column 4.
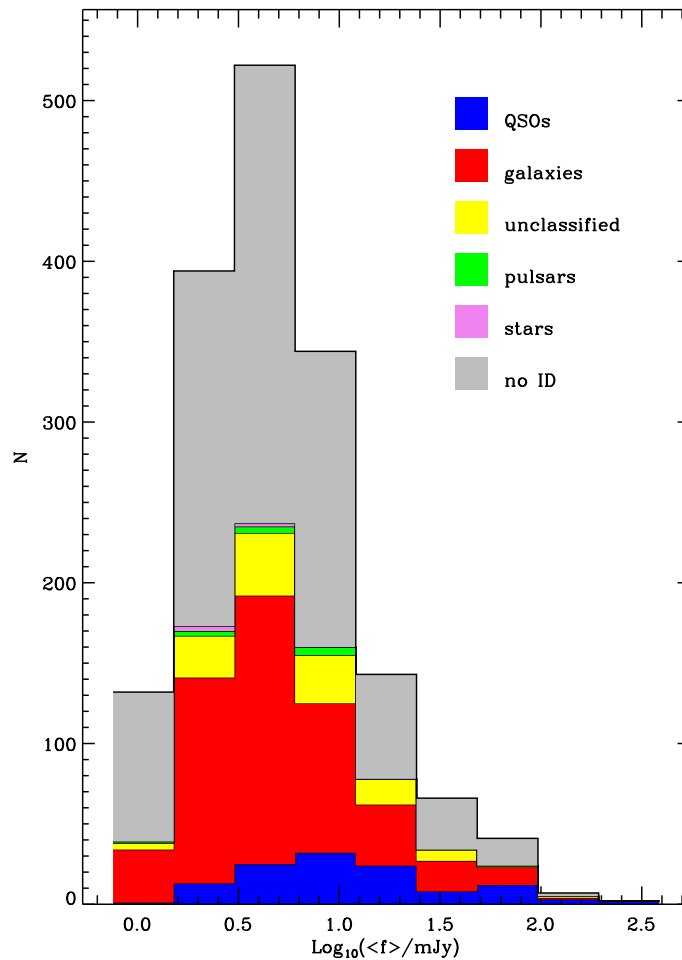
Figure 2.15: Composition of counterparts for the variables and transients as a function of the mean peak flux density.

In all cases, the rate of chance coincidences is low, typically less than one source per category with the exception of SDSS galaxies where up to seven chance coincidences (out of 443 matches) are possible. In summary, we find 5 bright stars, 13 radio pulsars, 120 quasars, and 490 galaxies among our variable sources, yielding firm identifications for 38% of our objects. An additional 119 objects are identified with unclassified stellar objects in the SDSS and GSC II databases; a total of 50 objects have X-ray counterparts, although only 5 of these are not also identified optically (mostly as quasars). This leaves 899 objects or 54% of the total without identifications in other wavelength bands (although 502 of these are found in other radio catalogs).
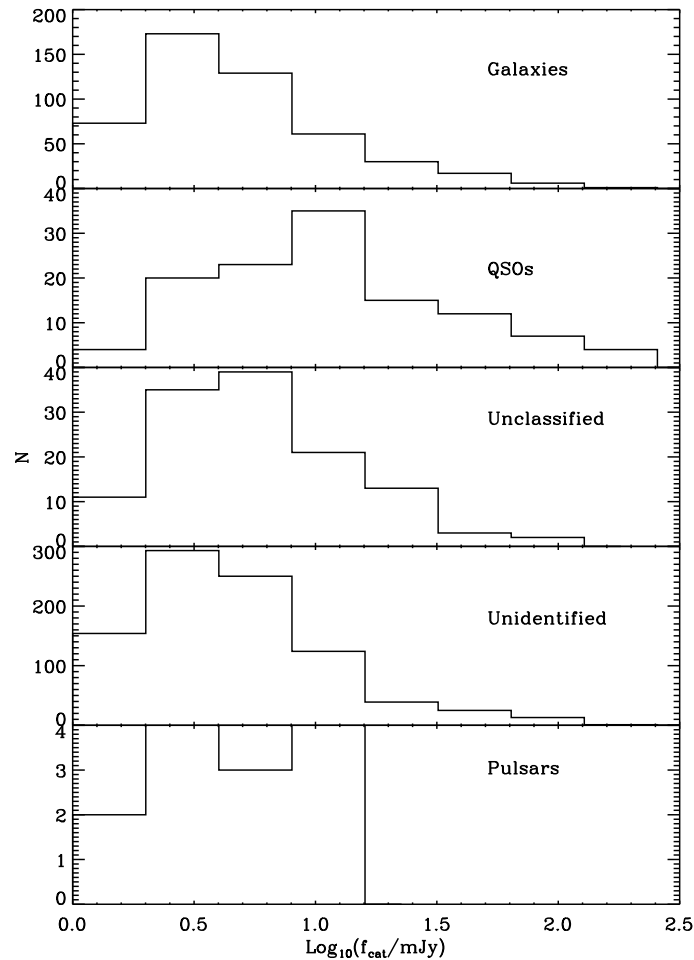
Figure 2.16: Histogram of *FIRST* catalog peak flux densities of different classes of variable objects.

We discuss below each class of objects in turn, and compare the properties of the identified objects to the unidentified ones in order to seek clues as to the identities of the latter sources.

Figure 2.15 illustrates the composition of the various identifications as a function of their mean peak flux densities. Expectedly, the relative fraction of QSOs with respect to galaxies increases with increasing mean peak flux density and vice versa with the dividing line being ~ 10 mJy. The pulsars and the stars are generally found to have mean peak flux densities of a few mJy. The distribution of unidentified objects appears to follow the trend shown by galaxies and interestingly, it also has a
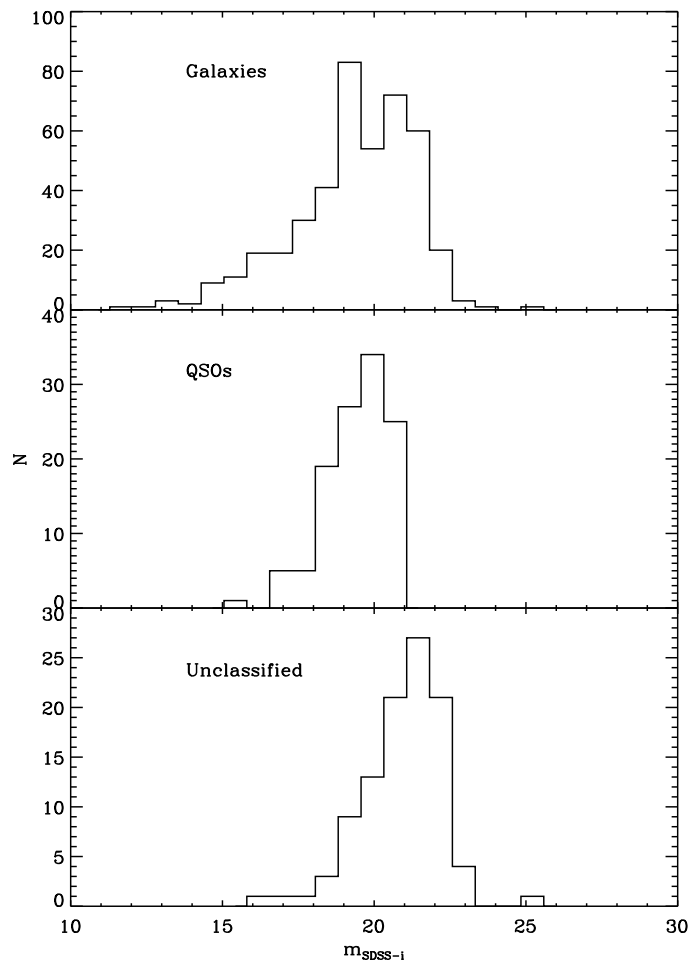
Figure 2.17: Histogram of SDSS i-band magnitudes of different classes of variable objects detected in SDSS.

significant tail at the high-mean peak flux density end.

2.6.1 Radio Pulsars

While ~ 70 known radio pulsars fall within our survey area, most are both faint and have steep radio spectra, leading to only 17 detections in the *FIRST* survey catalog (Table 2.3). Of these 9 ($\sim 50\%$) appear in our catalog of highly variable sources. By slightly relaxing our criterion for a point-source, we find an additional four pulsars that would have been classified as outliers by our algorithm; we add these to the total number of outliers quoted throughout the paper. Thus, more than three-quarters of

Table 2.2. Summary of Cross-ID Statistics for Variables & Transients.

Cross-ID	Catalog	Rank[a]	$\Delta\theta$ ('')	Matches		Match Rate	
				N	% of Variables	Variable %	% of *FIRST* sources[b]
STAR	HIPPARCOS	1	1.4	3 (3)	0.18 (0.18)	27.3 (27.3)	0.004 (0.004)
	TYCHO	2	1.4	4 (2)	0.24 (0.12)	22.2 (22.2)	0.006 (0.003)
PULSAR[c]	ATNF	3	3.0	13 (13)	0.79 (0.79)	76.48 (76.48)	0.006 (0.006)
QSO	SDSS (S)[d]	4	1.4	53 (53)	3.22 (3.22)	1.16 (1.16)	1.632 (1.632)
	SDSS (P)[e]	5	1.4	68 (67)	4.13 (4.07)	1.1 (1.09)	2.203 (2.239)
GALAXY	SDSS DR7	6	1.4	443 (432)	26.84 (26.17)	0.55 (0.54)	28.92 (29.68)
	GSC-2[g]	7	1.4	349 (56)	21.19 (3.40)	[g]	[g]
	2MASS[h]	8	1.4	121 (1)	8.99 (0.06)	[h]	[h]
	APMUKS(BJ)[i]	13	6.0	2 (1)	0.12 (0.06)	. . .	. . .
UNCLASSIFIED	SDSS DR7	6	1.4	228 (115)	13.84 (6.98)	0.92 (0.76)	8.9 (5.7)
	GSC-2[g]	7	1.4	111 (4)	6.74 (0.24)	[g]	[g]
	2MASS[h]	8	1.4	27 (0)	1.64 (0.00)	[h]	[h]
	CHANDRA	9	3.0	7 (1)	0.43 (0.06)	1.45 (1.23)	0.173 (0.048)
	XMM	10	15.0	15 (2)	0.91 (0.12)	1.52 (1.03)	0.353 (0.116)
	RASS-BSC	11	30.0	15 (0)	0.91 (0.00)	2.29 (0.00)	0.234 (0.011)
	RASS-FSC	12	60.0	13 (2)	0.79 (0.12)	0.70 (0.49)	0.664 (0.246)
UNIDENTIFIED	GB-87[i]	13	6.0	21 (7)	1.28 (0.43)	. . .	. . .
	VLSS[i]	13	6.0	5 (2)	0.30 (0.12)	. . .	. . .
	WB-92[i]	13	6.0	13 (1)	0.79 (0.06)	. . .	. . .
	ABELL-04[i]	13	6.0	1 (1)	0.06 (0.06)	. . .	. . .
	B3[i]	13	6.0	1 (1)	0.06 (0.06)	. . .	. . .
	WN[i]	13	6.0	2 (1)	0.12 (0.06)	. . .	. . .
	NVSS	14	7.1	992 (489)	60.23 (29.69)	0.75 (0.63)	47.46 (46.88)
	NONE	15	. . . [j]	397 (397)	24.10 (24.10)	0.45	. . . (100.0)
TOTAL				1647+4[c]	100.0		

[a]Rank indicates the order in which the matches are made with different catalogs.

[b]Only the isolated point-like sources from the *FIRST* catalog

[c]Four objects are slightly resolved but nevertheless included. More detailed data available in table 2.3

[d]Data obtained from SDSS DR7 spectroscopic QSO sample

[e]Data obtained from SDSS DR7 photometric QSO sample

[f]Has also made use of SDSS cross-match information available in the *FIRST* catalog which may not be up to date compared to DR7

[g]Has solely made use of the Guide Star Catalog II cross-match information available in the *FIRST* catalog

[h]Has solely made use of the 2 Micron All-Sky Survey cross-match information available in the *FIRST* catalog

[i]Data obtained from the NASA Extragalactic Database

[j]Search radius varies depending on the catalog being searched

[k]4 additional pulsars included upon relaxation of the point-source criterion

the detected radio pulsars in the survey are found to be highly variable.

While the intrinsic radio luminosity of a pulsar is steady, its emission suffers from interstellar scintillation which arises when signals traveling in slightly different directions are alternately scattered into, and out of, our line of sight by the fluctuating electron density distribution of the interstellar medium. The effect is largest when the number of scattering centers is small, so the highest variability is seen for the nearest pulsars; indeed, 11 of our 13 variable objects have dispersion measures (DM) of $\lesssim 20$ cm^{-3}pc; the other two have DM values of 27 cm^{-3}pc and 41 cm^{-3}pc. Of

Table 2.3.   Summary of the Properties of Pulsars.

Coordinates (J2000)	Δ ($''$)	PSR Name	f_{cat} (mJy)	Period (s)	DM (cm^{-3}pc)	Distance (kpc)
Pulsar matches with the sample of outliers						
10 24 38.698 -07 19 19.07	0.17	J1024-0719	5.21	0.005	6.49	0.53
09 22 14.008 +06 38 22.84	0.51	J0922+0638	10.33	0.431	27.27	1.20
10 22 58.011 +10 01 52.85	0.40	J1022+1001	3.69	0.016	10.25	0.40
12 39 40.386 +24 53 49.87	1.19	J1239+2453	11.53	1.382	9.24	0.86
08 26 51.438 +26 37 22.83	1.19	J0826+2637	11.14	0.531	19.45	0.36
16 52 03.080 +26 51 39.85	0.56	J1652+2651	6.27	0.916	40.80	2.93
15 18 16.831 +49 04 34.19	0.31	J1518+4904	5.03	0.041	11.61	0.70
10 12 33.387 +53 07 02.09	0.66	J1012+5307	2.20	0.005	9.02	0.52
15 09 25.675 +55 31 32.90	0.62	J1509+5531	10.02	0.740	19.61	2.13
Pulsar matches passing variability criteria but not strictly point-like						
16 07 12.078 -00 32 40.98	0.42	J1607-0032	3.93	0.422	10.68	0.59
10 23 47.622 +00 38 41.60	1.09	J1023+0038	3.12	0.002	14.32	0.90
09 43 30.092 +16 31 34.67	2.32	J0943+1631	1.51	1.087	20.32	1.76
16 40 16.699 +22 24 08.98	0.60	J1640+2224	1.92	0.003	18.43	1.19
Other pulsar matches in the *FIRST* survey						
09 53 09.287 +07 55 35.94	0.38	J0953+0755	83.22	0.253	2.96	0.26
15 43 38.837 +09 29 16.52	0.26	J1543+0929	6.17	0.748	35.24	7.69
07 51 09.148 +18 07 38.73	0.17	J0751+1807	1.42	0.003	30.25	0.62
11 15 38.456 +50 30 12.68	0.67	J1115+5030	1.00	1.656	9.20	0.54

Note. — Data obtained from the ATNF Pulsar Catalog

the four pulsars not seen to vary significantly, two have flux densities < 1.5 mJy, too close to our threshold to detect variability, and a third has a $DM > 35$.

The typical time scale for scintillation is $\sim$ 1 min at 20 cm (to be compared with our 165 s integration time) and the decorrelation bandwidth is typically smaller than our 50 MHz bandwidth, so our observational parameters largely smooth over the fluctuations. Nonetheless, pulsars are among the most variable objects in our sample, with 8 out of 13 varying by more than a factor of 4 (see figure 2.12). Interestingly, 23 of the 899 variables which lack optical counterparts entirely also vary by this large factor; this is to be contrasted to the fact that none of the 120 variables identified as quasars are this variable, and only 1% of the sources coincident with galaxies vary by such large factors. All but one of these 23 sources have flux densities less than 4 mJy and most appear only once or twice, falling below our detection threshold in the other observations. An examination of the radio spectrum and polarization of these sources

could provide candidates for pole-on, very short period, and/or intermittent pulsars worthy of further study.

2.6.2 Optical Counterparts

A total of 734 radio variables have an optical counterpart in one or more of the catalogs used in the identification program summarized in table 2.2; the vast majority of these are from a match to the SDSS DR7 catalog. Figures 2.12 through 2.19 show variability amplitudes, SDSS i-band magnitudes, radio peak flux densities from the *FIRST* catalog, and the SDSS colors of our sample. We discuss each sample of objects in turn below.

2.6.2.1 Stars

Most stars are very faint at radio wavelengths. Of the more than 800,000 sources in the *FIRST* catalog, only 37 match objects in the bright star catalogs we examined to within $1\overset{''}{.}4$. To check that high proper motions of these (mostly) nearby stars have not obviated any true matches, we expanded the search radius to $5''$; no additional matches were found when proper-motion-corrected positions were used. Helfand et al. (1999) conducted a more exhaustive search of the first 4,760 $\deg^2$ of the *FIRST* survey and found a total of 26 radio-detected stars, 5 of which were at flux densities below the survey limit of 1.0 mJy. One of the detections reported in that earlier survey, the flare star (08 08 55.47 +32 49 06.0), is found in our catalog of highly variable objects. It has a fluctuating light curve with variability on timescales of days, months and years. In total, we find only 5 stars both bright enough and variable enough to make our sample of variables and transients. All are previously known variables.

2.6.2.2 Quasars

A total of 53 quasars from the SDSS DR5 spectroscopic quasar catalog (Schneider et al. 2007) are found in our list of variables. In addition, another 67 objects in the DR6 photometric quasar catalog of Richards et al. (2009) are in our list, making a total of 120 quasars in the sample or 7% of all variables. For the whole *FIRST* catalog there are 8396 and 10,025 matches from the spectroscopic and photometric catalogs, respectively, accounting for nearly 2.5% of all *FIRST* sources. Table 2.2, however, includes only matches with isolated point-like sources from the *FIRST* catalog.

The quasars have the highest mean radio flux density (> 10 mJy) among our identified source classes (figure 2.16) and the lowest mean max-to-min flux density ratio. This is in part a selection effect, in that only in bright sources does modest variability exceed our significance threshold. Nonetheless, with our coarse and uneven sampling, we have found only a dozen quasars that vary by more than a factor of 2.5.

2.6.2.3 Galaxies

The largest identified segment of our sample is coincident with an object classified as a galaxy in SDSS (with a few additional galaxies contributed from GSC II, 2MASS, NED, etc.). The 490 galaxies comprise roughly 30% of our sample. The galaxies have a broad spread in absolute magnitudes (figure 2.17) and a lower mean radio flux density than the quasars but somewhat higher amplitude of variability (Figure 2.12).

AGN are undoubtedly the source of variable radio emission in these objects. Optical spectroscopy (and/or hard X-ray imaging) of this sample could be interesting, in that it could reveal the fraction of buried AGN which show no optical evidence of an accreting black hole.

2.6.2.4   Unclassified Stellar Counterparts

A total of 114 radio variables are coincident with unclassified stellar objects in the SDSS DR7 catalog; a few additional such objects are found in the GSC II catalog in areas lying outside of the SDSS coverage. Figure 2.19 shows the SDSS color-color diagrams for these stellar objects; comparison with figure 2.18 shows a large majority of these objects have colors consistent with quasars, while virtually all of the remainder fall within the galaxy contours in color-color space. The majority of these objects fall below the $m_i = 21.0$ cutoff for the SDSS quasar catalogs, but nearly 60 objects lie above this threshold. Spectroscopic follow-up of these objects could provide insight into the completeness of the photometric quasar catalog[1].

2.6.2.5   Unidentified Sources

There are no optical (or X-ray) counterparts for 899 sources comprising 54% of our sample. Figures 2.12 and 2.18 show that these sources mostly cohabit the parameter-space of galaxies and QSOs, although there are a few notable outliers with very high variability amplitudes as noted above.

2.7   Summary

After analyzing about 56,000 snapshot images from the *FIRST* survey of the radio sky covering 8,444 deg^2 with sensitivity down to 1 mJy for variability and transient phenomena, we have assembled a sample of 1651 sources that are significantly variable. This sample was matched with multi-wavelength catalogs to identify counterparts. We found 13 radio pulsars, 53 SDSS spectroscopic QSOs, 67 SDSS photometric QSOs, 490 galaxies, 5 stars, 124 optically detected but unclassified sources and 899

---

[1]The three brightest objects with $m_i < 18$ include one source with no spectrum and two with spectra classified as 'STAR'.

optically undetected sources. The unidentified sources mostly seem to occupy the parameter-space of galaxies and QSOs but there are a few notable outliers which are worthy of follow-up.

Our study has shown that there is much to be discovered in the dynamic radio sky. Exploration by the next-generation instruments sampling different portions of the spectral and temporal domains will prove to be highly productive.
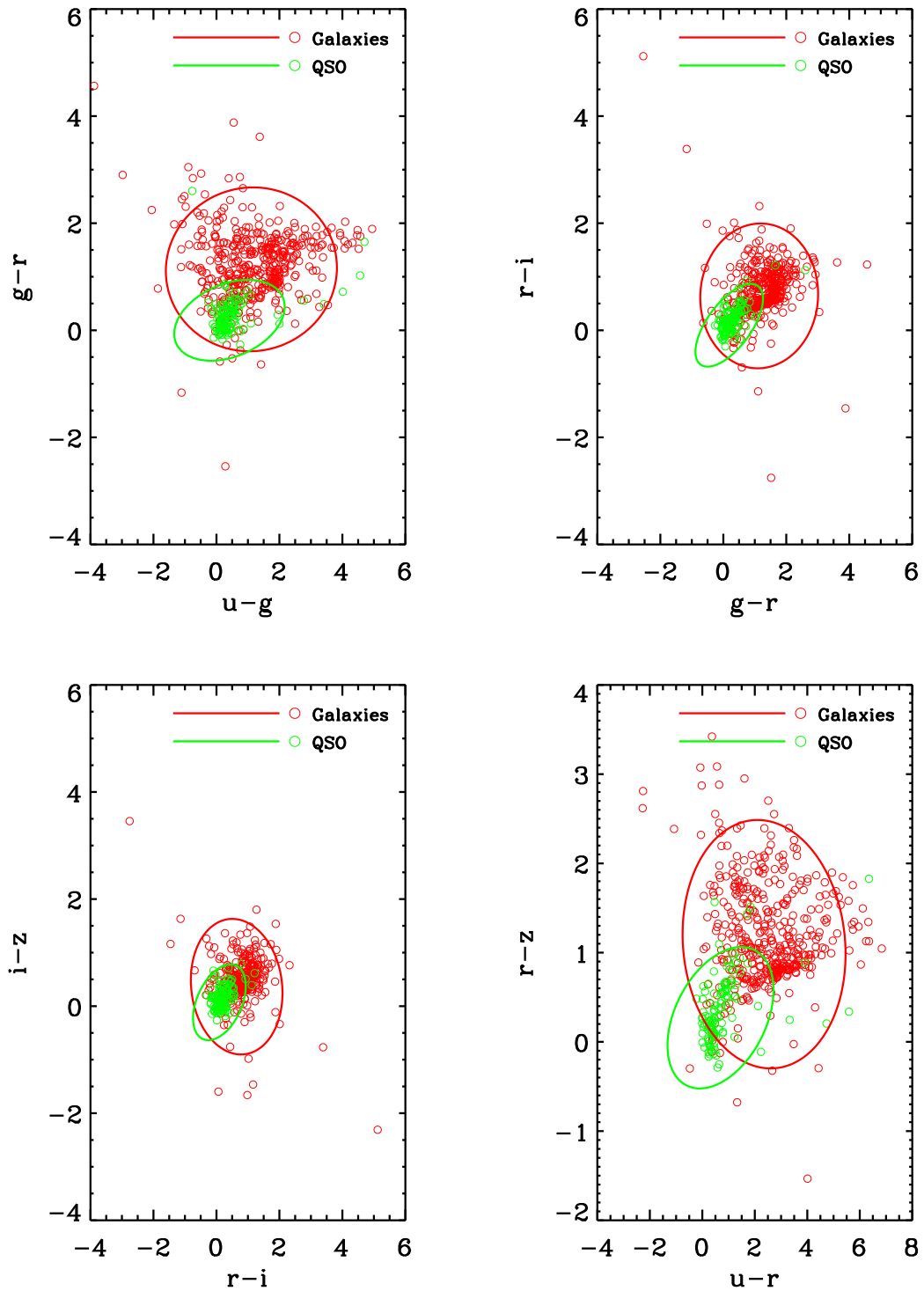
Figure 2.18: Scatter plot of SDSS colors of variable objects detected and classified as galaxies and QSOs in SDSS. The red and green ellipses denote the color-color distribution of galaxies and QSOs respectively.
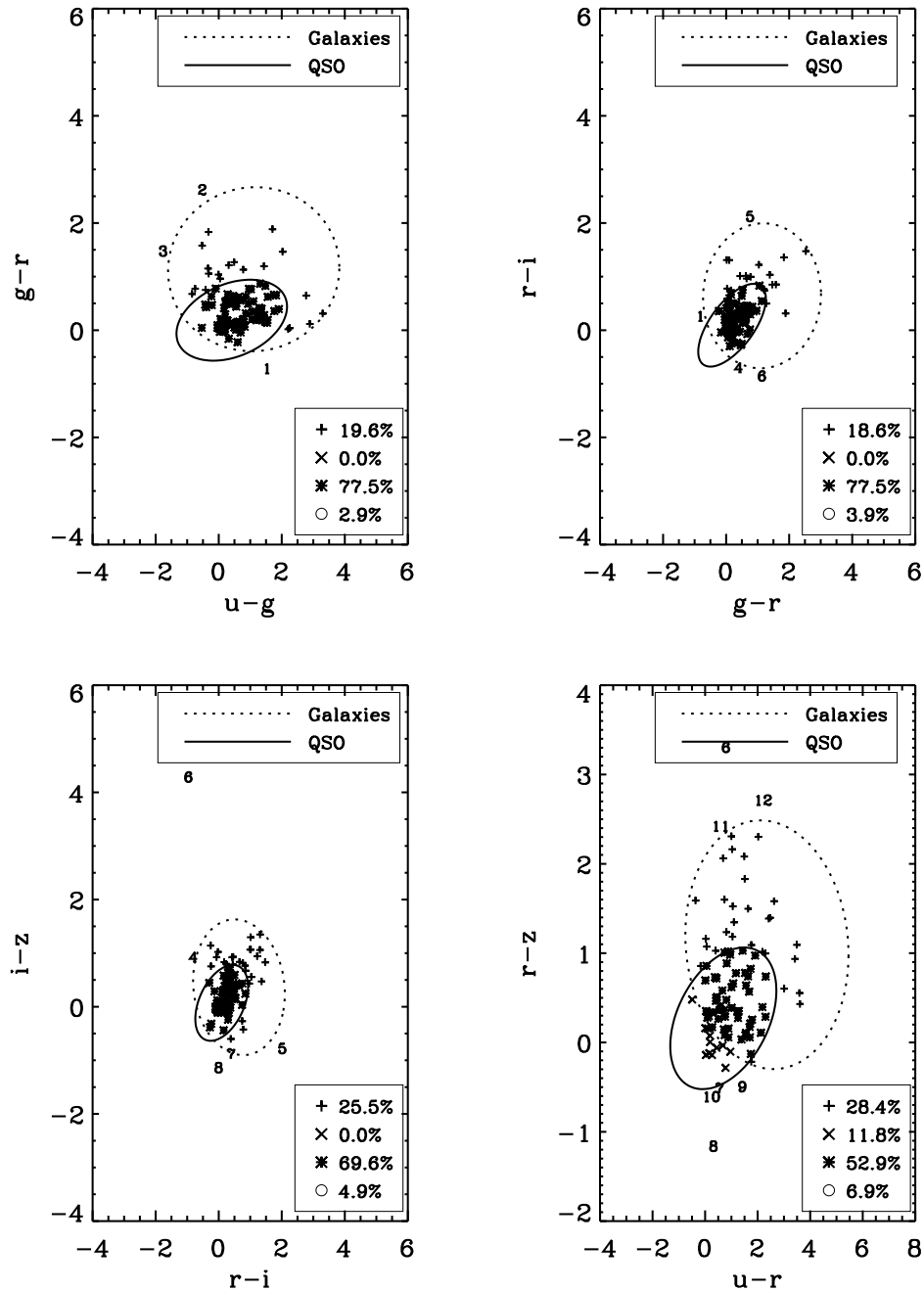
Figure 2.19: Scatter plot of SDSS colors of variable objects detected but unclassified in SDSS. The dotted and dashed ellipses denote the color-color distribution of galaxies and QSOs respectively, identical to those in figure 2.18. The open circles in the legend represent the numbers in the plot indicating the unclassified objects that fall outside of both ellipses. The numbering scheme is used for easy identification of objects that consistently fall outside of the QSO and galaxy ellipses.

Chapter 3

Size Evolution of FR II Quasars

3.1 Background

Early work (Miley 1971; Wardle & Miley 1974; Hooley et al. 1978) that used the sizes of double-lobed radio sources showed that plotting Largest Angular Sizes (LAS) against redshift was consistent with the Euclidean model for the universe. Subsequent studies (Kapahi 1985, 1989; Singal 1988, 1993; Barthel & Miley 1988; Onuora 1989; Ubachukwu & Onuora 1993; Nilsson et al. 1993) that investigated the variation of binned mean or median angular sizes as a function of redshift showed that the observed data was very consistent with a Euclidean model after trying to compensate for possible orientation and evolutionary effects.

These authors have presented various explanations for these observations. The intrinsic length scale of these double-lobed objects are expected to be determined, in no small part, by the density of the IGM which changes with cosmological epoch. This could give rise to an inverse correlation between observed angular size and redshift resulting in the selection of intrinsically smaller sources at higher redshifts. Other possibilities of size evolution have also been discussed. For instance, Inverse Compton losses against the microwave background which increase rapidly at large redshifts, combined with the synchrotron losses, could limit the radiative lifetime of a source (Van der Laan & Perola 1969), thereby introducing a correlation between size and redshift. In flux-limited surveys, the luminosity of the source is positively correlated with redshift and including a negative power-law correlation between luminosity of the object and its size thus results in selection of a sample that appears to contain

preferentially smaller objects at higher redshifts. Many observers found that the observed $\theta - z$ data were consistent with Friedmann models if these effects are taken into account with varying degrees of weight. Further, if the unification models for radio galaxies and quasars are correct, the classification of an object as a radio galaxy or a quasar depends entirely on its orientation to line-of-sight (Barthel 1989; Lister et al. 1994), with quasars which are relatively highly inclined dominating the high-redshift population. In studies that include both, there could be possible orientation effects, thereby revealing a deficit of larger sources at higher redshifts. The understanding of these effects in these studies and their significance concerning the observed results have largely remained unclear and disputed.

In more recent work, Buchalter et al. (1998) used the *FIRST* survey and available redshift information to construct a carefully defined set of 103 double-lobed quasars with $z > 0.3$. After addressing the selection effects and correlations in the data mentioned above, and considering a subset with no significant evolution, thereby increasing the integrity of the data set, they find no decrease in apparent angular size in the redshift range of $1.0 \lesssim z \lesssim 2.7$ consistent with standard Friedmann models rather than the Euclidean model. However, lack of a larger data set has rendered the constraints inadequate to distinguish between the various Friedmann cosmologies.

Gurvits et al. (1999) studied the $\theta - z$ relation using the compact radio jets from a sample of 330 quasars and AGN from 5 GHz VLBI data. The jets lie well within the host environment unaffected by the IGM, and are believed to be short-lived and hence independent of evolutionary effects at reasonable redshifts. With the help of multi-parameter regression analysis (Gurvits 1994), this data is found to be consistent with standard FRW cosmologies with $0 \lesssim q_0 \lesssim 0.5$ and $\Lambda = 0$ without the need to invoke evolution of the population or to appeal to selection effects. They note however that their results are based on very inhomogeneous data obtained by many different observers using different instruments and imaging techniques.

We restrict ourselves to FR II type radio sources (Fanaroff & Riley 1974) which have edge-brightened morphologies characterized by radio hot-spots near the outer edges of the lobes. The measure of angular size is defined as the angular distance between the hot spots. Such a definition is thus fairly robust to the details of the observation.

The completed *FIRST* survey catalog (Becker et al. 2003) contains $\sim$816,000 radio objects covering $\sim 9{,}033$ deg^2 of the sky at 1.4 GHz to a sensitivity of ~ 1 mJy with a $5\rlap{.}''4$ FWHM gaussian beam. The Sloan Digital Sky Survey (SDSS) (York et al. 2000) had, at that time, imaged $\sim 8{,}420$ deg^2 in the Northern Galactic Cap and ~ 200 deg^2 in the Southern Galactic Hemisphere with a r-band sensitivity of 22.5 (Ivezić et al. 2003). The spectroscopic catalog from the SDSS Data Release 5 (DR5) contains $\sim 140{,}000$ quasars with luminosities larger than $M_i = -22.0$, fainter than $m_i \approx 15.0$ and brighter than $m_i \approx 19.1$ (Schneider et al. 2007). In this paper, we investigate the $\theta - z$ relation for double-lobed FR II quasars in the completed *FIRST* survey with optical counterparts in the SDSS DR5 spectroscopic quasar catalog. We also make use of the photometric QSO catalog (Richards et al. 2009) from SDSS DR6 which has imaged quasars down to $m_i \approx 21.3$, in order to increase our sample size.

In §3.2, we describe the semi-automated algorithm and selection criteria used to construct the sample and summarize the properties of the sample (§3.3). We compare the spectroscopic and photometric samples of FR II in §3.3. In §3.4, we explore how the properties of the data are correlated using both parametric and non-parametric methods, some of which include size-power correlation, power-redshift correlation (arising due to the flux-limited nature of the survey) and a size-redshift correlation (arising due to apparent or intrinsic effects). In brief, we find evidence for mild apparent evolution arising due to power-redshift and power-size correlations but none for intrinsic evolution. In §3.5, we investigate the multi-dimensional χ^2-surface. We note that it is degenerate in its parameters and requires additional,

independent information to be resolved. We also perform a χ^2-minimization using the Levenberg-Marquardt algorithm (which is optimized for non-linear functions) with different constraints on the parameters to confirm the nature of the χ^2-surface. Hence, the optimal parameters are subject to certain degeneracies. In §3.6, the size distributions of these objects are investigated for any dependence on redshift. We compare the results to some basic modeling of FR II sources found in the literature in §3.7. In §3.8, we present our conclusions.

3.2   The Sample

3.2.1   Selection Criteria

Daly (1995) has computed the ambient densities of radio galaxies and radio-loud quasars based on the strong jump conditions and concluded they are found in similar environments. In contrast, the 'k' parameter that characterizes the environmental factors suggest different trends with redshift. The conclusions also come with caution about selection effects and small samples. In order to ensure homogeneity of our sample, we generally follow the prescriptions of Buchalter et al. (1998). This $\theta - z$ study utilizes only those double-lobed radio sources that are spectroscopically confirmed as quasars. This prevents potential contamination from those classified as radio galaxies and hence avoids different mean orientations and power-size-redshift correlations affecting the $\theta - z$ plane. Moreover, since $\theta - z$ curves for different cosmological parameters are easily distinguishable around their minima which occur at $z \sim 1.5$ (see figure 3.1), quasars which generally dominate the population of radio sources at higher redshifts than radio galaxies should be the preferred candidates for this sample. More specifically, we imposed a lower limit on redshift, $z > 0.3$. Moreover, Heckman et al. (1992) & Hes et al. (1995) have shown that the properties of low-z and high-z radio sources exhibit different behaviors, with the cutoff occurring
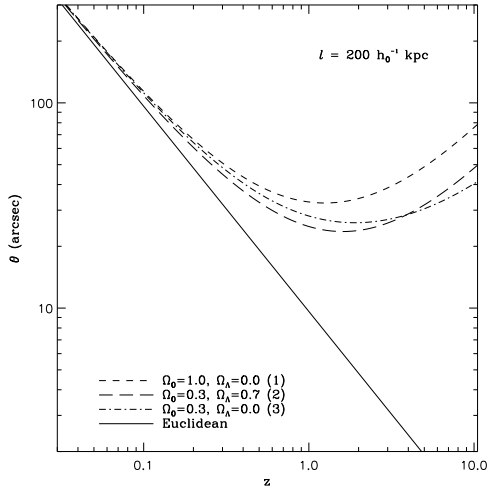
Figure 3.1: The angular diameter vs. redshift $(\theta - z)$ relation for a standard rod of length $200\,h_0^{-1}\,\mathrm{kpc}$.

roughly at $z = 0.3$.

3.2.2   Selection Algorithm

We follow the selection procedure described by de Vries et al. (2006) called '*Environment Matching*'. Basically, this procedure looks for multiple (≥ 2) radio sources in the *FIRST* survey within a specified radius ($180''$) around the optical positions of the spectroscopically confirmed QSOs from the SDSS DR5 catalog. It should be noted that this procedure has the following advantages. Firstly, it is equally sensitive to quasars with both detected and undetected radio cores. Secondly, it is robust to non-collinear lobe-core-lobe geometry. If some of these quasars are in dense environments, high ram pressure may cause the lobes to appear bent. Any selection procedure that requires the presence of a central core while matching positions will be biased against radio sources whose lobes are slightly bent. This effect is particularly pronounced for the larger sources where even a slightly bend (deviation from $180°$) causes significant non-collinearity.

Additional criteria were applied to the candidates to reduce contaminants to the

sample and make the selection procedure efficient. These criteria are described in sequence.

The candidate lobe's flux density must exceed 3 mJy. This helps in selecting lobes that are prominent enough so their morphology can be easily identified as resembling a FR II quasar lobe's morphology. The candidate's lobes are required to have no optical counterpart. This helps to eliminate unrelated sources from contaminating our sample.

The flux density ratio of the core to the lobes should not exceed 20. This criterion intends to remove sources that have very bright cores which could be beamed, thereby systematically skewing the sample and introducing projection effects. This criterion was also found to efficiently weed out contaminants like very bright objects with sidelobes that could be confused for radio lobes.

The flux ratio between the lobes is constrained to remain between 0.1 and 10. Sources outside of this contrast range were found not to have well-defined FR II morphologies.

The distance ratio of the lobes from the core (optical QSO position) was restricted to lie between 0.5 and 2 thereby eliminating lobes that were placed too asymmetrically, indicative of a dense environment, a chance alignment, or other confounding effects.

One of the main reasons for false positives was found to be the presence of randomly placed sources unrelated to the QSO in question that could be confused for being a radio lobe of the central QSO. We subsequently carried out a thorough visual inspection of each of these objects using cutouts of their images from the *FIRST* database server. We paid particular attention to the morphologies and the total extents of these objects. Generally, only those sources were included that allowed an accurate morphological classification. For instance, possibly genuine FR II type objects that had a lobe separation roughly equal to the beam size were discarded. Potential candidate FR II type objects that were embedded in maps that were noisy

and/or dominated by sidelobes were also discarded. Thus, we carefully examined individual images and removed the false positives for such objects.

There were some objects where the angular extent of the possible lobes was large. In order to ensure that the high-resolution *FIRST* beam was not resolving out the flux from these extended sources, we followed up such objects with the NRAO VLA Sky Survey (NVSS) (Condon et al. 1998). NVSS has a sensitivity of ~ 2.5 mJy with $45''$ FWHM resolution. In such cases, we used the NVSS images for confirmation. From this selected set of images, an object was selected only if it exhibited a clear edge-brightened morphology characteristic of FR II type objects.

The efficiency of the overall algorithm at the end of the application of the objective criteria was such that about two out of every three candidates were FR II quasars.

Since the matching procedure involves matching two different catalogs, we carried out a procedure to estimate the rate of inclusion of false positives due to positional coincidence of possibly unrelated objects. The positions of the objects in the optical QSO catalog were displaced by $3'$. A set of candidates were again chosen by the algorithm described above. This was used to estimate a quantitative measure of the rate of inclusion of false positives purely due to random positional coincidence. Figure 3.2 shows the histograms of the opening angle of these candidate lobes with the central QSO as a function of the total angular size. This analysis can also be used to determine an effective upper limit to the angular size that can be reliably used from this database for the $\theta - z$ study. The matching procedure was repeated to pick objects that resemble the FR II morphology purely because they happen to be centered around the position of a displaced object. This estimate for the rate of inclusion of false positives was found to be not more than 5%. We also note that despite including or discarding a few possibly genuine objects in the above procedure, we have not introduced any additional systematic bias with redshift or flux density.

The complete sample of spectroscopic and photometric FR II quasars is provided
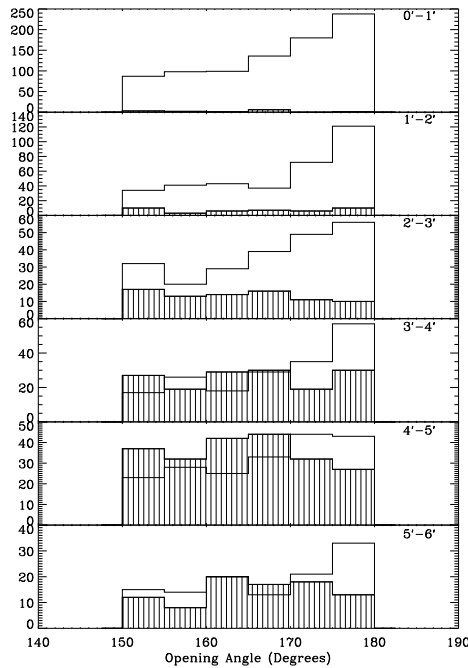
Figure 3.2: The histogram of opening angles for candidates selected by the *environment matching* algorithm. Each panel represents a range of total linear angular sizes of the candidate objects. The shaded histograms are for the simulated false matches. This demonstrates that angular sizes beyond the $3'$- $4'$ range have relatively high contamination from random matches either from foreground or background sources. This also sets a natural upper limit on reliable angular sizes that is well below the sizes of our image cutouts implying that we do not miss reliable candidates bigger than the size of our image cutouts.

in tables B.1 and B.2, respectively, in appendix B, which are subsequently subjected to the selection criteria described in §3.2.1. In these tables, column 1 provides the optical QSO position (J2000), column 2 gives the sum of the angular distances of the "hot spots" in the lobes from the optical QSO position, and column 3 gives the redshift of the QSO derived from the spectroscopic or photometric QSO catalogs from the SDSS as the case may be.

3.3   Spectroscopic vs. Photometric Sample

Using the selection procedure described above, we created two samples of FR II quasars, one from the SDSS spectroscopic QSO catalog and the other from the photometric catalog. One of the original motivations of using both these samples was to increase the sample size hoping it would reduce the size of the error bars and help in distinguishing between the cosmological models. In this section, it will be demonstrated how much the two samples differ.

This is illustrated by the distributions of physical parameters such as redshift (z), projected physical size ($l \sin \phi$), 1.4 GHz radio luminosity ($L_{1.4\mathrm{GHz}}$) and optical luminosity (M_i). Prompted by the significant lack of similarity in these physical parameters between the two distributions, the photometric sample was randomly sampled to match its redshift distribution to that of the spectroscopic sample. Consequently, the random sampling keeps only 35-40% of the photometric sample. As expected, we see in figure 3.3 that the redshift distributions match very well (within the limits allowed taking into account the random sampling). However, the distributions of projected physical sizes remain significantly dissimilar.

It must be pointed out that the SDSS targeted some objects for spectroscopic follow-up simply because they coincided with *FIRST* sources despite them being fainter than the survey limit of $m_\mathrm{i} \lesssim 19.1$. Since there is the possibility that any sort of radio selection might introduce a bias in the sample, the SDSS targets that came from *FIRST* have been removed before comparing the distributions in redshift, projected physical size, and radio and optical luminosity space. The radio luminosity distributions show some similarity (significant to a few percent) but the optical luminosities remain very different (figure 3.4).

Having demonstrated the lack of similarity even after matching the redshift distributions, it should be emphasized that one must not try to combine the two samples and interpret the results while not understanding the apparent lack of statistical

(a) Redshift (b) Projected Physical Size
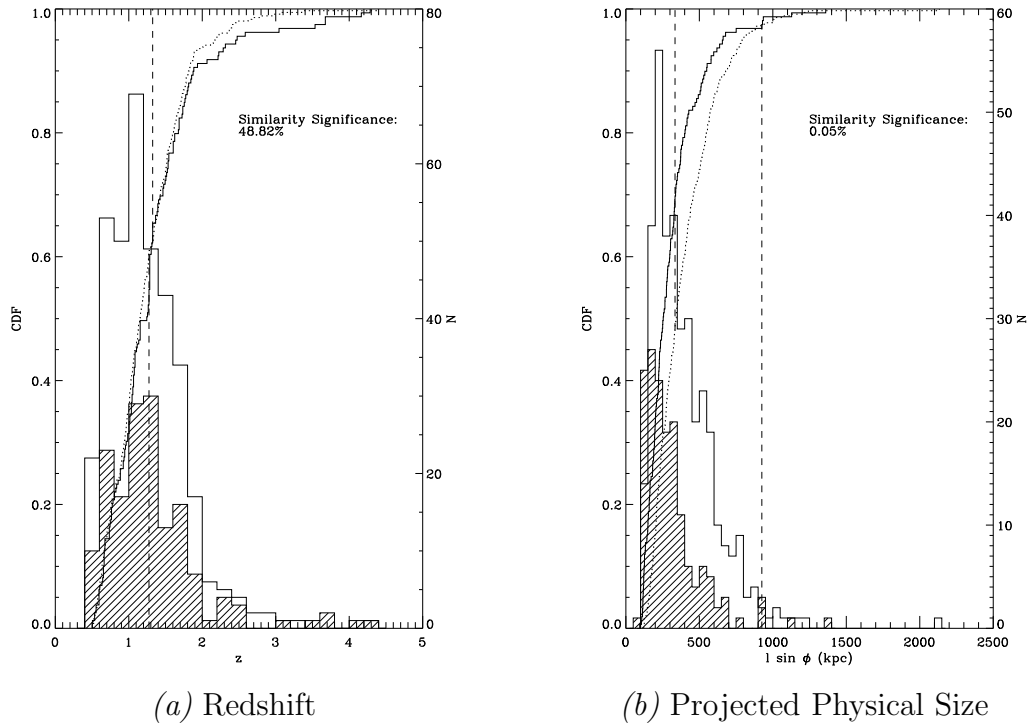
Figure 3.3: Histogram of redshifts and projected physical sizes of FR II quasars in the spectroscopic and randomly sampled redshift-matched photometric samples. The unshaded histogram and the dotted line correspond to the spectroscopic sample while the shaded histogram and the solid line correspond to the photometric sample. The significance from the two-sided K-S test is recorded in the plot (in percent). The higher this value, the higher the similarity between the two distributions.

similarity between them; this would not offer any more credibility than those of the earlier studies, many of which were plagued by selection effects due to non-uniform and inhomogeneous sample composition.

Hereafter, the analysis of the two samples is kept separate.

3.3.1 Properties of the Sample

While the text hereafter mostly addresses the spectroscopic sample, there are some figures and tables from the photometric sample for comparison.

A total of 682 objects passed the basic criteria described in §3.2.2 which constitutes, hereafter, the parent sample. The peak-to-peak angular size for the parent

(a) Radio Luminosity   *(b)* Optical Luminosity
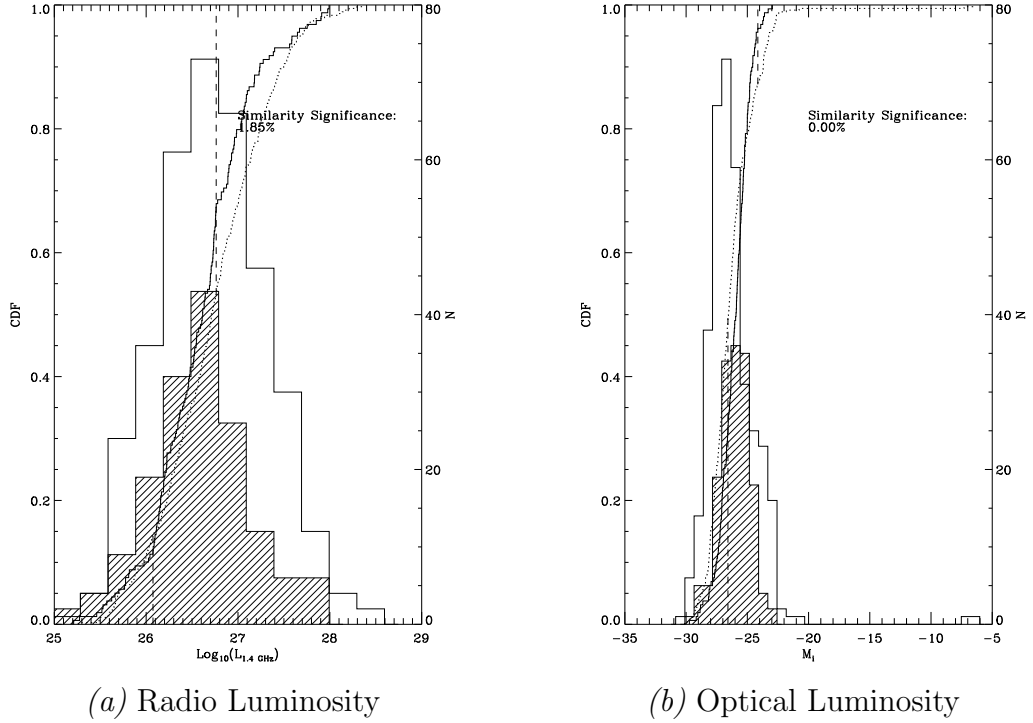
Figure 3.4: Histogram of radio and optical luminosities of FR II quasars in the spectroscopic and randomly sampled, redshift-matched photometric samples. The unshaded histogram and the dotted line correspond to the spectroscopic sample, while the shaded histogram and the solid line correspond to the photometric sample. The significance from the two-sided K-S test is noted on the plots (in percent). The higher this value, the higher the similarity between the two distributions.

sample was measured as the sum of the angular distances between the peaks of the gaussian model fits of the lobes and the optical QSO position. Since the gaussian model fitting underestimates the sizes of these non-gaussian, edge-brightened profiles, we also added one-half of the FWHM of the two Gaussian peaks to obtain the final estimates of the peak-to-peak angular sizes. As explained in §3.2.2, for the objects that were followed up with NVSS, we used an identical definition applied to the NVSS maps for angular size.

Throughout this paper, we assume $H_0 = 70 \, \mathrm{km \, s^{-1} \, Mpc^{-1}}$. Figure 3.5 shows the scatter plot of the θ-z data. The errors in the measured values of θ are typically $\sim 1''$, less than the scatter in the angular sizes at any redshift. The data are binned with a roughly equal number of data points per bin and we calculate both the mean values,

(a) Spectroscopic Sample   *(b)* Photometric Sample
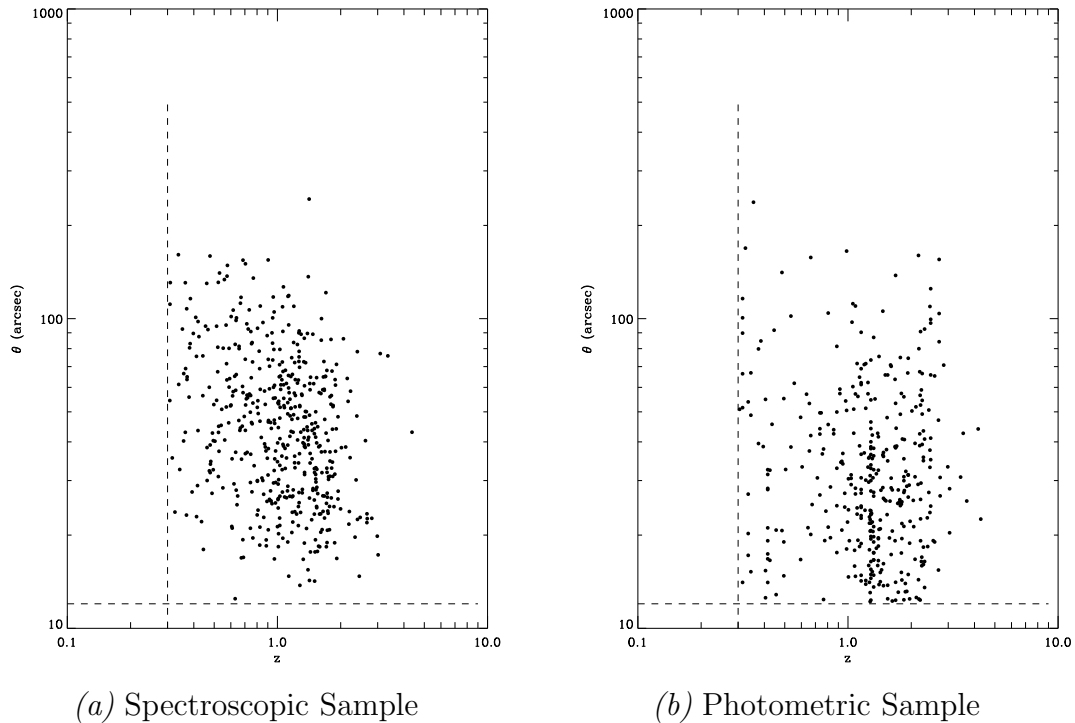
Figure 3.5: Scatter plot of the peak-to-peak angular sizes, θ, vs. redshift. The vertical dashed line represents the redshift limit above which the radio source population is dominated by quasars. The horizontal dashed line represents the effective resolution limit at $12''$, below which accurate morphological classifications could not be determined.

$\langle\theta\rangle$, and median values, θ_{med}, with the standard errors of the mean values, and median absolute deviations, respectively, for each bin. From figure 3.6, it can immediately be seen that the data are generally consistent with Friedmann models than with a static Euclidean model and that the uncertainties are considerably reduced when compared with the work of Buchalter et al. (1998), so that the data should be able to distinguish between the different models reasonably well.

Figure 3.3 shows the redshift distribution of the parent sample. The redshift selection we used means that there are no data with $z \leq 0.3$. The shape of this distribution is primarily determined by the sensitivity of the SDSS. We considered augmenting the parent sample at the high-redshift end using data from NED that was not present in the SDSS. However, since we failed to detect significantly different
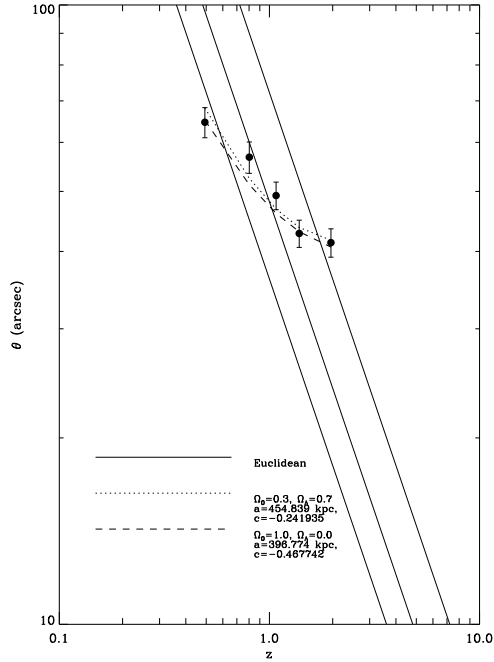
Figure 3.6: Mean binned data points along with a demonstration that Euclidean models are incapable of providing a reasonable fit to the data. The figure also visually illustrates the degeneracy of parameters in the χ^2-contours.

results, we use the results from only the parent sample in this paper. The photometric sample has an inexplicably high redshift spike at $z \sim 1.3$ visible in figure 3.5(b). The most likely reason could be stellar contaminants.

The distribution of angular sizes is shown in figure 3.7. In order to ensure only those objects are included whose FR II type morphologies are clearly identified and not affected by the survey's resolution, the angular size cutoff is fixed at $\theta_{\min} \approx 12''$. From the sharp fall-off observed in this histogram, it can be inferred that we have not missed any significant fraction of objects whose lobe separation might be greater than $360''$. Buchalter et al. (1998) have shown that the analysis can be performed without loss of generality by considering any arbitrary upper and lower limits on the intrinsic physical sizes, l.

The opening angles (angle made by the lobes with the central QSO position) are distributed as shown in figure 3.8. Figure 3.9 shows the distribution of the ratio

(a) Spectroscopic Sample   *(b)* Photometric Sample
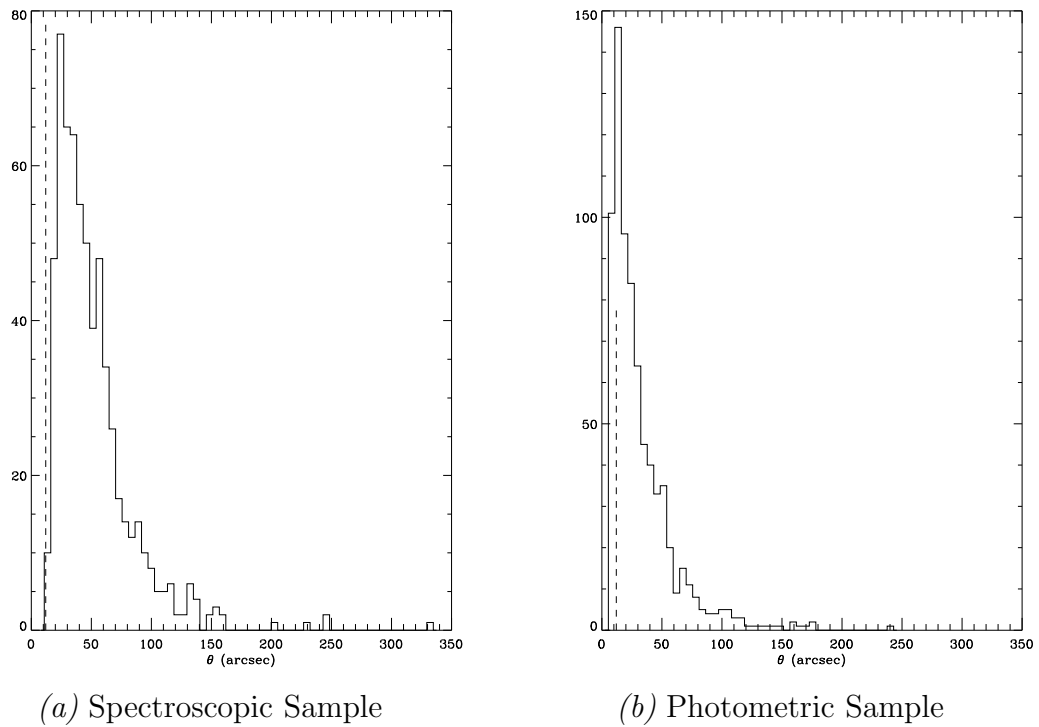
Figure 3.7: Distribution of angular sizes. The vertical dashed line represents the lower limit used, below which an accurate morphological classification was not possible.

(a) Spectroscopic Sample   *(b)* Photometric Sample
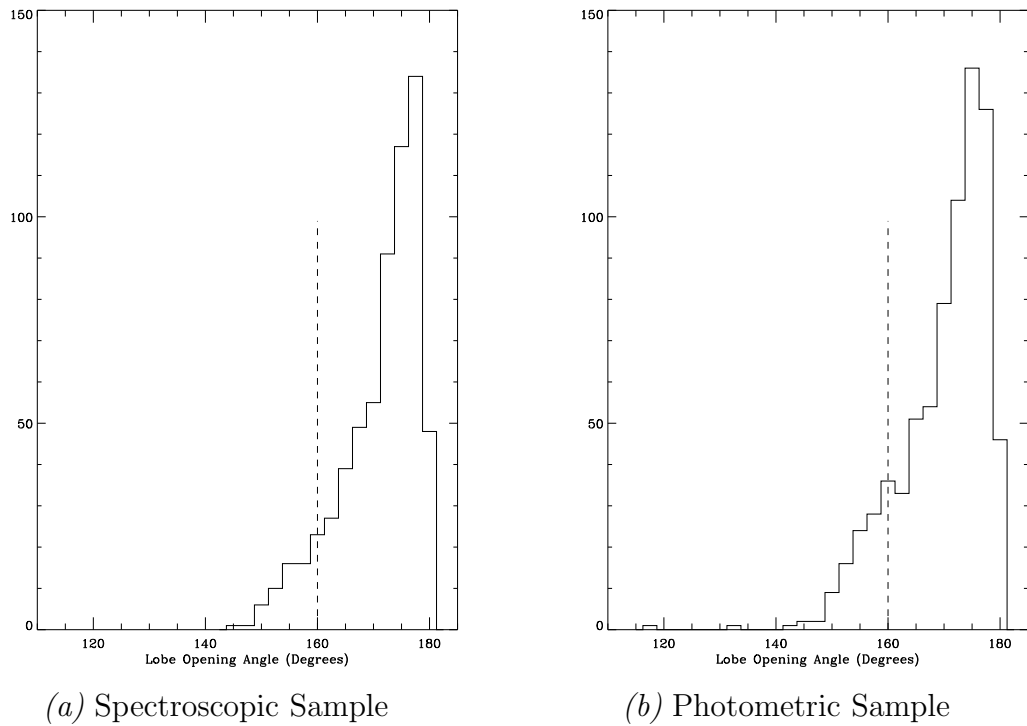
Figure 3.8: Distribution of opening angles. The vertical dashed line represents the lower limit used, below which the lobe-core-lobe geometry was assumed to be bent.

(a) Spectroscopic Sample   *(b)* Photometric Sample
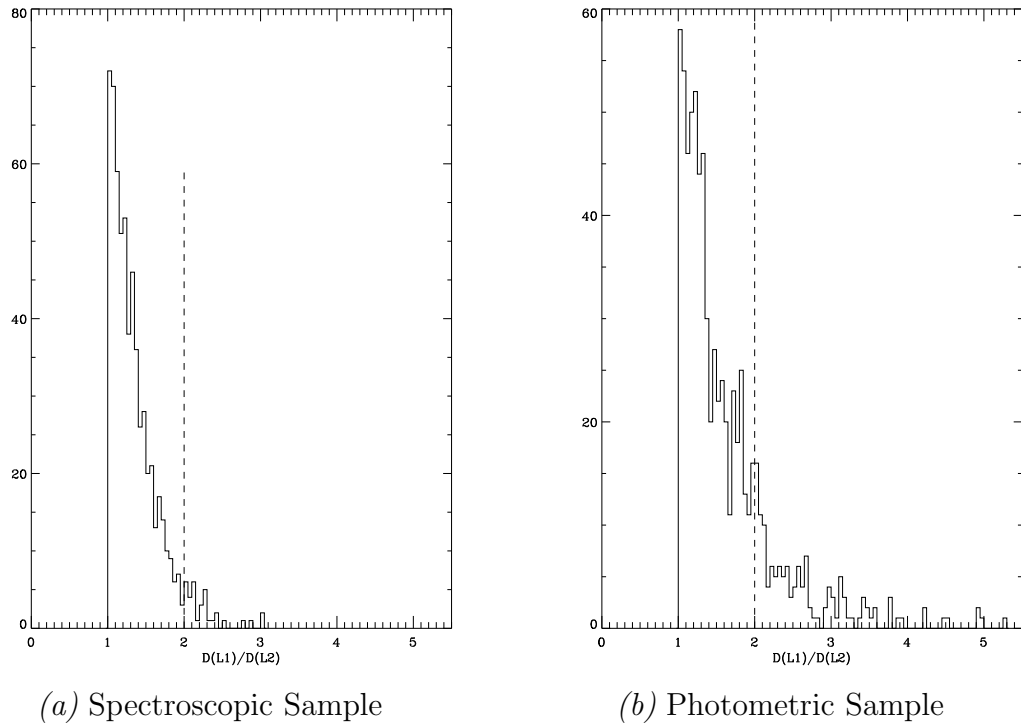
Figure 3.9: Distribution of ratio of distances of lobes from the core. The vertical dashed line represents the upper limit used, above which the lobe-core-lobe geometry was taken as being too far from being symmetrical.

of the distances between the lobes and the core. It is a one-sided distribution with ratios greater than unity since it is a ratio of the distance of the farther lobe to the nearer one. The opening angles and the ratio of core-to-lobe distances are useful observational diagnostics of interactions of the lobes with the IGM.

Figure 3.10 shows the distribution of the Lobe-to-Core flux ratio, $f_{C/L}$. To ensure we select only FR II type radio sources, characterized by prominent lobes, we discarded objects with $f_{C/L} \geq 20$. Moreover, objects with a high $f_{C/L}$ are very likely to be relativistically beamed, aligned close to the line of sight, introducing a strong orientation effect.

Figures 3.11 and 3.12 show the distribution of apparent and absolute magnitudes of this sample in the SDSS i-band respectively. Figure 3.13 shows a scatter plot of the absolute magnitude, M_i, versus redshift.

(a) Spectroscopic Sample   *(b)* Photometric Sample
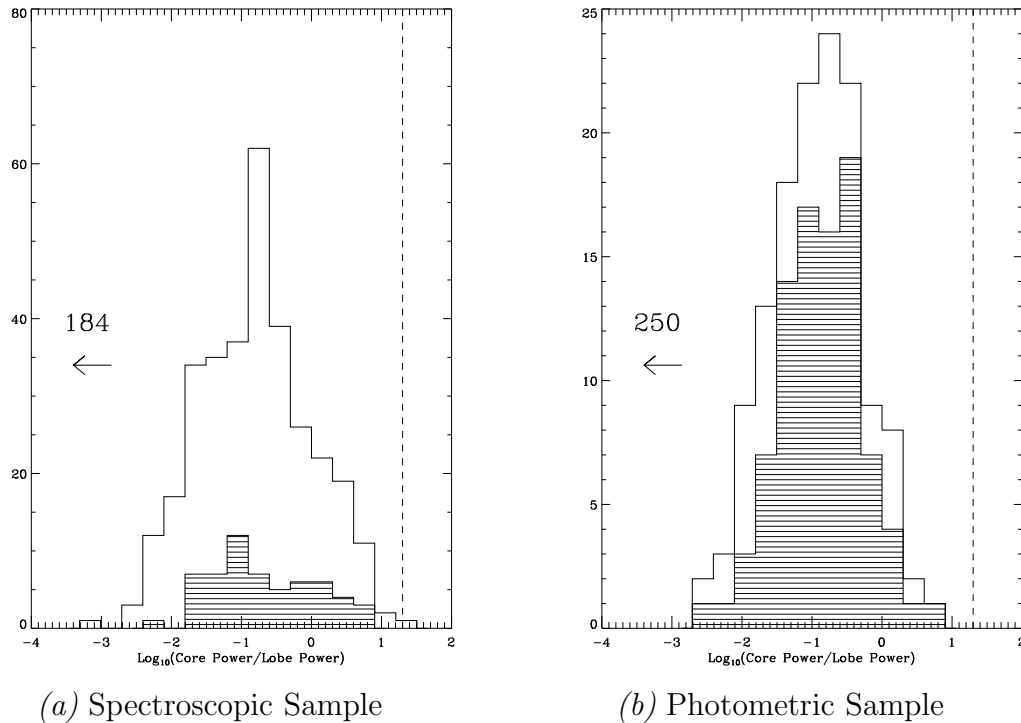
Figure 3.10: Distribution of ratio of fluxes of cores to lobes. The vertical dashed line represents the upper limit used, above which relativistic beaming effects due to close inclination to line of sight may be significant. The shaded histogram represents known FIRST sources targetted by the SDSS fainter than the SDSS i-band limit of 19.1. The number shown above the leftward arrow in the plot represents the number of FR II quasars with no detected radio core.

In the context of the unified scheme for AGN, excluding objects classified as radio galaxies helps to avoid introducing non-cosmological effects into the θ-z plane because FR II sources and radio galaxies have different mean orientations. However, our parent sample of FR II quasars are composed of both Core-Dominated QSOs (CDQs) and Lobe-Dominated QSOs (LDQs) with a wide range of values in $f_{C/L}$. The observed median values of $f_{C/L}$ for these objects are ~ 10 and ~ 0.1 respectively (Ubachukwu 1996). Although we have selected FR II quasars that have prominent lobes, we still performed a two-sided K-S test on the redshift distributions of objects on either side of the median of the $f_{C/L}$ distribution (see figure 3.10). The two distributions were not even different at the 1σ level. Thus, we believe the core-lobe flux ratio does not introduce any systematic effects with redshift. There has

(a) Spectroscopic Sample   *(b)* Photometric Sample
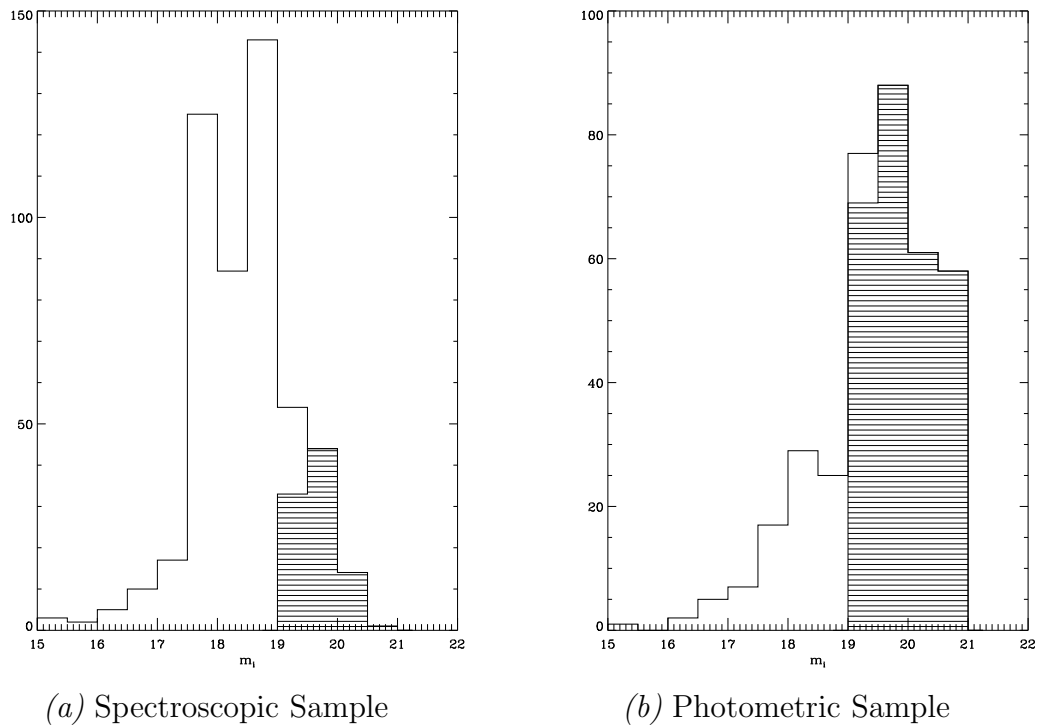
Figure 3.11: Distribution of the SDSS i-band apparent magnitudes, m_i, for the sample. The shaded histogram represents known FIRST sources targetted by the SDSS fainter than the SDSS i-band limit of 19.1.

also been some evidence suggesting the unification scheme is either incomplete in its simple form or is incorrect (Heckman et al. 1992; Singal 1996). Assuming there is no systematic variation of orientations with redshift, however, using a statistical sample of the observed projected sizes can still be valuable and informative.

Finally, the limits on intrinsic linear size in this parameter space merits some discussion. An effective angular resolution cutoff has to be imposed for an accurate classification of morphologies but it should be noted that a constant minimum resolvable angular size does not translate into a constant minimum intrinsic linear size and, in fact, varies with redshift. To avoid this redshift dependence in the sample, it is desirable to restrict the sample to linear sizes in the range $l_{min} < l < l_{max}$ where l_{min} and l_{max} do not vary with redshift. We follow the self-consistent selection of the sample based on the intrinsic linear size range described by Buchalter et al. (1998) by aligning the minimum of the θ-z curve for the particular model under investigation

(a) Spectroscopic Sample   (b) Photometric Sample
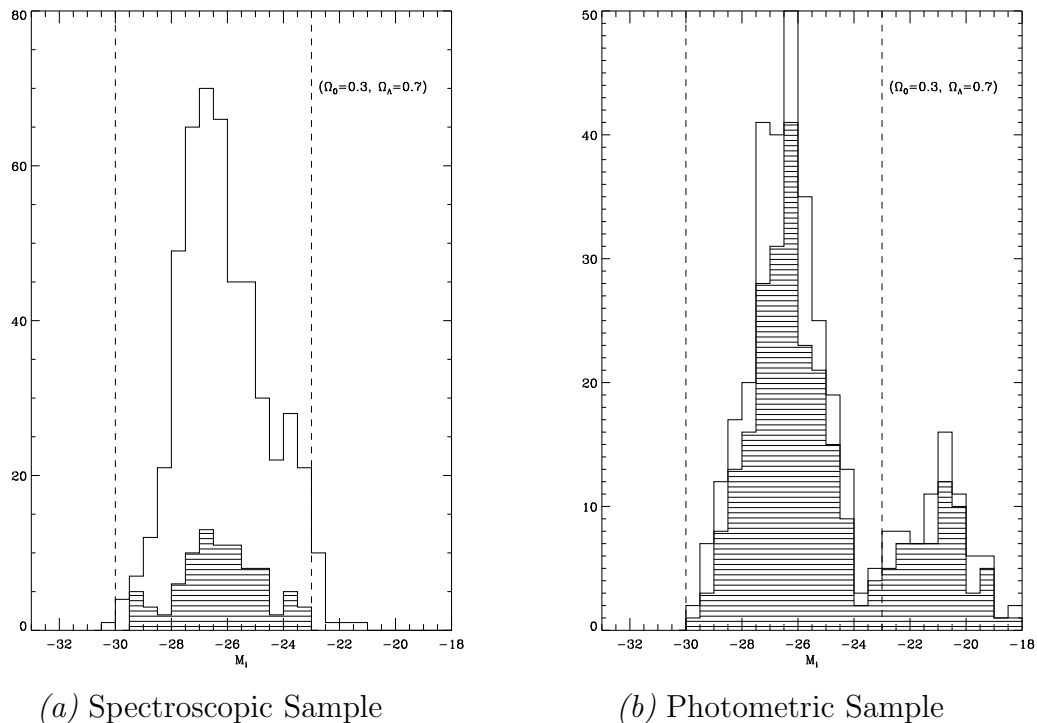
Figure 3.12: Distribution of the SDSS i-band absolute magnitudes, M_i, for the sample. The objects included between the two vertical dashed lines only are used. The shaded histogram represents known FIRST sources targetted by the SDSS fainter than the SDSS i-band limit of 19.1.

with the smallest observable angular size at which morphologies can be accurately determined and including only points above this curve. As long as it can be assumed that the distribution of intrinsic linear sizes does not change or evolve with redshift, the results and the discussion presented in this paper are valid for any choice of $l_{\min}$ and $l_{\max}$. In §3.6, we indeed show using two-sided K-S tests that there is no evidence for a size distribution that evolves with redshift, thereby validating this assumption.

Since our sample is selected from two uniformly sensitive, large-scale surveys, the effects due to inhomogeneity are expected to be minimal. Due to the rigorous parameter space restrictions imposed above, the effects from contamination and inconsistencies are also expected to be negligible.

(a) Spectroscopic Sample   *(b)* Photometric Sample
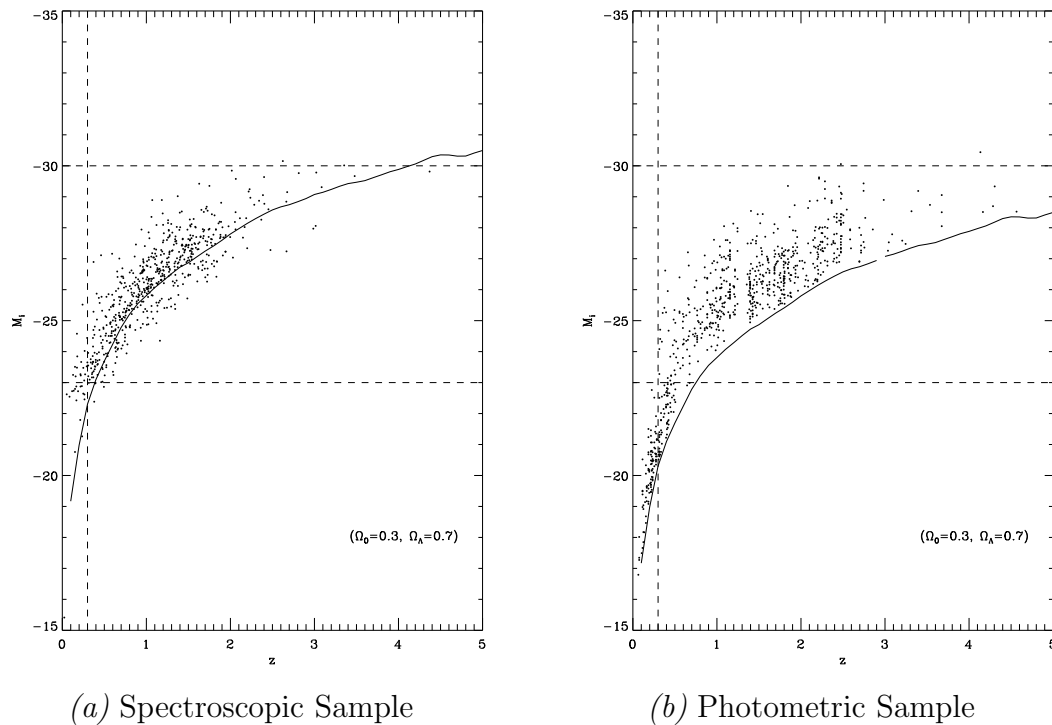
Figure 3.13: Scatter plot of the SDSS i-band absolute magnitudes, M_i, versus redshift. The vertical and the horizontal dashed lines represent the limits on z and M_i respectively. The solid line represents the absolute magnitude corresponding to the SDSS-i band apparent magnitude limit as a function of redshift.

3.4 Correlations Between Power, Size and Redshift

We consider a 199-point grid for the cosmological parameters for open and flat universes. The grid consists of values of Ω_0 from 0.01 to 0.99 inclusive, in intervals of 0.01 for a flat universe ($\Omega_0 + \Omega_\Lambda = 1$) and an open universe ($\Omega_\Lambda = 0$). Finally, the grid also includes the Einstein-de Sitter universe ($\Omega_0 \equiv 1$ and $\Omega_\Lambda = 0$).

Before best-fit models are computed, any correlations in the source properties that may be present must be understood. These may not only be important for determining the best-fit cosmological parameters but also for understanding the characteristics of the host AGN and the IGM. We parameterize these correlations after the manner described in Buchalter et al. (1998). For each set of cosmological parameters, one can

calculate the intrinsic power and the projected linear size respectively,

$$P = 4\pi S_{1.4} D_{\rm A}^2 (1+z)^{3+\alpha}, \quad s = l \sin\phi = \theta D_{\rm A}, \tag{3.1}$$

of each double-lobed quasar assuming a spectral index of $\alpha = 0.5$ for any core components, $\alpha = 0.8$ for lobe components, and P to be the total power in the core and the lobes. The orientation angle ϕ is independent of the distributions of P and l. From the discussion in §3.3.1, ϕ and z are not correlated.

3.4.1 Parametric Analysis

Consistent with Buchalter et al. (1998), the different quantities in (3.1) maybe assumed to have the following relationships, parameterized by n, β and x,

$$l \propto (1+z)^n, \tag{3.2}$$

$$l \propto P^\beta, \tag{3.3}$$

$$P \propto (1+z)^x, \tag{3.4}$$

Relation (3.2) denotes the intrinsic size evolution with redshift. Relation (3.4) is the correlation between the source power and redshift expected in any flux-limited survey. It can be seen that relations (3.3) and (3.4) give rise to an apparent size evolution with redshift of the form $l \propto (1+z)^c$, where $c = \beta x + n$. The data let us measure the best fit values of the parameters c, β and x for each set of the cosmological parameters, from which the intrinsic size evolution parameter, n, can be estimated. The evolutionary effects that determine β and n could include changes in the ram pressure exerted by the IGM, synchrotron and Inverse Compton losses, etc.

Tables 3.1 and 3.2 list the best-fit values for c, β, x and n, along with 1σ errors obtained from the diagonal elements of the covariance matrix for the χ^2 fit of

(a) Spectroscopic Sample   *(b)* Photometric Sample
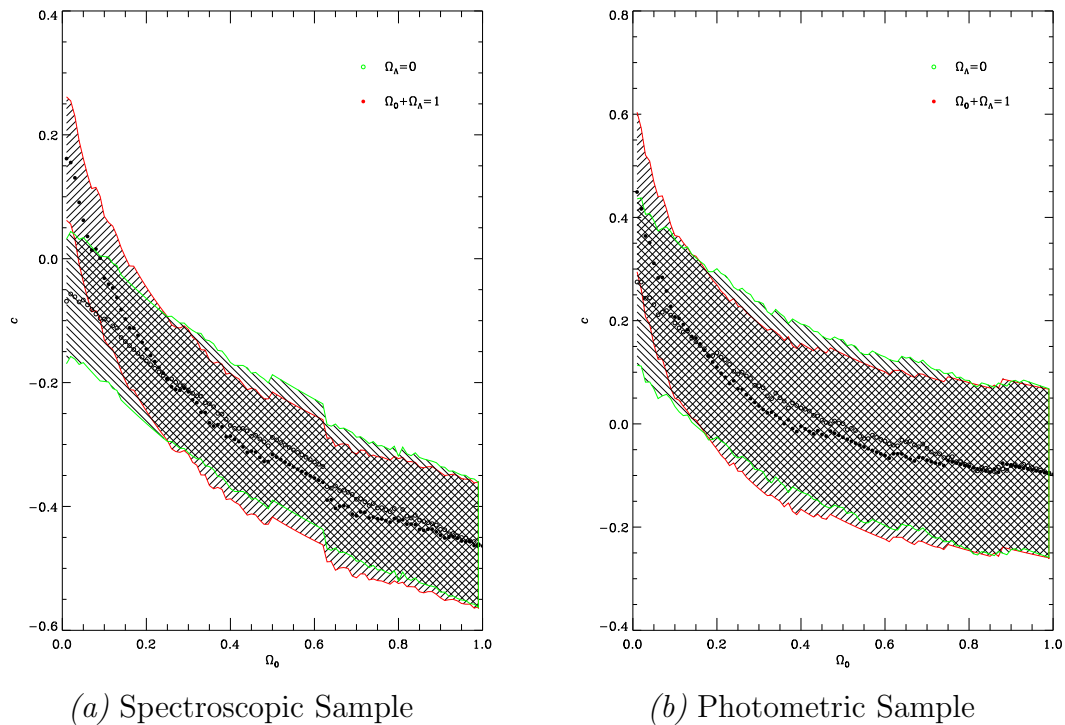
Figure 3.14: Dependence of c (see Relations 3.2-3.4) on the cosmological models. The hatched bands represent the 1σ uncertainties.

the spectroscopic and photometric samples respectively, for a sample of cosmological parameters.

Investigating the best-fit parameter values for these correlations reveals that c, β, x and n are not independent of the cosmological models (see figures 3.14 through 3.17).

The parameter x is extremely significant while the parameter β is moderately significant. On the other hand, the parameter n, which represents the intrinsic size evolution with redshift, is roughly consistent with zero within the listed uncertainties (to within $\sim 2 - 3\sigma$). In other words, we do not find significant evidence in this population of FR II quasars for intrinsic changes in size with redshift. It should be further noted that these result are consistent with, and the uncertainties greatly reduced from, the values obtained by Buchalter et al. (1998).

Table 3.1.   Selected Results of Parametric Fits for c, β, x and n (Spectroscopic Sample)

Model	Ω_0	c	β	x	n	β_l	x_l	n_l
1...	1.00	-0.462 ± 0.101	-0.130 ± 0.017	3.840 ± 0.087	0.038 ± 0.120	-0.118 ± 0.016	3.763 ± 0.099	-0.019 ± 0.118
2...	0.10	-0.013 ± 0.101	-0.064 ± 0.014	4.871 ± 0.086	0.297 ± 0.122	-0.065 ± 0.015	4.793 ± 0.098	0.297 ± 0.123
2...	0.30	-0.216 ± 0.101	-0.093 ± 0.015	4.371 ± 0.087	0.192 ± 0.120	-0.090 ± 0.015	4.291 ± 0.098	0.168 ± 0.121
2...	0.90	-0.443 ± 0.101	-0.126 ± 0.016	3.858 ± 0.087	0.041 ± 0.119	-0.116 ± 0.016	3.781 ± 0.099	-0.004 ± 0.117
3...	0.10	-0.080 ± 0.101	-0.074 ± 0.015	4.711 ± 0.087	0.267 ± 0.123	-0.071 ± 0.015	4.627 ± 0.097	0.250 ± 0.123
3...	0.30	-0.187 ± 0.102	-0.094 ± 0.015	4.420 ± 0.086	0.229 ± 0.123	-0.087 ± 0.015	4.338 ± 0.097	0.192 ± 0.122
3...	0.90	-0.436 ± 0.101	-0.124 ± 0.016	3.900 ± 0.087	0.049 ± 0.120	-0.115 ± 0.016	3.823 ± 0.099	0.004 ± 0.118

Note. — The quantities c, β, x and n are as defined by relations 3.2-3.4. The subscript l denotes that only the power in the lobes were used.

Table 3.2.   Selected Results of Parametric Fits for c, β, x and n (Photometric Sample)

Model	Ω_0	c	β	x	n	β_l	x_l	n_l
1...	1.00	-0.098 ± 0.163	-0.015 ± 0.030	2.300 ± 0.072	-0.063 ± 0.177	-0.011 ± 0.029	2.369 ± 0.076	-0.072 ± 0.178
2...	0.10	0.207 ± 0.158	0.022 ± 0.026	3.039 ± 0.074	0.141 ± 0.177	0.033 ± 0.027	3.058 ± 0.078	0.106 ± 0.178
2...	0.30	0.035 ± 0.160	-0.003 ± 0.028	2.659 ± 0.074	0.043 ± 0.176	0.000 ± 0.028	2.675 ± 0.078	0.034 ± 0.177
2...	0.90	-0.080 ± 0.163	-0.013 ± 0.029	2.330 ± 0.072	-0.050 ± 0.177	-0.009 ± 0.029	2.400 ± 0.076	-0.059 ± 0.177
3...	0.10	0.196 ± 0.162	0.018 ± 0.027	3.047 ± 0.075	0.141 ± 0.181	0.029 ± 0.027	3.069 ± 0.079	0.108 ± 0.182
3...	0.30	0.074 ± 0.163	0.003 ± 0.028	2.792 ± 0.075	0.066 ± 0.180	0.006 ± 0.028	2.810 ± 0.079	0.057 ± 0.181
3...	0.90	-0.081 ± 0.163	-0.012 ± 0.029	2.399 ± 0.071	-0.052 ± 0.178	-0.009 ± 0.029	2.472 ± 0.075	-0.059 ± 0.178

Note. — The quantities c, β, x and n are as defined by relations 3.2-3.4. The subscript l denotes that only the power in the lobes were used.

(a) Spectroscopic Sample

(b) Photometric Sample
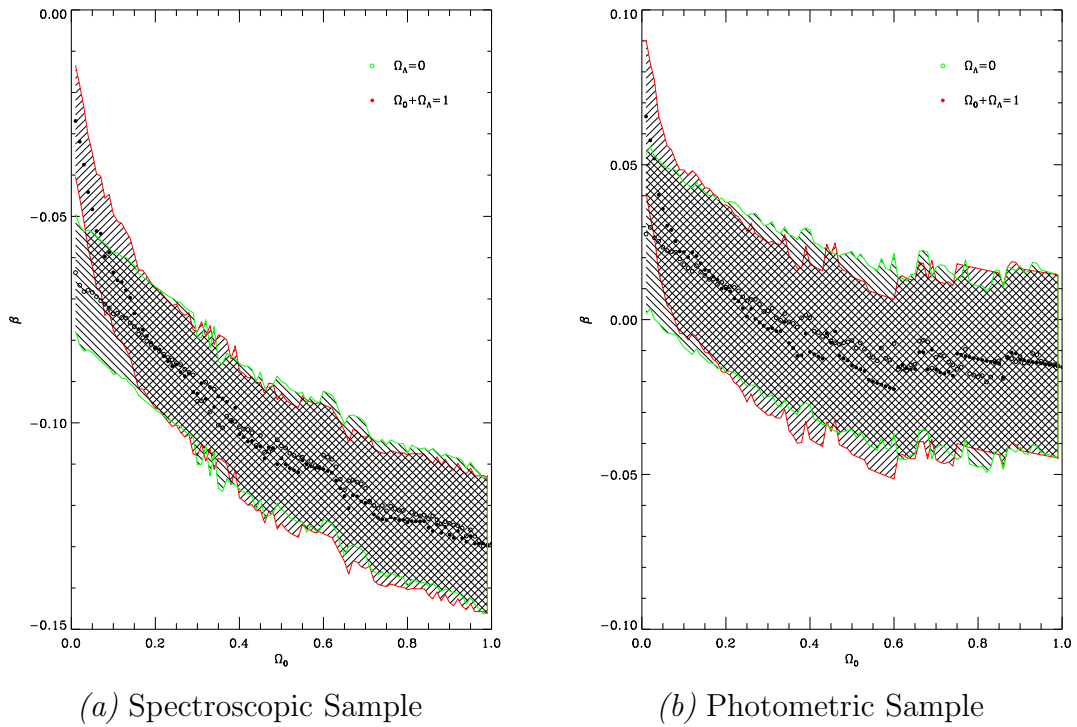
Figure 3.15: Dependence of β (see Relations 3.2-3.4) on the cosmological models. The hatched bands represent the 1σ uncertainties.

(a) Spectroscopic Sample

(b) Photometric Sample
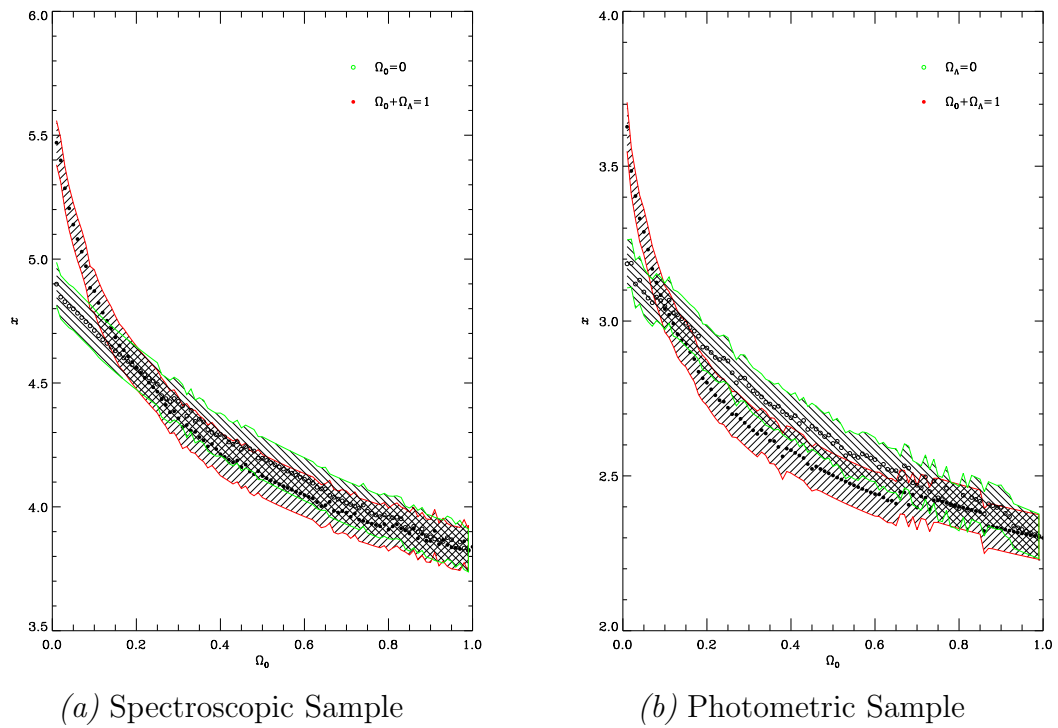
Figure 3.16: Dependence of x (see Relations 3.2-3.4) on the cosmological models. The hatched bands represent the 1σ uncertainties.

(a) Spectroscopic Sample   (b) Photometric Sample
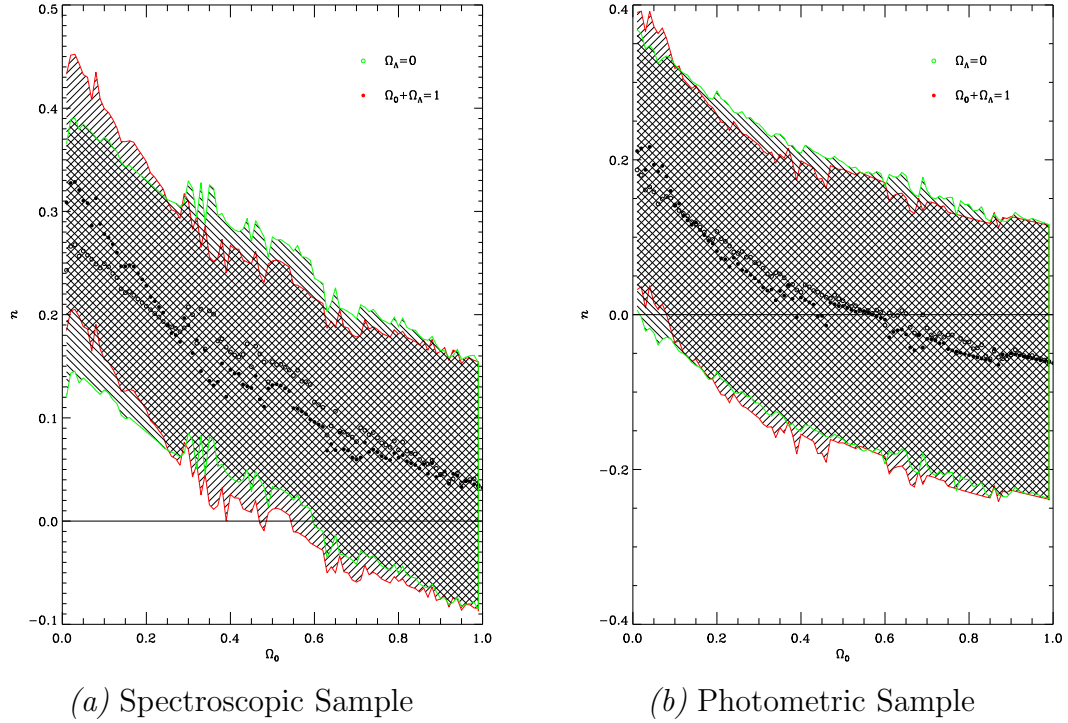
Figure 3.17: Dependence of n (see Relations 3.2-3.4) on the cosmological models. The hatched bands represent the 1σ uncertainties. The horizontal solid line is the reference for no intrinsic evolution of size with redshift.

3.4.2   Non-parametric Analysis

The parametric analysis in §3.4.1 assumes that specific functional forms hold relating the source properties. If these parameterizations are not accurate, they could introduce spurious correlations. Thus it is advisable to perform a correlation analysis that is independent of functional forms. Non-parametric methods have the added advantage that they are independent of the details of binning. The Spearman rank correlation coefficient (r) is a robust non-parametric diagnostic that is commonly used.

The statistic r_{ab} measures the Spearman rank correlation between the quantities a and b. Thus, r_{sz}, r_{sP} and r_{Pz} denote the size-redshift, size-power and power-redshift correlations respectively. It can be shown that these are the non-parametric analogues

Table 3.3.   Selected Results of Nonparametric Analysis between s, P and z
(Spectroscopic Sample)

Model	Ω_0	r_{sz}	r_{sP}	r_{sP_1}	r_{Pz}	$r_{sz,P}$
1...	1.00	-0.1875 ($< 10^{-4}$)	-0.3243 ($< 10^{-12}$)	-0.3225 ($< 10^{-11}$)	0.6442 ($< 10^{-15}$)	0.0227 (0.623)
2...	0.10	-0.0005 (0.991)	-0.1889 ($< 10^{-4}$)	-0.1968 ($< 10^{-4}$)	0.7307 ($< 10^{-15}$)	0.1400 (0.002)
2...	0.30	-0.0829 (0.069)	-0.2518 ($< 10^{-7}$)	-0.2557 ($< 10^{-7}$)	0.6952 ($< 10^{-15}$)	0.0952 (0.036)
2...	0.90	-0.1793 ($< 10^{-4}$)	-0.3193 ($< 10^{-11}$)	-0.3176 ($< 10^{-11}$)	0.6490 ($< 10^{-15}$)	0.0295 (0.522)
3...	0.10	-0.0274 (0.546)	-0.2094 ($< 10^{-5}$)	-0.2169 ($< 10^{-5}$)	0.7202 ($< 10^{-15}$)	0.1263 (0.005)
3...	0.30	-0.0742 (0.102)	-0.2494 ($< 10^{-7}$)	-0.2543 ($< 10^{-7}$)	0.6977 ($< 10^{-15}$)	0.1030 (0.023)
3...	0.90	-0.1760 ($< 10^{-3}$)	-0.3176 ($< 10^{-11}$)	-0.3161 ($< 10^{-11}$)	0.6504 ($< 10^{-15}$)	0.0322 (0.484)

Note. — The quantities r_{ab} and $r_{ab,c}$ respectively denote the Spearman rank correlation and partial rank correlation coefficients between quantities a, b, and c. In each case, the number in parenthesis denotes the two-sided probability that a random data set could achieve the associated value of $|r|$ and thus gives the significance of the result.

of the relations (3.2)-(3.4). The Spearman partial-rank statistic,

$$r_{sz,P} = \frac{r_{sz} - r_{sP}\, r_{Pz}}{\sqrt{(1 - r_{sP}^2)(1 - r_{Pz}^2)}}$$

denotes the correlation between size and redshift when power is held fixed. In other words, it represents any intrinsic size-redshift correlation that exists when the effects of apparent correlation arising out of individual size-power and power-redshift correlations are removed.

For an identical grid in the cosmological parameter space, tables 3.3 and 3.4 list the different Spearman rank correlation statistics for the spectroscopic and photometric samples respectively. Values in the parenthesis indicate the significance of the correlations; i.e., probabilities that these correlations could have arisen entirely by chance. Thus, a small value in the parenthesis implies a significant amount of correlation.

Examination of table 3.3 reveals that there is a very significant correlation between power and redshift (as expected), and a moderately significant correlation between power and projected size. However, the partial rank correlation between projected size and redshift with power held fixed is found to be insignificant (not significant

Table 3.4. Selected Results of Nonparametric Analysis between s, P and z
(Photometric Sample)

Model	Ω_0	r_{sz}	r_{sP}	r_{sP_1}	r_{Pz}	$r_{sz,P}$
1...	1.00	-0.0490 (0.347)	-0.0273 (0.601)	-0.0252 (0.630)	0.5935 ($< 10^{-15}$)	-0.0328 (0.529)
2...	0.10	0.0630 (0.230)	0.0421 (0.423)	0.0414 (0.431)	0.6705 ($< 10^{-15}$)	0.0348 (0.508)
2...	0.30	-0.0070 (0.893)	-0.0109 (0.835)	-0.0085 (0.870)	0.6313 ($< 10^{-15}$)	-0.0002 (1.000)
2...	0.90	-0.0414 (0.427)	-0.0227 (0.663)	-0.0205 (0.695)	0.5971 ($< 10^{-15}$)	-0.0278 (0.594)
3...	0.10	0.0680 (0.197)	0.0395 (0.454)	0.0400 (0.448)	0.6788 ($< 10^{-15}$)	0.0412 (0.435)
3...	0.30	0.0145 (0.782)	0.0044 (0.934)	0.0047 (0.929)	0.6462 ($< 10^{-15}$)	0.0117 (0.824)
3...	0.90	-0.0394 (0.449)	-0.0255 (0.624)	-0.0236 (0.650)	0.6009 ($< 10^{-15}$)	-0.0241 (0.644)

Note. — The quantities r_{ab} and $r_{ab,c}$ respectively denote the Spearman rank correlation and partial rank correlation coefficients between quantities a, b, and c. In each case, the number in parenthesis denotes the two-sided probability that a random data set could achieve the associated value of $|r|$ and thus gives the significance of the result.

at the $\sim 2 - 3\sigma$ level in an equivalent normal distribution). The relative values of the Spearman rank correlation statistic are also found to vary with the cosmological parameters in a fashion similar to that seen in §3.4.1.

3.5 Exploring the χ^2-surface

Before we examine the χ^2-surface, it can easily be seen from figure 3.6 that the data favor the Friedmann models and that the Euclidean model is incapable of providing a reasonable fit to the dataset.

The χ^2-surface is a 3-dimensional surface in the parameter space given by

$$\chi^2 = \chi^2(a, c, \Omega_0) = \sum_{i=1}^{N} \left\{ \frac{[\langle\theta_p\rangle(a, c, \Omega_0; z_i) - \langle\theta_i\rangle]^2}{\sigma_{\langle\theta_i\rangle}^2} \right\} , \quad \langle\theta_p\rangle = \frac{a(1+z)^c}{D_A(\Omega_0; z)}, \quad (3.5)$$

where $\langle\theta_p\rangle$ is the mean angular size predicted by the model at z_i, and, given a, c, $a = h_0 \langle l \sin\phi\rangle_{z=0}$ (measured in kpc throughout) fixes the overall amplitude of the θ-z curve; D_A (measured in kpc) is the familiar angular diameter distance in cosmology. The quantity $\sigma_{\langle\theta_i\rangle} = \sigma_{l\sin\phi}/D_A$ is the square root of the observed variance in each bin

i arising out of the spread in the intrinsic projected sizes, given by $\sigma_{l\sin\phi}$, as well as from curvature effects. Since the survey's astrometric accuracy is better than $1''$, the error arising out of uncertainties in individual measurements is negligible compared to $\sigma^2_{\langle\theta_i\rangle}$.

For this project, we used a grid of 199 cosmological models, 32 values for a and 32 values for c. It should be noted that while the coarseness of these grids may be varied, this does not alter either the results or the overall nature/shape of χ^2.

Figure 3.18 shows the contours of χ^2 in the a-c plane for a fixed cosmology. Figure 3.19 shows the contours of χ^2 in the c-Ω_0 plane for a fixed value of a while figure 3.20 displays the χ^2 contours on the a-Ω_0 for a fixed c. The contours are the percentage confidence levels. In each of the plots of χ^2 with different parameters, a degeneracy is strikingly obvious. From the shapes of these degeneracies and based on the results from the parametric analysis and Equation (3.5), it is clear that these quantities are interlinked and we need additional independent information to untangle them.

Figure 3.6 actually demonstrates this effect. While it is apparent that the Euclidean models (with different physical size parameters) cannot provide a good fit to the data, two different Friedmann models with different apparent evolutions and projected physical sizes (parameterized by c and a) as shown are virtually indistinguishable.

3.6 Distribution of Sizes & Evolution with Redshift

Figure 3.21 shows the distribution of projected sizes for a given cosmological model in each of the redshift bins. In order to evaluate any difference between these distributions, we performed a two-sided K-S test. The results are shown in table 3.5. It is
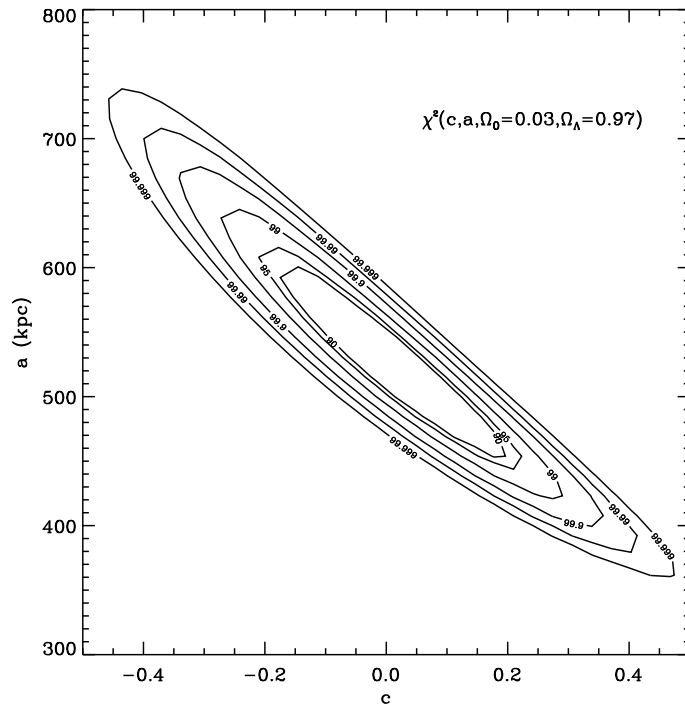
(a) Spectroscopic Sample
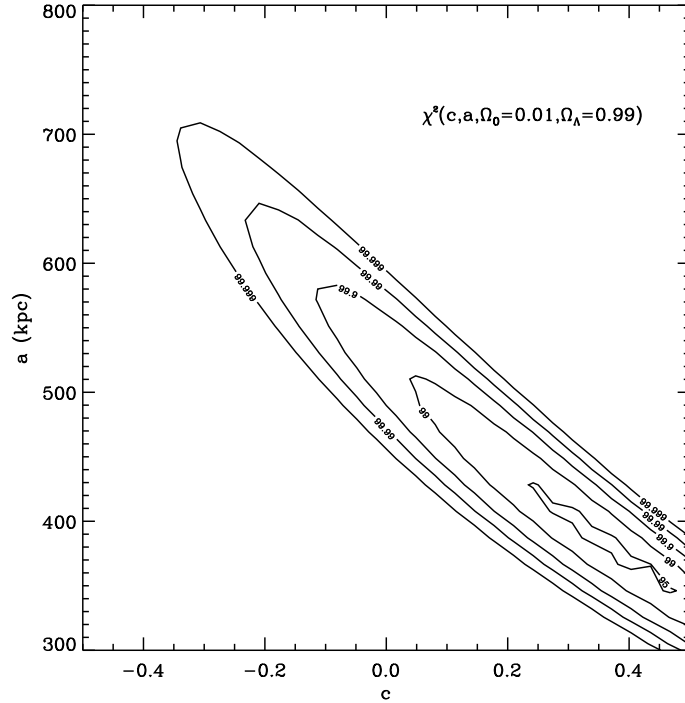
(b) Photometric Sample

Figure 3.18: χ^2 contours in the $a - c$ plane for a fixed cosmological model. The numbers alongside the contours represent the confidence levels (in percent).
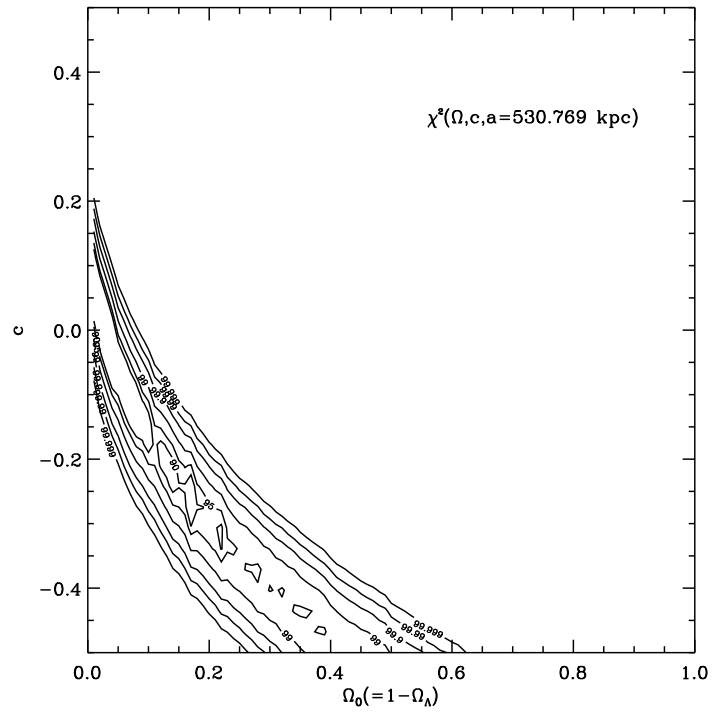
(a) Spectroscopic Sample
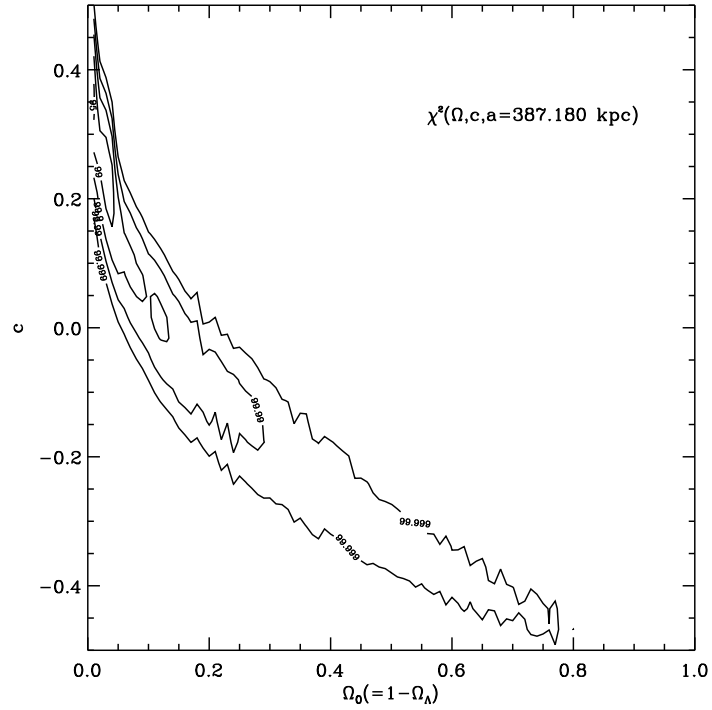
(b) Photometric Sample

Figure 3.19: χ^2 contours in the $\Omega_0 - c$ plane for a fixed a. The numbers alongside the contours represent the confidence levels (in percent).
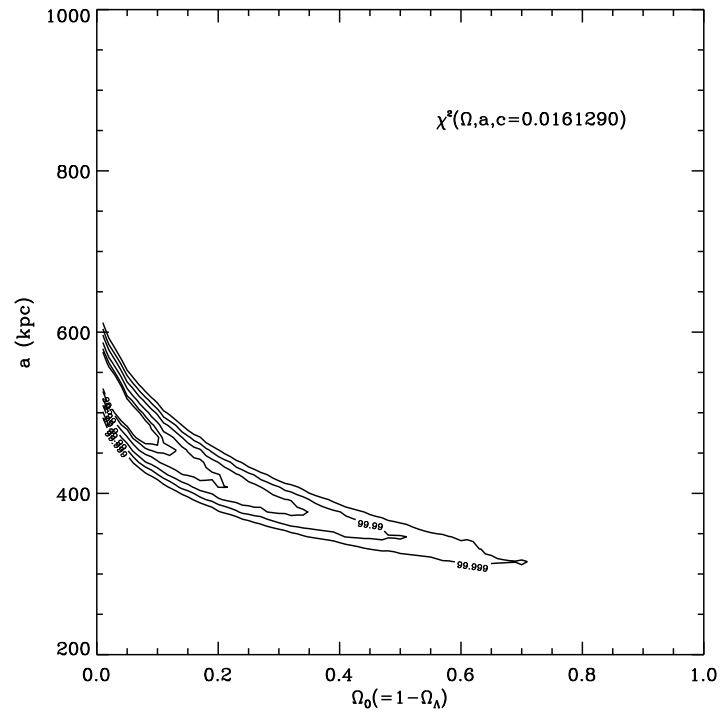
(a) Spectroscopic Sample
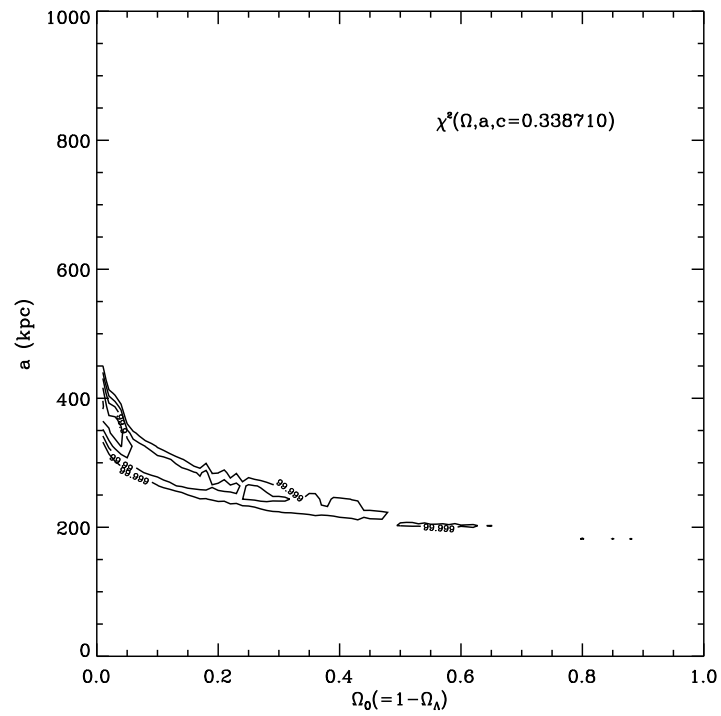
(b) Photometric Sample

Figure 3.20: χ^2 contours in the $\Omega_0 - a$ plane for a fixed c. The numbers alongside the contours represent the confidence levels (in percent).

Table 3.5.   Two-sided significance of the K-S test between distributions of
projected physical sizes in different redshift bins for $\Omega_0 = 0.3$, $\Omega_\Lambda = 0.7$
(Spectroscopic Sample).

Bin	2	3	4	5
1	0.858984	0.647081	0.340539	0.262976
2	$\cdots$	0.262976	0.199169	0.199168
3	$\cdots$	$\cdots$	0.148044	0.431944
4	$\cdots$	$\cdots$	$\cdots$	0.758685

Note. — The values $(0 \leq p \leq 1)$ in the table denote
the significance $(1 - p)$ of the difference in the distribu-
tions in any two bins. Thus, a small value of p indicates
that the distributions in the two bins are significantly
different.

seen that any two bins have different distributions with at most 85% significance. In
other words, the sizes in no two bins are drawn from distributions that differ signifi-
cantly. This result has a two-fold significance. Firstly, it would have been interesting
if the distributions had been significantly different. Apart from implications for mod-
eling, it could signify changes in the physics of FR II objects in different cosmological
epochs resulting either from changes in the IGM or from the sources' intrinsic pow-
ers. Secondly, and most important for our purposes, it addresses the issue of using
FR II objects as standard rods in cosmology. As explained earlier, the definition of
a standard rod can be relaxed from being one with a fixed length to a constraint on
the statistics of the rods' distributions. In other words, in our analysis, we do not
require that all these objects have a fixed intrinsic size but only have nearly identical
distributions of intrinsic sizes in different redshift intervals. In such a scenario, any
statistic should be a robust measure. The two-sided K-S test results from table 3.5
validates the assumption that the distributions of projected physical sizes are not
significantly different.
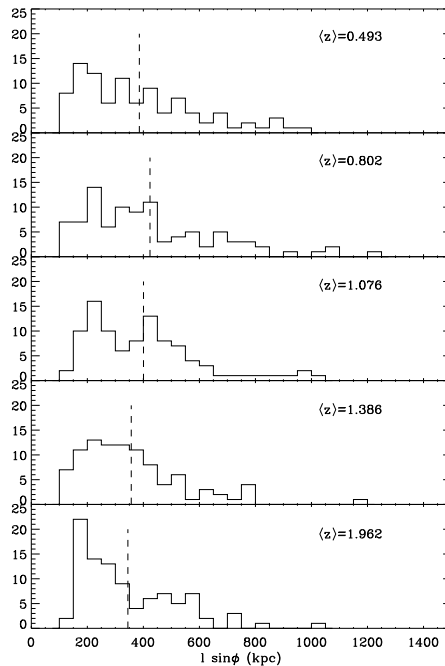
Figure 3.21: A panel of histograms of the projected physical sizes (lobe-core-lobe) of the FR II sample assuming $\Omega_0 = 0.3$, $\Omega_\Lambda = 0.7$ for different redshift bins with each bin's average redshift as indicated. The dashed line indicates the average projected physical size in each of the redshift bins.

3.7   Comparison with FR II Modeling

Modeling of FR II sources has been undertaken by many authors. In this section we will take up a few simple models that predict the sizes of FR II sources as a function of redshift, ambient density, mass of the source, the luminosity of the source, etc. One of the earliest models by De Young (1971) is the single ejection model which involved time-dependent multi-dimensional calculations of the evolution of extended radio sources. These models neglect the effect of magnetic fields and only consider the dominant thermal component of the gas. There are no *a priori* constraints on ram-pressure confinement but it is taken into account that the radio source is injected into a uniform IGM of density $\rho = \rho_0 (1 + z)^3$, and temperature $T = T_0 (1 + z)^2$. The distance of the ejecta from the central object at the end of a rapid deceleration is

taken as a measure of the size of the FR II object and is given by

$$l \sim 65 \, (M_6)^{1/5} (\rho_0/\rho_c)^{-1/4} (1+z)^{-4/5} \, \text{kpc}.$$

where, M_6 is the total mass of the radio source powering the jets in units of $10^6 M_\odot$, ρ_0 is the density of the IGM at $z = 0$ and ρ_c is the critical closure density of the universe. Subsequent modeling by Nepveu (1979) has concluded that the single ejection model seems 'tenable' using a non-uniform radial density distribution around the parent galaxy while neglecting magnetic fields and relativistic particles. On the other hand, data analysis of observations compiled by Eder & Oster (1979) indicated that single ejection models were inadequate to explain the rapid decrease of linear size with increasing redshift. Refinements such as re-supply of relativistic electrons and multiple-ejection models were favored. An extensive review of the theory of extragalactic sources is given in Begelman, Blandford & Rees (1984).

More recently, Gopal-Krishna & Wiita (1987) have proposed a simple analytical model where the radio source expands in two phases, first through the gaseous halo of the parent galaxy and then through a much hotter IGM, incorporating cosmological evolution of the linear size. Barai & Wiita (2006) have tested different models that include relativistic particles and magnetic fields with observations from radio surveys and conclude none of these models can give acceptable fits to all the data simultaneously.

For the purposes of this chapter, we will compare the data with the prediction for "stopping" distance in the models of De Young (1971). The redshift dependence of M_6 is unclear. If it can be assumed that M_6 scales linearly with radio power, then the expression can be conveniently re-written as $l \sim P^{1/5}(1+z)^{-4/5}$. This can be immediately identified with $l \sim P^\beta (1+z)^n$, in terms of the parametric coefficients used in this paper. Table 3.1 shows that both β and n are significantly different from

the predictions of the simple model. The conclusions are true even if M_6 is assumed to be constant. Refinements to the model, or the hypothesis that FR II quasars are different from the generalized class of extragalactic double radio sources in their intrinsic features or environment may be able to explain some of the above difference.

3.8 Summary

The main findings from this study are as follows:

1. The results clearly show that the data are consistent with standard Friedmann models and not with a static Euclidean model. From the χ^2-contours, we find that the parameters suffer from degeneracies. Additional independent information is required to break the degeneracies.

2. In addition to being consistent with the results of Buchalter et al. (1998), our analysis provides much improved error bars.

3. The data show no strong evidence for a significant intrinsic evolution of the size of FR II quasars.

4. A parallel analysis was performed for the photometric sample of FR II quasars. As demonstrated in §3.3 and §3.3.1, there seems to be some fundamental differences in their physical properties. Until these differences can be understood, combining the two samples cannot be undertaken. However, individually, the two samples show some important similarities: both exhibit no significant intrinsic projected physical size evolution with redshift within their respective populations.

Chapter 4

Conclusions & Future Work

The projects in the preceding chapters have revealed valuable information, sometimes in ways that one would not have expected. In line with the summary of the contributions of *FIRST* in chapter 1, it must be emphasized that the projects in this thesis have expanded the breadth of science achievable with the *FIRST* and demonstrated its potential in discovery space. What follows is a recap of some of these important new revelations which could be useful for radio source modeling and are relevant to the next-generation of radio instruments.

It was pointed out earlier in chapter 2 that the *FIRST* survey was not specifically designed for studying variability of the radio sky. Even with this apparent handicap, the data and the results have shown an unprecedented amount of radio variability. This variability is seen on a wide range of timescales, from intra-day to years. Upcoming radio instruments will specifically target radio transients and variables with a much more complete sampling of timescales and sky coverage. While one could speculate about how much the discovery space will be extended, one can be certain that it will be enormously impactful.

In the search for radio transients and variables with the *FIRST* survey, 1651 objects have been found with significant transient or variable behaviour with a wide range of timescales. This by far overshadows any other search of a similar nature, as it does not compromise breadth for the depth and vice versa; it is deeper in flux density sensitivity (~ 1 mJy) and broader in sky coverage ($\sim 9,000$ deg^2) than most searches undertaken so far and provide rich statistics to very good levels of sensitivity. It is thus an important point of reference for future surveys planned with the next-

generation of radio instruments such as ASKAP, MWA, LOFAR, etc. Having shown that $\sim 54\%$ of the sample does not have counterparts in other wavelengths, it provides a wide scope for multi-wavelength follow-up observations to classify and understand the nature of these undetected systems.

An interesting characteristic of this search is that it is self-consistent without the need for external information or models. In fact, such self-consistent analysis has shed some valuable light on the survey itself. This is notable from three things. First, an empirical primary beam was determined specifically for the *FIRST* data. It is found to be slightly different from the standard expression for the VLA primary beam. We thus avoided the need to rely on an external model for the primary beam correction. Second, variability criteria are defined from the data alone. Besides determining the primary beam function from the data, we defined our variability criteria such as $\Delta_{\max}$, $\sigma_{\max}$ and $P(\chi^2, \nu)$ without making use of any external information. In fact, even the peak flux density information in the *FIRST* catalog from coadded images was not explicitly used (although the major and minor axes, and the position angle of the sources were taken from the *FIRST* catalog only due to the catalog's superior reliability and not out of necessity). Third, the data made it possible to estimate fluctuations in the overall amplitude calibration scale throughout the survey.

Another important finding is the non-ideal nature of big surveys and instrumental behaviour. False source contamination can arise from a number of reasons some of which might not be obvious. For instance, the non-physical clustering of outliers seen in figure 2.2 is yet to be understood. In this case, simple checks for abnormal noise or sidelobes in the snapshot images alone did not help beyond a certain point. Besides highlighting such non-ideal behaviour, solving for such non-ideal behaviour also leads to more efficient and intelligent algorithms which are bound to become indispensable for future surveys and instruments.

Although interesting in its own way, the nature of results from the project on the

evolution FR II quasars has been understandably different from the one above. Work on the evolution of radio sources has had a long history, is still debated and is yet to be completely resolved. This study, with improved error bars, shows the data on FR II quasars to be having no significant evidence for intrinsic evolution of projected physical size with redshift further strengthening the view that these objects behave as standard rods in a statistical sense. Such an input will provide invaluable constraints for models and simulations of these radio sources.

As expected, the bigger size of the sample resulted in a decrease of the size of the error bars. But unexpectedly strong degeneracies were found between the different parameters namely, a, c and the cosmological models (see §3.5), and to resolve them, additional independent information is required.

Another significant finding has been the difference between the spectroscopic and photometric samples of FR II quasars from the SDSS as illustrated in §3.3. The fact that the photometric sample is relatively at a higher redshift than the spectroscopic sample is understandable owing to the fainter flux limit of the photometric survey. However, the highly significant smaller sizes of the photometric sample relative to the spectroscopic sample is difficult to explain. The optical luminosity is not biased clearly towards one side or the other of the spectroscopic sample but the distributions are indeed very different. Could there be other factors not yet accounted for that could imply the two samples are drawn from different populations? Could they be powered by different mechanisms? Could they be sampling different environments in a way their physical sizes are affected? With an enormous volume of data available from *FIRST*, SDSS and other optical surveys, it will be interesting to investigate further the nature of quasars from these two samples.

Bibliography

Aller, M. F., Aller, H. D., Hughes, P. A., 2003, ApJ, 586, 33

Altschuler, D. R., Broderick, J. J., Dennison, B., Mitchell, K. J., O'dell, S. L., Condon, J. J., Payne, H. E., 1984, AJ, 89, 1784

Antonucci, R., 1993, ARA&A, 31, 473

Barai, P., Wiita, P. J., 2006, MNRAS, 372, 381

Barthel, P. D., 1989, ApJ, 336, 606

Barthel, P. D., Miley, G. K., 1988, Nature, 333, 319

Becker, R. H., White, R. L., Helfand, D. J., 1995, ApJ, 450, 559

Becker, R. H., Gregg, M. D., Hook, I. M., McMahon, R. G., White, R. L., Helfand, D. J., 1997, ApJ, 479, 93

Becker, R. H., White, R. L., Gregg, M. D., Brotherton, M. S., Laurent-Muehleisen, S. A., Arav, N., 2000, ApJ, 538, 72

Becker, R. H., Helfand, D. J., White, R. L., Gregg, M. D., Brotherton, M. S., Laurent-Muehleisen, S. A., 2003, VizieR On-line Data Catalog: VIII/71

Begelman, M. C., Blandford, R. D., Rees, M. J., 1984, Rev. Mod. Phys., 56, 255

Blake, C., Wall, J., 2002, MNRAS, 337, 993

Blanton, E. L., Gregg, M. D., Helfand, D. J., Becker, R. H., White, R. L., 2000, ApJ, 531, 118

Blanton, E. L., Gregg, M. D., Helfand, D. J., Becker, R. H., Leighly, K. M., 2001, AJ, 121, 2915

Blanton, E. L., Gregg, M. D., Helfand, D. J., Becker, R. H., White, R. L., 2003, AJ, 125, 1635

Bower, G. C. et al., 2005, ApJ, 633, 218

Bower, G. C. et al., 2007, ApJ, 666, 346

Brinkmann, W., Laurent-Muehleisen, S. A., Voges, W., Siebert, J., Becker, R. H., Brotherton, M. S., White, R. L., Gregg, M. D., 2000, A&A, 356, 445

Brotherton, M. S., Gregg, M. D., Becker, R. H., Laurent-Muehleisen, S. A., White, R. L., Stanford, S. A., 1999, ApJ, 514, 61

Brotherton, M. S., Tran, H. D., Becker, R. H., Gregg, M. D., Laurent-Muehleisen, S. A., White, R. L., 2001, ApJ, 546, 775

Buchalter, A., Helfand, D. J., Becker, R. H., White, R. L., 1998, ApJ, 494, 503

Burke-Spolaor, S., Bailes, M., 2010, MNRAS, 402, 855

Carballo, R., González-Serrano, J. I., Benn, C. R., Jiménez-Luján, F., 2008, MNRAS, 391, 369

Carilli, C. L., Ivison, R. J., Frail, D. A., 2003, ApJ, 590, 192

Chang, T.-C., Refregier, A., 2002, ApJ, 570, 447

Chang, T.-C., Refregier, A., Helfand, D. J., 2004, ApJ, 617, 794

Cheung, C. C., 2007, AJ, 133, 2097

Cirasuolo, M., Magliocchetti, M., Celotti, A., Danese, L., 2003, MNRAS, 341, 993

Clewley, L.; Jarvis, M. J., 2004, MNRAS, 352, 909

Condon, J. J., Cotton, W. D., Greisen, E. W., Yin, Q. F., Perley, R. A., Taylor, G. B., Broderick, J. J., 1998, AJ, 115, 1693

Cordes, J. M., Lazio, T. J. W., McLaughlin, M. A., 2004, NewAR, 48, 1459

Cordes, J. M, 2008, ASPC, 395, 225

Cress, C. M., Helfand, D. J., Becker, R. H., Gregg, M. D., White, R. L., 1996, ApJ, 473, 7

Croft, S., de Vries, W., Becker, R. H., 2007, ApJ, 667, 13

Daly, R. A., 1995, ApJ, 454, 580

De Breuck, C., van Breugel, W., Röttgering, H. J. A., Miley, G., 2000, A&AS, 143, 303

del Rizzo, D. A., Gray, A. D., Dougherty, S. M., Taylor, A. R., 2007, Proceedings of "Bursts, Pulses and Flickering: wide-field monitoring of the dynamic radio sky", 25D

Deneva, J. S. et al., 2009, ApJ, 703, 2259

de Vries, W. H., Becker, R. H., White, R. L., Helfand, D. J., 2004, AJ, 127, 2565

de Vries, W. H., Becker, R. H., White, R. L., 2006, AJ, 131, 666

de Vries, W. H., Hodge, J. A., Becker, R. H., White, R. L., Helfand, D. J., 2007, AJ, 134, 457

De Young, D. S., 1971, ApJ, 167, 541

Djorgovski, S. G., Baltay, C., Mahabal, A. A., Drake, A. J., Williams, R., Rabinovitz, D., Graham, M. J., Donalek, C., Glikman, E., Bauer, A., Scalzo, R., Ellman, N., Jerke, J., 2008, AN, 329, 263

Eder, D. C., Oster, L., 1979, ApJ, 233, 780

Fanaroff, B. L., Riley, J. M., 1974, MNRAS, 167, 31

Fender, R. P., Bell Burnell, S. J., Waltman, E. B., Pooley, G. G., Ghigo, F. D., Foster, R. S., 1997, MNRAS, 288, 849

Fender, R. et al., 2008, preprint (astro-ph/0805.4349)

Flesch, E.; Hardcastle, M. J., 2004, A&A, 427, 387

Frail, D. A., Kulkarni, S. R., Bloom, J. S., 1999, Nature, 398, 127

Frey, S., Paragi, Z., Campbell, R. M., Moór, A., 2010, A&A, 513, 18

Gaensler, B. M. et al., 2005, Nature, 434, 1104

Gal-Yam, A. et al., 2006, ApJ, 639, 331

Gawroński, M. P., Marecki, A., Kunert-Bajraszewska, M., Kus, A. J., 2006, A&A, 447, 63

Georgakakis, A., Georgantopoulos, I., Leonidaki, I., Akylas, A., Stewart, G. C., Goudis, C., 2004, MNRAS, 352, 1005

Glikman, E., Helfand, D. J., White, R. L., Becker, R. H., Gregg, M. D., Lacy, M., 2007, ApJ, 667, 673

Gopal-Krishna., Wiita, P. J., 1987, MNRAS, 226, 531

Gregg, M. D., Becker, R. H., White, R. L., Helfand, D. J., McMahon, R. G., Hook, I. M., 1996, AJ, 112, 407

Gregg, M. D., Becker, R. H., Brotherton, M. S., Laurent-Muehleisen, S. A., Lacy, M., White, R. L., 2000, ApJ, 544, 142

Gregg, M. D., Lacy, M., White, R. L., Glikman, E., Helfand, D. J., Becker, R. H., Brotherton, M. S., 2002, ApJ, 564, 133

Gregg, M. D., Becker, R. H., de Vries, W., 2006, ApJ, 641, 210

Gregorini, L., Ficarra, A., Padrielli, L., 1986, A&A, 168, 25

Guerra, E. J., Newlander, S. M., Haarsma, D. B., Bruce P. R., 2002, NewAR, 46, 303

Gurvits, L. I., 1994, ApJ, 425, 442

Gurvits, L. I., Kellerman, K. I., Frey. S., 1999, A&A, 342, 378

Han, J. L., Tian, W. W., 1999, AAS, 136, 571

Harwitt, M., 1998, Astrophysical Concepts (New York: Springer)

Heckman, T. M., Chambers, K. C., Postman, M., 1992, ApJ, 391, 39

Helfand, D. J., Schnee, S., Becker, R. H., White, R. L., McMahon, R. G., 1999, AJ, 117, 1568

Helfand, D. J., Stone, R. P. S., Willman, B., White, R. L., Becker, R. H., Price, T., Gregg, M. D., McMahon, R. G., 2001, AJ, 121, 1872

Hes, R., Barthel, P. D., Hoekstra, H., 1995, A&A, 303, 8

Hessels, J. W. T., Stappers, B. W., van Leeuwen, J., 2009, ASPC, 407, 318

Hey, J. S., 1946, Nature, 157, 47

Hodge, J. A., Becker, R. H., White, R. L., de Vries, W. H., 2008, AJ, 136, 1097

Hooley, A., Longair, M. S., Riley, J. M., 1978, MNRAS, 182, 127

Hopkins, A., Windhorst, R., Cram, L., Ekers, R., 2000, Exp. Astron., 10, 419

Hopkins, A. M. et al., 2003, ApJ, 599, 971

Hughes, P. A., Aller, H. D., Aller, M. F., 1992, ApJ, 396, 469

Hyman, S. D., Lazio, T. J. W., Kassim, N. E., Bartleson, A. L., 2002, AJ, 123, 1497

Hyman, S. D., Lazio, T. J. W., Kassim, N. E., Ray, P. S., Markwardt, C. B., Yusef-Zadeh, F., 2005, Nature, 434, 50

Hyman, S. D., Wijnands, R., Lazio, T. J. W., Pal, S., Starling, R., Kassim, N. E., Ray, P. S., 2009, ApJ, 696, 280

Ivezić, Ž. et al., 2002, AJ, 124, 2364

Ivezić, Ž. et al., 2003, Mem. Soc. Astron. Italiana, 74, 978

Ivezić, Ž. et al., 2008, preprint (astro-ph/0805.2366)

Jackson, P. D., Kundu, M. R., White, S. M., 1989, A&A, 210, 284

Johnston, S. et al., 2007, PASA, 24, 174

Johnston, S. et al., 2008, Exp. Astron., 22, 151

Kaiser, N., 2004, SPIE, 5489, 11

Kamionkowski, M., Babul, A., Cress, C. M., Refregier, A., 1998, MNRAS, 301, 1064

Kapahi, V. K., 1985, MNRAS, 214, 19

Kapahi, V. K., 1989, AJ, 97, 1

Kaplan, D. L., Condon, J. J., Arzoumanian, Z., Cordes, J. M., 1998, ApJS, 119, 75

Kunert-Bajraszewska, M., Marecki, A., Thomasson, P., Spencer, R. E., 2005, A&A, 440, 93

Kunert-Bajraszewska, M., Marecki, A., Thomasson, P., 2006, A&A, 450, 945

Lacy, M., Laurent-Muehleisen, S. A., Ridgway, S. E., Becker, R. H., White, R. L., 2001, ApJ, 551, 17

Lacy, M., Gregg, M. D., Becker, R. H., White, R. L., Glikman, E., Helfand, D. J., Winn, J. N., 2002, AJ, 123, 2925

Lainela, M., 1994, A&A, 286, 408

Lehár, J., Buchalter, A., McMahon, R. G., Kochanek, C. S., Muxlow, T. W. B., 2001, ApJ, 547, 60

Levinson, A., Ofek, E. O, Waxman, E., Gal-Yam, A., 2002, ApJ, 576, 923

Lister, M. L., Hutchings, J. B., Gower, A. C., 1994, ApJ, 427, 125

Lister, M. L., Tingay, S. J., Preston, R. A., 2001, ApJ, 554, 964

Lonsdale, C. J. et al., 2009, IEEEP, 97, 1497

Lovell, J. E. J. et al., 2003, AJ, 126, 1699

Machalski, J., Jamrozy, M., Zola, S., 2001, A&A, 371, 445

Magliocchetti, M., Maddox, S. J., Lahav, O., Wall, J. V., 1998, MNRAS, 300, 257

Magliocchetti, M., Maddox, S. J., Wall, J. V., Benn, C. R., Cotter, G., 2000, MNRAS, 318, 1047

Magliocchetti, M. et al., 2002, MNRAS, 333, 100

Magliocchetti, M. et al., 2004, MNRAS, 350, 1485

Manchester, R. N., Hobbs, G. B., Teoh, A., Hobbs, M., 2005, AJ, 129, 1993

Marecki, A., Thomasson, P., Mack, K.-H., Kunert-Bajraszewska, M., 2006, A&A, 448, 479

Marecki, A., Kunert-Bajraszewska, M., Spencer, R. E., 2006, A&A, 449, 985

McGreer, I. D.; Becker, R. H.; Helfand, D. J.; White, R. L., 2006, ApJ, 652, 157

McLaughlin, M. A. et al., 2006, Nature, 439, 817

McMahon, R. G., White, R. L., Helfand, D. J., Becker, R. H., 2002, ApJS, 143, 1

Menou, K. et al., 2001, ApJ, 561, 645

Mickaelian, A. M., Hovhannisyan, L. R., Engels, D., Hagen, H.-J., Voges, W., 2006, A&A, 449, 425

Miley, G. K., 1971, MNRAS, 152, 477

Mitchell, K. J., Dennison, B., Condon, J. J., Altschuler, D. R., Payne, H. E., O'dell, S. L., Broderick, J. J., 1994, ApJS, 93, 441

Napier, P. J., 2006, ASPC, 356, 65

Nepveu, M., 1979, A&A, 75, 149

Nice, D. J., 1999, ApJ, 513, 927

Nilsson, K., Valtonen, M. J., Kotilainen, J., Jaakkola, T., 1993, ApJ, 413, 453

Onuora, L. I., 1989, Ap&SS, 162, 343

Overzier, R. A.; Röttgering, H. J. A.; Rengelink, R. B.; Wilman, R. J., 2003, A&A, 405, 53

Padrielli et al., 1987, A&AS, 67, 63

Proctor, D. D., 2006, ApJS, 165, 95

Quirrenbach, A., Witzel, A., Krichbaum, T. P., Hummel, C. A., Wegner, R., Schalinski, C. J., Ott, M., Alberdi, A., Rioja, M., 1992, A&A, 258, 279

Rau, A. et al., 2009, PASP, 121, 1334

Richards, E. A., Fomalont, E. B., Kellermann, K. I., Windhorst, R. A., Partridge, R. B., Cowie, L. L., Barger, A. J., 1999, ApJ, 526, 73

Richards, G. T. et al., 2002, AJ, 123, 2945

Richards, G. T. et al., 2009, ApJS, 180, 67

Rickett, B. J., 1986, ApJ, 307, 564

Rickett, B. J., Quirrenbach, A., Wegner, R., Krichbaum, T. P., Witzel, A., 1995, A&A, 293, 479

Rupen, M. P., 2000, AAS, 196.3002

Ryan, R. E. Jr., Cohen, S. H., Windhorst, R. A., Keeton, C. R., Veach, T. J., 2008, ApJ, 688, 43

Sánchez-Sutil, J. R., Muñoz-Arjonilla, A. J., Martí, J., Garrido, J. L., Pérez-Ramírez, D., Luque-Escamilla, P., 2006, A&A, 452, 739

Schechter, P. L., Gregg, M. D., Becker, R. H., Helfand, D. J., White, R. L., 1998, AJ, 115, 1371

Schneider, D. P. et al., 2007, AJ, 134, 102

Singal, A. K., 1988, MNRAS, 233, 87

Singal, A. K., 1993, MNRAS, 263, 139

Singal, A. K., 1996, MNRAS, 278, 1069

Sullivan, M., 2009, AIPC, 1111, 539

Totani, T., Panaitescu, A., 2002, ApJ, 576, 120

Tyson, A., Angel, R., 2001, ASPC, 232, 347

Ubachukwu, A. A., Onuora, L. I., 1993, Ap&SS, 209, 169

Ubachukwu, A. A., 1996, Ap&SS, 236, 167

Urry, C. M., Padovani, P., 1995, PASP, 107, 803

van Breugel, W., 1999, Ap&SS, 266, 23

van der Laan, H., Perola, G. C., 1969, A&A, 3, 468

Waltman, E. B., Ghigo, F. D., Johnston, K. J., Foster, R. S., Fiedler, R. L., Spencer, J. H., 1995, AJ, 110, 290

Wang, T.-G, Zhou, H.-Y., Wang, J.-X., Lu, Y.-J., Lu, Y., 2006, ApJ, 645, 856

Wardle, J. F. C., Miley, G. K., 1974, A&A, 30, 305

Weiler, K. W., Panagia, N., Montes, M. J., Sramek, R. A., 2002, ARA&A, 40, 387

Whalen, D. J., Laurent-Muehleisen, S. A., Moran, E. C., Becker, R. H., 2006, AJ, 131, 1948

White, R. L., Becker, R. H., Helfand, D. J., Gregg, M. D., 1997, ApJ, 475, 479

White, R. L. et al., 2000, ApJS, 126, 133

White, R. L., Helfand, D. J., Becker, R. H., Glikman, E., de Vries, W., 2007, ApJ, 654, 99

Wilkinson, P. N., Kellermann, K. I., Ekers, R. D., Cordes, J. M, Lazio, T. J. W., 2004, NewAR, 48, 1551

Windhorst, R. A., Hopkins, A., Richards, E. A., Waddington, I., 1999, ASPC, 193, 55

York, D. G. et al., 2000, AJ, 120, 1579

Zakamska, N. L., Strauss, M. A., Heckman, T. M., Ivezić, Ž., Krolik, J. H., 2004, AJ, 128, 1002

Appendix A

Complete Sample of Variables & Transients

Table A.1 presents the complete sample of 1651 highly variable and transient radio sources identified in our study. Column 1 provides the source position derived from the *FIRST* catalog. Columns 2 and 3 give, respectively, the *FIRST* catalog peak flux density and the mean peak flux density derived from the light curves. The range of flux densities for the source derived from the grid images are in column 4, while column 5 provides the NVSS catalog peak flux density. Note that, while *FIRST* and NVSS have very different angular resolutions, our restriction of this study to isolated point sources in the higher-resolution *FIRST* survey means resolution effects should not be a factor in most cases.

These data are followed by the number of observations available (col. 6). The next three columns provide the three measures of variability: $P(\chi^2, \nu)$ for the light curve (col. 7), the maximum deviation of a single data point from the mean flux density in the light curve (col. 8), and the difference (in σ) between the most significantly different pair of data points (col. 9). The maximum-to-minimum flux density ratio is provided in column 10. The $T_{\min}$ (days) in column 11 denotes the minimum timescale at which two data points differ by at least 6σ. In cases where the maximum absolute difference of any pair of data points never reaches a value 6σ, the value denotes the timescale at which the maximum absolute difference in column 10 is attained. In a few cases where the date of observation cannot be reliably obtained from the snapshot header, the entry is left without a numerical value. Column 12 contains a flag 'BN' if the outlier is found to be in the vicinity of a source brighter than 500 mJy within

$31'$. Column 13 provides the distance of the mean normalized peak flux density of the neighbours corresponding to each outlier from the mean of the distribution of such normalized neighbour peak flux densities corresponding to all outliers and is a proxy for the quality of the field. The higher the absolute value in this column, the less ideal the quality of field surrounding the outlier and hence, the less reliable the physical variability of the outlier.

The type of light curve is denoted in column 14 by V (Variable) and T (Transient). The apparent SDSS-i band magnitudes are provided in column 15 where a SDSS match is available. Finally, column 16 gives the best ranked counterpart at other wavelengths. This ranking is explained in §2.6.

Table A.1: Summary of Properties of Variables & Transients

Coordinates (J2000)	f (mJy)				N	Measures			$\frac{\text{Max.}}{\text{Min.}}$	T_{min}	Flags	σ_{nbr}	Type	i	Cross-ID
	Cat.	$\overline{f}$	Range	NVSS		$P(\chi^2,\nu)$	σ_{max}	$\Delta_{max}(\sigma)$		(days)				Mag.	
06 53 51.960 +60 29 07.03	3.94	3.93	<2.56 - 4.34	$\cdots$	2	1.779e-10	6.17	6.13	>1.69	404	$\cdots$	0.42	T	$\cdots$	$\cdots$
06 57 38.503 +61 05 53.97	11.24	6.21	<3.67 - 8.15	9.33	3	5.030e-12	6.42	6.96	>2.22	3	$\cdots$	0.13	V	$\cdots$	$\cdots$
06 58 24.412 +54 54 46.01	7.34	7.22	4.72 - 7.62	6.11	3	7.718e-12	5.97	5.02	1.61	64	$\cdots$	0.25	V	$\cdots$	$\cdots$
07 00 38.036 +63 17 17.81	3.17	3.39	1.45 - 3.99	2.69	3	3.059e-07	4.97	5.28	2.75	8	$\cdots$	2.43	V	$\cdots$	$\cdots$
07 01 13.235 +61 51 35.18	8.89	8.74	6.73 - 10.77	7.40	3	1.875e-10	4.81	5.63	1.60	4	$\cdots$	-0.93	V	$\cdots$	$\cdots$
07 02 31.115 +48 17 29.96	1.32	1.51	<1.07 - 2.43	$\cdots$	3	4.034e-10	4.87	6.16	>2.27	12	$\cdots$	0.44	T	$\cdots$	$\cdots$
07 06 12.017 +58 21 12.02	10.32	11.00	6.39 - 18.89	11.21	5	1.971e-07	5.29	4.52	1.74	54	$\cdots$	0.78	V	$\cdots$	$\cdots$
07 07 14.456 +37 22 41.88	48.78	41.26	40.98 - 65.30	49.49	3	2.442e-09	5.59	5.11	1.59	1	$\cdots$	-0.09	V	$\cdots$	GSC2-FIRST-G
07 07 27.070 +60 42 02.19	7.12	6.59	2.93 - 8.26	4.49	4	6.328e-09	4.01	4.64	2.59	404	$\cdots$	1.39	V	$\cdots$	$\cdots$
07 10 11.147 +57 19 31.62	5.68	6.14	4.24 - 7.60	6.88	4	2.516e-09	5.66	5.93	1.79	5	$\cdots$	1.39	V	$\cdots$	GSC2-FIRST-G
07 11 00.421 +37 37 13.03	3.12	2.81	1.33 - 4.26	$\cdots$	3	6.668e-09	4.58	6.07	3.21	59	$\cdots$	-4.03	V	$\cdots$	GSC2-FIRST-G
07 13 23.159 +60 15 12.69	2.15	2.31	1.11 - <3.68	$\cdots$	4	2.923e-08	4.68	5.81	2.88	391	$\cdots$	0.38	V	$\cdots$	GSC2-FIRST-G
07 13 47.093 +56 30 06.69	1.44	1.18	<0.98 - <5.31	$\cdots$	3	3.427e-10	4.70	6.18	>2.61	415	$\cdots$	0.02	V	$\cdots$	GSC2-FIRST-G
07 14 03.920 +33 56 34.67	10.36	10.40	7.95 - 12.98	8.54	3	1.352e-07	4.84	4.72	1.63	8	$\cdots$	0.16	V	$\cdots$	GSC2-FIRST-G
07 17 05.376 +51 37 01.89	14.19	14.64	13.42 - 18.68	13.94	5	5.167e-07	3.80	4.16	1.39	2	$\cdots$	0.88	V	$\cdots$	$\cdots$
07 17 40.540 +57 26 49.35	35.23	34.14	33.51 - 49.58	35.66	4	1.054e-06	5.19	4.71	1.48	0	$\cdots$	1.35	V	$\cdots$	$\cdots$
07 17 49.021 +57 26 10.32	61.86	61.70	60.53 - 91.10	62.46	4	3.245e-11	5.36	4.88	1.51	0	$\cdots$	0.63	V	$\cdots$	$\cdots$
07 17 50.275 +45 18 32.52	2.65	2.78	1.40 - 3.75	$\cdots$	4	2.559e-07	4.44	4.63	2.68	15	$\cdots$	-0.18	V	$\cdots$	$\cdots$
07 18 08.619 +38 29 33.11	16.45	15.88	14.91 - 23.75	16.71	4	2.108e-11	5.31	5.15	1.59	0	$\cdots$	-1.56	V	$\cdots$	$\cdots$
07 18 15.969 +38 18 30.31	5.75	5.86	4.37 - 8.26	4.70	4	4.989e-08	4.84	4.48	1.50	3	$\cdots$	2.33	V	$\cdots$	$\cdots$
07 18 19.017 +30 58 09.80	3.65	3.77	2.48 - 4.98	3.94	3	1.037e-08	3.75	5.27	2.01	419	$\cdots$	0.54	V	21.39	SDSS-G
07 20 06.053 +28 37 13.90	3.26	3.12	1.35 - 3.44	$\cdots$	3	9.030e-07	5.08	5.06	2.55	893	$\cdots$	1.45	V	$\cdots$	$\cdots$
07 20 11.777 +64 12 52.28	2.80	2.81	<1.79 - 3.84	$\cdots$	3	1.301e-08	5.77	5.64	>1.70	23	$\cdots$	0.99	V	$\cdots$	$\cdots$
07 20 29.149 +54 09 24.72	2.49	2.45	<1.44 - <8.25	$\cdots$	4	3.557e-07	5.08	5.11	>1.89	0	$\cdots$	1.06	V	$\cdots$	$\cdots$
07 21 44.720 +46 32 40.57	1.69	1.57	<1.25 - 2.06	$\cdots$	2	7.617e-08	4.67	5.21	>1.65	1	$\cdots$	1.05	T	$\cdots$	GSC2-FIRST-G
07 22 10.036 +28 42 20.62	34.43	31.93	30.65 - 68.21	38.65	3	0.000	8.47	8.26	2.23	893	$\cdots$	0.76	V	$\cdots$	$\cdots$
07 23 15.350 +51 25 39.27	22.90	20.42	17.31 - 34.31	22.39	4	1.048e-10	5.46	6.27	1.98	0	$\cdots$	0.25	V	$\cdots$	$\cdots$
07 23 52.460 +37 31 15.70	7.94	7.87	7.20 - <14.44	8.22	5	5.427e-06	5.01	4.92	1.57	1	$\cdots$	-1.62	V	$\cdots$	$\cdots$
07 24 21.171 +54 00 14.80	3.32	3.30	1.34 - 3.83	3.49	3	2.469e-07	5.07	5.26	2.86	0	$\cdots$	-0.08	V	$\cdots$	GSC2-FIRST-G
07 24 47.831 +31 39 43.07	3.23	3.13	2.06 - 3.87	$\cdots$	3	2.756e-08	4.46	5.20	1.88	0	$\cdots$	0.11	V	21.45	SDSS-G

Coordinates (J2000)	f (mJy)				N	Measures			$\frac{\text{Max.}}{\text{Min.}}$	$T_{\min}$	Flags	σ_{nbr}	Type	i	Cross-ID
	Cat.	$\overline{f}$	Range	NVSS		$P(\chi^2,\nu)$	$\sigma_{\max}$	$\Delta_{\max}(\sigma)$		(days)				Mag.	
07 24 53.712 +30 18 32.90	8.39	8.45	5.79 - 10.39	9.65	3	2.220e-15	6.66	6.68	1.79	7	$\cdots$	-0.09	V	17.31	SDSS-G
07 25 02.776 +54 50 56.47	11.08	9.72	9.29 - 15.70	9.70	4	1.725e-10	5.69	5.58	1.69	428	$\cdots$	-0.47	V	$\cdots$	$\cdots$
07 25 37.678 +32 11 46.65	2.24	2.54	1.36 - 4.16	$\cdots$	4	1.787e-07	4.79	5.06	3.05	0	$\cdots$	-0.41	V	19.44	SDSS-G
07 26 45.159 +64 17 29.33	30.54	30.03	22.21 - 45.56	35.03	5	2.665e-15	5.73	5.77	1.63	23	$\cdots$	0.74	V	$\cdots$	GSC2-FIRST-G
07 27 22.657 +38 28 40.88	12.04	11.85	9.50 - 17.03	12.99	4	1.324e-09	4.43	5.37	1.79	0	$\cdots$	-0.32	V	$\cdots$	$\cdots$
07 29 07.313 +61 49 54.47	2.08	2.00	<1.48 - <6.33	$\cdots$	4	5.641e-07	4.80	5.04	>1.70	4	$\cdots$	0.25	V	$\cdots$	$\cdots$
07 30 22.192 +26 10 59.45	8.83	9.67	<6.04 - 10.14	$\cdots$	4	1.580e-08	5.73	5.47	>1.68	2	$\cdots$	-0.38	V	$\cdots$	$\cdots$
07 30 52.321 +51 59 24.79	9.96	9.47	9.05 - <16.82	11.61	6	1.091e-09	6.16	6.02	1.79	3	BN	1.65	V	$\cdots$	GSC2-FIRST-G
07 31 32.888 +39 51 43.07	4.58	4.80	<3.39 - <6.89	3.79	5	1.014e-06	5.42	5.18	>1.47	0	$\cdots$	-0.09	V	$\cdots$	$\cdots$
07 31 38.058 +43 00 50.21	14.34	14.62	5.75 - 14.98	7.65	5	6.041e-10	5.55	5.23	2.60	2	$\cdots$	0.36	V	20.50	SDSS-*
07 33 13.989 +58 07 18.62	6.68	6.92	3.60 - 8.86	5.63	5	2.097e-11	6.60	5.94	2.33	61	$\cdots$	-0.12	V	$\cdots$	GSC2-FIRST-G
07 35 08.271 +25 38 04.00	2.01	2.04	1.13 - 3.66	$\cdots$	3	1.393e-07	4.69	5.49	3.25	8	$\cdots$	0.71	V	$\cdots$	$\cdots$
07 35 59.821 +59 54 24.37	14.32	13.20	6.81 - 14.16	12.91	5	9.251e-08	4.62	4.22	>1.95	2	$\cdots$	0.11	V	$\cdots$	$\cdots$
07 36 28.815 +36 22 37.80	4.08	4.15	1.87 - 4.91	3.60	3	2.284e-08	5.43	5.75	2.63	5	BN	0.54	V	20.68	SDSS-G
07 36 45.760 +36 03 31.98	2.22	2.13	<1.57 - 2.99	$\cdots$	3	2.946e-09	4.58	5.69	>1.91	0	BN	-1.18	T	$\cdots$	$\cdots$
07 36 56.669 +19 36 19.04	7.94	8.08	4.85 - 14.81	5.74	4	1.156e-10	5.34	6.24	3.06	$\cdots$	$\cdots$	0.11	V	21.50	SDSS-*
07 37 36.277 +36 04 17.40	3.22	3.47	1.86 - 4.34	5.67	4	4.294e-07	3.89	4.67	>2.33	5	BN	-0.36	V	$\cdots$	$\cdots$
07 37 46.155 +59 25 24.38	6.60	6.35	4.11 - 6.86	2.09	4	1.868e-07	5.45	4.71	1.67	8	$\cdots$	-1.28	V	$\cdots$	GSC2-FIRST-G
07 37 54.452 +28 00 31.53	1.32	1.18	0.60 - 2.28	$\cdots$	3	7.178e-08	4.05	5.45	3.84	485	$\cdots$	-0.11	V	$\cdots$	$\cdots$
07 38 13.026 +57 22 38.36	21.40	21.74	16.01 - 26.06	18.61	4	5.773e-09	5.73	5.60	1.63	411	$\cdots$	0.21	V	$\cdots$	$\cdots$
07 38 26.371 +29 46 28.92	38.90	38.35	36.02 - 55.76	50.30	3	1.994e-08	5.40	5.34	1.55	10	$\cdots$	0.10	V	21.03	SDSS-G
07 38 46.432 +64 16 47.09	20.42	19.88	9.30 - 45.29	21.62	6	1.910e-12	5.60	6.09	2.60	23	$\cdots$	-0.42	V	$\cdots$	$\cdots$
07 38 49.526 +18 35 10.56	2.88	3.01	1.63 - 3.96	2.18	3	9.949e-08	5.12	4.78	2.08	$\cdots$	$\cdots$	0.24	V	$\cdots$	$\cdots$
07 39 13.460 +18 02 22.75	7.38	7.81	<6.75 - 13.22	2.86	4	3.465e-10	5.01	5.97	>1.96	$\cdots$	BN	0.26	V	17.00	SDSS-QSO(P)
07 39 51.588 +59 35 45.22	13.54	11.79	10.79 - 17.29	13.01	4	6.892e-08	3.47	3.91	1.41	12	$\cdots$	1.76	V	$\cdots$	$\cdots$
07 40 01.126 +60 04 17.97	10.64	10.78	10.04 - 16.52	9.70	4	9.376e-09	4.75	4.93	1.65	391	$\cdots$	0.63	V	$\cdots$	$\cdots$
07 40 10.686 +18 31 49.13	39.68	39.53	37.33 - 54.60	50.71	4	6.567e-10	4.67	4.62	1.46	$\cdots$	$\cdots$	0.11	V	20.71	SDSS-QSO(P)
07 40 14.299 +51 28 37.36	29.92	31.01	23.53 - 33.86	28.74	3	1.843e-07	5.35	4.46	1.44	0	BN	-2.69	V	$\cdots$	$\cdots$
07 40 55.809 +54 19 40.73	1.29	1.12	<1.19 - <10.01	$\cdots$	4	2.550e-07	4.80	5.46	>2.36	428	$\cdots$	-0.73	V	$\cdots$	GSC2-FIRST-G
07 40 56.777 +51 46 10.99	9.25	8.60	7.41 - 12.53	8.42	3	1.128e-07	4.61	5.43	1.69	0	BN	0.28	V	$\cdots$	$\cdots$
07 42 05.242 +21 35 06.03	5.58	5.55	<3.95 - <8.53	4.61	5	1.425e-07	5.23	5.01	>1.45	2	$\cdots$	-0.70	V	$\cdots$	$\cdots$

Continued on next page...

Coordinates (J2000)	f (mJy)				N	Measures			$\frac{\text{Max.}}{\text{Min.}}$	$T_{\min}$	Flags	σ_{nbr}	Type	i	Cross-ID
	Cat.	$\overline{f}$	Range	NVSS		$P(\chi^2,\nu)$	$\sigma_{\max}$	$\Delta_{\max}(\sigma)$		(days)				Mag.	
07 42 17.130 +43 55 46.68	2.26	2.33	<1.63 - <7.80	$\cdots$	5	4.137e-07	4.28	4.47	>1.58	1	$\cdots$	0.13	V	$\cdots$	$\cdots$
07 42 41.180 +38 10 02.26	3.75	4.14	2.76 - 4.75	$\cdots$	3	3.263e-07	4.42	4.73	>1.72	15	BN	0.93	V	$\cdots$	SDSS-UNKNOWN
07 42 50.457 +61 09 26.29	3.88	4.13	<3.14 - 7.31	2.04	4	3.772e-12	5.74	6.17	>2.33	6	$\cdots$	-0.10	V	$\cdots$	HIP-STAR
07 42 51.634 +43 57 36.18	1.64	1.72	<1.19 - 2.39	$\cdots$	3	2.376e-09	4.98	5.56	>2.01	1	$\cdots$	0.76	T	$\cdots$	$\cdots$
07 43 18.647 +28 53 02.22	1.99	2.08	<1.03 - 4.74	5.77	4	0.000	7.57	8.38	>4.10	5	$\cdots$	0.86	V	$\cdots$	HIP-STAR
07 43 58.039 +30 47 35.25	1.76	1.49	0.89 - 2.49	$\cdots$	3	5.553e-07	4.14	4.87	>2.79	8	$\cdots$	0.43	V	$\cdots$	$\cdots$
07 44 15.516 +55 06 50.70	3.48	3.45	<1.67 - <11.91	$\cdots$	4	1.087e-09	6.30	6.16	>2.18	428	$\cdots$	-4.42	V	$\cdots$	$\cdots$
07 45 01.564 +15 38 04.88	61.57	61.53	55.98 - 88.57	68.14	6	1.882e-10	5.13	4.91	1.50	2	$\cdots$	0.45	V	16.89	SDSS-QSO(P)
07 45 06.844 +55 04 55.85	14.76	14.68	9.23 - 15.10	11.97	3	0.000	6.20	5.06	1.64	428	$\cdots$	0.65	V	$\cdots$	GSC2-FIRST-G
07 45 20.211 +41 57 25.44	20.67	19.84	18.51 - 27.56	18.94	4	3.779e-08	4.59	4.66	1.49	413	$\cdots$	0.21	V	19.04	SDSS-QSO(S)
07 45 35.436 +31 44 03.70	3.74	4.29	1.82 - 5.06	$\cdots$	3	6.097e-12	5.34	5.64	>2.78	500	BN	-2.72	V	19.09	SDSS-G
07 45 48.636 +38 18 23.77	1.33	1.17	<0.83 - 3.37	$\cdots$	3	1.995e-10	5.20	4.78	>4.07	1	BN	0.86	T	$\cdots$	$\cdots$
07 45 49.109 +55 34 16.23	122.97	121.80	118.44 - 164.61	109.65	4	2.511e-07	3.57	3.45	1.39	2	$\cdots$	-0.24	V	$\cdots$	$\cdots$
07 46 33.395 +19 30 10.85	41.66	39.47	38.95 - 54.26	43.59	5	4.419e-10	4.21	3.81	1.39	$\cdots$	$\cdots$	0.17	V	19.00	SDSS-QSO(S)
07 46 40.521 +32 45 03.12	15.42	15.41	10.44 - 18.14	15.91	6	7.560e-12	4.97	5.14	1.74	86	$\cdots$	0.98	V	22.07	SDSS-G
07 47 03.543 +30 13 02.41	4.20	4.60	2.97 - 5.32	$\cdots$	5	7.189e-12	6.35	5.50	1.79	10	$\cdots$	-0.59	V	$\cdots$	$\cdots$
07 47 50.715 +29 13 19.97	11.55	11.46	5.53 - 14.03	11.69	5	1.243e-14	7.58	7.07	2.54	5	$\cdots$	0.57	V	17.59	SDSS-G
07 47 54.818 +31 34 36.75	3.88	4.06	2.17 - <12.65	6.02	5	1.035e-12	4.40	5.02	>1.44	506	BN	0.74	V	$\cdots$	$\cdots$
07 48 34.783 +54 16 12.84	2.94	3.03	1.45 - <4.55	2.71	4	1.154e-09	5.69	6.18	2.63	440	$\cdots$	-0.83	V	$\cdots$	$\cdots$
07 49 13.013 +44 43 55.85	10.02	10.33	9.98 - 16.28	13.68	5	4.997e-06	5.13	4.88	1.61	2	$\cdots$	0.60	V	20.76	SDSS-QSO(P)
07 49 42.182 +57 20 52.15	2.18	2.08	<0.95 - <11.89	$\cdots$	4	1.275e-13	6.58	7.65	>3.23	24	$\cdots$	1.19	V	$\cdots$	$\cdots$
07 49 49.171 +27 31 47.70	3.92	3.93	2.56 - 4.55	$\cdots$	3	4.298e-07	4.87	4.99	1.78	1	BN	-1.00	V	21.30	SDSS-G
07 50 09.512 +37 14 03.87	23.83	23.41	21.60 - 43.21	22.75	4	1.505e-10	6.71	6.84	2.00	7	$\cdots$	-0.74	V	$\cdots$	$\cdots$
07 50 22.097 +33 18 34.60	8.40	9.42	5.34 - 10.62	8.23	3	5.734e-10	5.84	5.81	1.99	482	BN	-0.07	V	$\cdots$	$\cdots$
07 50 36.832 +15 57 48.94	1.97	1.60	<1.23 - 2.74	$\cdots$	2	6.986e-11	4.73	6.51	>2.23	7	BN	1.41	T	$\cdots$	$\cdots$
07 50 42.448 +60 00 07.64	11.24	11.28	5.93 - <19.64	4.02	4	0.000	9.31	7.21	1.89	407	$\cdots$	0.61	V	$\cdots$	GSC2-FIRST-G
07 52 01.489 +62 05 18.19	1.98	2.23	<1.85 - 3.31	2.62	3	1.096e-08	4.18	5.44	>1.67	50	$\cdots$	0.96	V	$\cdots$	$\cdots$
07 52 01.663 +54 46 14.16	12.07	12.34	11.92 - 20.04	$\cdots$	4	2.172e-10	5.16	5.04	1.68	436	$\cdots$	-1.75	V	$\cdots$	GSC2-FIRST-G
07 53 07.619 +48 34 29.74	1.27	1.39	0.96 - <4.58	$\cdots$	4	3.794e-07	4.37	5.08	2.66	3	$\cdots$	0.64	V	$\cdots$	$\cdots$
07 53 52.908 +24 33 31.37	1.52	1.48	1.20 - <12.57	$\cdots$	5	5.531e-07	5.02	5.29	>3.10	2	$\cdots$	1.11	V	$\cdots$	$\cdots$
07 53 54.957 +13 09 16.98	12.36	14.13	6.18 - 14.43	7.26	4	0.000	7.19	5.90	1.91	13	$\cdots$	-1.27	V	13.79	SDSS-G

Coordinates (J2000)	f (mJy)				N	Measures			$\frac{\text{Max.}}{\text{Min.}}$	$T_{\min}$	Flags	σ_{nbr}	Type	i	Cross-ID
	Cat.	$\overline{f}$	Range	NVSS		$P(\chi^2,\nu)$	$\sigma_{\max}$	$\Delta_{\max}(\sigma)$		(days)				Mag.	
07 53 59.130 +50 31 09.85	3.09	3.10	<2.33 - 3.92	2.37	3	2.241e-07	5.01	5.04	>1.44	1	$\cdots$	0.97	V	$\cdots$	$\cdots$
07 53 59.594 +36 14 50.52	12.08	12.19	11.17 - 18.24	8.79	4	1.023e-09	4.77	5.08	1.63	7	$\cdots$	0.57	V	$\cdots$	$\cdots$
07 54 29.982 +30 59 20.98	5.34	5.24	3.23 - 6.27	3.39	3	1.610e-14	7.50	6.20	1.94	417	$\cdots$	0.77	V	22.06	SDSS-*
07 55 12.999 +18 57 03.42	6.21	6.39	4.01 - 8.62	6.29	4	8.172e-10	5.00	4.64	1.59	$\cdots$	$\cdots$	-2.12	V	$\cdots$	$\cdots$
07 55 20.120 +15 52 39.60	33.12	30.74	29.61 - 43.76	33.79	4	3.966e-09	4.97	4.70	1.48	7	$\cdots$	0.99	V	21.56	SDSS-G
07 55 39.899 +18 23 54.46	1.70	1.63	<0.98 - 4.41	$\cdots$	3	2.953e-14	5.64	6.94	>4.50	$\cdots$	BN	1.20	V	$\cdots$	$\cdots$
07 55 49.265 +18 23 37.55	1.81	1.81	<1.30 - 2.98	$\cdots$	3	1.010e-09	4.87	6.02	>2.29	$\cdots$	BN	0.64	V	$\cdots$	$\cdots$
07 56 19.913 +31 26 45.98	2.00	1.81	0.85 - 2.56	$\cdots$	3	3.005e-08	5.35	4.74	2.46	97	$\cdots$	-0.24	V	$\cdots$	$\cdots$
07 56 58.140 +32 25 53.54	2.44	2.39	1.42 - 3.49	$\cdots$	4	1.915e-09	4.21	5.63	>2.45	2	$\cdots$	0.17	V	18.20	SDSS-G
07 57 05.526 +29 08 28.75	34.75	36.74	25.49 - 47.41	31.29	4	0.000	7.63	7.40	1.86	501	$\cdots$	-0.72	V	21.23	SDSS-*
07 57 21.733 +14 02 15.80	6.96	6.37	<4.41 - 6.60	4.39	4	4.195e-07	5.12	5.04	>1.50	13	$\cdots$	-1.01	V	22.00	SDSS-G
07 57 47.569 +32 34 07.93	1.21	1.14	<0.70 - <4.43	$\cdots$	5	2.102e-12	5.45	6.88	>3.05	1	$\cdots$	0.92	V	$\cdots$	$\cdots$
07 58 44.500 +37 25 45.86	5.94	6.45	3.02 - <13.67	3.66	5	5.868e-08	4.54	4.53	2.03	6	BN	1.17	V	21.85	SDSS-G
07 59 36.143 +13 21 17.92	3.85	3.78	2.73 - 7.50	4.36	3	0.000	7.21	8.16	2.69	13	$\cdots$	1.15	V	18.23	SDSS-QSO(P)
07 59 55.150 +57 56 51.04	1.19	1.16	<1.08 - 2.08	$\cdots$	3	4.798e-08	4.16	5.24	>1.93	0	$\cdots$	0.07	T	$\cdots$	$\cdots$
08 00 19.098 +18 35 56.80	1.83	1.98	1.26 - 3.17	2.31	3	1.995e-07	4.04	5.32	2.51	$\cdots$	$\cdots$	-1.34	V	18.27	SDSS-G
08 01 28.845 +54 55 11.77	29.40	28.53	24.35 - 48.77	30.75	3	0.000	7.31	8.06	2.00	428	$\cdots$	-0.07	V	20.87	SDSS-*
08 01 29.127 +22 26 11.45	6.38	6.51	4.80 - 8.48	7.55	4	2.807e-12	5.45	6.39	1.77	6	$\cdots$	-0.48	V	19.96	SDSS-G
08 01 59.352 +60 02 22.40	10.81	10.69	10.17 - 17.34	10.13	4	5.584e-07	5.36	5.32	1.71	409	$\cdots$	0.38	V	$\cdots$	GSC2-FIRST-G
08 02 53.983 +32 53 36.84	1.70	1.62	0.79 - 2.09	$\cdots$	5	1.007e-07	4.37	5.23	>2.64	85	$\cdots$	-0.78	V	19.50	SDSS-G
08 03 34.872 +15 52 03.19	1.68	1.68	<1.41 - <3.70	$\cdots$	4	1.444e-07	4.13	5.25	>1.68	5	BN	-0.63	V	21.64	SDSS-G
08 03 48.073 +36 18 30.80	1.81	1.75	1.06 - 3.52	2.70	3	3.740e-12	5.55	6.86	3.33	5	$\cdots$	-0.24	V	18.74	SDSS-G
08 03 53.207 +33 03 48.83	1.48	1.37	<0.59 - 3.29	$\cdots$	4	0.000	6.93	9.53	>5.54	84	$\cdots$	0.21	V	$\cdots$	$\cdots$
08 05 18.437 +32 55 59.74	1.34	1.33	1.03 - 2.09	$\cdots$	4	2.496e-07	4.02	5.29	>1.69	84	$\cdots$	-1.05	V	$\cdots$	$\cdots$
08 05 41.662 +42 54 55.17	2.41	2.26	1.89 - <13.01	$\cdots$	5	7.023e-08	4.08	4.69	>2.02	1	$\cdots$	-0.31	V	17.06	SDSS-G
08 06 23.978 +44 42 47.12	3.50	3.46	2.43 - 5.03	3.24	4	2.222e-08	4.46	5.65	1.86	1	$\cdots$	0.88	V	18.44	SDSS-G
08 06 54.163 +18 43 04.20	8.43	9.47	7.17 - 13.72	8.84	4	2.703e-08	3.60	4.56	1.91	$\cdots$	$\cdots$	-0.44	V	19.14	SDSS-G
08 07 06.323 +44 38 36.93	42.26	41.02	39.41 - 61.41	44.17	4	1.310e-07	4.78	4.67	1.56	2	$\cdots$	0.93	V	19.02	SDSS-G
08 07 16.093 +38 41 57.32	1.58	1.43	<1.13 - 2.36	$\cdots$	4	4.184e-10	4.02	5.51	>2.09	5	$\cdots$	0.14	T	$\cdots$	$\cdots$
08 07 24.886 +27 16 36.26	8.41	8.14	4.24 - 12.39	9.01	5	4.568e-08	5.12	4.75	2.92	4	$\cdots$	1.49	V	19.86	SDSS-QSO(P)
08 07 39.108 +28 20 58.41	4.71	4.77	3.98 - 7.67	5.07	4	1.119e-08	5.48	5.95	1.86	909	$\cdots$	-0.33	V	17.92	SDSS-G

Continued on next page...

Coordinates (J2000)	f (mJy)				N	Measures			$\frac{\text{Max.}}{\text{Min.}}$	$T_{\min}$	Flags	σ_{nbr}	Type	i	Cross-ID
	Cat.	$\overline{f}$	Range	NVSS		$P(\chi^2,\nu)$	$\sigma_{\max}$	$\Delta_{\max}(\sigma)$		(days)				Mag.	
08 07 39.335 +42 14 10.48	2.05	2.07	<1.53 - 3.14	$\cdots$	4	2.518e-11	5.23	6.33	>2.04	58	BN	0.69	V	$\cdots$	$\cdots$
08 07 56.402 +53 29 53.97	2.99	2.94	<2.22 - <6.61	$\cdots$	4	1.500e-07	4.76	5.59	>1.64	1	$\cdots$	1.19	V	16.05	SDSS-G
08 08 52.916 +15 59 31.39	3.01	3.09	<2.15 - 3.49	3.54	3	2.749e-07	5.22	5.27	>1.63	2	$\cdots$	0.66	V	$\cdots$	$\cdots$
08 08 53.793 +23 50 41.66	9.99	9.94	6.09 - 11.74	9.08	5	8.272e-07	5.65	4.67	1.65	3	$\cdots$	0.31	V	19.04	SDSS-G
08 08 55.470 +32 49 06.03	2.47	2.42	<0.45 - <11.24	$\cdots$	6	0.000	16.10	16.37	>12.58	1	$\cdots$	0.27	V	$\cdots$	2MASS-FIRST-G
08 09 17.574 +14 12 55.55	6.63	6.71	4.95 - 8.26	5.75	3	4.816e-08	4.79	5.37	1.67	527	$\cdots$	2.04	V	$\cdots$	$\cdots$
08 09 24.194 +12 50 47.00	2.15	2.44	1.32 - 3.79	$\cdots$	3	1.190e-13	4.69	6.58	>1.96	498	$\cdots$	-1.74	V	20.23	SDSS-G
08 09 35.259 +21 14 40.76	4.72	4.86	2.77 - <8.47	3.27	4	1.564e-09	4.50	5.74	2.26	4	$\cdots$	0.16	V	$\cdots$	$\cdots$
08 09 57.524 +19 48 04.89	3.48	3.57	2.09 - 4.52	$\cdots$	3	1.226e-08	5.06	5.64	2.17	$\cdots$	$\cdots$	1.08	V	$\cdots$	SDSS-UNKNOWN
08 10 07.178 +14 09 07.48	5.96	5.29	4.90 - 8.54	5.68	3	3.819e-09	5.08	5.26	1.74	527	$\cdots$	-3.25	V	$\cdots$	$\cdots$
08 10 58.043 +63 31 09.57	7.28	7.75	3.83 - 8.11	8.04	3	6.680e-07	5.10	4.84	2.12	3	$\cdots$	-1.71	V	$\cdots$	$\cdots$
08 11 23.871 +32 44 12.13	6.05	6.10	4.07 - 8.83	5.86	4	6.295e-14	6.72	5.80	1.84	84	BN	0.63	V	18.55	SDSS-QSO(S)
08 11 33.408 +63 31 59.81	4.75	4.89	2.37 - <13.35	3.72	5	5.038e-08	5.38	5.04	2.18	0	$\cdots$	-2.27	V	$\cdots$	GSC2-FIRST-G
08 11 45.908 +33 52 02.51	1.36	1.33	<1.26 - <4.39	$\cdots$	4	3.927e-07	3.61	4.81	>1.71	6	$\cdots$	-0.20	V	$\cdots$	$\cdots$
08 11 59.473 +35 28 04.40	4.98	5.12	2.85 - 5.81	$\cdots$	4	1.110e-16	7.14	7.15	>1.91	1	$\cdots$	-0.77	V	17.97	SDSS-G
08 12 07.242 +31 36 25.70	3.90	3.99	1.84 - <23.77	2.76	6	4.936e-07	5.30	5.11	2.30	409	$\cdots$	0.49	V	21.90	SDSS-G
08 12 24.071 +33 04 51.15	1.29	1.26	0.64 - <5.39	$\cdots$	4	1.540e-07	4.00	5.53	3.37	403	BN	-0.81	V	$\cdots$	$\cdots$
08 12 30.297 +19 42 15.78	5.95	6.01	5.31 - 9.73	6.36	3	5.409e-11	4.79	5.35	1.67	$\cdots$	$\cdots$	0.26	V	20.80	SDSS-G
08 13 17.953 +07 21 53.46	1.35	1.17	<0.96 - 2.44	$\cdots$	3	3.867e-09	4.62	6.10	>2.56	4	$\cdots$	0.00	V	20.16	SDSS-G
08 13 22.152 +37 06 19.66	4.21	4.34	2.96 - 5.96	$\cdots$	4	8.204e-08	4.04	5.30	1.96	2	$\cdots$	1.06	V	15.91	SDSS-G
08 13 46.595 +07 22 53.13	6.20	6.56	4.93 - 7.83	$\cdots$	3	1.312e-07	4.71	4.61	1.53	4	$\cdots$	0.41	V	20.68	SDSS-G
08 14 28.290 +13 26 56.78	13.73	14.13	8.04 - 16.91	13.31	4	6.124e-10	6.41	5.37	1.85	488	$\cdots$	0.20	V	$\cdots$	$\cdots$
08 14 34.677 +63 08 32.20	9.27	9.14	6.83 - 14.62	11.29	4	3.895e-09	5.88	5.98	1.73	5	$\cdots$	0.63	V	$\cdots$	$\cdots$
08 15 04.431 +38 01 37.94	27.79	27.64	21.61 - 37.34	34.10	5	4.422e-09	4.35	4.26	1.42	5	$\cdots$	-0.72	V	19.07	SDSS-G
08 15 23.194 +62 46 20.04	6.56	6.83	3.12 - 6.99	6.58	3	1.543e-07	5.43	4.99	2.24	2	$\cdots$	-1.36	V	$\cdots$	$\cdots$
08 16 07.993 +62 02 19.73	2.44	2.29	1.62 - <6.44	2.16	4	4.097e-07	3.43	4.48	>1.84	22	$\cdots$	0.74	V	$\cdots$	$\cdots$
08 16 27.228 +21 54 09.90	8.61	8.50	7.35 - 16.84	6.24	5	6.661e-16	8.07	8.59	>2.29	951	$\cdots$	0.42	V	$\cdots$	$\cdots$
08 16 27.394 +31 14 18.63	5.39	5.47	3.27 - 7.32	$\cdots$	4	0.000	5.87	6.85	2.24	411	$\cdots$	-0.85	V	21.52	SDSS-*
08 16 31.190 +03 33 53.43	2.65	2.48	<1.66 - <6.14	$\cdots$	4	1.654e-07	5.04	5.17	>1.65	5	$\cdots$	0.50	V	$\cdots$	$\cdots$
08 17 16.628 +17 52 47.76	1.82	1.80	<1.57 - <4.11	$\cdots$	4	4.566e-07	3.92	5.04	>1.54	$\cdots$	$\cdots$	-0.88	V	$\cdots$	$\cdots$
08 17 56.457 +45 31 18.02	14.38	14.55	11.17 - 20.83	12.95	5	1.333e-07	4.77	4.59	1.49	9	$\cdots$	0.66	V	18.19	SDSS-QSO(S)

Coordinates (J2000)	f (mJy)				N	Measures			$\frac{\text{Max.}}{\text{Min.}}$	$T_{\min}$	Flags	σ_{nbr}	Type	i	Cross-ID
	Cat.	$\overline{f}$	Range	NVSS		$P(\chi^2,\nu)$	$\sigma_{\max}$	$\Delta_{\max}(\sigma)$		(days)				Mag.	
08 18 58.235 +35 08 31.56	4.20	4.25	2.59 - 5.08	2.83	3	1.288e-10	6.07	5.80	1.92	1	$\cdots$	-0.01	V	$\cdots$	$\cdots$
08 19 18.157 +18 07 56.01	6.48	6.37	2.78 - 6.56	7.02	3	9.485e-10	5.92	5.42	2.36	$\cdots$	BN	0.58	V	$\cdots$	$\cdots$
08 19 29.566 +22 52 35.50	4.34	4.41	<3.22 - 5.31	$\cdots$	4	1.917e-06	5.05	5.08	>1.52	4	BN	0.39	V	$\cdots$	$\cdots$
08 19 41.689 +52 02 49.99	5.43	5.65	5.36 - 9.60	6.87	3	1.006e-08	4.35	4.42	1.68	2	$\cdots$	1.38	V	$\cdots$	$\cdots$
08 19 52.791 +56 03 45.87	3.92	4.07	2.06 - <6.78	$\cdots$	4	7.434e-13	6.55	7.01	2.57	418	$\cdots$	0.04	V	$\cdots$	$\cdots$
08 20 00.807 +12 57 24.82	2.61	2.59	2.37 - 7.00	$\cdots$	4	6.012e-06	5.09	5.12	2.84	486	$\cdots$	0.45	V	20.81	SDSS-*
08 21 07.610 +34 28 26.56	16.62	16.38	11.86 - 17.41	14.67	4	4.677e-10	6.27	4.80	1.46	5	$\cdots$	0.50	V	21.93	SDSS-G
08 21 13.901 +56 44 18.11	3.21	3.43	3.22 - 7.36	$\cdots$	4	3.331e-08	4.03	4.16	2.15	0	$\cdots$	1.17	V	$\cdots$	$\cdots$
08 21 17.714 +29 48 41.71	4.74	5.38	2.03 - 5.55	4.57	3	5.200e-07	5.35	5.06	2.74	0	$\cdots$	-0.36	V	$\cdots$	$\cdots$
08 21 53.842 +29 47 10.77	2.10	2.24	<1.77 - 3.14	$\cdots$	3	1.110e-07	4.37	5.62	>1.77	0	$\cdots$	-1.01	V	$\cdots$	$\cdots$
08 21 56.230 +59 20 13.17	3.49	3.34	<2.32 - <4.51	$\cdots$	4	1.838e-08	5.31	5.54	>1.64	4	$\cdots$	-0.04	V	18.60	SDSS-*
08 22 02.040 +33 00 44.71	21.90	21.86	17.41 - 27.64	22.36	4	6.926e-09	4.59	5.82	1.59	403	$\cdots$	-0.29	V	19.50	SDSS-G
08 22 31.855 +21 11 11.22	5.03	5.01	3.27 - <12.14	3.82	5	3.359e-09	5.37	5.38	>1.61	33	$\cdots$	0.60	V	20.44	SDSS-QSO(P)
08 23 14.031 +28 29 10.61	1.41	1.46	0.74 - <2.53	$\cdots$	3	3.329e-10	4.69	6.01	3.40	901	$\cdots$	-0.62	V	21.42	SDSS-G
08 23 18.627 +47 15 07.02	10.46	10.25	9.04 - 15.20	8.97	4	8.236e-09	5.13	5.73	1.61	5	$\cdots$	0.38	V	22.50	SDSS-*
08 23 34.880 +08 52 29.59	1.22	0.91	<0.68 - 3.17	$\cdots$	3	9.870e-14	6.48	7.70	>4.65	3	$\cdots$	0.56	T	$\cdots$	$\cdots$
08 25 00.670 +03 40 15.13	3.81	3.84	1.48 - 4.17	$\cdots$	3	1.300e-09	5.83	5.70	2.82	1	$\cdots$	0.43	V	$\cdots$	$\cdots$
08 25 06.185 +03 10 55.93	3.08	2.95	<1.65 - 3.39	$\cdots$	4	6.696e-13	6.37	6.02	>2.05	7	BN	0.41	T	$\cdots$	$\cdots$
08 25 22.830 +02 53 16.89	4.78	4.92	<2.78 - <12.38	$\cdots$	4	1.422e-11	5.92	5.89	>1.88	3	BN	-4.13	V	19.96	SDSS-G
08 26 08.035 +01 41 49.15	1.73	1.77	<1.62 - 2.81	$\cdots$	3	5.104e-08	3.89	5.26	>1.74	0	$\cdots$	-0.05	T	19.48	SDSS-G
08 26 22.015 +02 16 14.92	2.10	1.94	0.86 - <3.22	2.19	4	3.018e-07	4.64	5.27	2.95	3	$\cdots$	-0.06	V	18.90	SDSS-G
08 26 26.017 +31 32 01.17	2.24	2.18	<1.31 - 2.83	$\cdots$	3	1.049e-10	6.02	6.46	>2.16	96	$\cdots$	-1.39	V	$\cdots$	$\cdots$
08 26 27.424 +18 02 37.95	6.89	7.25	2.75 - 7.71	5.73	4	2.932e-08	5.89	5.59	2.77	$\cdots$	$\cdots$	0.74	V	$\cdots$	$\cdots$
08 26 37.615 +31 29 42.92	22.19	22.65	16.63 - 25.14	19.60	3	1.728e-11	6.69	5.29	1.51	505	$\cdots$	-0.76	V	$\cdots$	$\cdots$
08 26 51.438 +26 37 22.83	11.14	10.49	<1.28 - <14.49	16.07	6	0.000	24.63	16.08	>9.12	2	$\cdots$	0.57	V	$\cdots$	PSR
08 27 49.182 +33 15 40.22	4.57	4.54	2.75 - 6.44	$\cdots$	4	0.000	8.15	8.40	2.35	483	$\cdots$	0.02	V	20.27	SDSS-G
08 27 54.225 +13 39 36.35	3.82	3.94	<2.63 - <4.53	$\cdots$	4	1.371e-07	5.01	5.28	>1.68	8	$\cdots$	0.79	V	$\cdots$	$\cdots$
08 28 27.806 +08 58 07.85	10.29	10.93	<7.77 - 14.35	10.32	5	4.691e-12	5.34	5.40	>1.85	0	$\cdots$	-0.78	V	$\cdots$	$\cdots$
08 28 46.608 +01 29 27.80	7.18	7.74	<4.95 - 7.88	4.28	3	3.381e-09	6.20	5.75	>1.59	0	$\cdots$	0.13	V	$\cdots$	$\cdots$
08 28 49.352 +29 39 50.89	12.35	12.15	7.35 - 13.24	7.41	4	1.337e-09	5.69	4.61	1.48	0	$\cdots$	0.02	V	$\cdots$	$\cdots$
08 29 33.051 +56 13 05.04	8.23	8.65	5.76 - <14.86	8.74	4	2.460e-08	5.76	4.67	1.58	418	$\cdots$	1.25	V	17.59	SDSS-G

Coordinates (J2000)	f (mJy)				N	Measures			$\frac{\text{Max.}}{\text{Min.}}$	$T_{\min}$	Flags	σ_{nbr}	Type	i	Cross-ID
	Cat.	$\overline{f}$	Range	NVSS		$P(\chi^2,\nu)$	$\sigma_{\max}$	$\Delta_{\max}(\sigma)$		(days)				Mag.	
08 29 40.204 +56 04 05.31	14.05	13.35	7.98 - 17.56	11.85	4	8.736e-09	4.14	5.05	2.20	418	$\cdots$	-1.53	V	$\cdots$	$\cdots$
08 29 43.733 +30 57 04.41	2.47	2.85	1.54 - 3.60	$\cdots$	4	1.213e-08	5.01	5.34	2.34	414	$\cdots$	-1.32	V	21.28	SDSS-*
08 31 42.676 +31 23 46.03	4.73	4.20	1.88 - <14.30	3.82	5	2.165e-14	6.54	6.01	>2.40	96	$\cdots$	-4.90	V	$\cdots$	$\cdots$
08 31 52.460 +38 06 29.12	3.14	2.97	<2.83 - 4.47	$\cdots$	4	5.265e-09	4.93	5.07	>1.58	5	BN	0.65	V	$\cdots$	$\cdots$
08 32 09.836 +31 24 26.43	3.02	2.82	1.53 - 4.31	$\cdots$	3	2.027e-13	7.03	6.26	2.14	96	$\cdots$	-3.65	V	$\cdots$	$\cdots$
08 32 17.355 +29 19 09.63	5.39	5.32	2.35 - 6.13	$\cdots$	3	0.000	9.36	8.08	2.61	11	$\cdots$	1.99	V	10.24	HIP-STAR
08 32 59.169 +19 52 55.47	33.71	32.63	29.61 - 48.18	34.16	4	1.898e-14	5.42	5.75	1.63	$\cdots$	$\cdots$	0.61	V	$\cdots$	$\cdots$
08 33 16.600 +48 59 23.90	1.40	1.32	<1.06 - 3.22	$\cdots$	3	4.457e-07	4.07	4.83	>3.03	0	$\cdots$	1.46	V	19.28	SDSS-G
08 33 45.370 +13 47 34.15	2.34	2.36	1.98 - 4.85	$\cdots$	3	4.356e-07	5.11	5.16	2.30	5	$\cdots$	1.64	V	$\cdots$	$\cdots$
08 33 58.883 +31 29 05.16	3.46	3.60	1.28 - 5.20	2.34	3	2.670e-12	6.56	6.39	4.05	505	$\cdots$	-0.25	V	$\cdots$	$\cdots$
08 36 11.565 +08 56 26.67	1.60	1.78	1.36 - 2.95	$\cdots$	3	1.071e-08	4.32	5.45	>2.10	2	$\cdots$	0.52	V	17.48	SDSS-G
08 37 07.874 +45 02 14.39	3.92	4.22	2.48 - 4.59	$\cdots$	4	3.688e-06	5.12	4.58	1.86	24	$\cdots$	-0.11	V	19.25	SDSS-G
08 37 15.018 +32 36 10.07	5.34	5.98	3.41 - <16.32	5.45	6	2.982e-06	5.05	4.83	1.88	2	$\cdots$	1.12	V	18.44	SDSS-G
08 37 41.583 +45 05 15.75	5.37	5.42	3.27 - 6.65	3.77	4	1.047e-07	3.59	4.36	2.03	26	$\cdots$	-1.16	V	19.01	SDSS-G
08 37 47.655 +07 21 49.30	3.01	2.80	1.12 - 3.67	$\cdots$	3	2.144e-13	6.80	7.14	3.29	4	$\cdots$	-0.35	V	$\cdots$	$\cdots$
08 38 28.059 +39 07 53.36	3.62	3.54	<2.45 - 5.21	4.05	3	7.103e-09	5.26	5.86	>2.13	2	$\cdots$	0.35	V	$\cdots$	$\cdots$
08 38 56.404 +32 06 46.01	23.63	23.57	11.43 - 30.36	25.11	5	5.647e-08	4.85	5.78	2.58	2	$\cdots$	-0.40	V	20.39	SDSS-G
08 39 00.601 +02 10 26.50	38.41	35.97	35.68 - 50.76	39.69	5	5.840e-09	3.94	3.63	1.42	0	$\cdots$	1.61	V	21.39	SDSS-G
08 39 24.939 +45 08 09.94	5.70	4.94	4.34 - 8.73	5.17	3	1.094e-08	4.24	4.75	2.01	6	$\cdots$	-1.20	V	18.12	SDSS-G
08 39 51.010 +02 23 01.15	2.02	1.92	1.47 - 4.35	$\cdots$	3	4.068e-09	5.65	6.21	2.97	0	$\cdots$	0.31	V	18.07	SDSS-G
08 40 13.004 +19 28 03.89	2.95	2.82	<2.03 - <3.44	2.33	3	5.205e-07	4.93	4.89	>1.48	$\cdots$	$\cdots$	-0.04	V	20.89	SDSS-G
08 40 35.193 +28 32 52.10	4.80	4.57	2.59 - <13.27	4.36	6	3.829e-09	4.79	4.88	>1.56	909	$\cdots$	0.62	V	18.91	SDSS-G
08 40 38.474 +33 01 09.65	2.12	2.06	1.56 - <13.73	$\cdots$	7	1.118e-10	3.81	4.63	>2.48	487	$\cdots$	1.40	V	$\cdots$	$\cdots$
08 40 56.049 +37 21 05.65	17.75	18.29	17.06 - 29.93	19.91	4	1.980e-13	6.58	6.54	1.75	6	$\cdots$	-0.20	V	18.74	SDSS-QSO(S)
08 41 21.541 +53 30 22.80	4.83	5.09	3.55 - <9.80	$\cdots$	4	2.416e-07	4.27	5.43	1.79	1	$\cdots$	1.59	V	$\cdots$	$\cdots$
08 41 25.455 +51 55 39.60	57.89	52.12	50.77 - 94.97	60.22	4	1.822e-09	6.12	5.92	1.87	3	$\cdots$	0.34	V	$\cdots$	$\cdots$
08 41 54.987 +53 35 25.59	8.72	8.67	7.99 - 13.89	12.56	3	1.984e-09	5.79	5.87	1.74	1	$\cdots$	0.19	V	$\cdots$	$\cdots$
08 42 01.718 +62 49 39.60	4.16	4.41	2.71 - 5.25	$\cdots$	4	9.829e-08	4.51	4.83	1.73	2	$\cdots$	0.39	V	$\cdots$	$\cdots$
08 42 06.031 +26 24 36.67	14.40	13.12	12.21 - 20.18	16.10	5	4.707e-08	3.72	3.95	1.40	6	$\cdots$	0.47	V	$\cdots$	$\cdots$
08 42 20.903 +21 12 55.58	2.14	2.01	<1.81 - <11.03	$\cdots$	4	3.488e-07	3.56	4.24	>1.37	0	$\cdots$	-0.58	V	21.23	SDSS-G
08 43 04.281 +53 32 28.32	2.49	2.44	<2.06 - <9.12	$\cdots$	4	3.377e-09	4.20	5.85	>1.69	1	$\cdots$	3.46	V	$\cdots$	$\cdots$

Coordinates (J2000)	f (mJy)				N	Measures			$\frac{\text{Max.}}{\text{Min.}}$	$T_{\min}$	Flags	σ_{nbr}	Type	i	Cross-ID
	Cat.	$\overline{f}$	Range	NVSS		$P(\chi^2,\nu)$	$\sigma_{\max}$	$\Delta_{\max}(\sigma)$		(days)				Mag.	
08 43 34.131 -02 59 55.83	2.90	2.76	2.51 - 6.40	3.36	3	1.409e-06	5.07	5.16	2.55	1	$\cdots$	0.35	V	15.66	SDSS-G
08 43 47.029 +54 03 30.57	13.79	14.23	<8.63 - 16.69	12.73	5	5.538e-06	5.17	5.01	>1.81	5	$\cdots$	0.33	V	$\cdots$	$\cdots$
08 45 38.357 +06 17 42.09	1.39	1.58	1.19 - 2.34	$\cdots$	3	2.408e-07	4.45	5.31	>1.94	2	$\cdots$	-0.37	V	$\cdots$	$\cdots$
08 45 43.923 +30 58 23.91	6.02	6.03	2.84 - 6.46	4.41	3	0.000	10.07	7.53	2.27	411	$\cdots$	-0.06	V	$\cdots$	$\cdots$
08 46 55.334 +00 15 40.26	4.97	4.70	2.73 - 8.10	4.88	3	1.060e-08	4.72	5.43	2.97	2	$\cdots$	0.61	V	$\cdots$	$\cdots$
08 48 04.171 -01 48 03.11	4.93	4.94	<3.41 - <11.06	5.84	4	2.314e-06	5.03	4.86	>1.48	1	$\cdots$	0.21	V	$\cdots$	$\cdots$
08 48 33.065 +05 48 47.03	6.17	6.37	3.78 - 7.49	4.89	3	2.986e-14	7.42	6.65	1.98	1	$\cdots$	-1.89	V	$\cdots$	$\cdots$
08 49 04.900 +06 12 29.43	6.75	6.98	4.19 - 7.46	$\cdots$	4	2.869e-08	4.76	4.25	1.48	2	$\cdots$	-1.36	V	$\cdots$	$\cdots$
08 49 07.639 +51 16 50.10	176.22	178.25	132.48 - 242.39	182.18	5	1.349e-10	4.52	6.00	1.83	0	$\cdots$	0.31	V	20.11	SDSS-G
08 49 11.700 +58 31 32.05	1.61	1.52	0.79 - 4.67	$\cdots$	5	3.102e-07	4.78	5.57	5.89	54	$\cdots$	0.46	V	$\cdots$	$\cdots$
08 49 47.230 +15 11 41.97	54.64	49.39	46.41 - 64.72	55.58	4	4.063e-07	4.25	4.26	1.39	22	BN	0.37	V	18.92	SDSS-G
08 51 27.869 +63 55 07.20	4.43	4.66	3.04 - 6.82	3.62	4	3.153e-13	5.86	6.62	2.24	4	$\cdots$	-0.87	V	$\cdots$	$\cdots$
08 52 03.311 +36 55 10.40	1.46	1.36	<0.84 - 3.48	$\cdots$	3	6.252e-08	4.89	4.85	>1.86	1	$\cdots$	0.80	V	$\cdots$	$\cdots$
08 52 42.448 +63 54 55.25	5.97	6.35	4.17 - 7.24	4.72	3	2.160e-08	5.64	4.87	1.62	4	$\cdots$	-0.74	V	$\cdots$	$\cdots$
08 52 59.846 -01 22 40.33	1.10	1.19	<0.88 - <6.16	$\cdots$	4	3.229e-08	4.33	5.13	>2.10	0	$\cdots$	0.60	V	$\cdots$	$\cdots$
08 53 41.818 +33 50 37.27	4.32	4.50	2.15 - 5.47	$\cdots$	4	3.722e-09	5.50	6.02	2.54	6	BN	-0.72	V	16.25	SDSS-G
08 54 09.954 -03 13 56.66	1.81	1.56	<1.03 - <2.65	$\cdots$	3	1.037e-11	5.64	6.62	>2.33	4	BN	-0.30	V	$\cdots$	$\cdots$
08 54 18.962 +20 03 46.61	16.10	14.75	<8.63 - 16.22	12.87	4	7.204e-08	5.74	5.88	>1.88	$\cdots$	BN	0.82	V	$\cdots$	$\cdots$
08 55 05.610 +51 38 06.72	2.75	3.06	1.22 - 3.56	2.29	4	3.519e-08	5.21	5.33	2.93	2	$\cdots$	-0.23	V	15.77	SDSS-G
08 55 46.809 +20 41 45.88	3.43	3.73	1.20 - 4.38	$\cdots$	3	3.952e-14	7.51	7.20	3.64	8	$\cdots$	-0.55	V	$\cdots$	$\cdots$
08 55 56.173 +37 13 42.49	13.32	11.93	10.26 - 16.31	48.98	4	6.329e-08	4.01	4.95	1.50	1	$\cdots$	0.33	V	19.10	SDSS-QSO(P)
08 56 06.097 +31 39 43.95	5.31	5.21	3.67 - 7.45	3.41	3	1.332e-15	6.09	7.69	2.03	409	$\cdots$	0.45	V	20.95	SDSS-*
08 56 09.089 +24 05 55.68	10.69	10.66	9.11 - 15.98	15.19	4	1.967e-09	4.37	5.40	1.54	1	$\cdots$	1.56	V	19.91	SDSS-QSO(S)
08 56 17.366 +27 36 51.04	8.87	8.64	<5.77 - 9.36	8.58	4	8.016e-08	5.92	5.48	>1.52	508	BN	0.29	V	$\cdots$	$\cdots$
08 56 41.565 +42 42 53.95	20.09	20.16	19.04 - 28.34	19.39	4	5.877e-08	4.51	4.53	1.49	478	$\cdots$	0.61	V	18.41	SDSS-QSO(S)
08 57 19.691 +46 28 41.91	2.18	2.15	1.35 - 3.60	$\cdots$	4	3.883e-08	4.42	5.92	2.67	1	$\cdots$	1.07	V	17.88	SDSS-G
08 57 28.539 +09 54 42.64	1.53	1.53	<0.97 - 4.70	$\cdots$	4	1.070e-07	4.78	5.07	>1.88	1	$\cdots$	0.94	V	16.56	SDSS-G
08 58 34.966 +15 07 20.14	64.44	61.63	60.91 - 94.10	67.30	5	8.564e-11	4.54	4.27	1.54	1	$\cdots$	0.15	V	$\cdots$	$\cdots$
08 58 56.411 +08 28 25.69	1.17	1.19	0.97 - 4.07	$\cdots$	3	6.140e-07	5.15	5.35	4.21	1	$\cdots$	0.24	V	12.49	SDSS-G
08 59 06.361 -02 38 38.07	1.27	1.24	1.17 - 3.25	$\cdots$	3	2.381e-07	4.67	5.50	>2.59	2	$\cdots$	0.02	V	$\cdots$	$\cdots$
08 59 53.602 +33 36 53.57	8.36	8.55	<4.51 - 13.58	8.46	5	5.006e-09	5.88	5.97	>2.22	2	$\cdots$	-0.64	V	$\cdots$	$\cdots$

Coordinates (J2000)	f (mJy)				N	Measures			$\frac{\text{Max.}}{\text{Min.}}$	$T_{\min}$	Flags	σ_{nbr}	Type	i	Cross-ID
	Cat.	$\overline{f}$	Range	NVSS		$P(\chi^2,\nu)$	$\sigma_{\max}$	$\Delta_{\max}(\sigma)$		(days)				Mag.	
09 00 31.304 +51 52 29.34	9.98	9.79	6.40 - 12.08	8.34	4	5.481e-07	3.52	4.38	1.42	3	$\cdots$	-2.57	V	$\cdots$	$\cdots$
09 02 02.545 +29 15 04.54	6.71	6.75	5.62 - 11.57	9.87	4	1.629e-08	5.22	5.89	2.06	21	BN	-0.23	V	$\cdots$	$\cdots$
09 02 05.164 -05 31 03.40	4.69	5.08	<3.26 - 5.29	4.98	4	4.663e-07	5.63	5.38	>1.62	7	BN	-3.55	V	$\cdots$	$\cdots$
09 02 09.038 -05 25 05.96	6.36	6.97	2.39 - 7.99	7.13	3	0.000	12.99	10.01	3.34	7	BN	-0.78	V	$\cdots$	GSC2-FIRST-G
09 02 46.666 +13 54 07.34	21.27	20.39	19.80 - 29.89	18.61	4	2.005e-09	4.47	4.22	1.44	4	$\cdots$	NA	V	$\cdots$	$\cdots$
09 03 12.180 +42 15 51.18	8.09	7.81	4.73 - 9.02	7.10	5	8.680e-08	5.06	4.91	>1.39	52	BN	-0.30	V	$\cdots$	$\cdots$
09 04 26.880 +32 52 49.91	50.07	51.49	49.65 - 76.45	46.65	7	2.433e-12	5.08	4.87	1.54	487	$\cdots$	0.29	V	19.98	SDSS-QSO(P)
09 04 27.294 +41 26 23.28	6.11	6.45	3.17 - 8.39	$\cdots$	5	1.454e-08	4.90	4.57	>2.09	1	$\cdots$	-1.32	V	$\cdots$	$\cdots$
09 04 42.502 +25 15 37.99	13.31	13.65	12.40 - 19.15	8.30	4	8.829e-09	4.95	5.27	1.54	7	$\cdots$	0.31	V	21.12	SDSS-G
09 04 50.511 +50 10 04.73	2.57	2.74	1.50 - 3.22	$\cdots$	3	8.543e-08	3.98	4.32	>2.15	26	BN	-0.58	V	$\cdots$	$\cdots$
09 05 43.564 +21 30 41.56	6.22	6.43	3.54 - 6.66	4.64	3	1.150e-07	4.63	4.36	1.88	5	$\cdots$	-0.51	V	$\cdots$	$\cdots$
09 06 08.324 +42 41 48.04	7.63	7.86	4.13 - 9.61	5.40	3	6.184e-09	5.56	5.79	2.33	0	BN	-0.86	V	$\cdots$	$\cdots$
09 06 20.782 +57 33 20.82	29.28	26.68	25.13 - 43.52	32.43	4	0.000	6.55	6.41	1.72	1396	$\cdots$	-0.45	V	$\cdots$	$\cdots$
09 06 43.513 +58 00 06.34	2.23	2.16	<1.38 - <4.53	2.18	4	3.533e-10	5.59	5.51	>2.82	7	$\cdots$	0.45	V	$\cdots$	$\cdots$
09 07 16.271 +43 00 58.63	9.03	8.57	6.69 - <16.78	5.89	6	1.693e-07	4.73	5.63	1.57	2504	BN	-0.44	V	$\cdots$	$\cdots$
09 07 43.191 +06 36 03.34	1.26	1.23	0.83 - <10.24	$\cdots$	4	1.859e-07	4.57	5.05	4.53	1	$\cdots$	1.39	V	17.04	SDSS-G
09 08 06.174 +36 30 32.04	1.18	1.16	<0.99 - <2.84	$\cdots$	3	1.214e-07	3.79	5.29	>1.98	2	$\cdots$	0.12	V	$\cdots$	$\cdots$
09 08 53.489 +62 33 59.50	2.08	2.09	1.48 - 3.13	$\cdots$	4	2.746e-07	3.72	4.60	>2.11	2	$\cdots$	-0.39	V	$\cdots$	$\cdots$
09 08 57.964 +32 50 58.73	5.51	6.29	3.09 - 6.75	2.54	4	3.843e-12	7.18	6.42	2.19	484	$\cdots$	0.08	V	22.49	SDSS-G
09 09 02.498 +18 10 27.71	5.58	5.96	2.42 - 6.76	4.13	4	6.247e-09	6.24	5.74	2.62	28	$\cdots$	0.53	V	23.26	SDSS-*
09 09 09.844 +30 58 04.42	1.41	1.48	<0.99 - <2.72	$\cdots$	4	3.691e-10	5.64	5.59	>2.16	414	$\cdots$	0.92	V	$\cdots$	$\cdots$
09 09 17.084 +00 08 23.98	3.27	2.84	1.94 - <13.75	3.27	4	3.613e-08	4.84	5.35	>1.63	2	$\cdots$	0.81	V	20.16	SDSS-QSO(S)
09 09 18.918 +59 31 55.34	2.39	2.28	1.49 - 4.34	$\cdots$	3	3.434e-11	4.79	5.56	2.45	4	$\cdots$	0.42	V	$\cdots$	$\cdots$
09 10 02.498 -00 02 25.46	3.49	3.45	1.61 - 3.95	3.64	3	2.168e-07	5.03	5.07	2.45	2	$\cdots$	1.10	V	21.08	SDSS-*
09 10 24.346 -07 02 43.08	2.49	2.51	<1.24 - <15.56	$\cdots$	3	3.494e-10	6.05	6.18	>2.27	4	BN	0.06	V	$\cdots$	$\cdots$
09 10 43.693 +31 11 56.96	3.01	3.26	2.50 - 3.99	2.52	4	2.126e-07	3.65	4.43	>1.35	411	$\cdots$	-0.98	V	20.87	SDSS-G
09 11 29.799 -04 04 00.41	23.80	21.94	10.27 - 24.33	19.04	4	2.825e-07	5.35	5.44	2.37	934	$\cdots$	-0.34	V	$\cdots$	$\cdots$
09 11 37.434 +01 26 30.24	2.53	2.56	<1.72 - <7.15	2.90	4	1.592e-12	5.65	6.43	>1.91	1	$\cdots$	-2.58	V	22.50	SDSS-*
09 12 02.856 +33 38 18.02	8.13	8.00	4.49 - 8.21	6.72	5	3.219e-09	5.07	4.98	>1.55	1	$\cdots$	0.96	V	$\cdots$	$\cdots$
09 12 19.600 +58 01 45.08	6.59	7.18	4.51 - <9.28	$\cdots$	4	1.040e-10	5.01	6.07	1.99	7	$\cdots$	0.80	V	$\cdots$	$\cdots$
09 12 19.871 +12 39 03.24	3.97	4.11	<2.82 - 4.27	3.76	3	9.046e-07	5.19	5.02	>1.51	3	$\cdots$	-0.45	V	$\cdots$	$\cdots$

Continued on next page. . .

Coordinates (J2000)	f (mJy)				N	Measures			$\frac{\text{Max.}}{\text{Min.}}$	$T_{\min}$	Flags	σ_{nbr}	Type	i	Cross-ID
	Cat.	$\overline{f}$	Range	NVSS		$P(\chi^2,\nu)$	$\sigma_{\max}$	$\Delta_{\max}(\sigma)$		(days)				Mag.	
09 12 44.337 +08 54 07.76	3.30	3.43	<2.64 - 4.10	3.25	3	1.647e-07	4.79	5.40	>1.55	0	$\cdots$	0.11	V	17.95	SDSS-G
09 13 02.014 +04 26 24.05	1.39	1.33	<0.84 - <5.33	$\cdots$	4	9.244e-08	4.73	4.71	>2.18	380	$\cdots$	-0.04	V	$\cdots$	$\cdots$
09 14 09.650 +42 14 51.13	1.32	1.13	<0.91 - <1.64	$\cdots$	3	3.338e-07	3.90	4.98	>1.73	58	$\cdots$	-0.05	V	$\cdots$	$\cdots$
09 14 11.609 -06 16 26.88	2.11	2.13	1.21 - 2.70	$\cdots$	3	1.325e-08	4.25	4.99	>1.66	4	$\cdots$	-0.41	V	$\cdots$	GSC2-FIRST-G
09 15 05.142 -05 04 07.72	5.35	5.35	<2.07 - 6.39	$\cdots$	3	0.000	12.93	11.00	>3.08	6	$\cdots$	0.37	T	$\cdots$	$\cdots$
09 17 35.922 -05 21 00.69	1.72	1.43	0.88 - <6.84	$\cdots$	4	6.409e-08	4.22	5.19	3.26	7	$\cdots$	0.82	V	$\cdots$	$\cdots$
09 17 39.254 -07 30 25.33	4.85	4.53	1.96 - <9.81	$\cdots$	4	7.632e-08	5.52	5.14	2.40	459	$\cdots$	-0.78	V	$\cdots$	$\cdots$
09 17 48.900 +01 52 27.49	1.89	1.83	<1.10 - <10.62	$\cdots$	4	3.856e-07	5.01	5.18	>1.93	3	$\cdots$	0.20	V	20.79	SDSS-G
09 18 33.442 +56 51 17.09	8.75	9.14	6.73 - 10.26	7.16	4	3.624e-10	5.54	5.02	1.52	21	$\cdots$	-1.14	V	20.51	SDSS-*
09 19 15.502 +22 30 58.27	3.37	3.46	<2.51 - <14.19	$\cdots$	4	3.288e-07	5.04	5.38	>1.57	4	BN	1.15	V	$\cdots$	$\cdots$
09 19 15.612 -05 57 09.09	5.58	5.62	2.61 - 8.63	5.41	4	2.031e-08	5.66	5.21	2.63	2	$\cdots$	0.47	V	$\cdots$	$\cdots$
09 19 16.461 +22 21 30.20	3.59	3.55	<2.34 - <16.17	2.72	4	5.202e-08	5.52	5.71	>1.70	2	BN	-0.26	V	$\cdots$	$\cdots$
09 19 20.211 +31 20 18.57	3.38	3.50	2.04 - <13.40	$\cdots$	5	7.846e-09	5.34	5.43	>1.78	96	$\cdots$	0.21	V	20.47	SDSS-G
09 20 21.962 +41 15 53.61	1.07	1.09	<1.08 - 3.25	$\cdots$	3	1.219e-08	5.11	5.86	>3.02	1	$\cdots$	2.40	T	$\cdots$	$\cdots$
09 20 23.533 +01 34 44.39	3.47	3.40	1.85 - <8.95	3.64	4	4.531e-07	3.56	4.72	2.34	5	$\cdots$	0.50	V	19.46	SDSS-G
09 20 27.389 -03 25 43.78	3.97	4.05	2.98 - 4.42	$\cdots$	3	1.365e-07	4.66	4.79	>1.43	4	$\cdots$	-1.11	V	$\cdots$	$\cdots$
09 20 43.557 -07 29 43.54	3.88	3.80	2.39 - <8.52	$\cdots$	4	9.257e-09	4.94	5.03	>1.44	459	$\cdots$	-0.57	V	$\cdots$	$\cdots$
09 21 10.605 +03 19 20.67	4.48	4.32	<2.86 - <24.09	$\cdots$	4	2.368e-07	5.42	5.39	>1.61	4	$\cdots$	-0.19	V	$\cdots$	$\cdots$
09 21 31.838 -01 32 30.09	7.14	7.29	5.09 - 8.11	8.27	3	1.264e-08	5.68	4.98	1.59	5	$\cdots$	0.53	V	$\cdots$	$\cdots$
09 22 14.008 +06 38 22.84	10.33	10.49	<2.12 - 11.43	6.01	4	0.000	21.28	14.39	>5.34	1	$\cdots$	0.67	V	$\cdots$	PSR
09 22 30.077 +31 15 24.78	5.97	6.24	3.73 - 7.76	5.55	3	1.042e-12	5.40	6.20	2.08	96	BN	0.47	V	$\cdots$	$\cdots$
09 23 43.513 +34 30 21.13	24.11	23.99	22.90 - 34.73	26.21	5	3.229e-07	3.62	3.71	1.52	1	$\cdots$	-0.06	V	$\cdots$	$\cdots$
09 24 05.273 +31 57 46.32	5.36	5.71	3.92 - 7.52	4.39	4	4.653e-11	5.63	5.66	1.81	499	$\cdots$	0.25	V	21.33	SDSS-G
09 24 17.413 +28 28 47.72	3.94	3.83	1.65 - 4.14	$\cdots$	3	1.066e-08	5.30	5.10	>2.52	398	$\cdots$	-0.41	V	$\cdots$	$\cdots$
09 24 17.944 +02 57 56.19	14.32	13.72	13.34 - 29.88	17.89	4	7.394e-13	7.55	7.30	2.22	4	$\cdots$	0.74	V	$\cdots$	SDSS-UNKNOWN
09 24 49.017 +17 04 16.93	7.23	6.83	4.51 - 7.81	7.02	3	1.845e-09	5.89	5.20	1.73	28	$\cdots$	-0.16	V	$\cdots$	$\cdots$
09 25 03.472 +63 58 23.05	2.69	2.75	<1.99 - 3.10	2.34	3	2.319e-07	5.19	5.36	>1.56	0	BN	1.03	V	$\cdots$	$\cdots$
09 25 28.894 -00 07 11.75	4.52	4.77	<2.53 - <21.59	5.06	5	1.881e-10	6.60	6.44	>2.01	2	BN	0.61	V	$\cdots$	$\cdots$
09 25 30.007 +35 49 29.59	195.96	187.09	183.81 - 241.66	192.83	5	4.890e-08	3.60	3.27	1.31	1	$\cdots$	0.30	V	$\cdots$	$\cdots$
09 25 44.297 +21 55 59.78	7.60	7.47	5.17 - 7.99	6.05	3	4.156e-07	5.28	4.60	1.54	29	$\cdots$	-0.65	V	20.47	SDSS-QSO(P)
09 25 51.544 -00 32 10.89	6.74	6.43	3.34 - 6.77	7.04	4	1.589e-07	5.78	5.32	2.02	4	$\cdots$	0.23	V	$\cdots$	$\cdots$

Coordinates (J2000)	f (mJy)				N	Measures			$\frac{\text{Max.}}{\text{Min.}}$	$T_{\min}$	Flags	σ_{nbr}	Type	i	Cross-ID
	Cat.	$\overline{f}$	Range	NVSS		$P(\chi^2,\nu)$	$\sigma_{\max}$	$\Delta_{\max}(\sigma)$		(days)				Mag.	
09 26 13.081 +01 30 01.43	2.41	2.58	<1.65 - 3.18	2.69	3	3.824e-09	5.70	6.10	>1.93	6	$\cdots$	-1.48	V	21.82	SDSS-G
09 26 18.640 +18 55 55.40	1.52	1.59	<1.20 - <4.18	$\cdots$	4	1.802e-07	4.75	5.20	>1.77	$\cdots$	$\cdots$	0.59	V	20.08	SDSS-G
09 26 26.990 +51 36 15.70	25.92	24.43	23.21 - 42.60	26.79	4	7.159e-13	6.76	6.62	1.84	0	$\cdots$	-1.32	V	19.19	SDSS-G
09 26 35.900 +13 42 07.57	1.89	1.93	1.38 - 4.00	$\cdots$	3	8.789e-10	5.73	6.42	2.91	1	$\cdots$	0.70	V	$\cdots$	$\cdots$
09 26 42.429 +45 01 00.03	3.16	3.13	2.86 - <8.10	2.40	5	6.126e-08	5.11	5.34	2.39	2	$\cdots$	0.54	V	$\cdots$	$\cdots$
09 26 45.593 +03 07 13.03	4.39	4.32	<2.44 - 8.25	$\cdots$	4	5.680e-11	6.66	6.26	>1.84	7	$\cdots$	0.62	V	$\cdots$	$\cdots$
09 26 52.039 +57 16 32.07	4.12	4.10	3.03 - 5.86	5.90	3	2.122e-09	3.91	5.11	1.94	24	$\cdots$	0.40	V	20.40	SDSS-QSO(P)
09 27 34.915 +19 53 24.86	1.56	1.57	1.01 - <4.39	$\cdots$	4	5.361e-09	4.75	5.11	2.37	$\cdots$	$\cdots$	-1.22	V	$\cdots$	$\cdots$
09 28 04.999 -00 58 33.95	5.45	5.58	2.21 - 7.46	3.43	4	7.727e-11	6.20	6.76	3.38	2	$\cdots$	-0.04	V	20.91	SDSS-G
09 28 07.042 +19 56 30.13	2.59	2.63	1.29 - 2.76	$\cdots$	3	8.941e-07	5.21	4.64	2.15	$\cdots$	$\cdots$	-0.36	V	19.51	SDSS-G
09 29 59.264 +38 44 26.53	3.83	3.87	<2.69 - <14.04	3.70	5	1.118e-07	5.08	5.27	>1.57	5	$\cdots$	1.57	V	19.52	SDSS-G
09 30 22.181 +44 29 35.65	124.81	121.67	118.28 - 191.15	125.54	5	1.597e-09	5.75	5.42	1.62	1	$\cdots$	0.77	V	20.35	SDSS-QSO(P)
09 30 28.561 -06 01 18.10	5.59	5.43	<4.14 - 5.62	5.77	4	4.000e-07	4.75	4.61	>1.36	2	$\cdots$	0.74	V	$\cdots$	GSC2-FIRST-G
09 30 35.837 +10 36 06.29	2.26	2.21	0.82 - <4.20	$\cdots$	4	7.527e-14	6.31	7.47	3.93	1	$\cdots$	0.88	V	13.35	HIP-STAR
09 30 54.818 +58 41 15.10	9.48	9.74	5.36 - 10.95	10.87	5	2.362e-09	6.49	6.00	2.04	436	BN	-0.05	V	$\cdots$	$\cdots$
09 31 30.308 +19 29 09.82	9.30	9.69	4.41 - 11.08	9.68	5	1.471e-07	4.34	4.08	2.22	$\cdots$	$\cdots$	0.26	V	$\cdots$	$\cdots$
09 31 34.962 +27 42 31.62	6.35	6.45	<3.71 - <9.09	7.00	5	1.406e-06	5.39	5.28	>1.78	1	$\cdots$	0.65	V	$\cdots$	$\cdots$
09 32 00.443 +38 51 37.35	1.44	1.40	1.03 - 3.23	$\cdots$	3	2.918e-08	4.24	4.77	3.13	5	$\cdots$	0.71	V	$\cdots$	$\cdots$
09 32 17.289 +00 09 22.98	1.39	1.39	0.88 - <6.13	$\cdots$	4	4.611e-07	4.18	4.47	2.49	38	$\cdots$	-1.35	V	20.49	SDSS-G
09 33 12.122 +39 18 31.73	1.13	1.01	<0.85 - 3.23	$\cdots$	4	5.648e-07	3.79	4.97	>3.79	0	$\cdots$	0.83	V	21.92	SDSS-G
09 33 30.201 +03 01 54.06	6.56	6.67	3.37 - 7.10	6.07	3	8.468e-09	5.38	5.18	2.10	7	$\cdots$	0.60	V	$\cdots$	$\cdots$
09 34 17.710 +02 32 32.94	3.32	3.41	1.82 - <28.92	$\cdots$	4	5.409e-07	5.07	5.08	2.11	4	$\cdots$	-0.19	V	$\cdots$	$\cdots$
09 34 33.003 +33 10 18.79	3.67	3.86	<2.45 - <6.77	$\cdots$	6	1.252e-07	5.58	5.88	>1.86	487	$\cdots$	0.32	V	22.69	SDSS-G
09 34 40.931 +63 35 13.66	4.57	4.60	3.34 - 6.75	4.90	4	3.904e-07	3.69	4.36	>1.63	0	$\cdots$	1.00	V	$\cdots$	$\cdots$
09 35 18.234 +03 15 07.97	3.49	3.84	1.35 - 4.57	3.85	3	8.105e-15	7.59	6.95	3.38	7	$\cdots$	-1.75	V	20.97	SDSS-G
09 35 45.234 +01 03 40.16	1.66	1.58	<1.19 - 2.35	$\cdots$	3	2.224e-07	4.68	4.99	>1.76	20	$\cdots$	-1.09	V	$\cdots$	$\cdots$
09 36 02.673 +03 30 26.59	23.17	24.79	<15.84 - 24.92	21.94	3	2.257e-08	5.71	5.38	>1.57	4	$\cdots$	-0.40	V	$\cdots$	$\cdots$
09 36 38.130 +28 17 11.49	1.33	1.16	<0.62 - <3.46	$\cdots$	4	2.503e-11	5.74	6.26	>3.22	511	$\cdots$	0.98	V	$\cdots$	$\cdots$
09 36 47.600 +50 16 49.57	2.46	2.41	<1.76 - <9.62	2.16	4	1.021e-07	4.89	5.67	>1.70	1	$\cdots$	0.35	V	$\cdots$	$\cdots$
09 36 53.152 -04 06 49.04	1.69	1.78	1.31 - 3.83	2.50	3	5.418e-08	4.38	5.01	2.93	12	$\cdots$	-0.65	V	$\cdots$	$\cdots$
09 36 56.056 +04 45 36.32	2.66	2.84	1.89 - 4.14	$\cdots$	3	4.304e-08	3.88	5.19	2.19	0	BN	-0.10	V	$\cdots$	$\cdots$

Coordinates (J2000)	Cat.	$\overline{f}$	Range	NVSS	N	$P(\chi^2,\nu)$	$\sigma_{\max}$	$\Delta_{\max}(\sigma)$	$\frac{\text{Max.}}{\text{Min.}}$	$T_{\min}$ (days)	Flags	σ_{nbr}	Type	i Mag.	Cross-ID
09 37 00.439 +19 45 16.30	11.46	11.76	8.98 - 15.19	9.29	3	4.191e-11	5.10	6.24	1.69	$\cdots$	$\cdots$	-0.07	V	21.05	SDSS-*
09 37 11.667 -02 23 50.71	15.14	13.56	13.19 - 19.88	13.86	3	8.836e-08	4.27	4.12	1.51	2	$\cdots$	-0.06	V	$\cdots$	$\cdots$
09 37 18.245 +31 04 43.76	13.72	13.60	12.92 - 19.72	15.71	5	1.266e-12	5.23	5.05	>1.51	411	$\cdots$	0.11	V	19.96	SDSS-*
09 37 35.087 +27 36 42.06	10.27	9.82	5.05 - 13.80	11.07	6	1.667e-07	5.05	5.98	2.73	1	$\cdots$	-1.33	V	$\cdots$	$\cdots$
09 37 51.321 +03 30 58.12	2.28	2.44	<1.77 - 3.35	$\cdots$	3	5.347e-08	4.24	5.43	>1.89	5	$\cdots$	-0.41	V	18.47	SDSS-QSO(S)
09 37 53.679 +42 26 08.50	1.69	1.58	0.80 - 1.89	$\cdots$	3	6.619e-08	4.72	4.42	>2.37	52	$\cdots$	0.90	V	21.22	SDSS-G
09 38 09.957 -06 20 47.66	3.00	2.79	1.34 - 3.47	$\cdots$	3	7.141e-09	5.63	5.56	2.42	4	$\cdots$	-0.41	V	$\cdots$	GSC2-FIRST-G
09 38 53.698 +00 19 33.32	8.14	7.47	4.28 - <17.46	7.60	4	1.707e-06	5.05	4.42	1.76	0	$\cdots$	-0.25	V	16.21	SDSS-G
09 39 23.752 +03 14 18.01	19.60	20.32	15.18 - 21.90	25.60	3	4.896e-07	5.05	4.34	1.44	7	$\cdots$	-0.47	V	$\cdots$	$\cdots$
09 39 24.554 +49 54 39.84	3.54	3.58	2.56 - 4.53	4.29	3	9.587e-08	3.45	4.85	>1.77	4	$\cdots$	-0.23	V	$\cdots$	$\cdots$
09 39 38.364 +03 08 46.90	14.64	14.46	9.01 - 17.31	14.35	4	2.665e-14	5.69	6.02	1.67	7	$\cdots$	-0.69	V	$\cdots$	$\cdots$
09 39 43.824 +00 57 18.42	1.89	2.03	0.88 - <4.06	$\cdots$	4	4.465e-12	5.69	6.70	3.38	13	$\cdots$	1.27	V	20.20	SDSS-G
09 39 47.333 +05 56 17.40	72.94	71.26	68.58 - 110.53	93.44	4	2.710e-08	6.11	5.72	1.61	1	$\cdots$	0.64	V	$\cdots$	$\cdots$
09 40 04.094 +02 29 28.32	6.03	5.96	2.14 - 6.44	4.06	4	2.617e-13	7.04	6.62	>3.01	4	$\cdots$	-0.39	V	$\cdots$	$\cdots$
09 40 19.307 +58 19 51.17	1.34	1.30	1.04 - 6.91	$\cdots$	5	2.182e-06	5.06	5.33	>4.09	436	$\cdots$	-2.84	V	20.51	SDSS-G
09 40 22.463 +61 48 26.27	9.25	9.58	5.30 - 11.09	10.68	4	2.362e-08	5.44	5.75	2.09	50	$\cdots$	0.53	V	17.13	SDSS-G
09 40 34.969 +27 40 27.52	7.67	7.71	<4.92 - 9.53	7.35	5	1.249e-08	6.20	5.79	>1.60	1	$\cdots$	0.25	V	$\cdots$	SDSS-UNKNOWN
09 40 51.599 +07 16 02.78	3.88	4.15	<3.04 - 4.63	4.34	4	4.528e-06	5.04	4.94	>1.44	4	$\cdots$	0.58	V	20.37	SDSS-QSO(P)
09 41 00.875 +02 52 39.80	26.28	24.51	11.77 - 30.89	25.16	4	2.460e-08	5.26	6.11	2.62	6	$\cdots$	0.18	V	$\cdots$	$\cdots$
09 41 04.373 +03 33 25.78	14.20	13.63	6.97 - 16.01	14.04	4	2.650e-07	5.50	5.06	2.04	4	$\cdots$	0.97	V	21.10	SDSS-*
09 41 05.024 -03 53 55.57	1.44	1.48	<0.98 - 3.21	$\cdots$	2	2.331e-15	5.78	7.56	>3.28	921	$\cdots$	0.44	T	$\cdots$	GSC2-FIRST-G
09 41 19.629 +18 45 20.80	1.82	2.14	<0.68 - 3.63	$\cdots$	4	0.000	9.66	9.68	>5.31	$\cdots$	$\cdots$	1.61	T	$\cdots$	$\cdots$
09 41 23.254 +11 23 46.91	3.57	3.68	2.10 - <6.37	3.38	4	1.825e-09	5.50	5.57	2.04	2	$\cdots$	-0.49	V	22.76	SDSS-G
09 41 40.653 +58 25 30.86	7.68	7.98	5.22 - 16.39	10.34	5	0.000	9.37	11.73	3.14	436	$\cdots$	-0.58	V	21.43	SDSS-*
09 41 47.010 +11 19 34.19	5.74	5.71	3.64 - 5.85	5.29	3	2.226e-07	4.90	4.75	>1.42	2	$\cdots$	-1.12	V	21.59	SDSS-G
09 41 57.239 -05 28 19.90	3.71	3.45	1.90 - 4.00	3.11	4	9.747e-08	5.52	5.56	2.11	9	$\cdots$	0.93	V	$\cdots$	$\cdots$
09 42 01.381 +13 19 50.34	8.68	8.59	6.51 - 11.41	4.79	4	5.181e-09	3.92	4.92	1.69	15	BN	1.56	V	$\cdots$	$\cdots$
09 42 03.940 +64 03 11.24	67.26	67.50	60.99 - 101.38	70.34	6	2.811e-09	4.28	4.28	1.57	4	$\cdots$	1.35	V	19.96	SDSS-QSO(P)
09 42 06.299 -00 44 51.15	3.47	3.60	<2.36 - <11.00	3.88	4	1.460e-08	5.65	5.47	>1.63	2	$\cdots$	-0.14	V	17.14	SDSS-G
09 42 39.558 -07 17 47.77	6.21	6.19	3.06 - 6.81	4.94	4	4.211e-07	4.11	4.39	2.23	2	BN	-1.73	V	$\cdots$	GSC2-FIRST-G
09 42 42.268 +39 45 17.88	3.35	3.35	2.55 - 4.68	$\cdots$	3	1.614e-07	3.83	5.28	1.79	1	$\cdots$	-1.23	V	19.54	SDSS-G

Continued on next page. . .

Coordinates (J2000)	f (mJy)				N	Measures			$\frac{\text{Max.}}{\text{Min.}}$	$T_{\min}$	Flags	σ_{nbr}	Type	i	Cross-ID
	Cat.	$\overline{f}$	Range	NVSS		$P(\chi^2,\nu)$	$\sigma_{\max}$	$\Delta_{\max}(\sigma)$		(days)				Mag.	
09 42 45.897 -00 46 58.28	1.56	1.44	<1.32 - <3.07	$\cdots$	4	4.458e-08	4.08	5.47	>1.86	2	$\cdots$	-0.81	V	19.39	SDSS-G
09 42 48.666 -01 30 06.86	6.30	6.62	3.52 - 7.31	6.28	3	4.099e-13	7.30	6.38	2.07	0	$\cdots$	-1.65	V	$\cdots$	$\cdots$
09 43 29.213 +25 42 32.56	5.39	5.37	<3.09 - 5.91	$\cdots$	4	4.005e-08	5.94	5.83	>1.82	2	BN	0.10	V	$\cdots$	$\cdots$
09 43 29.381 +26 43 35.38	10.18	9.69	<6.24 - 12.40	9.12	5	1.847e-06	5.33	5.10	>1.56	1	BN	-1.33	V	20.48	SDSS-G
09 44 12.239 +09 13 23.22	13.48	13.28	4.95 - 13.65	12.79	4	2.124e-07	5.79	5.40	2.76	3	$\cdots$	-0.21	V	$\cdots$	$\cdots$
09 44 46.227 +07 09 23.84	2.75	2.85	1.99 - 4.14	$\cdots$	3	1.650e-07	4.08	5.48	2.08	2	$\cdots$	0.74	V	$\cdots$	$\cdots$
09 45 07.299 +10 14 58.08	2.76	2.61	<2.32 - 3.82	3.73	3	2.990e-07	3.78	5.06	>1.50	5	$\cdots$	-0.23	V	21.09	SDSS-*
09 45 14.663 +49 28 57.76	6.99	7.45	6.09 - 10.28	6.43	4	1.484e-09	4.81	5.69	1.63	2	$\cdots$	1.29	V	22.09	SDSS-*
09 45 25.338 +17 32 15.25	4.64	5.02	2.78 - 5.31	4.40	3	5.234e-07	4.62	4.47	1.91	1	$\cdots$	-0.39	V	$\cdots$	SDSS-QSO(P)
09 45 27.070 +00 28 01.06	4.39	4.21	2.81 - 4.50	4.52	3	2.920e-08	4.73	4.86	>1.46	40	$\cdots$	-1.09	V	$\cdots$	$\cdots$
09 45 33.380 +03 27 25.26	4.84	4.92	1.67 - 5.94	$\cdots$	3	4.447e-11	6.60	6.25	3.15	4	$\cdots$	2.33	V	18.85	SDSS-G
09 45 34.376 -02 05 53.67	7.66	7.28	<5.11 - 7.47	6.85	4	5.209e-06	5.11	4.89	>1.45	5	$\cdots$	0.23	V	$\cdots$	$\cdots$
09 45 41.210 +32 56 22.15	6.84	6.45	2.26 - 7.15	3.26	4	0.000	12.99	9.89	3.17	484	$\cdots$	-1.34	V	$\cdots$	$\cdots$
09 45 46.099 -04 48 08.77	2.89	2.97	<1.78 - 3.51	2.34	2	9.138e-11	6.16	6.18	>1.97	2	$\cdots$	-0.11	T	$\cdots$	$\cdots$
09 45 52.251 +00 30 55.13	1.26	1.18	<0.53 - <4.07	$\cdots$	4	5.218e-15	6.90	7.00	>3.88	42	$\cdots$	-1.56	V	$\cdots$	$\cdots$
09 46 07.178 +32 46 46.00	18.58	17.72	<12.18 - 20.16	18.45	5	9.523e-08	5.67	5.81	>1.66	489	$\cdots$	-3.85	V	20.66	SDSS-G
09 46 11.265 +25 33 17.14	1.78	3.92	<1.90 - 6.13	$\cdots$	2	4.441e-16	7.06	7.73	>3.24	2	BN	-1.06	T	$\cdots$	$\cdots$
09 46 23.661 +36 09 40.24	1.36	1.37	<0.76 - 1.89	$\cdots$	4	3.870e-07	5.40	4.61	>2.48	1	$\cdots$	0.66	V	18.39	SDSS-G
09 47 31.567 +15 36 06.96	6.91	7.00	3.55 - 8.17	3.38	4	1.221e-15	6.68	6.81	>2.30	5	$\cdots$	0.51	V	21.51	SDSS-*
09 47 37.313 +49 41 26.51	15.14	15.61	4.73 - <17.99	16.73	5	1.776e-15	8.46	7.31	3.34	4	$\cdots$	0.80	V	18.83	SDSS-QSO(S)
09 47 43.462 +03 02 05.33	8.77	8.06	<4.47 - 8.44	7.75	3	2.276e-11	6.97	6.49	>1.84	7	$\cdots$	-0.88	V	21.51	SDSS-*
09 47 51.196 +00 19 00.26	2.09	2.20	<1.45 - <10.83	$\cdots$	4	3.079e-07	4.84	5.11	>1.70	38	BN	-1.05	V	$\cdots$	$\cdots$
09 48 47.900 +46 16 45.07	2.09	2.11	1.38 - <4.39	$\cdots$	3	3.320e-07	3.64	5.09	2.17	2	$\cdots$	0.79	V	$\cdots$	$\cdots$
09 49 03.732 +50 12 35.97	1.79	1.89	1.17 - 3.89	$\cdots$	3	2.909e-08	3.57	4.68	2.36	1	$\cdots$	0.49	V	17.91	SDSS-G
09 49 09.518 +31 09 50.34	3.38	3.36	2.18 - 3.85	3.05	3	2.188e-08	5.62	5.05	1.76	411	$\cdots$	0.19	V	21.05	SDSS-G
09 50 56.224 +14 18 50.90	14.11	6.78	<6.10 - <20.41	10.29	4	1.049e-13	6.48	7.05	>2.41	0	BN	NA	V	18.49	SDSS-*
09 51 18.442 -02 55 21.44	4.09	4.16	2.20 - <8.13	$\cdots$	4	1.546e-07	4.99	4.90	2.06	6	$\cdots$	-0.87	V	$\cdots$	$\cdots$
09 51 53.643 +49 49 44.99	3.87	3.85	2.33 - 4.64	2.56	3	9.421e-10	5.83	5.98	1.99	4	$\cdots$	0.64	V	18.74	SDSS-G
09 52 09.653 +24 28 15.43	3.28	3.28	<2.36 - 3.51	$\cdots$	3	2.331e-07	4.69	4.75	>1.49	1	BN	0.02	T	$\cdots$	$\cdots$
09 52 19.402 -05 18 53.44	6.52	6.75	4.11 - <9.70	6.26	4	5.665e-09	5.29	5.46	2.25	0	$\cdots$	0.27	V	$\cdots$	$\cdots$
09 52 43.052 +34 36 38.74	2.52	2.61	1.70 - 3.72	$\cdots$	4	1.827e-07	3.78	5.05	>2.18	5	$\cdots$	0.34	V	18.70	SDSS-G

Table A.1 – Continued

Coordinates (J2000)	f (mJy)				N	Measures			$\frac{\text{Max.}}{\text{Min.}}$	$T_{\min}$	Flags	σ_{nbr}	Type	i	Cross-ID
	Cat.	$\overline{f}$	Range	NVSS		$P(\chi^2,\nu)$	$\sigma_{\max}$	$\Delta_{\max}(\sigma)$		(days)				Mag.	
09 54 08.972 +58 18 09.78	6.79	6.12	2.40 - 6.29	7.54	4	1.429e-06	5.36	5.07	2.63	450	$\cdots$	0.95	V	19.37	SDSS-G
09 54 26.122 +14 06 47.29	2.41	2.22	1.34 - <6.46	$\cdots$	4	4.354e-07	3.75	4.47	>1.40	13	$\cdots$	0.53	V	20.51	SDSS-G
09 54 27.074 -05 12 05.75	4.64	4.73	<3.15 - 5.74	4.42	3	2.714e-09	6.05	5.56	>1.54	7	$\cdots$	-0.38	V	$\cdots$	$\cdots$
09 54 31.241 -01 03 24.49	1.62	1.62	<1.36 - 2.73	$\cdots$	3	1.672e-08	4.27	5.97	>2.02	4	$\cdots$	-0.54	V	$\cdots$	$\cdots$
09 55 47.670 -08 02 58.50	10.18	9.97	5.49 - 10.11	10.47	2	1.341e-08	5.67	4.91	1.84	443	$\cdots$	1.21	V	$\cdots$	GSC2-FIRST-G
09 56 29.473 +12 10 31.75	5.09	5.26	2.35 - 5.80	3.67	3	0.000	8.35	7.36	2.47	4	$\cdots$	0.83	V	20.77	SDSS-QSO(P)
09 58 35.402 +00 44 33.80	5.74	6.32	3.42 - <14.16	6.24	4	1.606e-08	5.82	4.98	1.89	13	$\cdots$	-0.50	V	15.11	SDSS-G
09 59 01.941 +05 36 26.87	3.28	3.22	1.16 - 3.75	$\cdots$	3	1.282e-10	6.33	5.80	3.15	2	$\cdots$	1.41	V	18.07	SDSS-G
09 59 21.698 +60 48 19.37	15.53	14.18	9.76 - 14.47	15.49	3	4.101e-07	4.39	3.80	1.48	3	$\cdots$	0.16	V	$\cdots$	$\cdots$
10 00 06.013 +38 37 14.08	10.49	10.89	<6.73 - 13.60	9.51	5	2.506e-09	6.45	5.91	>1.63	5	$\cdots$	-0.19	V	$\cdots$	$\cdots$
10 00 06.119 +20 05 33.48	7.33	6.96	5.48 - <19.24	7.07	6	2.624e-10	6.74	6.66	2.01	$\cdots$	$\cdots$	0.27	V	$\cdots$	$\cdots$
10 00 13.209 +12 32 47.86	48.75	47.40	44.90 - 64.01	49.41	4	2.968e-10	4.53	4.44	1.43	14	$\cdots$	0.30	V	21.03	SDSS-G
10 00 34.592 +24 32 20.94	5.81	5.76	3.66 - 7.74	$\cdots$	3	0.000	8.39	8.02	2.11	1	$\cdots$	0.37	V	21.97	SDSS-*
10 00 58.960 -03 32 44.40	2.74	2.75	<2.08 - <6.11	5.06	4	1.766e-08	4.76	5.45	>1.62	1	$\cdots$	-0.45	V	$\cdots$	GSC2-FIRST-S
10 01 03.428 +42 38 40.71	2.71	2.67	1.28 - <3.67	$\cdots$	4	2.484e-08	5.49	5.67	2.41	478	$\cdots$	0.10	V	19.83	SDSS-G
10 01 25.269 +14 00 44.34	5.75	5.79	2.62 - 7.53	4.96	4	5.629e-07	5.16	4.86	2.87	0	BN	0.81	V	$\cdots$	$\cdots$
10 01 40.983 +28 57 10.63	5.96	6.25	2.39 - <13.78	$\cdots$	5	1.282e-10	5.86	5.89	3.05	6	BN	-0.38	V	$\cdots$	$\cdots$
10 01 41.642 +13 56 40.83	2.24	2.06	<1.40 - 3.28	$\cdots$	3	2.517e-10	5.58	5.86	>1.82	9	BN	0.88	V	$\cdots$	$\cdots$
10 01 49.607 +10 52 05.01	10.18	9.87	7.42 - 13.37	11.77	3	2.331e-14	5.77	6.63	1.80	2	$\cdots$	1.11	V	18.54	SDSS-QSO(S)
10 01 53.481 +02 11 52.31	2.09	2.03	1.06 - 3.44	$\cdots$	3	1.306e-09	4.76	5.69	3.24	5	$\cdots$	-0.45	V	19.27	SDSS-G
10 02 34.556 +50 37 09.90	1.31	1.31	<1.03 - 2.00	$\cdots$	3	1.210e-07	4.00	4.95	>1.93	1	$\cdots$	1.44	T	$\cdots$	$\cdots$
10 02 52.936 -02 58 34.04	6.92	7.13	3.32 - <10.63	6.78	4	2.106e-06	5.10	4.69	2.18	8	$\cdots$	-0.38	V	$\cdots$	$\cdots$
10 03 13.575 +28 45 26.87	69.36	69.34	49.08 - 78.47	88.65	5	1.536e-07	5.74	4.47	1.60	11	BN	-1.51	V	19.89	SDSS-QSO(P)
10 03 30.297 +29 04 34.47	2.27	2.15	<1.95 - 3.48	$\cdots$	3	2.929e-07	3.57	5.03	>1.78	5	BN	-1.04	V	21.59	SDSS-*
10 03 31.227 +50 52 24.16	5.68	5.66	<3.40 - 5.90	4.63	3	4.926e-07	5.34	5.20	>1.70	2	$\cdots$	0.15	V	$\cdots$	$\cdots$
10 03 59.436 +22 49 32.85	10.60	10.67	7.71 - 11.61	8.36	3	3.040e-07	5.28	4.56	1.50	4	$\cdots$	-1.43	V	$\cdots$	$\cdots$
10 04 06.284 +57 57 36.50	26.24	23.59	22.59 - 33.69	29.43	4	7.207e-10	4.89	4.71	1.49	0	$\cdots$	-0.04	V	$\cdots$	$\cdots$
10 04 41.667 -07 22 48.95	1.31	1.26	<1.00 - <2.54	$\cdots$	3	1.655e-08	4.26	5.50	>2.31	11	$\cdots$	0.69	V	$\cdots$	$\cdots$
10 04 59.271 +56 08 23.57	1.63	1.38	<0.97 - <2.85	$\cdots$	4	2.876e-08	4.78	5.47	>2.01	418	$\cdots$	1.07	V	$\cdots$	$\cdots$
10 05 14.857 -02 59 17.57	7.15	7.05	5.13 - 8.21	9.27	3	2.072e-10	5.60	5.44	1.60	6	$\cdots$	-0.40	V	20.54	SDSS-G
10 05 20.109 +51 46 09.89	55.42	53.66	52.22 - 80.97	55.97	4	7.159e-09	5.59	5.18	1.55	0	$\cdots$	1.60	V	22.24	SDSS-G

Continued on next page. . .

Coordinates (J2000)	f (mJy)				N	Measures			$\frac{\text{Max.}}{\text{Min.}}$	$T_{\min}$	Flags	σ_{nbr}	Type	i	Cross-ID
	Cat.	$\overline{f}$	Range	NVSS		$P(\chi^2,\nu)$	$\sigma_{\max}$	$\Delta_{\max}(\sigma)$		(days)				Mag.	
10 06 03.234 +28 09 43.79	4.47	4.44	2.10 - 5.12	$\cdots$	4	1.324e-08	5.76	5.68	2.44	511	$\cdots$	0.89	V	$\cdots$	$\cdots$
10 06 08.145 -04 12 31.75	2.92	2.73	<1.71 - <10.83	$\cdots$	4	1.985e-08	5.78	5.65	>1.77	924	$\cdots$	0.69	V	$\cdots$	GSC2-FIRST-G
10 07 33.032 +40 19 43.36	2.96	3.18	<2.19 - <9.03	3.13	5	6.820e-07	5.05	4.88	>1.51	5	$\cdots$	0.18	V	$\cdots$	$\cdots$
10 07 45.846 +07 14 54.27	42.89	46.14	19.31 - 48.34	69.03	3	4.282e-12	7.20	6.26	2.44	4	BN	-1.50	V	$\cdots$	$\cdots$
10 07 54.470 +31 21 11.82	2.32	2.37	<1.66 - <6.67	$\cdots$	4	1.058e-09	5.43	6.04	>1.77	97	$\cdots$	0.36	V	19.35	SDSS-G
10 08 04.281 +50 49 36.00	1.30	1.14	<0.92 - <5.70	$\cdots$	4	2.089e-13	5.11	6.59	>2.46	2	$\cdots$	0.55	V	17.95	SDSS-G
10 09 06.182 +43 19 00.90	10.63	10.46	10.14 - 16.65	9.97	5	7.783e-09	4.13	4.11	1.64	2	$\cdots$	0.23	V	14.55	SDSS-G
10 09 15.337 +62 12 44.87	7.69	7.58	4.54 - <16.45	7.75	5	4.275e-07	4.67	4.98	2.06	0	$\cdots$	-0.37	V	21.09	SDSS-G
10 09 37.844 +36 42 24.49	3.10	3.07	2.32 - 5.37	2.10	3	1.899e-08	4.06	5.45	1.87	5	$\cdots$	0.03	V	$\cdots$	SDSS-QSO(P)
10 09 58.385 +05 59 28.39	7.55	7.69	<5.39 - 8.77	4.49	4	7.821e-09	4.57	4.97	>1.63	1	BN	1.09	V	$\cdots$	$\cdots$
10 10 12.792 +14 23 35.86	4.41	4.29	3.48 - 6.35	$\cdots$	3	4.228e-07	4.36	5.32	1.83	9	BN	1.04	V	21.83	SDSS-*
10 10 27.155 +21 13 08.58	6.04	5.93	2.60 - <21.76	5.61	6	2.793e-12	5.74	5.60	>1.57	7	$\cdots$	0.86	V	$\cdots$	$\cdots$
10 10 33.940 -00 07 56.85	6.91	6.67	2.63 - 9.11	5.89	4	9.482e-08	5.17	5.70	3.33	2	$\cdots$	-0.70	V	$\cdots$	$\cdots$
10 12 07.804 +13 45 20.45	4.26	4.36	2.69 - 6.09	$\cdots$	3	2.554e-15	6.88	7.44	2.26	8	$\cdots$	1.74	V	19.76	SDSS-G
10 12 17.582 +41 02 16.55	7.43	7.39	5.89 - 11.63	5.59	4	1.422e-11	4.84	6.10	1.97	6	$\cdots$	-0.45	V	21.33	SDSS-*
10 12 20.237 +36 09 02.11	95.55	95.24	92.18 - 132.86	98.06	5	7.002e-08	3.73	3.67	1.44	1	$\cdots$	0.14	V	20.17	SDSS-QSO(P)
10 12 33.387 +53 07 02.09	2.20	2.15	<1.36 - 4.10	3.71	4	1.339e-09	5.56	5.85	>1.89	1	$\cdots$	0.59	V	19.69	PSR
10 12 59.158 -01 50 44.98	6.18	6.12	2.86 - 9.80	5.84	4	1.082e-08	5.45	5.12	2.25	1	$\cdots$	-0.35	V	16.75	SDSS-G
10 13 03.812 +58 16 42.96	6.56	6.23	3.80 - 6.51	3.37	4	2.697e-08	6.05	5.09	1.72	450	$\cdots$	0.56	V	14.78	SDSS-G
10 15 00.399 +24 49 12.68	10.40	7.62	2.88 - <20.53	8.44	5	1.270e-12	6.54	6.63	3.39	2	BN	-0.22	V	$\cdots$	$\cdots$
10 15 08.394 +02 13 25.76	16.28	13.76	<7.11 - 16.75	14.67	3	5.148e-11	6.43	6.75	>2.36	4	$\cdots$	-2.01	V	$\cdots$	$\cdots$
10 15 41.243 +38 49 30.32	2.39	2.28	1.54 - 3.54	3.05	3	4.563e-07	4.20	4.92	2.30	5	BN	0.30	V	$\cdots$	$\cdots$
10 15 52.745 +02 29 20.88	10.33	10.46	4.78 - 14.70	$\cdots$	3	7.916e-13	6.53	6.78	3.08	5	$\cdots$	-1.82	V	$\cdots$	$\cdots$
10 16 01.685 -04 15 16.27	7.49	7.37	5.41 - 8.51	8.73	4	1.203e-07	4.01	4.51	>1.44	924	$\cdots$	0.85	V	$\cdots$	$\cdots$
10 16 02.662 +64 07 10.69	1.21	1.10	0.69 - <3.58	$\cdots$	4	7.658e-08	4.51	5.35	>4.09	0	$\cdots$	-0.82	V	$\cdots$	$\cdots$
10 16 31.696 +35 08 14.34	10.74	10.84	9.11 - 14.03	9.10	4	2.127e-07	4.02	5.21	1.54	2	$\cdots$	-0.24	V	19.81	SDSS-QSO(P)
10 16 50.343 +52 03 59.63	6.50	6.59	6.15 - 10.17	7.55	3	2.226e-08	5.15	5.24	1.65	2	$\cdots$	1.70	V	20.94	SDSS-G
10 16 53.511 +01 38 03.92	2.32	2.20	<1.60 - <9.27	2.09	4	3.727e-07	4.70	5.03	>1.63	1	$\cdots$	-1.13	V	$\cdots$	$\cdots$
10 16 57.327 +01 13 33.10	6.13	6.10	3.68 - <10.96	3.87	4	9.339e-07	5.07	4.83	1.80	1	$\cdots$	-1.51	V	19.00	SDSS-G
10 17 02.454 -01 45 48.68	3.26	3.20	2.11 - 4.39	3.94	3	6.467e-08	3.90	4.93	2.08	1	$\cdots$	-1.13	V	$\cdots$	$\cdots$
10 17 05.306 -02 04 32.80	2.54	2.40	1.34 - <4.98	$\cdots$	4	5.490e-07	4.43	5.27	2.30	4	$\cdots$	0.17	V	14.45	SDSS-G

Coordinates (J2000)	f (mJy)				N	Measures			$\frac{\text{Max.}}{\text{Min.}}$	$T_{\min}$	Flags	σ_{nbr}	Type	i	Cross-ID
	Cat.	$\overline{f}$	Range	NVSS		$P(\chi^2,\nu)$	$\sigma_{\max}$	$\Delta_{\max}(\sigma)$		(days)				Mag.	
10 17 10.474 -05 01 58.20	2.51	2.26	1.70 - 3.85	2.76	3	9.178e-08	4.62	5.61	2.27	0	$\cdots$	0.63	V	$\cdots$	$\cdots$
10 17 46.996 +54 38 20.87	2.41	2.20	1.26 - 2.96	2.60	3	2.505e-07	4.62	5.24	2.36	8	$\cdots$	-0.85	V	15.75	SDSS-G
10 17 54.858 +47 05 29.10	8.58	8.76	4.40 - 9.84	7.23	4	4.667e-08	5.75	5.59	2.23	1	$\cdots$	0.13	V	18.70	SDSS-QSO(S)
10 17 55.781 -07 06 50.94	2.41	2.61	1.81 - 6.87	5.13	3	2.276e-14	5.33	5.96	3.80	2	$\cdots$	0.06	V	$\cdots$	$\cdots$
10 18 16.476 +35 42 18.23	5.03	4.77	1.77 - <27.57	$\cdots$	5	1.935e-10	6.07	6.20	3.02	4	BN	-0.45	V	$\cdots$	$\cdots$
10 18 32.311 +36 34 38.76	3.30	3.46	<2.29 - 3.73	$\cdots$	3	4.224e-07	5.21	5.21	>1.63	5	$\cdots$	-0.62	V	$\cdots$	SDSS-UNKNOWN
10 18 32.710 -07 01 02.15	3.69	4.03	3.40 - 6.26	6.35	4	1.152e-07	4.94	5.32	1.84	2	$\cdots$	0.25	V	$\cdots$	$\cdots$
10 18 47.113 +29 55 03.70	2.55	2.61	1.82 - <4.15	$\cdots$	4	6.543e-08	3.94	5.35	1.94	10	$\cdots$	0.33	V	$\cdots$	$\cdots$
10 19 20.588 +59 07 29.56	3.42	3.60	1.32 - 4.82	$\cdots$	4	1.243e-14	7.57	7.58	3.40	0	$\cdots$	2.37	V	18.04	SDSS-G
10 19 22.423 +32 09 21.81	6.07	6.21	3.83 - 7.11	6.96	4	1.443e-14	6.87	6.12	1.86	1	$\cdots$	NA	V	16.03	SDSS-G
10 19 48.486 +58 28 06.76	6.87	6.91	4.35 - 7.92	8.02	4	1.141e-07	5.45	4.94	1.77	450	$\cdots$	-0.41	V	$\cdots$	$\cdots$
10 20 01.791 +03 42 07.47	4.20	4.40	2.17 - 4.80	4.45	3	3.671e-07	4.42	4.53	2.21	0	BN	0.11	V	22.15	SDSS-*
10 20 25.924 +29 24 42.14	4.02	3.86	2.64 - 4.34	4.11	3	4.274e-07	3.99	4.21	>1.64	11	$\cdots$	0.21	V	$\cdots$	$\cdots$
10 20 43.444 +25 12 29.40	5.91	5.66	2.89 - 5.87	$\cdots$	3	2.246e-07	4.52	4.19	1.70	7	$\cdots$	1.33	V	16.14	SDSS-G
10 20 55.748 -06 07 07.35	9.22	8.39	8.27 - 19.75	9.81	3	2.530e-07	4.89	4.86	2.39	2	$\cdots$	0.30	V	$\cdots$	$\cdots$
10 20 57.817 -03 41 48.82	1.61	1.53	<1.35 - <3.75	$\cdots$	4	4.078e-07	3.81	5.06	>1.67	9	$\cdots$	0.09	V	$\cdots$	$\cdots$
10 21 08.683 +21 53 41.72	15.26	15.48	<11.64 - 19.77	17.20	6	1.640e-09	4.99	6.04	>1.70	5	BN	0.44	V	$\cdots$	$\cdots$
10 21 21.218 +47 31 42.37	6.79	6.87	3.14 - 7.61	$\cdots$	4	8.505e-07	5.11	5.26	2.43	5	$\cdots$	1.48	V	$\cdots$	$\cdots$
10 21 32.336 +41 09 06.01	1.62	1.67	1.29 - <4.67	$\cdots$	4	9.533e-08	4.77	5.34	2.46	5	$\cdots$	0.10	V	19.13	SDSS-G
10 21 51.932 -06 27 53.76	2.95	2.76	1.00 - 4.07	2.91	3	0.000	7.91	8.50	4.08	4	$\cdots$	1.18	V	$\cdots$	$\cdots$
10 22 02.194 +06 35 42.83	2.07	2.05	1.50 - 6.40	$\cdots$	4	2.783e-07	3.38	4.27	2.48	2	$\cdots$	0.32	V	21.75	SDSS-*
10 22 13.367 +51 02 54.97	1.57	1.44	1.36 - 5.42	$\cdots$	4	9.983e-09	5.55	6.26	>3.74	4	$\cdots$	0.54	V	21.01	SDSS-G
10 22 29.612 -06 04 03.46	1.42	1.17	<0.98 - <3.81	$\cdots$	4	3.603e-07	3.74	5.08	>1.96	2	$\cdots$	0.53	V	$\cdots$	$\cdots$
10 22 30.593 +31 16 29.82	18.84	18.54	15.95 - 23.42	23.47	4	4.613e-08	3.68	4.78	1.46	507	$\cdots$	-2.08	V	19.82	SDSS-QSO(S)
10 22 33.219 +16 57 17.91	9.03	9.53	6.51 - <17.57	6.28	6	2.144e-08	5.50	4.47	1.51	29	$\cdots$	0.82	V	$\cdots$	$\cdots$
10 22 41.938 +36 51 25.55	7.97	7.90	2.99 - 8.24	4.49	5	3.997e-15	7.17	6.52	>2.75	1	$\cdots$	-0.99	V	$\cdots$	$\cdots$
10 22 49.299 -06 03 37.03	3.10	2.75	<1.40 - 3.86	3.22	3	0.000	7.99	8.33	>2.71	0	$\cdots$	0.53	V	$\cdots$	$\cdots$
10 22 52.017 +11 53 15.40	1.14	0.93	<1.01 - <6.98	$\cdots$	4	6.584e-08	4.87	5.46	>2.43	6	$\cdots$	0.35	V	$\cdots$	$\cdots$
10 22 58.011 +10 01 52.85	3.69	3.54	<1.54 - 6.86	2.57	3	0.000	10.52	12.52	>4.46	1	$\cdots$	-0.04	V	$\cdots$	PSR
10 23 12.949 -06 09 17.04	2.28	2.05	1.16 - <6.30	3.08	4	8.144e-08	4.15	4.76	3.30	2	$\cdots$	0.21	V	$\cdots$	$\cdots$
10 23 17.952 +18 37 36.01	4.26	4.20	2.39 - 4.94	$\cdots$	3	3.119e-08	5.39	5.02	2.07	$\cdots$	BN	-0.25	V	20.16	SDSS-G

Coordinates (J2000)	f (mJy)				N	Measures			$\frac{\text{Max.}}{\text{Min.}}$	$T_{\min}$	Flags	σ_{nbr}	Type	i	Cross-ID
	Cat.	$\overline{f}$	Range	NVSS		$P(\chi^2, \nu)$	$\sigma_{\max}$	$\Delta_{\max}(\sigma)$		(days)				Mag.	
10 23 30.978 +01 43 39.81	3.85	3.57	3.24 - 7.07	3.32	3	3.975e-09	5.98	6.18	2.18	1	$\cdots$	0.28	V	$\cdots$	$\cdots$
10 24 16.707 +58 56 00.79	3.41	3.52	1.76 - <20.79	$\cdots$	4	2.237e-07	4.73	4.77	2.29	9	BN	1.37	V	20.22	SDSS-QSO(P)
10 24 23.339 +45 33 27.22	6.02	5.87	4.48 - 10.57	7.24	5	1.513e-09	5.49	5.50	1.72	9	$\cdots$	0.84	V	21.54	SDSS-G
10 24 24.844 +21 36 18.77	5.71	5.61	3.39 - 6.04	5.51	4	2.854e-08	4.21	4.13	>1.58	5	$\cdots$	1.06	V	$\cdots$	$\cdots$
10 24 38.698 -07 19 19.07	5.21	5.47	<3.05 - 9.10	$\cdots$	4	0.000	6.73	9.34	>2.99	0	$\cdots$	1.00	V	$\cdots$	PSR
10 26 33.149 -02 36 03.38	6.56	6.76	3.82 - 6.97	4.58	3	1.696e-06	5.13	4.60	1.82	2	$\cdots$	-0.13	V	$\cdots$	GSC2-FIRST-S
10 27 00.238 +56 30 08.23	2.51	2.48	1.71 - 3.88	$\cdots$	3	1.582e-09	4.15	5.33	2.27	415	$\cdots$	0.39	V	19.51	SDSS-*
10 27 09.166 -07 08 36.26	3.46	4.34	<2.79 - 5.08	$\cdots$	2	4.860e-11	6.22	6.28	>1.82	0	$\cdots$	-1.97	T	$\cdots$	$\cdots$
10 27 13.462 +58 29 04.15	7.86	7.60	3.10 - 7.73	6.26	5	4.783e-06	5.33	4.96	2.49	0	$\cdots$	-0.17	V	$\cdots$	$\cdots$
10 27 30.989 +55 06 27.79	2.52	2.69	<1.76 - <7.06	2.20	4	9.045e-07	5.21	5.05	>1.61	47	$\cdots$	-0.08	V	$\cdots$	$\cdots$
10 27 41.547 +18 31 44.36	1.19	0.90	<0.71 - <3.64	$\cdots$	4	2.221e-08	4.12	5.57	>2.53	$\cdots$	$\cdots$	0.47	V	$\cdots$	$\cdots$
10 27 58.674 -06 47 55.71	11.65	11.79	7.27 - 16.63	11.40	3	4.078e-09	4.86	6.01	2.29	10	$\cdots$	0.58	V	$\cdots$	GSC2-FIRST-G
10 28 16.414 +44 38 39.47	47.58	42.19	39.40 - 55.71	45.54	5	7.659e-10	4.15	4.24	1.39	1	$\cdots$	-0.06	V	19.49	SDSS-G
10 28 20.940 -01 52 08.08	6.12	6.15	<3.41 - <11.25	6.42	3	1.824e-12	7.02	6.55	>1.86	1	$\cdots$	0.60	V	$\cdots$	$\cdots$
10 28 36.625 -05 58 45.13	3.96	3.80	<2.13 - <12.31	$\cdots$	4	1.689e-09	5.55	5.69	>1.93	2	$\cdots$	-0.72	V	$\cdots$	$\cdots$
10 28 40.045 +57 57 57.47	30.09	25.91	24.75 - 36.55	28.71	4	1.897e-11	4.69	4.57	1.48	7	$\cdots$	-0.82	V	$\cdots$	$\cdots$
10 29 26.539 +21 58 00.74	11.75	13.45	9.26 - 14.36	9.11	3	1.832e-14	6.15	5.09	1.55	999	$\cdots$	-1.13	V	$\cdots$	$\cdots$
10 30 08.368 -07 19 11.41	13.11	12.29	8.10 - 12.49	13.31	4	1.296e-06	5.21	4.31	1.54	0	$\cdots$	0.44	V	$\cdots$	GSC2-FIRST-G
10 30 10.280 +00 44 43.72	3.00	3.09	<2.31 - <9.73	$\cdots$	4	5.070e-08	4.59	4.95	>1.52	7	BN	0.89	V	19.54	SDSS-G
10 30 22.800 +25 45 18.91	5.58	5.50	2.82 - <8.57	4.07	4	6.898e-07	5.21	4.95	2.07	3	$\cdots$	0.37	V	18.66	SDSS-G
10 31 33.340 +01 00 48.52	7.18	6.80	2.98 - 8.33	5.76	4	1.500e-06	5.36	4.95	2.33	13	$\cdots$	0.63	V	20.15	SDSS-G
10 31 38.544 +57 26 25.99	7.89	8.06	3.33 - 8.69	6.21	3	4.441e-16	8.30	7.10	2.61	22	$\cdots$	2.76	V	20.67	SDSS-QSO(P)
10 31 40.613 +23 47 29.45	7.98	8.14	3.73 - 9.12	3.33	4	5.846e-12	5.28	5.50	2.45	3	$\cdots$	0.41	V	21.89	SDSS-*
10 31 49.808 -06 34 52.62	4.54	4.54	2.75 - <17.39	$\cdots$	4	1.433e-07	5.47	4.89	1.78	4	$\cdots$	-1.76	V	$\cdots$	GSC2-FIRST-G
10 32 37.778 -01 56 15.68	3.33	4.93	2.89 - 6.16	3.47	2	9.007e-12	6.13	6.20	2.13	4	$\cdots$	2.33	V	20.87	SDSS-G
10 33 28.729 +10 55 16.62	10.17	10.05	7.21 - 12.25	10.67	3	1.997e-07	4.99	4.69	1.70	3	BN	-1.89	V	$\cdots$	$\cdots$
10 33 42.931 +17 45 52.45	2.71	2.71	<1.97 - 3.78	$\cdots$	3	2.387e-07	4.75	5.41	>1.92	11	BN	0.43	V	$\cdots$	$\cdots$
10 33 48.402 +17 15 06.16	6.99	6.81	6.38 - 10.98	6.57	3	1.412e-07	5.43	5.45	1.72	1	BN	1.02	V	$\cdots$	$\cdots$
10 34 13.542 +54 47 43.72	98.12	94.85	94.06 - 125.32	108.19	5	2.900e-08	3.90	3.43	1.33	47	$\cdots$	-0.80	V	$\cdots$	$\cdots$
10 34 47.684 +04 42 05.76	4.58	5.04	3.17 - <12.15	6.00	4	3.373e-09	4.68	6.02	2.38	1	$\cdots$	-4.40	V	$\cdots$	$\cdots$
10 35 10.693 +10 29 03.06	7.36	7.55	5.01 - 8.58	6.34	3	5.827e-10	6.01	5.64	1.71	5	$\cdots$	0.40	V	$\cdots$	$\cdots$

Coordinates (J2000)	f (mJy)				N	Measures			$\frac{\text{Max.}}{\text{Min.}}$	$T_{\min}$	Flags	σ_{nbr}	Type	i	Cross-ID
	Cat.	$\overline{f}$	Range	NVSS		$P(\chi^2,\nu)$	$\sigma_{\max}$	$\Delta_{\max}(\sigma)$		(days)				Mag.	
10 35 56.045 +02 49 15.47	8.47	8.51	6.79 - 10.22	$\cdots$	3	2.976e-07	3.99	4.77	1.49	1	$\cdots$	-0.28	V	19.65	SDSS-QSO(P)
10 36 23.661 +59 42 55.10	3.07	2.95	1.74 - 3.93	$\cdots$	3	6.406e-08	3.89	5.20	1.99	1	$\cdots$	0.63	V	$\cdots$	$\cdots$
10 36 33.135 -02 25 28.17	6.52	7.03	5.83 - 9.01	6.15	3	2.507e-07	3.70	4.89	1.54	0	$\cdots$	-1.64	V	$\cdots$	$\cdots$
10 36 46.974 -06 54 24.08	1.72	1.82	<1.56 - 2.59	$\cdots$	3	2.629e-07	3.97	5.20	>1.66	4	$\cdots$	0.42	T	$\cdots$	$\cdots$
10 36 50.911 +01 53 08.52	3.57	3.63	1.73 - 4.49	3.02	4	4.230e-14	6.93	7.03	2.59	3	$\cdots$	-1.40	V	21.59	SDSS-G
10 37 17.955 +05 19 50.25	3.74	3.59	<2.41 - <10.98	4.53	4	2.162e-06	5.04	4.94	>1.56	1	$\cdots$	0.21	V	20.70	SDSS-G
10 37 50.057 +62 17 10.23	1.12	1.15	<0.76 - <2.21	$\cdots$	3	1.097e-07	5.08	4.60	>1.92	44	$\cdots$	0.19	V	$\cdots$	$\cdots$
10 38 18.197 +42 44 42.85	78.28	76.60	60.15 - 116.22	164.10	3	1.110e-16	6.44	8.17	1.93	478	$\cdots$	-0.24	V	17.90	SDSS-G
10 38 40.803 +48 13 12.58	4.22	4.43	2.91 - 5.57	$\cdots$	4	1.948e-07	4.52	4.70	1.91	3	$\cdots$	0.17	V	$\cdots$	$\cdots$
10 38 42.363 +39 56 53.05	3.14	3.08	2.23 - 5.29	2.25	4	2.202e-07	4.85	5.66	2.30	2	BN	0.64	V	$\cdots$	$\cdots$
10 38 45.322 +33 09 15.02	25.20	24.93	15.92 - 32.08	23.33	5	1.134e-09	5.28	6.25	2.01	0	$\cdots$	-0.28	V	22.61	SDSS-*
10 39 58.517 +11 22 08.22	1.12	1.21	<1.03 - 2.14	$\cdots$	3	5.523e-07	3.74	5.28	>2.09	1	$\cdots$	0.56	T	$\cdots$	$\cdots$
10 40 36.332 +02 45 49.98	5.29	5.25	<3.04 - <8.20	3.82	4	2.946e-09	5.91	5.54	>1.80	4	BN	0.73	V	19.64	SDSS-G
10 41 05.559 +21 03 32.12	7.04	7.13	4.73 - 8.71	4.70	3	5.707e-14	7.06	6.67	1.84	8	$\cdots$	-0.21	V	$\cdots$	$\cdots$
10 41 17.080 +63 39 10.11	1.49	1.48	<1.00 - 2.42	$\cdots$	3	5.518e-09	4.44	5.74	>2.42	0	$\cdots$	-3.33	T	21.45	SDSS-*
10 41 40.309 +12 39 43.17	22.83	23.95	23.23 - 33.82	23.80	3	8.195e-09	4.76	4.46	1.46	7	$\cdots$	0.70	V	$\cdots$	$\cdots$
10 41 58.594 +33 00 04.45	1.51	1.51	<1.16 - <2.26	$\cdots$	5	3.401e-09	5.09	6.20	>1.86	484	$\cdots$	-0.95	V	$\cdots$	$\cdots$
10 42 29.055 -04 05 35.75	4.35	4.54	3.47 - 5.85	4.42	3	5.302e-08	3.46	4.79	1.68	924	$\cdots$	1.03	V	$\cdots$	$\cdots$
10 42 46.227 +31 08 34.10	1.27	1.04	<1.02 - <4.89	$\cdots$	4	1.895e-07	4.21	5.13	>1.84	410	$\cdots$	1.82	V	20.50	SDSS-G
10 43 07.720 +03 45 21.16	6.71	6.64	<3.56 - 7.17	7.29	4	1.336e-10	6.88	6.44	>1.91	983	$\cdots$	0.97	V	$\cdots$	$\cdots$
10 44 11.686 +36 10 02.70	2.03	2.06	0.97 - 2.60	$\cdots$	3	5.167e-07	4.73	5.13	2.67	5	$\cdots$	0.52	V	21.32	SDSS-G
10 44 15.813 -01 09 47.08	14.05	13.89	7.29 - 14.89	14.61	4	3.487e-09	6.28	5.75	2.04	5	$\cdots$	0.06	V	19.28	SDSS-G
10 44 56.191 +19 31 18.20	1.74	1.65	0.91 - <3.22	$\cdots$	4	1.085e-08	4.46	5.60	2.75	$\cdots$	$\cdots$	2.51	V	$\cdots$	SDSS-UNKNOWN
10 45 13.370 -00 49 29.51	5.24	4.87	<3.41 - 5.91	6.83	3	1.587e-07	5.50	5.17	>1.46	4	$\cdots$	1.37	V	18.48	SDSS-G
10 45 22.994 +42 47 18.47	7.78	7.91	7.38 - 11.49	7.97	5	1.602e-08	4.55	4.70	1.54	478	$\cdots$	-0.21	V	$\cdots$	$\cdots$
10 45 30.850 +43 25 37.45	48.00	47.93	46.24 - 66.23	54.51	5	7.269e-08	4.28	4.06	1.40	2	$\cdots$	0.97	V	19.42	SDSS-QSO(P)
10 45 46.626 +32 51 46.21	5.21	5.11	<2.95 - 5.73	4.26	4	9.220e-12	7.19	6.73	>1.94	484	$\cdots$	-0.82	V	$\cdots$	$\cdots$
10 46 03.149 +07 19 06.91	7.62	7.76	5.44 - 8.38	7.37	4	1.326e-09	4.99	4.51	>1.54	4	$\cdots$	0.55	V	19.61	SDSS-QSO(S)
10 46 30.077 +29 51 17.60	3.57	3.70	<2.33 - 4.57	$\cdots$	4	3.528e-11	5.66	6.42	>1.96	10	$\cdots$	0.08	V	21.15	SDSS-*
10 46 58.107 +36 43 54.23	1.94	2.06	<1.24 - <6.52	$\cdots$	4	3.754e-11	6.19	5.71	>2.27	5	$\cdots$	0.12	V	$\cdots$	$\cdots$
10 47 01.981 +47 25 09.82	1.76	1.62	<1.09 - <2.86	$\cdots$	3	1.693e-12	5.34	7.03	>2.46	2	BN	-2.79	V	$\cdots$	$\cdots$

123

Coordinates (J2000)	f (mJy)				N	Measures			$\frac{\text{Max.}}{\text{Min.}}$	$T_{\min}$	Flags	σ_{nbr}	Type	i	Cross-ID
	Cat.	$\overline{f}$	Range	NVSS		$P(\chi^2, \nu)$	$\sigma_{\max}$	$\Delta_{\max}(\sigma)$		(days)				Mag.	
10 47 12.085 -01 41 03.47	1.92	2.04	1.50 - <8.49	$\cdots$	4	3.833e-07	3.92	4.91	>1.62	1	$\cdots$	0.62	V	$\cdots$	$\cdots$
10 47 35.028 +31 40 00.61	2.46	2.76	<1.93 - 3.17	2.42	3	5.754e-08	5.62	5.36	>1.56	95	$\cdots$	0.23	V	19.81	SDSS-G
10 47 36.636 +47 22 58.61	3.19	3.10	<1.63 - <10.44	3.17	5	8.428e-12	6.57	6.64	>2.17	2	BN	-0.61	V	21.24	SDSS-G
10 48 30.322 +17 52 46.96	3.59	3.54	2.67 - 3.93	2.88	4	3.104e-07	3.73	4.05	>1.30	11	$\cdots$	0.72	V	$\cdots$	$\cdots$
10 48 59.758 +03 01 04.31	1.92	1.78	<0.72 - 3.02	$\cdots$	3	0.000	7.56	8.12	>4.20	3	$\cdots$	0.10	V	$\cdots$	$\cdots$
10 49 01.721 +00 55 34.10	5.73	5.94	3.33 - <8.96	$\cdots$	3	7.598e-12	6.59	6.00	2.00	13	$\cdots$	0.40	V	18.08	SDSS-QSO(S)
10 49 04.677 +09 43 49.09	6.36	6.05	<4.21 - 6.34	5.88	4	1.546e-07	5.23	5.16	>1.51	3	$\cdots$	0.52	V	20.95	SDSS-G
10 49 39.792 -02 35 53.12	3.31	3.53	2.48 - 4.72	$\cdots$	3	1.682e-09	4.58	5.70	1.90	2	$\cdots$	-0.45	V	17.94	SDSS-G
10 49 49.127 -00 03 18.04	5.07	5.02	2.75 - <17.29	$\cdots$	4	5.649e-07	5.15	5.00	2.00	2	$\cdots$	-1.98	V	20.13	SDSS-QSO(P)
10 49 50.021 +20 08 33.97	4.07	4.21	3.47 - 6.58	3.05	3	8.350e-08	4.81	5.60	1.89	$\cdots$	$\cdots$	-1.92	V	$\cdots$	$\cdots$
10 50 10.001 +20 45 32.82	16.83	16.98	6.96 - 18.41	14.37	3	4.536e-13	7.45	6.44	2.50	8	$\cdots$	-0.31	V	21.76	SDSS-G
10 50 10.851 +17 36 34.00	1.74	1.74	0.92 - 3.37	$\cdots$	4	1.083e-08	4.54	5.21	2.71	1	$\cdots$	0.68	V	20.57	SDSS-G
10 50 18.761 -00 13 42.42	10.62	10.69	7.08 - 11.64	8.26	3	3.282e-13	7.33	5.63	1.63	2	$\cdots$	-0.57	V	$\cdots$	$\cdots$
10 50 25.679 +24 16 57.46	3.36	3.05	2.62 - 4.61	$\cdots$	3	3.105e-07	3.93	4.58	1.76	1	$\cdots$	1.07	V	21.82	SDSS-*
10 50 37.053 +14 02 14.17	9.96	9.74	6.06 - 10.15	6.99	4	3.995e-09	4.66	4.07	1.67	13	$\cdots$	-0.08	V	19.20	SDSS-G
10 50 45.916 +34 32 57.59	15.80	17.62	9.72 - 18.14	15.82	5	6.445e-12	5.14	4.59	1.71	5	BN	1.10	V	$\cdots$	$\cdots$
10 50 47.692 +14 46 25.31	2.09	2.23	2.10 - <5.89	2.17	4	6.536e-08	5.00	5.57	>2.27	12	$\cdots$	0.47	V	21.26	SDSS-G
10 50 49.933 +31 33 58.42	32.14	30.21	25.49 - 45.77	36.88	4	0.000	5.81	6.84	1.75	95	$\cdots$	-0.65	V	20.74	SDSS-G
10 50 57.623 +05 05 01.05	2.01	2.10	<1.35 - <5.26	$\cdots$	4	1.957e-07	4.93	5.16	>1.79	2	$\cdots$	0.26	V	$\cdots$	$\cdots$
10 51 13.634 +38 50 15.42	4.95	4.92	2.64 - 5.93	5.68	4	2.023e-08	5.24	5.79	2.25	6	$\cdots$	0.78	V	17.54	SDSS-QSO(S)
10 51 44.553 +06 11 07.87	4.23	4.08	3.08 - 5.33	$\cdots$	4	2.009e-09	4.09	5.44	>1.73	2	$\cdots$	-0.51	V	17.75	SDSS-G
10 51 50.922 +32 57 49.89	7.16	7.12	4.86 - 8.53	7.96	4	3.590e-07	5.21	4.53	1.76	488	$\cdots$	-0.04	V	$\cdots$	$\cdots$
10 51 55.074 -00 03 16.79	3.05	2.92	<1.91 - <7.00	$\cdots$	4	5.895e-08	5.42	5.53	>1.78	4	$\cdots$	-0.73	V	20.77	SDSS-G
10 52 05.566 +21 08 37.95	4.26	4.62	2.01 - 5.80	3.36	2	3.328e-13	6.58	6.92	2.88	6	BN	-0.09	V	$\cdots$	$\cdots$
10 52 08.782 +37 00 53.28	3.65	3.71	2.51 - 4.87	2.64	4	9.906e-08	5.37	4.72	1.67	1	$\cdots$	0.02	V	19.05	SDSS-G
10 52 21.749 -00 23 55.97	1.55	1.45	<1.17 - <2.22	$\cdots$	3	2.145e-07	4.10	5.19	>1.76	4	$\cdots$	-0.70	V	$\cdots$	$\cdots$
10 53 22.936 +38 29 14.68	2.17	1.95	<1.54 - <4.81	$\cdots$	3	1.138e-10	4.67	6.36	>1.91	1	BN	-0.43	V	20.49	SDSS-QSO(P)
10 53 41.294 +01 00 16.08	5.66	5.70	3.40 - <9.16	$\cdots$	4	4.460e-07	4.75	4.77	1.85	8	$\cdots$	0.42	V	$\cdots$	RASS-FSC
10 54 36.511 -00 58 11.43	8.61	8.69	<5.24 - 9.24	$\cdots$	3	2.023e-11	6.95	6.41	>1.76	4	$\cdots$	0.45	V	$\cdots$	$\cdots$
10 54 43.407 +14 47 51.30	8.24	7.54	6.52 - 10.10	8.96	4	4.491e-07	3.86	4.99	>1.53	7	$\cdots$	0.25	V	$\cdots$	$\cdots$
10 54 52.775 +04 52 28.25	1.58	1.53	0.91 - <3.86	$\cdots$	4	2.280e-07	4.13	5.17	2.88	1	$\cdots$	1.28	V	$\cdots$	$\cdots$

Coordinates (J2000)	f (mJy)				N	Measures			Max./Min.	$T_{\min}$	Flags	σ_{nbr}	Type	i	Cross-ID
	Cat.	$\overline{f}$	Range	NVSS		$P(\chi^2,\nu)$	$\sigma_{\max}$	$\Delta_{\max}(\sigma)$		(days)				Mag.	
10 54 57.682 -07 00 36.87	2.31	2.26	1.47 - <6.78	$\cdots$	4	1.436e-07	4.28	5.14	2.23	2	$\cdots$	0.48	V	$\cdots$	$\cdots$
10 55 14.982 +36 41 53.58	4.80	4.90	3.90 - 7.98	$\cdots$	4	8.152e-11	3.92	5.18	1.73	5	$\cdots$	-0.05	V	$\cdots$	$\cdots$
10 55 20.951 +31 07 19.25	5.40	5.50	2.16 - <13.36	4.90	5	7.229e-12	6.36	5.88	2.67	410	$\cdots$	-0.86	V	21.06	SDSS-*
10 55 28.810 +31 24 11.65	9.07	9.02	6.11 - 10.84	9.08	5	1.036e-06	5.09	4.89	1.77	0	$\cdots$	-1.16	V	16.91	SDSS-*
10 55 39.792 +31 18 21.72	3.70	3.67	2.32 - 4.54	3.32	4	6.116e-07	5.15	4.29	1.67	97	$\cdots$	-3.28	V	$\cdots$	$\cdots$
10 55 46.553 +52 07 57.37	3.93	3.63	3.08 - 5.07	$\cdots$	3	2.574e-07	3.83	4.68	1.64	2	$\cdots$	-0.63	V	$\cdots$	$\cdots$
10 55 48.230 +14 53 13.25	1.78	1.64	0.81 - 2.54	$\cdots$	3	3.002e-11	4.48	5.90	>2.10	1	$\cdots$	0.60	V	$\cdots$	$\cdots$
10 55 50.793 +23 31 50.37	5.18	4.74	4.28 - 8.36	5.54	3	5.801e-08	5.59	5.70	1.89	2	$\cdots$	0.20	V	21.83	SDSS-*
10 55 56.030 +14 18 16.35	4.98	4.96	2.06 - 5.22	4.21	4	5.124e-08	5.98	5.60	2.53	6	$\cdots$	2.32	V	$\cdots$	$\cdots$
10 56 16.036 +21 07 08.51	4.16	4.24	2.20 - 4.77	2.78	3	4.884e-07	4.87	4.93	2.17	7	$\cdots$	-1.58	V	19.74	SDSS-*
10 56 19.958 -00 45 11.54	3.66	3.56	1.84 - 5.28	$\cdots$	4	0.000	7.82	7.68	2.52	4	$\cdots$	-1.19	V	21.62	SDSS-G
10 56 59.813 +59 11 43.98	18.21	17.70	16.95 - 25.82	19.19	6	3.464e-09	5.34	5.10	1.52	9	$\cdots$	-0.55	V	20.52	SDSS-G
10 57 09.847 +30 54 58.10	2.16	2.26	<1.59 - <3.58	$\cdots$	4	6.100e-07	5.23	4.98	>1.57	413	$\cdots$	0.16	V	$\cdots$	$\cdots$
10 57 40.525 -01 18 23.12	3.58	3.31	1.78 - 3.82	$\cdots$	3	4.659e-07	4.47	4.89	2.15	5	$\cdots$	-0.17	V	$\cdots$	$\cdots$
10 58 00.491 +02 15 58.28	9.60	9.76	<4.81 - 10.53	8.52	4	1.110e-16	8.50	7.96	>2.19	2	$\cdots$	0.67	V	$\cdots$	$\cdots$
10 58 04.259 +01 22 40.14	32.38	36.38	11.16 - 37.02	27.66	2	3.109e-15	7.88	6.84	3.32	2	BN	-0.50	V	$\cdots$	$\cdots$
10 58 26.096 +06 38 01.80	3.76	3.70	1.99 - <10.73	2.65	4	4.799e-07	3.93	4.04	>1.31	1	$\cdots$	-0.46	V	$\cdots$	$\cdots$
10 58 53.324 +08 51 30.47	1.93	1.79	1.62 - <4.06	$\cdots$	4	9.541e-07	5.04	4.93	1.96	24	$\cdots$	1.04	V	20.45	SDSS-QSO(P)
10 59 13.011 +07 16 04.69	1.26	1.29	<0.75 - <2.79	$\cdots$	4	3.403e-13	5.50	7.39	>3.18	2	$\cdots$	-0.27	V	$\cdots$	$\cdots$
10 59 41.305 -02 51 16.46	3.05	3.26	<1.47 - 4.01	5.16	2	2.220e-16	7.70	7.89	>2.73	6	$\cdots$	-2.59	T	$\cdots$	NED-APMUKS(BJ)-G
10 59 47.761 +20 10 31.79	11.71	11.74	<7.36 - 12.07	9.59	3	5.860e-10	6.11	5.83	>1.64	$\cdots$	BN	-0.46	V	18.42	SDSS-QSO(P)
10 59 59.081 +08 45 38.88	7.34	7.39	<5.23 - <12.35	6.26	6	1.623e-06	5.43	5.14	>1.44	24	$\cdots$	0.72	V	$\cdots$	$\cdots$
11 00 28.737 -07 37 51.26	1.80	1.43	1.15 - 2.74	$\cdots$	3	4.649e-08	4.50	5.73	>2.10	0	$\cdots$	0.14	V	$\cdots$	$\cdots$
11 00 33.347 +36 33 30.81	10.88	10.75	6.50 - 11.98	11.60	3	4.898e-09	5.94	5.44	1.84	7	$\cdots$	-0.88	V	20.20	SDSS-G
11 00 39.774 -01 16 34.01	4.80	4.96	<2.87 - 5.79	2.66	3	2.389e-09	5.64	6.18	>2.02	5	BN	0.08	V	$\cdots$	$\cdots$
11 01 38.800 +44 23 07.17	6.98	7.15	5.38 - 8.43	$\cdots$	4	3.752e-08	4.54	4.97	1.57	4	$\cdots$	0.42	V	19.32	SDSS-G
11 01 39.445 -05 16 19.04	3.37	3.64	2.49 - <14.72	$\cdots$	4	3.085e-08	4.38	4.83	>1.49	0	$\cdots$	0.17	V	$\cdots$	$\cdots$
11 01 51.896 +16 40 38.65	8.33	8.54	7.07 - 10.97	$\cdots$	3	6.371e-08	3.60	4.90	1.55	7	$\cdots$	-1.58	V	15.39	SDSS-G
11 02 45.037 +62 25 59.12	8.72	9.09	4.08 - 16.23	7.95	6	8.336e-10	6.88	6.07	>2.29	15	$\cdots$	0.76	V	21.50	SDSS-G
11 02 55.129 -06 10 37.43	10.63	9.30	7.25 - 15.19	10.90	4	8.507e-08	5.29	5.95	2.09	4	$\cdots$	-0.38	V	$\cdots$	$\cdots$
11 03 14.791 -06 19 33.59	1.81	1.82	0.81 - 2.45	$\cdots$	3	8.321e-08	4.79	5.41	3.01	4	$\cdots$	-1.44	V	$\cdots$	$\cdots$

Coordinates (J2000)	f (mJy)				N	Measures			$\frac{\text{Max.}}{\text{Min.}}$	$T_{\min}$	Flags	σ_{nbr}	Type	i	Cross-ID
	Cat.	$\overline{f}$	Range	NVSS		$P(\chi^2,\nu)$	$\sigma_{\max}$	$\Delta_{\max}(\sigma)$		(days)				Mag.	
11 03 33.618 -05 51 33.92	1.58	1.50	1.37 - 2.70	$\cdots$	3	3.624e-07	4.08	5.40	>1.95	4	$\cdots$	0.21	V	$\cdots$	$\cdots$
11 03 50.709 -03 08 25.84	10.94	10.51	6.26 - 10.85	13.70	4	3.149e-08	5.31	4.64	1.73	7	$\cdots$	0.01	V	$\cdots$	$\cdots$
11 04 24.089 +07 30 52.98	70.30	69.80	66.73 - 107.76	76.09	4	2.609e-14	5.95	5.70	1.61	2	$\cdots$	-0.90	V	16.68	SDSS-QSO(S)
11 04 27.810 +35 17 38.33	7.26	7.85	4.70 - 11.98	5.77	5	1.111e-06	5.09	4.47	1.71	1	$\cdots$	-0.33	V	17.06	SDSS-G
11 04 28.187 +33 07 14.50	2.92	3.12	<2.12 - <4.15	3.66	6	4.265e-06	5.16	5.00	>1.58	487	$\cdots$	0.24	V	$\cdots$	$\cdots$
11 04 57.081 +29 48 17.85	3.11	3.23	1.57 - 4.29	$\cdots$	3	5.332e-12	6.37	6.66	2.73	10	$\cdots$	-1.38	V	$\cdots$	$\cdots$
11 05 07.031 +03 18 30.52	6.62	6.51	3.41 - 6.95	6.62	4	9.263e-07	5.18	5.02	2.04	71	$\cdots$	-0.23	V	19.09	SDSS-G
11 05 46.458 +26 43 38.01	1.91	2.17	<1.64 - 4.96	$\cdots$	4	1.208e-08	4.83	5.09	>3.03	1	$\cdots$	1.16	V	18.62	SDSS-G
11 06 07.258 +28 12 47.05	211.47	221.58	182.75 - 321.28	220.87	4	4.609e-12	5.72	6.99	1.76	926	$\cdots$	0.73	V	17.77	SDSS-QSO(P)
11 06 13.572 +54 05 45.53	1.58	1.44	<1.11 - 2.17	$\cdots$	3	3.116e-08	4.25	4.93	>1.96	426	$\cdots$	-0.12	T	$\cdots$	$\cdots$
11 06 24.833 +07 44 09.44	6.14	6.85	3.22 - 7.12	5.35	4	2.501e-06	5.22	4.92	2.21	4	$\cdots$	0.26	V	$\cdots$	$\cdots$
11 06 31.230 +53 49 45.14	2.97	3.01	<2.10 - 3.98	3.31	4	2.581e-09	5.32	5.84	>1.73	430	$\cdots$	-0.24	V	$\cdots$	$\cdots$
11 07 04.805 +50 10 37.87	29.04	28.29	25.76 - 37.60	35.44	3	1.882e-07	4.14	4.56	1.46	25	$\cdots$	-0.02	V	18.90	SDSS-QSO(S)
11 07 10.250 +36 48 15.05	9.56	9.73	4.19 - <17.27	10.23	5	7.349e-07	5.36	5.30	2.59	6	$\cdots$	-1.15	V	$\cdots$	$\cdots$
11 07 20.409 +37 04 48.75	2.57	2.79	<2.28 - 3.75	$\cdots$	4	5.330e-08	4.31	5.25	>1.64	1	$\cdots$	0.85	V	20.08	SDSS-G
11 08 03.094 +03 23 55.79	1.74	1.61	<1.27 - <5.77	2.35	4	5.855e-08	4.32	5.42	>1.84	4	$\cdots$	-0.24	V	$\cdots$	$\cdots$
11 08 45.634 -04 54 48.04	2.50	2.44	<1.65 - <11.91	$\cdots$	4	2.942e-07	5.24	5.34	>1.67	46	$\cdots$	1.28	V	$\cdots$	$\cdots$
11 08 46.534 +01 49 53.88	3.11	3.14	<2.25 - <10.27	3.18	4	6.796e-08	4.55	4.86	>1.55	3	BN	-0.21	V	$\cdots$	$\cdots$
11 08 47.468 +31 42 31.30	38.91	40.35	39.47 - 56.22	43.08	5	6.834e-09	3.95	3.74	1.42	4	$\cdots$	1.37	V	$\cdots$	$\cdots$
11 08 49.178 -02 29 41.54	8.81	9.54	5.85 - <14.18	13.42	4	3.752e-09	6.16	5.09	1.68	3	$\cdots$	-0.79	V	$\cdots$	$\cdots$
11 08 50.804 +02 01 59.45	2.62	2.88	<1.80 - <20.85	$\cdots$	4	7.228e-10	5.53	5.48	>1.87	5	BN	1.42	V	$\cdots$	$\cdots$
11 08 51.995 +39 06 07.31	5.04	5.15	<2.89 - 9.54	5.33	5	6.428e-14	7.06	6.53	>1.85	1	BN	-0.87	V	$\cdots$	$\cdots$
11 09 30.154 -02 11 01.79	6.52	7.07	6.52 - 10.40	9.84	3	7.820e-08	4.67	4.86	1.60	1	$\cdots$	-0.15	V	$\cdots$	$\cdots$
11 09 36.943 +02 24 45.08	5.28	5.20	<3.33 - 6.63	6.23	3	1.636e-12	6.53	7.17	>1.99	3	BN	0.62	V	20.91	SDSS-G
11 09 44.568 +03 07 15.73	2.59	2.81	1.60 - <5.29	$\cdots$	4	1.581e-08	4.58	5.96	2.34	71	BN	0.29	V	$\cdots$	$\cdots$
11 09 48.669 -01 51 58.71	7.60	7.69	3.21 - 9.04	8.72	4	3.823e-11	6.59	6.36	2.63	4	$\cdots$	-0.29	V	$\cdots$	GSC2-FIRST-G
11 09 52.310 -05 02 58.94	1.52	1.57	<1.16 - <4.81	$\cdots$	4	4.246e-08	4.50	5.21	>1.80	40	$\cdots$	0.11	V	$\cdots$	$\cdots$
11 09 57.129 +02 01 38.50	6.31	6.30	3.55 - 7.08	5.20	4	5.839e-09	4.84	5.09	1.87	2	BN	1.79	V	14.89	SDSS-G
11 10 05.035 +36 53 36.12	18.62	15.94	11.83 - 26.47	22.09	4	9.537e-14	6.33	7.62	2.14	6	$\cdots$	-3.72	V	20.01	SDSS-QSO(S)
11 10 06.053 -02 21 16.53	2.00	1.97	<1.35 - 2.19	$\cdots$	3	2.329e-07	4.38	4.59	>1.63	1	$\cdots$	-0.33	T	$\cdots$	GSC2-FIRST-G
11 10 14.326 -02 31 14.32	2.52	2.59	<1.73 - <11.79	$\cdots$	4	1.515e-07	5.12	5.34	>1.71	2	$\cdots$	-0.49	V	$\cdots$	GSC2-FIRST-G

Coordinates (J2000)	f (mJy)				N	Measures			$\frac{\text{Max.}}{\text{Min.}}$	$T_{\min}$	Flags	σ_{nbr}	Type	i	Cross-ID
	Cat.	$\overline{f}$	Range	NVSS		$P(\chi^2,\nu)$	$\sigma_{\max}$	$\Delta_{\max}(\sigma)$		(days)				Mag.	
11 10 15.582 +34 25 00.47	70.68	64.00	62.21 - 84.08	72.71	5	7.520e-09	3.93	3.66	1.35	1	$\cdots$	-0.27	V	$\cdots$	$\cdots$
11 10 30.458 +03 48 32.91	15.37	15.23	10.85 - 15.83	11.07	4	7.620e-08	5.81	4.51	1.46	983	$\cdots$	-0.27	V	18.94	SDSS-QSO(S)
11 10 38.727 +11 02 29.31	7.69	7.36	<6.17 - 10.69	6.96	4	3.373e-07	3.86	5.29	>1.73	2	BN	0.04	V	18.43	SDSS-G
11 10 54.624 +08 09 47.42	13.92	14.19	6.63 - 15.88	15.10	4	4.872e-08	5.54	5.59	2.38	3	$\cdots$	-0.10	V	17.58	SDSS-G
11 10 56.840 +35 39 07.22	7.52	7.53	4.56 - 10.29	3.70	3	0.000	8.78	8.61	2.26	4	BN	-0.24	V	18.69	SDSS-QSO(S)
11 10 56.971 +01 11 20.28	15.35	15.28	9.45 - 15.80	16.00	4	2.102e-07	4.23	3.72	1.67	7	$\cdots$	0.61	V	$\cdots$	$\cdots$
11 11 19.032 +10 28 20.03	4.21	4.34	<3.06 - 6.06	$\cdots$	3	5.151e-10	5.32	6.26	>1.98	3	BN	0.84	V	$\cdots$	$\cdots$
11 11 24.888 +30 31 31.18	3.76	3.78	2.22 - 4.39	3.50	3	9.738e-08	5.30	5.19	1.98	3	$\cdots$	0.24	V	19.05	SDSS-G
11 11 40.928 +42 18 58.94	40.57	41.11	39.81 - 55.84	41.00	5	1.269e-09	4.06	3.87	1.40	5	$\cdots$	0.45	V	19.65	SDSS-QSO(S)
11 11 49.039 +35 57 58.19	3.60	3.57	<1.99 - 4.25	2.89	4	2.220e-15	7.75	7.68	>2.14	1	BN	-0.99	V	$\cdots$	$\cdots$
11 11 51.735 +35 46 03.56	5.83	5.78	<3.77 - 6.37	4.00	4	7.968e-10	6.18	6.11	>1.69	4	BN	-3.06	V	20.73	SDSS-G
11 12 38.965 +64 09 30.85	6.90	6.89	5.31 - 8.91	$\cdots$	4	1.089e-07	4.45	5.04	1.58	503	$\cdots$	1.04	V	21.64	SDSS-G
11 12 40.690 +05 57 52.96	2.94	3.22	2.37 - 4.09	3.29	4	4.388e-07	3.70	4.58	>1.73	2	$\cdots$	0.09	V	19.03	SDSS-G
11 12 42.938 +42 22 35.59	16.87	16.94	14.59 - 21.00	19.01	3	4.938e-07	3.65	4.78	1.44	5	$\cdots$	2.38	V	19.07	SDSS-QSO(S)
11 12 45.154 -02 29 26.09	6.19	6.14	<3.62 - 6.31	$\cdots$	3	1.831e-10	6.67	6.09	>1.74	1	BN	-1.25	V	$\cdots$	$\cdots$
11 13 01.311 -03 38 51.66	4.02	3.95	2.05 - 4.40	$\cdots$	3	2.220e-16	7.60	7.32	>2.00	0	$\cdots$	0.13	V	$\cdots$	GSC2-FIRST-G
11 13 19.189 +36 27 49.72	1.63	1.63	<1.30 - <14.81	$\cdots$	5	2.301e-07	3.94	5.17	>3.30	0	$\cdots$	2.92	V	16.36	SDSS-G
11 13 22.006 +38 05 58.57	3.89	4.19	2.56 - 5.03	2.48	4	1.212e-08	5.74	5.23	1.97	5	$\cdots$	0.14	V	20.77	SDSS-QSO(P)
11 13 49.248 +21 00 53.18	4.76	4.68	2.07 - <15.54	5.80	4	6.138e-09	5.45	5.91	2.85	7	$\cdots$	-0.08	V	$\cdots$	$\cdots$
11 14 02.765 -03 44 55.53	2.31	2.16	<1.56 - <4.66	$\cdots$	4	1.479e-08	5.18	4.96	>1.53	1	$\cdots$	-1.29	V	$\cdots$	$\cdots$
11 14 04.838 +16 28 55.54	7.49	7.29	5.45 - 9.73	6.94	4	6.280e-12	5.00	5.17	>1.69	13	$\cdots$	-0.07	V	21.40	SDSS-G
11 14 47.999 +29 51 55.50	3.89	4.45	4.13 - <16.97	7.79	5	9.144e-08	4.93	5.06	1.91	10	$\cdots$	1.10	V	$\cdots$	$\cdots$
11 14 53.254 +21 54 22.94	8.02	7.89	3.62 - 10.93	8.03	6	2.691e-07	4.76	4.52	2.24	2	$\cdots$	0.06	V	21.58	SDSS-G
11 15 23.291 -04 06 40.79	2.18	2.19	0.81 - 3.36	2.73	3	8.660e-15	6.63	6.40	3.83	917	$\cdots$	-2.94	V	$\cdots$	$\cdots$
11 15 40.063 +21 46 54.33	2.55	2.52	<1.68 - 3.00	$\cdots$	3	9.591e-08	5.33	5.44	>1.78	2	$\cdots$	0.35	V	$\cdots$	$\cdots$
11 16 24.141 -03 50 58.26	9.30	11.32	5.24 - 12.75	10.94	2	0.000	9.51	7.71	2.43	917	$\cdots$	-4.39	V	$\cdots$	$\cdots$
11 16 24.917 -04 54 25.66	4.02	3.95	<2.69 - <15.51	3.04	4	4.410e-07	5.18	5.10	>1.53	8	$\cdots$	0.72	V	$\cdots$	$\cdots$
11 16 25.020 +12 52 41.71	26.28	23.97	23.70 - 36.29	26.18	3	3.966e-10	4.95	4.57	1.53	3	$\cdots$	-0.39	V	$\cdots$	$\cdots$
11 16 34.468 +07 16 53.73	24.95	25.86	24.21 - 38.85	29.66	4	9.488e-13	5.82	5.76	1.61	4	$\cdots$	0.50	V	19.44	SDSS-G
11 16 44.312 +60 47 24.31	2.87	2.91	<1.90 - 3.63	$\cdots$	3	1.587e-07	5.21	5.21	>1.67	0	$\cdots$	0.80	V	$\cdots$	SDSS-G
11 16 50.636 +29 47 37.72	1.49	1.43	<0.96 - 2.28	$\cdots$	3	5.467e-10	5.13	5.70	>2.38	19	$\cdots$	0.76	V	20.26	SDSS-G

Coordinates (J2000)	f (mJy)				N	Measures			$\frac{\text{Max.}}{\text{Min.}}$	$T_{\min}$	Flags	σ_{nbr}	Type	i	Cross-ID
	Cat.	$\overline{f}$	Range	NVSS		$P(\chi^2, \nu)$	$\sigma_{\max}$	$\Delta_{\max}(\sigma)$		(days)				Mag.	
11 17 01.436 -06 48 32.50	3.43	3.51	1.91 - <4.63	2.56	4	4.398e-08	5.13	5.20	2.09	4	$\cdots$	-0.81	V	$\cdots$	$\cdots$
11 17 09.089 +37 11 31.16	2.61	2.87	1.84 - 5.16	3.39	3	4.051e-09	3.87	5.38	2.15	1	$\cdots$	0.31	V	$\cdots$	$\cdots$
11 17 13.539 +05 37 13.66	2.07	1.99	<1.37 - 2.85	$\cdots$	3	2.036e-07	4.82	5.41	>2.09	2	$\cdots$	-1.00	V	18.57	SDSS-G
11 17 32.739 +22 02 57.67	3.47	3.60	3.31 - 5.69	4.06	3	1.709e-07	4.81	4.89	>1.72	999	$\cdots$	-1.02	V	20.25	SDSS-QSO(P)
11 17 49.878 -02 14 59.55	9.97	10.33	5.67 - 11.45	9.28	4	4.591e-10	6.61	5.47	1.86	3	BN	-1.19	V	$\cdots$	$\cdots$
11 17 53.577 +07 42 13.97	4.78	5.11	2.66 - <12.70	$\cdots$	4	1.630e-07	5.24	4.93	2.05	4	$\cdots$	0.08	V	21.26	SDSS-*
11 18 18.354 +12 16 53.86	6.19	6.22	<4.33 - 6.72	5.73	4	2.987e-08	5.26	5.40	>1.55	2	BN	-0.32	V	$\cdots$	$\cdots$
11 18 33.278 -03 29 30.66	5.69	6.71	4.64 - 7.45	5.88	3	1.268e-09	4.48	4.57	>1.39	3	BN	-0.16	V	$\cdots$	$\cdots$
11 18 51.277 +14 02 14.03	3.70	3.58	2.82 - <8.34	$\cdots$	4	8.647e-07	5.02	4.85	2.26	3	BN	0.16	V	$\cdots$	$\cdots$
11 18 56.737 +13 04 08.80	12.90	13.59	10.24 - 16.39	11.46	3	1.108e-08	5.09	5.59	1.60	1	BN	1.20	V	$\cdots$	XMM
11 19 25.082 +32 48 29.01	12.45	12.34	11.62 - 16.27	13.06	8	1.270e-08	3.54	3.98	>1.39	489	$\cdots$	-0.00	V	19.14	SDSS-QSO(P)
11 19 48.534 +21 37 25.43	2.36	2.58	<1.92 - <7.85	$\cdots$	4	2.428e-07	5.19	4.85	>1.49	2	$\cdots$	0.39	V	$\cdots$	$\cdots$
11 20 03.127 +53 54 02.77	1.19	1.40	<0.74 - <4.55	$\cdots$	4	3.180e-10	5.63	5.95	>2.83	4	$\cdots$	0.76	V	$\cdots$	$\cdots$
11 20 15.399 -05 57 57.87	5.73	5.73	<3.13 - 6.16	4.23	4	5.472e-11	6.42	6.25	>1.97	6	BN	-0.23	V	$\cdots$	$\cdots$
11 20 43.154 +38 28 37.88	3.41	3.53	<2.66 - 3.89	2.74	4	1.125e-07	4.49	4.71	>1.46	2	$\cdots$	-1.58	V	21.49	SDSS-G
11 20 52.441 -05 20 30.34	5.77	5.89	2.36 - <11.86	3.07	4	8.891e-07	5.08	4.92	2.80	31	BN	0.09	V	$\cdots$	$\cdots$
11 20 55.844 -01 06 31.46	1.47	1.50	<1.24 - <2.25	$\cdots$	3	4.816e-07	4.09	4.99	>1.73	2	$\cdots$	-0.40	V	$\cdots$	$\cdots$
11 21 24.342 -03 16 49.74	2.27	2.51	1.01 - 3.41	$\cdots$	3	1.968e-08	5.58	4.60	2.70	3	$\cdots$	0.07	V	$\cdots$	$\cdots$
11 22 16.545 +31 57 18.73	17.67	17.62	11.57 - 24.76	19.35	5	3.663e-08	3.87	4.88	1.90	5	$\cdots$	NA	V	19.35	SDSS-*
11 22 21.530 +05 43 16.58	4.65	4.62	2.27 - <21.22	4.32	4	6.306e-08	5.01	5.04	2.80	1	BN	-0.54	V	$\cdots$	$\cdots$
11 22 35.570 +31 35 09.36	6.72	6.62	3.70 - <12.76	5.12	6	5.610e-12	6.86	5.61	>1.85	95	$\cdots$	-0.43	V	15.94	SDSS-G
11 23 34.362 -01 30 13.75	2.03	1.79	<1.31 - 2.76	$\cdots$	3	6.249e-10	5.23	5.83	>2.12	5	$\cdots$	0.74	V	$\cdots$	$\cdots$
11 24 06.841 +32 36 28.67	8.67	8.93	8.26 - 13.06	11.67	6	3.950e-09	3.95	4.21	1.45	4	$\cdots$	0.31	V	19.61	SDSS-QSO(P)
11 24 58.158 +19 11 12.46	9.87	10.07	4.49 - 11.15	8.34	3	8.493e-13	7.39	6.40	2.32	$\cdots$	BN	-0.51	V	$\cdots$	$\cdots$
11 25 47.476 +12 20 02.40	14.65	15.01	<10.34 - 17.12	10.79	4	5.447e-08	5.72	5.84	>1.66	4	BN	0.04	V	$\cdots$	$\cdots$
11 25 48.333 +12 42 24.13	2.11	2.20	<1.64 - 2.72	$\cdots$	3	1.973e-07	4.86	5.27	>1.66	3	BN	-0.89	V	20.49	SDSS-G
11 27 06.401 +21 56 48.80	4.70	4.99	<3.45 - <14.34	3.70	5	1.660e-09	5.29	5.12	>1.50	4	$\cdots$	-0.49	V	$\cdots$	$\cdots$
11 27 06.603 -07 22 07.16	8.82	7.84	<5.25 - 7.98	8.32	3	9.226e-12	6.01	5.58	>1.52	13	$\cdots$	-0.32	T	$\cdots$	$\cdots$
11 27 27.620 +21 53 51.08	1.88	1.92	<1.23 - <3.44	$\cdots$	4	1.884e-09	5.23	5.68	>1.97	4	$\cdots$	0.37	V	$\cdots$	$\cdots$
11 27 31.128 +27 20 26.48	1.31	1.26	<0.62 - <3.61	$\cdots$	4	9.992e-12	6.09	6.40	>3.10	1	$\cdots$	1.12	V	$\cdots$	$\cdots$
11 27 37.980 +03 17 06.15	3.49	3.50	<2.19 - 4.39	$\cdots$	3	1.389e-10	5.99	6.70	>2.01	7	$\cdots$	0.55	V	19.54	SDSS-G

Coordinates (J2000)	f (mJy)				N	Measures			$\frac{\text{Max.}}{\text{Min.}}$	$T_{\min}$	Flags	σ_{nbr}	Type	i	Cross-ID
	Cat.	$\overline{f}$	Range	NVSS		$P(\chi^2,\nu)$	$\sigma_{\max}$	$\Delta_{\max}(\sigma)$		(days)				Mag.	
11 28 09.536 -02 27 07.57	2.70	2.60	<1.40 - <4.64	$\cdots$	4	8.403e-09	5.58	5.69	>2.07	2	$\cdots$	1.29	V	$\cdots$	$\cdots$
11 28 22.548 +33 04 27.65	4.39	4.63	<2.80 - 6.92	$\cdots$	6	1.750e-09	5.75	6.66	>2.47	483	$\cdots$	-0.73	V	19.80	SDSS-G
11 28 41.459 +28 46 16.47	2.67	2.80	<1.78 - <11.38	2.85	5	3.598e-08	5.50	5.69	>1.81	5	BN	0.82	V	19.68	SDSS-G
11 28 57.382 +37 03 19.98	1.27	1.13	<0.93 - 2.29	$\cdots$	3	1.018e-07	4.01	5.49	>2.45	1	$\cdots$	1.01	T	$\cdots$	$\cdots$
11 28 57.429 +33 46 49.44	1.83	1.73	<0.77 - <4.54	$\cdots$	4	7.128e-14	6.72	7.31	>3.12	1	$\cdots$	1.14	V	$\cdots$	$\cdots$
11 29 05.779 +00 34 42.05	11.67	11.38	6.05 - 13.18	10.51	4	1.506e-08	5.54	5.70	2.14	1	$\cdots$	-0.11	V	21.50	SDSS-G
11 29 10.012 -02 48 46.50	3.42	3.54	1.59 - 3.93	3.15	3	5.683e-08	5.59	5.31	2.48	6	$\cdots$	1.67	V	22.55	SDSS-G
11 29 11.426 +58 38 39.42	6.23	6.08	3.32 - 7.96	4.37	3	9.667e-09	5.42	5.45	2.40	52	$\cdots$	0.16	V	21.39	SDSS-G
11 29 20.911 -05 51 09.47	5.67	5.42	4.02 - 8.85	3.85	3	2.220e-16	6.47	8.03	2.20	4	$\cdots$	-0.19	V	20.94	SDSS-*
11 29 22.104 +60 34 29.56	1.16	1.10	<0.72 - 2.76	$\cdots$	3	2.307e-11	4.56	6.31	>3.80	3	$\cdots$	1.13	T	$\cdots$	$\cdots$
11 29 22.969 +02 18 38.62	3.14	3.21	<2.33 - <7.79	3.73	4	2.776e-07	4.72	5.45	>1.72	1	$\cdots$	0.45	V	18.56	SDSS-G
11 29 52.101 +31 56 38.31	1.73	1.91	1.56 - <2.98	$\cdots$	4	1.218e-07	4.04	5.55	>1.81	5	$\cdots$	-0.27	V	$\cdots$	$\cdots$
11 30 15.256 +38 05 55.33	11.58	12.50	5.87 - 15.58	10.78	5	7.356e-07	5.08	5.20	2.45	6	BN	0.60	V	$\cdots$	$\cdots$
11 30 50.197 +30 18 31.41	1.51	1.35	<0.92 - 1.77	$\cdots$	3	4.619e-07	4.88	5.07	>1.93	3	$\cdots$	0.25	V	$\cdots$	$\cdots$
11 31 09.327 +25 19 54.13	9.40	8.93	5.13 - 9.25	7.89	3	1.182e-07	4.25	4.07	1.80	6	$\cdots$	0.35	V	21.82	SDSS-G
11 31 14.993 +28 20 12.96	4.79	4.80	3.29 - 5.43	4.24	3	5.523e-07	4.54	4.71	1.65	921	$\cdots$	1.20	V	$\cdots$	$\cdots$
11 31 25.858 +18 33 30.77	78.37	78.94	77.53 - 100.12	77.88	6	1.575e-07	3.19	2.89	1.27	$\cdots$	$\cdots$	-0.01	V	$\cdots$	$\cdots$
11 31 37.965 +31 31 21.67	27.79	25.63	25.26 - 40.51	27.51	5	5.408e-09	4.90	4.64	1.60	96	$\cdots$	0.41	V	20.83	SDSS-G
11 31 43.652 +37 17 23.93	3.71	3.71	<2.80 - <15.83	4.12	5	2.738e-08	4.79	4.98	>1.45	1	$\cdots$	-1.31	V	22.49	SDSS-*
11 32 54.521 +11 24 57.42	15.15	13.14	12.77 - 26.22	15.70	4	1.535e-10	5.10	4.92	1.63	1	$\cdots$	-0.83	V	$\cdots$	$\cdots$
11 33 08.236 +06 39 49.80	1.21	1.18	0.79 - <16.19	$\cdots$	4	6.688e-08	4.99	5.57	4.01	1	$\cdots$	0.00	V	$\cdots$	$\cdots$
11 33 14.114 +20 59 25.51	2.33	2.36	<1.84 - <5.72	$\cdots$	4	4.574e-07	4.09	4.40	>1.45	3	$\cdots$	-1.02	V	19.31	SDSS-G
11 33 54.049 -03 08 41.04	9.05	9.96	4.42 - 12.49	11.00	2	2.065e-13	6.82	6.55	2.83	10	$\cdots$	NA	V	$\cdots$	$\cdots$
11 34 02.889 +37 06 09.61	2.79	2.78	2.05 - 4.74	$\cdots$	3	1.677e-07	4.77	5.49	2.31	1	BN	0.80	V	$\cdots$	$\cdots$
11 34 55.865 +36 29 58.75	5.44	5.21	<3.72 - 5.42	4.13	3	2.283e-06	5.05	4.89	>1.45	7	$\cdots$	-0.69	V	$\cdots$	$\cdots$
11 35 06.178 +26 32 39.74	4.40	4.66	3.10 - 5.54	3.63	3	3.137e-08	5.36	4.96	1.79	7	$\cdots$	-0.72	V	16.91	SDSS-G
11 35 11.462 +15 27 48.60	3.59	3.94	2.59 - <8.26	2.84	4	2.947e-07	4.32	4.67	1.74	3	$\cdots$	0.37	V	$\cdots$	$\cdots$
11 35 46.901 -00 53 29.83	8.54	8.47	<5.85 - 8.61	8.54	3	4.603e-07	5.14	4.94	>1.47	6	$\cdots$	0.89	V	$\cdots$	$\cdots$
11 35 53.958 +13 42 14.71	6.86	6.65	5.04 - 9.19	5.64	3	1.198e-07	4.59	4.79	1.82	5	$\cdots$	-1.03	V	14.68	SDSS-G
11 36 03.179 +15 51 09.62	20.61	22.19	17.85 - 100.98	20.50	6	0.000	12.84	13.40	5.66	1	$\cdots$	0.20	V	$\cdots$	CHANDRA
11 36 32.450 +16 09 09.89	4.19	4.32	2.29 - 4.71	4.19	3	3.216e-07	3.83	3.92	1.62	17	$\cdots$	-1.06	V	$\cdots$	$\cdots$

Coordinates (J2000)	f (mJy)				N	Measures			$\frac{\text{Max.}}{\text{Min.}}$	$T_{\min}$	Flags	σ_{nbr}	Type	i	Cross-ID
	Cat.	$\overline{f}$	Range	NVSS		$P(\chi^2,\nu)$	$\sigma_{\max}$	$\Delta_{\max}(\sigma)$		(days)				Mag.	
11 37 16.934 -01 53 37.57	5.57	6.29	3.16 - 6.58	$\cdots$	4	4.520e-10	4.47	4.48	>1.35	1	$\cdots$	0.29	V	$\cdots$	$\cdots$
11 37 22.595 -02 56 53.57	6.14	6.82	2.79 - <14.80	5.49	3	1.234e-11	6.75	6.02	2.53	6	$\cdots$	-1.17	V	19.90	SDSS-G
11 37 22.679 +39 50 49.50	3.12	3.21	<1.77 - <6.67	$\cdots$	5	3.979e-12	5.77	5.75	>2.04	1	$\cdots$	0.71	V	$\cdots$	$\cdots$
11 38 37.148 +61 16 41.09	4.46	4.80	2.44 - 7.74	3.73	3	2.065e-14	5.48	7.56	3.17	4	$\cdots$	0.08	V	19.74	SDSS-*
11 38 53.536 +52 20 39.55	23.30	19.91	19.50 - 28.65	23.84	5	1.806e-11	4.20	3.90	1.42	1	$\cdots$	-0.04	V	20.37	SDSS-G
11 39 02.856 -02 42 15.20	5.43	5.34	2.68 - <13.48	5.32	4	9.836e-08	5.58	5.16	2.08	6	$\cdots$	-0.06	V	$\cdots$	$\cdots$
11 39 14.747 +19 11 19.99	3.12	3.14	<2.36 - <8.87	3.70	4	2.061e-06	5.00	4.90	>1.43	$\cdots$	$\cdots$	0.33	V	21.82	SDSS-G
11 39 33.801 -02 14 46.81	4.74	4.96	<3.15 - 5.45	$\cdots$	4	1.438e-06	5.33	5.29	>1.73	2	$\cdots$	-0.42	V	20.47	SDSS-G
11 40 04.164 +18 19 38.24	29.09	25.40	23.93 - 41.22	30.51	4	2.535e-07	4.64	4.77	1.72	20	BN	-0.14	V	$\cdots$	$\cdots$
11 40 37.896 +21 06 51.74	9.61	9.45	7.25 - 11.09	10.91	4	4.152e-08	5.10	4.47	1.44	3	$\cdots$	0.23	V	$\cdots$	$\cdots$
11 41 19.515 -03 30 45.41	6.11	6.92	3.26 - 7.35	$\cdots$	2	3.618e-13	7.19	6.31	2.26	3	$\cdots$	0.06	V	$\cdots$	$\cdots$
11 41 52.419 -02 15 51.72	6.18	6.56	3.48 - <15.91	5.43	4	6.574e-11	6.48	5.65	1.97	3	$\cdots$	-2.25	V	$\cdots$	$\cdots$
11 42 20.636 +04 29 27.03	1.91	1.93	<1.51 - <10.90	$\cdots$	4	1.472e-08	4.52	5.20	>1.63	388	$\cdots$	1.07	V	21.92	SDSS-G
11 42 44.008 +41 59 08.71	1.45	1.36	0.91 - 2.85	$\cdots$	3	3.005e-07	3.53	4.44	2.70	6	$\cdots$	0.99	V	$\cdots$	$\cdots$
11 42 45.278 +14 46 22.38	1.34	1.16	<0.85 - <3.35	$\cdots$	4	2.322e-09	4.29	5.97	>2.44	5	$\cdots$	1.18	V	$\cdots$	$\cdots$
11 43 15.209 +16 18 09.35	4.56	4.60	4.20 - <10.61	2.80	4	8.387e-09	5.03	5.32	1.93	23	$\cdots$	0.49	V	18.96	SDSS-QSO(P)
11 43 15.480 +21 27 32.89	8.52	8.82	3.54 - <17.07	7.56	4	2.213e-09	6.01	6.10	2.76	7	$\cdots$	-0.12	V	$\cdots$	$\cdots$
11 43 18.658 -03 25 52.43	4.56	4.62	<1.93 - 5.08	5.57	3	0.000	9.79	8.72	>2.64	0	$\cdots$	-0.02	V	17.72	SDSS-G
11 43 28.876 +31 27 11.61	9.54	9.07	4.04 - <16.13	8.48	5	3.311e-11	5.61	5.38	2.21	0	BN	0.21	V	19.12	SDSS-QSO(P)
11 43 30.948 +08 25 01.60	5.16	5.10	3.26 - <11.52	4.86	6	1.652e-07	5.19	5.07	>1.50	4	$\cdots$	-0.25	V	19.58	SDSS-G
11 43 40.012 +57 54 34.63	8.80	8.68	4.07 - 10.43	7.58	4	1.525e-10	5.56	4.99	2.15	7	$\cdots$	-2.01	V	$\cdots$	$\cdots$
11 43 40.474 +19 15 02.51	1.89	1.61	<1.14 - 2.05	$\cdots$	3	2.283e-07	4.91	5.49	>1.80	$\cdots$	$\cdots$	0.70	V	$\cdots$	$\cdots$
11 44 05.988 +33 20 45.16	3.35	3.23	1.65 - 3.89	3.53	3	9.853e-08	5.22	5.36	2.22	483	$\cdots$	-0.47	V	$\cdots$	$\cdots$
11 44 20.991 +08 07 01.94	4.95	4.91	<3.30 - <7.35	4.00	4	2.673e-09	5.92	6.10	>1.71	0	$\cdots$	1.78	V	25.14	SDSS-*
11 44 30.527 +30 53 00.24	6.22	6.71	3.15 - 6.89	6.85	4	3.151e-07	4.93	4.52	>2.18	414	$\cdots$	0.12	V	14.41	SDSS-G
11 44 37.614 +22 05 40.99	9.96	11.03	7.79 - 27.15	10.24	3	2.210e-10	5.24	6.10	3.48	997	BN	-0.76	V	20.80	SDSS-*
11 44 50.636 +41 44 20.93	10.15	9.81	5.55 - 11.86	8.50	5	1.499e-07	5.17	5.17	2.14	7	$\cdots$	0.06	V	$\cdots$	$\cdots$
11 45 25.507 +27 17 44.62	1.21	1.19	<0.87 - 2.06	$\cdots$	3	3.553e-10	4.43	5.67	>2.37	1	$\cdots$	0.78	T	$\cdots$	$\cdots$
11 45 32.230 +19 41 51.12	5.50	5.38	4.57 - 14.93	6.60	3	0.000	9.40	9.81	3.26	$\cdots$	$\cdots$	NA	V	$\cdots$	$\cdots$
11 45 35.588 +03 27 41.40	3.13	3.28	1.64 - 3.78	3.93	3	1.058e-07	3.90	4.42	2.31	4	$\cdots$	-0.51	V	$\cdots$	$\cdots$
11 45 39.976 +36 40 00.83	2.31	2.33	<1.66 - 2.92	3.24	3	4.710e-08	5.14	5.75	>1.75	5	$\cdots$	0.73	V	$\cdots$	$\cdots$

Coordinates (J2000)	f (mJy)				N	Measures			$\frac{\text{Max.}}{\text{Min.}}$	$T_{\min}$	Flags	σ_{nbr}	Type	i	Cross-ID
	Cat.	$\overline{f}$	Range	NVSS		$P(\chi^2,\nu)$	$\sigma_{\max}$	$\Delta_{\max}(\sigma)$		(days)				Mag.	
11 45 48.365 +07 43 50.91	2.13	2.11	1.00 - <5.59	$\cdots$	4	8.457e-09	4.12	5.76	3.11	2	$\cdots$	0.87	V	$\cdots$	$\cdots$
11 46 51.940 +21 21 52.48	5.45	5.12	<3.64 - 5.35	5.79	3	3.826e-08	5.02	4.97	>1.47	0	$\cdots$	-0.27	V	$\cdots$	$\cdots$
11 47 13.641 +36 53 39.71	7.10	6.86	4.86 - 8.47	6.05	3	9.050e-09	5.42	4.90	1.74	6	$\cdots$	-0.14	V	$\cdots$	$\cdots$
11 47 21.522 -06 49 57.19	1.33	1.38	<1.15 - <4.17	$\cdots$	4	6.048e-08	3.95	5.32	>1.89	4	$\cdots$	0.70	V	$\cdots$	$\cdots$
11 47 35.636 +07 31 24.77	9.13	8.81	4.78 - 10.87	10.32	4	9.904e-08	5.02	5.89	2.27	2	BN	-0.08	V	$\cdots$	$\cdots$
11 47 35.728 +62 48 05.92	7.36	7.70	5.28 - 9.90	8.65	3	1.110e-16	7.09	6.92	1.87	5	$\cdots$	0.01	V	$\cdots$	$\cdots$
11 48 02.465 +27 14 48.25	2.30	2.27	1.23 - 3.38	$\cdots$	4	3.565e-08	4.28	5.47	2.63	4	$\cdots$	0.61	V	$\cdots$	$\cdots$
11 48 08.364 +18 33 18.31	7.86	7.25	3.08 - <16.99	8.55	4	1.470e-08	5.62	5.63	2.56	$\cdots$	BN	-0.82	V	$\cdots$	$\cdots$
11 48 22.954 +18 42 31.43	6.35	6.43	3.84 - 9.76	7.22	4	9.452e-08	5.43	5.22	1.84	$\cdots$	BN	-1.05	V	$\cdots$	$\cdots$
11 48 36.138 -07 03 19.96	1.69	1.60	<0.85 - <3.43	$\cdots$	4	2.346e-11	5.87	6.55	>2.90	2	BN	-3.06	V	$\cdots$	$\cdots$
11 48 43.733 -07 16 09.54	11.09	10.42	<3.49 - 12.85	5.39	4	0.000	11.32	10.94	>3.68	2	BN	-1.01	V	$\cdots$	GSC2-FIRST-G
11 49 12.008 +20 52 25.22	5.36	5.69	2.88 - 5.84	5.40	3	5.708e-07	5.30	4.81	2.03	3	$\cdots$	0.13	V	$\cdots$	$\cdots$
11 49 37.731 +14 39 57.23	6.32	6.42	<4.40 - 7.46	5.14	3	4.866e-07	5.32	5.07	>1.48	5	$\cdots$	0.15	V	22.50	SDSS-*
11 49 40.770 +33 15 04.83	3.05	3.16	<2.34 - <16.02	3.00	6	1.318e-07	4.56	5.10	>1.58	483	$\cdots$	1.30	V	$\cdots$	$\cdots$
11 49 57.140 +32 54 36.01	6.31	6.12	<2.62 - 7.07	4.75	4	2.287e-14	7.64	7.73	>2.70	484	$\cdots$	-0.20	V	$\cdots$	$\cdots$
11 51 10.719 +53 37 52.65	34.40	32.58	31.50 - 44.46	32.24	3	5.604e-09	4.60	4.29	1.41	1	$\cdots$	0.12	V	$\cdots$	$\cdots$
11 51 20.233 +33 03 16.02	2.67	2.61	1.59 - <9.46	2.21	5	5.063e-11	4.94	6.59	2.27	484	$\cdots$	1.11	V	$\cdots$	$\cdots$
11 52 07.196 +20 57 20.98	4.52	4.59	2.48 - 5.01	4.35	4	2.890e-08	5.83	5.45	2.02	3	$\cdots$	0.36	V	16.36	SDSS-G
11 52 14.385 +03 36 46.94	3.36	3.54	<2.08 - 6.39	2.66	4	3.395e-07	5.31	5.22	>1.76	4	$\cdots$	0.54	V	20.56	SDSS-QSO(P)
11 52 17.988 -07 55 05.93	4.68	4.91	2.55 - 6.60	5.11	3	1.401e-07	4.85	5.21	2.59	383	$\cdots$	0.63	V	$\cdots$	$\cdots$
11 52 35.790 -04 48 27.90	2.01	1.98	<1.52 - <2.81	$\cdots$	3	1.138e-08	4.82	5.65	>1.74	8	$\cdots$	-0.00	V	$\cdots$	$\cdots$
11 53 11.151 +18 12 13.70	2.01	1.93	<1.22 - 2.37	$\cdots$	3	3.282e-08	5.41	5.61	>1.89	20	$\cdots$	1.00	V	22.64	SDSS-*
11 53 46.630 +38 51 26.92	4.01	4.05	2.08 - 4.56	2.39	4	3.921e-06	5.11	4.45	2.19	1	$\cdots$	-0.68	V	$\cdots$	$\cdots$
11 53 48.754 -04 04 41.76	3.87	3.56	<1.82 - 4.10	$\cdots$	3	6.407e-13	7.10	7.19	>2.25	905	$\cdots$	-0.48	V	$\cdots$	$\cdots$
11 53 51.097 +28 33 20.92	13.50	14.34	10.61 - 15.36	17.82	4	3.527e-10	5.49	4.56	1.45	12	$\cdots$	0.51	V	$\cdots$	$\cdots$
11 54 37.050 -04 05 18.40	1.64	1.43	<1.25 - 2.23	$\cdots$	3	2.366e-07	3.92	5.29	>1.78	905	$\cdots$	0.12	T	$\cdots$	GSC2-FIRST-G
11 55 54.609 -02 43 49.51	10.04	10.13	4.79 - 10.74	9.95	3	0.000	7.94	6.84	2.24	8	$\cdots$	0.30	V	$\cdots$	$\cdots$
11 56 46.553 +42 38 07.61	12.64	11.51	10.06 - 20.45	$\cdots$	3	2.220e-16	6.72	7.24	2.03	483	$\cdots$	0.50	V	16.68	SDSS-G
11 57 02.446 +21 02 28.29	5.18	4.96	<3.42 - <12.08	$\cdots$	5	8.067e-07	5.01	4.85	>1.48	1	$\cdots$	0.18	V	$\cdots$	$\cdots$
11 57 25.452 +41 51 19.55	5.75	5.84	<3.15 - 8.83	6.39	4	1.300e-10	5.79	6.56	>2.31	0	$\cdots$	0.26	V	$\cdots$	$\cdots$
11 58 46.776 +58 40 50.34	4.49	4.67	3.08 - 5.36	2.57	3	3.521e-07	3.72	4.27	>1.30	0	BN	0.38	V	$\cdots$	$\cdots$

Coordinates (J2000)	f (mJy)				N	Measures			$\frac{\text{Max.}}{\text{Min.}}$	$T_{\min}$	Flags	σ_{nbr}	Type	i	Cross-ID
	Cat.	$\overline{f}$	Range	NVSS		$P(\chi^2,\nu)$	$\sigma_{\max}$	$\Delta_{\max}(\sigma)$		(days)				Mag.	
11 58 50.768 -02 53 43.93	4.87	5.36	<4.26 - 6.67	4.95	4	7.102e-08	3.93	4.57	>1.45	0	$\cdots$	0.82	V	$\cdots$	$\cdots$
11 59 22.573 -05 52 17.18	2.38	2.29	1.09 - 2.95	$\cdots$	3	5.333e-07	4.76	4.53	2.48	2	$\cdots$	-0.01	V	$\cdots$	$\cdots$
11 59 25.118 +15 12 33.36	6.24	6.29	5.29 - 12.35	5.92	4	7.551e-08	5.33	5.90	2.33	25	$\cdots$	0.67	V	$\cdots$	$\cdots$
12 00 13.553 +43 06 42.70	1.45	1.31	<0.81 - 2.39	$\cdots$	4	4.918e-10	5.32	6.05	>2.96	2	$\cdots$	1.29	V	$\cdots$	$\cdots$
12 00 27.319 +32 58 10.69	1.93	2.03	<1.50 - 2.41	$\cdots$	4	1.237e-07	5.23	5.57	>1.61	1	$\cdots$	-0.05	V	20.56	SDSS-QSO(P)
12 01 02.933 +39 11 44.80	2.82	3.00	1.93 - <4.88	$\cdots$	4	4.344e-07	3.70	4.48	2.35	23	BN	-0.12	V	$\cdots$	$\cdots$
12 01 05.881 +20 23 10.85	5.91	5.85	2.56 - 6.19	4.28	3	1.173e-06	5.18	4.78	2.33	5	$\cdots$	0.10	V	21.24	SDSS-G
12 01 07.863 +24 53 33.32	8.78	8.96	3.04 - 9.15	8.08	3	3.141e-12	7.27	6.50	3.01	2	$\cdots$	-0.73	V	$\cdots$	$\cdots$
12 01 35.629 +33 12 33.28	4.75	4.53	<3.05 - <9.02	4.00	6	1.176e-08	5.61	5.35	>1.58	$\cdots$	$\cdots$	-1.50	V	$\cdots$	$\cdots$
12 01 49.193 +03 39 03.44	9.18	9.05	4.67 - 9.58	8.73	3	9.368e-07	5.22	4.64	1.95	1	$\cdots$	0.19	V	19.73	SDSS-G
12 02 10.433 +16 33 28.02	1.25	1.28	<1.05 - <3.75	$\cdots$	4	1.010e-07	4.06	5.25	>2.02	1	$\cdots$	0.23	V	21.28	SDSS-G
12 02 25.829 +30 37 38.12	4.44	4.46	<2.47 - <7.81	3.76	3	7.749e-11	6.39	6.17	>1.97	3	$\cdots$	0.64	V	19.39	SDSS-G
12 02 40.649 +21 56 20.99	8.40	7.14	6.76 - 11.24	9.19	3	1.356e-07	5.27	5.28	1.66	0	$\cdots$	-3.10	V	20.14	SDSS-G
12 02 49.673 +31 36 40.33	2.51	2.70	<1.67 - <15.62	$\cdots$	6	1.080e-09	5.48	5.70	>1.83	95	$\cdots$	-0.92	V	$\cdots$	$\cdots$
12 02 53.621 +34 31 29.70	4.54	4.47	1.43 - <15.83	4.61	5	1.110e-16	7.09	6.79	3.43	5	$\cdots$	0.68	V	$\cdots$	$\cdots$
12 02 55.734 +04 33 47.25	2.23	2.21	1.39 - 3.10	$\cdots$	3	2.049e-07	3.65	4.87	>2.24	388	BN	-0.25	V	$\cdots$	$\cdots$
12 03 02.267 +03 37 53.99	2.49	2.60	<1.66 - 3.29	$\cdots$	4	3.952e-11	5.99	6.56	>1.99	1	$\cdots$	-0.56	V	19.26	SDSS-QSO(P)
12 03 19.427 +04 38 15.57	3.64	3.58	2.24 - <13.88	3.39	4	2.063e-10	5.13	5.72	>1.73	388	BN	-0.11	V	$\cdots$	$\cdots$
12 03 57.217 -01 38 26.51	2.20	2.34	<1.73 - <7.93	$\cdots$	4	3.608e-08	5.28	5.61	>1.70	1	$\cdots$	1.18	V	16.02	SDSS-G
12 04 28.315 +03 52 59.25	5.38	5.42	<4.02 - 7.42	$\cdots$	4	1.167e-08	4.92	5.35	>1.53	1	BN	0.61	V	$\cdots$	$\cdots$
12 04 39.877 +50 28 20.71	2.32	2.32	1.43 - 3.59	$\cdots$	3	2.244e-09	4.80	5.94	2.50	27	$\cdots$	-0.09	V	$\cdots$	$\cdots$
12 04 50.878 +29 20 33.40	1.90	1.66	<1.40 - 2.96	$\cdots$	3	1.839e-08	4.35	5.92	>2.12	11	$\cdots$	-1.03	V	21.79	SDSS-G
12 04 53.441 -04 59 41.50	4.62	4.52	1.71 - 4.70	$\cdots$	3	3.036e-10	6.49	5.94	2.76	40	$\cdots$	-1.39	V	$\cdots$	$\cdots$
12 05 26.547 +32 54 33.42	3.53	3.39	1.80 - 4.03	4.21	4	3.240e-07	5.32	4.98	2.24	488	$\cdots$	0.44	V	15.29	SDSS-G
12 05 51.716 +21 11 20.45	10.99	11.12	6.29 - 13.44	8.62	5	9.746e-10	6.53	5.50	1.82	5	$\cdots$	0.23	V	$\cdots$	$\cdots$
12 06 06.530 +61 42 04.63	23.40	25.19	24.94 - 36.24	25.18	5	5.697e-08	3.92	3.61	1.41	0	$\cdots$	0.18	V	$\cdots$	$\cdots$
12 06 08.024 +36 43 31.29	3.11	3.01	<2.06 - <24.94	$\cdots$	6	1.294e-07	5.33	5.40	>1.62	5	$\cdots$	-0.40	V	21.89	SDSS-G
12 06 18.560 -07 36 45.19	6.53	7.24	4.32 - 8.39	9.55	2	2.444e-13	6.93	6.31	1.94	0	BN	-0.24	V	$\cdots$	$\cdots$
12 06 26.572 +00 09 31.41	4.44	4.35	2.60 - 10.80	4.47	4	2.249e-07	4.98	4.75	1.86	3	$\cdots$	0.92	V	18.13	SDSS-G
12 07 28.795 +25 30 18.66	17.03	16.69	16.41 - 38.70	13.66	6	6.677e-08	4.93	5.18	>1.96	0	$\cdots$	-0.06	V	19.62	SDSS-G
12 07 47.271 -06 08 57.51	4.11	4.08	1.87 - <13.68	$\cdots$	4	8.023e-12	6.63	5.92	2.87	2	$\cdots$	-0.93	V	$\cdots$	$\cdots$

Coordinates (J2000)	f (mJy)				N	Measures			Max. Min.	T_{min}	Flags	σ_{nbr}	Type	i	Cross-ID
	Cat.	$\overline{f}$	Range	NVSS		$P(\chi^2,\nu)$	σ_{max}	$\Delta_{max}(\sigma)$		(days)				Mag.	
12 08 06.423 +36 53 12.45	2.84	2.75	1.65 - 5.35	2.66	3	1.124e-07	4.85	5.64	3.24	6	$\cdots$	0.11	V	$\cdots$	$\cdots$
12 08 12.253 +33 13 22.10	2.37	2.61	1.50 - 4.22	3.29	4	3.759e-12	5.35	6.76	2.81	483	$\cdots$	0.35	V	$\cdots$	$\cdots$
12 08 15.370 +20 39 42.35	5.78	5.89	4.13 - 6.77	5.79	3	2.815e-09	4.93	5.11	1.64	6	$\cdots$	0.52	V	$\cdots$	$\cdots$
12 08 56.060 -03 19 45.75	1.82	1.82	<1.10 - <2.79	$\cdots$	3	1.072e-07	4.94	5.29	>1.99	3	$\cdots$	0.49	V	$\cdots$	$\cdots$
12 09 02.812 +43 57 49.59	9.73	9.80	<5.47 - 11.39	6.71	5	1.151e-06	5.38	5.63	>2.08	2	BN	-0.43	V	18.66	SDSS-G
12 10 11.177 +57 49 19.91	11.08	11.42	11.19 - 21.42	15.12	4	2.178e-09	6.44	6.19	1.91	1396	$\cdots$	0.31	V	15.01	SDSS-G
12 10 12.620 +33 18 34.10	2.64	2.92	<2.05 - <6.11	3.42	4	5.462e-08	5.11	5.38	>1.63	483	$\cdots$	0.70	V	22.14	SDSS-G
12 10 32.644 +44 59 27.86	5.47	5.91	4.44 - 7.69	5.89	4	6.225e-08	4.54	4.81	1.73	8	$\cdots$	-0.16	V	20.39	SDSS-QSO(P)
12 11 39.580 -07 40 05.06	8.24	7.99	6.93 - 12.61	8.42	4	4.448e-10	6.16	6.73	1.82	386	$\cdots$	-0.62	V	$\cdots$	GSC2-FIRST-G
12 12 02.904 +25 48 44.88	3.90	4.08	<2.50 - 4.95	$\cdots$	4	1.721e-08	5.64	5.95	>1.98	1	$\cdots$	0.13	V	20.86	SDSS-G
12 12 29.934 +43 51 44.01	1.73	1.70	<1.12 - <11.42	$\cdots$	5	4.016e-07	4.75	5.04	>1.77	1	$\cdots$	1.05	V	21.45	SDSS-G
12 12 45.319 +17 27 40.94	1.39	1.40	0.94 - 2.55	$\cdots$	3	3.327e-07	3.79	4.62	2.73	1	$\cdots$	1.36	V	$\cdots$	$\cdots$
12 12 48.300 -06 08 58.20	3.09	3.12	<2.09 - <6.62	3.44	4	2.650e-07	5.10	5.43	>1.75	2	$\cdots$	1.13	V	$\cdots$	GSC2-FIRST-G
12 13 10.620 +59 52 15.22	4.45	4.23	<3.00 - 5.55	4.69	4	1.683e-06	5.06	5.09	>1.62	1	$\cdots$	-0.20	V	20.70	SDSS-G
12 13 29.290 +50 44 29.44	99.65	93.32	90.29 - 135.94	94.20	5	3.142e-14	4.77	4.45	1.51	27	$\cdots$	-1.10	V	11.98	SDSS-G
12 13 49.783 +54 10 32.80	18.71	18.85	13.70 - 19.92	10.79	3	4.996e-15	5.93	4.58	1.43	1	$\cdots$	-0.34	V	21.00	SDSS-*
12 14 30.385 -01 34 05.78	4.42	4.54	2.23 - <10.00	3.60	4	1.043e-09	6.14	5.62	2.25	6	$\cdots$	-0.16	V	$\cdots$	$\cdots$
12 14 46.340 +14 05 33.07	6.26	6.82	3.09 - 7.29	4.58	3	4.441e-16	8.15	7.00	2.36	15	BN	-1.12	V	15.46	SDSS-G
12 15 05.281 +19 11 23.38	67.91	67.78	65.32 - 87.10	67.77	5	1.052e-08	3.64	3.44	1.31	$\cdots$	$\cdots$	0.38	V	$\cdots$	$\cdots$
12 15 39.042 +27 16 26.38	3.48	3.37	1.89 - 5.52	4.15	3	2.001e-11	5.06	6.61	2.91	4	$\cdots$	-0.09	V	$\cdots$	$\cdots$
12 15 41.210 +32 01 01.00	4.29	4.38	1.77 - 4.84	2.79	3	3.340e-07	5.21	5.20	2.73	4	$\cdots$	0.61	V	19.30	SDSS-G
12 16 03.823 +16 47 21.19	13.84	14.67	13.73 - 20.34	12.47	4	8.437e-09	4.02	4.14	1.40	6	$\cdots$	-1.00	V	$\cdots$	$\cdots$
12 16 24.192 +19 05 42.67	17.36	17.70	17.24 - 28.82	19.86	5	1.959e-06	5.09	4.80	1.64	$\cdots$	$\cdots$	-0.46	V	$\cdots$	$\cdots$
12 16 39.419 +03 36 46.24	2.10	2.24	2.09 - <8.24	2.39	4	8.626e-07	5.20	5.28	>2.99	0	$\cdots$	1.44	V	$\cdots$	$\cdots$
12 16 53.719 +10 28 06.82	1.92	1.87	1.27 - 3.32	$\cdots$	3	3.760e-07	4.59	5.27	2.60	0	$\cdots$	0.96	V	20.61	SDSS-G
12 16 55.851 -00 53 42.53	1.71	1.69	<1.17 - 2.97	$\cdots$	3	1.211e-13	4.90	6.77	>2.54	4	$\cdots$	1.22	T	$\cdots$	$\cdots$
12 17 21.628 +27 44 18.75	6.28	6.28	3.72 - 6.95	7.03	3	6.781e-09	5.89	5.49	1.87	1	$\cdots$	0.71	V	$\cdots$	$\cdots$
12 17 35.248 +63 54 51.68	4.75	4.56	<3.28 - <7.05	$\cdots$	5	1.519e-07	4.45	4.51	>1.46	4	BN	-2.16	V	$\cdots$	$\cdots$
12 17 36.262 +33 07 03.06	2.10	2.18	<1.16 - <4.01	$\cdots$	4	0.000	7.72	8.38	>2.73	484	$\cdots$	-0.58	V	$\cdots$	$\cdots$
12 18 06.339 +63 47 47.03	6.99	6.86	3.64 - <15.91	3.84	5	4.416e-06	5.01	4.61	2.16	0	BN	-0.25	V	20.08	SDSS-G
12 19 07.207 +05 38 56.90	10.08	10.78	4.44 - 15.98	$\cdots$	3	0.000	19.86	12.54	3.60	1	$\cdots$	0.52	V	21.15	SDSS-G

Coordinates (J2000)	f (mJy)				N	Measures			$\frac{\text{Max.}}{\text{Min.}}$	$T_{\min}$	Flags	σ_{nbr}	Type	i	Cross-ID
	Cat.	$\overline{f}$	Range	NVSS		$P(\chi^2,\nu)$	$\sigma_{\max}$	$\Delta_{\max}(\sigma)$		(days)				Mag.	
12 19 43.689 +00 36 19.42	5.34	5.65	2.70 - 5.78	4.06	3	5.715e-07	5.25	4.78	2.14	1	$\cdots$	-1.00	V	20.79	SDSS-G
12 19 57.711 -07 42 07.82	6.87	7.14	4.02 - 7.95	5.06	4	3.331e-16	8.32	6.95	1.98	386	$\cdots$	0.94	V	$\cdots$	GSC2-FIRST-G
12 20 23.339 +14 41 32.69	15.51	15.32	11.95 - 19.83	12.29	3	5.407e-11	5.18	5.92	1.66	8	$\cdots$	0.85	V	19.66	SDSS-G
12 21 16.069 +58 06 52.43	5.61	5.82	2.52 - 7.58	6.47	5	9.567e-08	5.24	5.61	3.01	457	$\cdots$	0.28	V	$\cdots$	$\cdots$
12 21 17.465 -06 30 39.09	6.38	6.23	2.85 - 6.39	6.40	3	1.510e-07	5.13	4.80	2.24	4	$\cdots$	-0.24	V	$\cdots$	$\cdots$
12 21 26.096 +61 37 19.82	2.55	2.61	1.27 - 4.20	$\cdots$	3	1.901e-07	3.91	5.41	3.31	461	$\cdots$	-0.68	V	$\cdots$	$\cdots$
12 21 35.116 -06 53 57.87	2.75	2.84	1.90 - <6.48	$\cdots$	4	1.064e-07	4.09	4.44	>1.41	2	$\cdots$	-2.21	V	$\cdots$	$\cdots$
12 21 41.942 +01 55 12.08	4.19	4.07	2.70 - 4.82	$\cdots$	3	3.519e-07	4.89	4.65	1.71	4	$\cdots$	-1.09	V	$\cdots$	$\cdots$
12 22 01.249 +05 15 45.48	31.83	31.72	17.80 - 33.48	26.39	4	2.935e-06	5.11	4.80	1.88	1	$\cdots$	0.41	V	21.10	SDSS-*
12 22 11.642 +01 37 14.19	8.31	8.17	5.50 - 8.63	7.63	4	2.361e-09	5.54	4.73	1.57	2	$\cdots$	-0.48	V	21.37	SDSS-G
12 22 16.959 +15 49 01.61	14.32	14.15	13.12 - 28.45	16.00	4	4.113e-08	4.09	4.30	2.17	17	$\cdots$	0.52	V	21.83	SDSS-G
12 22 29.557 +01 22 23.24	1.75	1.74	<1.01 - <4.49	$\cdots$	4	1.921e-09	5.89	5.62	>1.95	56	$\cdots$	-0.05	V	$\cdots$	$\cdots$
12 22 52.548 +19 51 34.59	2.84	2.83	1.20 - <7.21	$\cdots$	4	1.207e-08	4.70	5.14	>2.72	$\cdots$	$\cdots$	0.26	V	$\cdots$	$\cdots$
12 23 04.691 +28 32 47.62	10.66	10.83	3.88 - 11.28	9.54	4	2.461e-09	6.27	5.91	2.91	909	BN	-0.77	V	18.96	SDSS-QSO(P)
12 23 29.835 +04 37 53.52	2.21	1.98	0.99 - <5.44	$\cdots$	4	2.389e-11	4.67	5.84	>2.20	388	BN	0.70	V	$\cdots$	$\cdots$
12 23 44.996 +46 24 32.44	2.58	2.55	1.37 - 3.55	$\cdots$	4	4.089e-07	3.89	5.28	2.59	2	$\cdots$	-0.99	V	$\cdots$	$\cdots$
12 23 58.993 +40 44 09.20	9.56	9.38	<5.84 - 11.89	$\cdots$	5	1.698e-09	5.86	6.12	>2.04	2	$\cdots$	-0.27	V	15.53	SDSS-QSO(S)
12 24 24.902 +57 25 28.06	6.57	7.72	<5.15 - 8.60	6.78	4	1.391e-09	4.98	4.85	>1.53	24	$\cdots$	-1.33	V	$\cdots$	$\cdots$
12 24 55.477 -00 51 11.15	1.18	1.20	<0.94 - 2.26	$\cdots$	3	8.018e-08	3.87	5.45	>2.40	4	$\cdots$	-0.15	T	$\cdots$	$\cdots$
12 24 55.829 +57 50 34.97	16.14	15.54	9.47 - 25.83	15.93	4	6.646e-08	5.30	5.55	2.73	0	$\cdots$	0.68	V	$\cdots$	$\cdots$
12 25 04.552 +50 27 04.03	1.97	1.93	1.16 - 2.95	$\cdots$	3	5.420e-08	3.76	5.26	2.55	27	$\cdots$	1.17	V	$\cdots$	$\cdots$
12 25 12.931 +12 18 36.11	19.09	18.77	7.49 - 20.05	$\cdots$	4	1.986e-06	5.30	5.16	2.68	4	$\cdots$	-1.07	V	17.25	SDSS-QSO(S)
12 25 41.799 +36 58 04.25	3.04	3.12	<1.79 - <14.51	$\cdots$	5	8.115e-07	5.21	5.16	>1.84	1	$\cdots$	-0.70	V	$\cdots$	$\cdots$
12 26 02.816 +56 22 54.88	13.11	12.40	11.63 - 18.25	15.15	4	6.374e-08	5.13	4.88	1.53	2	$\cdots$	0.18	V	19.32	SDSS-QSO(S)
12 26 26.741 +02 33 37.54	7.74	7.67	2.44 - 8.75	$\cdots$	3	1.110e-16	7.90	7.52	3.58	65	$\cdots$	1.05	V	$\cdots$	$\cdots$
12 26 50.431 +02 39 32.63	6.76	6.71	3.08 - 10.54	$\cdots$	4	1.431e-13	6.60	6.73	>3.43	67	$\cdots$	-1.01	V	19.14	SDSS-G
12 27 11.495 -04 02 25.47	5.14	5.28	4.92 - <15.88	3.93	4	6.578e-07	5.16	5.25	1.78	916	$\cdots$	0.29	V	$\cdots$	$\cdots$
12 27 17.135 +10 24 01.55	4.07	3.97	<2.88 - <5.22	$\cdots$	4	3.141e-07	5.00	5.00	>1.47	3	$\cdots$	0.35	V	$\cdots$	$\cdots$
12 27 19.116 +21 37 37.57	5.43	5.57	<3.69 - 5.96	5.30	4	2.129e-09	5.90	5.50	>1.55	6	$\cdots$	-0.06	V	20.97	SDSS-G
12 27 31.805 +18 51 10.54	3.93	3.53	3.03 - 6.42	$\cdots$	3	3.151e-09	4.80	5.33	2.12	$\cdots$	$\cdots$	-0.20	V	$\cdots$	$\cdots$
12 28 08.309 +21 05 49.80	3.02	3.11	2.25 - 4.72	$\cdots$	3	2.070e-09	4.80	5.76	2.01	6	$\cdots$	0.28	V	$\cdots$	$\cdots$

Coordinates (J2000)	f (mJy)				N	Measures			$\frac{\text{Max.}}{\text{Min.}}$	$T_{\min}$	Flags	σ_{nbr}	Type	i	Cross-ID
	Cat.	$\overline{f}$	Range	NVSS		$P(\chi^2,\nu)$	$\sigma_{\max}$	$\Delta_{\max}(\sigma)$		(days)				Mag.	
12 28 18.435 +61 46 22.19	4.83	4.87	<3.20 - 5.68	$\cdots$	4	1.910e-07	4.57	5.07	>1.77	4	$\cdots$	-0.08	V	18.14	SDSS-G
12 28 26.429 +39 47 54.17	5.72	4.91	4.47 - <15.02	40.89	4	2.669e-11	6.47	6.64	2.26	1	$\cdots$	-0.36	V	20.08	SDSS-QSO(S)
12 28 45.132 +20 40 39.31	2.64	2.84	<2.00 - 3.51	$\cdots$	3	6.969e-09	5.53	5.89	>1.76	5	BN	-0.40	V	$\cdots$	$\cdots$
12 28 53.423 -01 05 26.19	3.67	3.70	<2.34 - 3.85	3.44	3	1.853e-06	5.09	5.02	>1.64	4	$\cdots$	0.86	V	$\cdots$	$\cdots$
12 29 02.937 +21 32 10.95	1.90	1.71	<1.09 - 2.29	3.09	3	7.237e-09	5.29	5.70	>2.10	4	$\cdots$	-0.17	V	17.85	SDSS-G
12 29 46.348 +09 11 50.44	5.52	5.83	2.19 - 7.40	5.52	4	1.972e-12	7.06	6.22	>2.74	1	$\cdots$	-0.61	V	$\cdots$	$\cdots$
12 29 51.987 +43 31 28.87	2.82	2.99	2.29 - 3.47	3.06	3	1.697e-07	4.64	5.10	>1.49	2	$\cdots$	0.43	V	$\cdots$	$\cdots$
12 30 16.531 +26 20 15.88	3.95	4.17	3.02 - 5.56	2.93	3	3.527e-09	4.61	5.32	1.84	5	$\cdots$	-0.82	V	19.93	SDSS-QSO(P)
12 30 40.825 +37 28 37.20	90.56	88.00	85.45 - 130.43	92.39	3	5.255e-07	5.34	4.95	1.53	7	$\cdots$	0.26	V	$\cdots$	$\cdots$
12 31 35.973 -02 38 47.56	4.11	4.26	<2.89 - 4.69	$\cdots$	3	1.252e-07	5.52	5.09	>1.50	6	BN	0.65	V	$\cdots$	$\cdots$
12 32 00.366 +40 25 46.55	4.40	4.36	3.89 - <11.61	5.14	5	1.998e-10	6.28	6.58	2.18	5	$\cdots$	0.15	V	22.34	SDSS-*
12 32 19.362 -01 08 03.46	3.37	3.68	1.98 - <5.52	$\cdots$	4	4.504e-13	6.50	6.96	2.52	6	$\cdots$	-0.36	V	21.61	SDSS-G
12 32 46.622 -01 36 39.48	4.53	4.58	2.40 - <9.12	$\cdots$	4	8.327e-15	6.35	6.45	>1.77	7	$\cdots$	-0.39	V	$\cdots$	SDSS-QSO(S)
12 32 47.124 -02 20 09.11	4.16	4.00	<1.77 - 4.62	2.69	3	2.063e-11	6.78	6.67	>2.61	5	BN	-0.87	V	$\cdots$	$\cdots$
12 32 47.238 +61 48 50.00	19.99	18.72	10.18 - 23.00	20.25	6	3.648e-07	3.88	4.81	2.26	7	$\cdots$	0.26	V	21.84	SDSS-G
12 33 20.424 +02 02 12.25	42.47	36.58	32.41 - 84.42	52.77	3	0.000	7.91	8.19	2.60	2	$\cdots$	3.24	V	$\cdots$	$\cdots$
12 34 04.841 -02 13 01.62	37.47	38.62	12.35 - 40.09	34.22	4	0.000	9.23	7.88	3.25	2	$\cdots$	0.27	V	$\cdots$	$\cdots$
12 34 07.756 +02 22 20.83	24.75	25.13	<11.68 - 26.38	20.28	3	5.762e-14	7.72	7.38	>2.25	2	$\cdots$	-0.19	V	21.30	SDSS-G
12 34 09.554 +34 55 58.26	1.83	1.81	1.65 - <13.08	$\cdots$	5	2.073e-06	5.27	5.35	4.29	1	$\cdots$	1.35	V	19.96	SDSS-G
12 34 29.703 +01 38 14.37	9.01	8.83	<3.26 - 9.06	8.29	2	4.441e-16	8.12	7.66	>2.78	2	$\cdots$	0.04	T	$\cdots$	$\cdots$
12 34 39.056 +39 53 01.28	2.69	3.14	<1.81 - <5.65	$\cdots$	5	8.146e-07	5.31	5.22	>1.81	1	$\cdots$	-0.13	V	$\cdots$	$\cdots$
12 35 17.501 +51 25 17.34	3.89	4.04	2.64 - 5.99	2.63	4	3.671e-09	5.60	4.71	2.27	2	$\cdots$	-0.40	V	$\cdots$	$\cdots$
12 36 06.636 +00 46 40.15	3.62	3.79	<2.38 - <7.45	3.67	4	4.102e-09	5.94	5.74	>1.68	6	$\cdots$	-0.29	V	$\cdots$	$\cdots$
12 36 18.402 +58 28 22.39	35.81	36.20	33.40 - 50.15	39.51	4	1.570e-08	4.29	4.51	1.45	0	$\cdots$	0.55	V	$\cdots$	$\cdots$
12 36 26.968 +02 43 25.45	2.37	2.26	1.71 - <6.47	$\cdots$	4	1.708e-07	3.54	4.53	2.03	67	$\cdots$	0.11	V	$\cdots$	$\cdots$
12 36 39.144 +26 15 38.33	4.72	4.89	2.29 - 5.29	4.30	3	9.253e-08	5.55	5.21	2.31	5	$\cdots$	-0.73	V	21.14	SDSS-G
12 37 07.767 +13 34 50.71	1.72	1.71	<1.62 - 2.33	$\cdots$	3	2.564e-07	3.35	4.45	>1.44	6	$\cdots$	0.37	T	$\cdots$	$\cdots$
12 37 27.587 +36 37 45.16	2.57	2.39	<1.89 - 4.25	2.26	4	2.948e-13	4.55	6.35	>2.06	5	BN	0.46	V	$\cdots$	$\cdots$
12 37 29.711 -06 32 33.32	2.54	2.72	1.87 - 3.41	$\cdots$	4	2.705e-07	3.30	4.32	>1.82	4	$\cdots$	-0.05	V	$\cdots$	GSC2-FIRST-G
12 37 30.311 +16 39 58.30	5.57	5.25	<2.40 - 6.80	3.57	4	1.050e-13	6.85	7.50	>2.84	0	$\cdots$	-1.16	V	20.85	SDSS-G
12 38 07.782 +53 25 55.83	42.04	38.44	36.61 - 55.10	46.94	4	4.952e-09	4.45	4.43	1.50	1	$\cdots$	1.12	V	17.30	SDSS-QSO(S)

Continued on next page. . .

Coordinates (J2000)	f (mJy)				N	Measures			$\frac{\text{Max.}}{\text{Min.}}$	$T_{\min}$	Flags	σ_{nbr}	Type	i	Cross-ID
	Cat.	$\overline{f}$	Range	NVSS		$P(\chi^2,\nu)$	$\sigma_{\max}$	$\Delta_{\max}(\sigma)$		(days)				Mag.	
12 38 47.703 -04 42 21.30	4.30	4.06	<2.30 - <6.47	$\cdots$	4	2.088e-07	5.50	5.46	>1.83	53	$\cdots$	0.71	V	$\cdots$	$\cdots$
12 38 50.087 +39 59 05.89	4.41	4.57	3.50 - 6.62	2.49	4	6.183e-10	4.07	4.85	1.67	1	$\cdots$	0.83	V	19.85	SDSS-QSO(S)
12 38 56.100 -00 59 30.89	13.43	12.04	11.37 - <28.71	14.75	4	5.615e-07	3.87	3.91	1.38	2	$\cdots$	-2.03	V	17.88	SDSS-QSO(S)
12 39 35.420 -01 15 01.17	9.42	9.24	<6.58 - 9.47	9.94	4	2.546e-06	5.28	5.03	>1.44	2	$\cdots$	-0.13	V	$\cdots$	$\cdots$
12 39 40.386 +24 53 49.87	11.53	11.37	3.36 - 23.14	19.59	3	0.000	19.41	15.21	6.88	1	$\cdots$	-0.46	V	$\cdots$	PSR
12 40 04.047 +21 35 43.39	4.30	4.16	2.26 - 4.98	2.41	3	2.000e-08	5.53	5.38	2.20	4	$\cdots$	-0.69	V	20.25	SDSS-G
12 40 21.581 +27 12 24.83	9.32	9.10	<6.88 - 12.89	30.97	5	9.920e-10	4.43	5.52	>1.76	0	$\cdots$	0.01	V	19.13	SDSS-G
12 40 42.037 +29 17 06.72	2.03	2.23	<1.72 - 3.02	2.15	4	2.293e-09	4.61	5.50	>1.70	2	$\cdots$	-0.93	V	$\cdots$	$\cdots$
12 40 42.543 -02 59 08.85	1.75	1.80	<1.45 - 2.31	$\cdots$	3	3.089e-08	4.19	4.87	>1.60	35	$\cdots$	-1.12	T	20.52	SDSS-G
12 40 54.584 -04 39 17.38	8.92	9.33	3.07 - 10.56	7.96	4	2.986e-14	7.74	7.57	3.40	2	BN	0.26	V	19.78	SDSS-G
12 41 56.862 -07 56 51.50	7.35	7.32	2.79 - 17.24	7.71	4	1.683e-11	5.16	4.91	2.69	383	$\cdots$	-1.16	V	$\cdots$	$\cdots$
12 42 08.489 +32 59 37.92	2.44	2.38	1.48 - 3.04	$\cdots$	5	7.939e-09	4.86	5.75	>2.06	484	$\cdots$	-0.15	V	18.18	SDSS-G
12 42 30.959 -00 42 16.06	2.45	2.29	1.43 - <10.83	2.57	4	9.112e-08	4.11	5.54	2.43	4	$\cdots$	-0.17	V	21.98	SDSS-*
12 42 31.696 -04 23 39.15	7.83	7.88	4.56 - <9.64	6.51	4	6.088e-09	5.38	5.46	1.93	5	BN	-0.33	V	$\cdots$	$\cdots$
12 42 37.181 +28 07 46.00	3.06	3.04	<1.77 - 3.83	3.36	3	4.546e-12	6.38	7.08	>2.16	921	$\cdots$	1.22	V	$\cdots$	$\cdots$
12 42 43.568 -05 33 54.40	1.14	1.16	<1.02 - <3.19	$\cdots$	4	6.640e-08	3.92	5.26	>2.36	0	$\cdots$	0.36	V	$\cdots$	$\cdots$
12 42 58.458 +57 32 05.51	3.74	3.83	3.14 - 8.53	3.42	4	1.168e-09	5.01	5.87	1.93	0	$\cdots$	-0.22	V	$\cdots$	$\cdots$
12 43 22.123 -05 06 50.85	4.99	5.31	2.38 - <59.72	$\cdots$	4	1.787e-09	6.15	5.18	2.35	9	BN	0.63	V	$\cdots$	$\cdots$
12 43 23.156 +23 58 41.93	57.65	50.51	49.59 - 69.24	60.16	5	8.956e-11	4.21	3.86	1.40	3	$\cdots$	-0.13	V	19.60	SDSS-QSO(P)
12 44 22.844 +32 54 16.59	4.47	4.27	<1.37 - 5.38	3.11	4	0.000	11.69	10.70	>3.91	484	$\cdots$	-0.52	V	20.67	SDSS-G
12 44 47.256 +32 58 52.10	2.89	2.85	1.64 - 4.31	2.80	5	2.094e-12	6.43	6.06	2.62	487	$\cdots$	-1.30	V	$\cdots$	$\cdots$
12 44 50.372 +01 57 43.10	2.85	2.98	2.05 - 4.56	$\cdots$	3	4.677e-08	4.93	4.36	1.69	5	$\cdots$	0.97	V	$\cdots$	$\cdots$
12 45 14.410 +59 21 27.67	5.00	5.07	4.77 - <12.62	4.65	4	3.141e-08	4.47	4.59	1.80	4	$\cdots$	-0.07	V	22.36	SDSS-G
12 45 14.692 -05 21 47.42	5.96	5.82	3.06 - <17.55	$\cdots$	4	4.315e-09	5.14	6.09	2.52	0	$\cdots$	-0.29	V	$\cdots$	$\cdots$
12 46 03.256 +33 11 18.12	1.90	1.90	<1.27 - 3.06	2.90	4	1.182e-12	5.65	6.36	>2.14	483	$\cdots$	-1.56	V	18.69	SDSS-G
12 46 11.605 +00 51 28.43	1.74	1.95	0.87 - 2.83	2.48	3	8.762e-09	5.05	5.84	3.24	62	$\cdots$	-0.90	V	$\cdots$	$\cdots$
12 46 20.024 +01 48 15.22	2.83	3.26	<2.48 - <15.50	$\cdots$	4	3.323e-07	4.91	5.14	>1.72	2	$\cdots$	-0.86	V	$\cdots$	$\cdots$
12 46 20.167 +32 54 37.92	5.71	5.41	<3.52 - <7.10	3.81	7	2.071e-06	5.49	5.34	>1.67	484	$\cdots$	0.02	V	15.65	SDSS-G
12 46 27.195 +33 10 39.99	5.32	5.37	<2.19 - 7.10	4.73	6	0.000	10.76	9.39	>2.87	0	$\cdots$	-1.03	V	$\cdots$	$\cdots$
12 46 34.720 +33 16 17.92	15.38	15.67	11.14 - 27.46	15.01	7	6.782e-07	5.12	4.00	2.44	482	$\cdots$	-0.36	V	20.82	SDSS-QSO(P)
12 46 44.539 +62 48 32.37	1.63	1.62	<0.93 - 2.14	$\cdots$	3	1.190e-07	5.24	5.02	>2.07	0	$\cdots$	0.24	V	$\cdots$	$\cdots$

Coordinates (J2000)	f (mJy)				N	Measures			$\frac{\text{Max.}}{\text{Min.}}$	$T_{\min}$	Flags	σ_{nbr}	Type	i	Cross-ID
	Cat.	$\overline{f}$	Range	NVSS		$P(\chi^2,\nu)$	$\sigma_{\max}$	$\Delta_{\max}(\sigma)$		(days)				Mag.	
12 47 32.996 +00 50 42.48	5.07	4.24	<3.41 - 6.43	4.36	3	2.139e-07	4.43	5.42	>1.88	62	$\cdots$	-1.92	V	$\cdots$	$\cdots$
12 48 24.803 -05 20 50.29	9.32	9.12	5.48 - 10.76	10.00	4	1.155e-12	6.98	6.11	1.96	0	$\cdots$	1.13	V	19.25	SDSS-G
12 49 00.421 +14 52 57.55	1.60	1.71	1.41 - 2.66	$\cdots$	3	1.178e-07	4.10	5.56	>1.83	0	$\cdots$	0.80	V	18.92	SDSS-G
12 49 16.534 +17 55 44.74	1.74	1.75	1.03 - 2.82	$\cdots$	3	1.068e-07	3.85	5.04	2.73	18	$\cdots$	0.83	V	14.88	SDSS-G
12 49 19.204 +18 55 09.17	2.39	2.33	2.23 - 21.83	$\cdots$	4	2.541e-09	4.96	5.24	>9.35	$\cdots$	$\cdots$	0.79	T	19.60	SDSS-G
12 49 25.770 +09 36 38.80	2.10	1.85	<1.27 - 2.53	$\cdots$	3	8.041e-09	5.27	6.01	>1.99	2	$\cdots$	-0.86	V	$\cdots$	$\cdots$
12 49 27.740 +09 05 58.25	7.78	7.45	3.79 - 8.52	7.46	4	9.701e-12	4.96	5.29	2.22	2	$\cdots$	1.76	V	$\cdots$	$\cdots$
12 50 02.780 +03 23 19.07	2.29	2.18	1.55 - <8.09	$\cdots$	4	3.171e-08	3.85	4.67	>1.50	4	$\cdots$	0.21	V	$\cdots$	$\cdots$
12 50 35.164 +34 43 10.81	2.09	2.23	<0.96 - <3.59	$\cdots$	3	8.260e-14	7.01	7.19	>2.95	1	$\cdots$	0.67	V	$\cdots$	$\cdots$
12 51 16.644 +05 52 55.28	1.13	1.12	<0.72 - 1.79	$\cdots$	3	1.266e-07	4.68	5.57	>2.50	3	$\cdots$	1.46	V	$\cdots$	$\cdots$
12 51 18.351 +28 52 48.46	4.42	4.47	<2.48 - 4.65	4.02	3	7.597e-09	6.07	5.88	>1.87	5	$\cdots$	-0.36	V	$\cdots$	$\cdots$
12 51 31.403 +56 32 46.40	11.20	11.75	6.17 - 13.35	10.82	3	1.064e-11	6.62	6.29	2.16	2	BN	-0.47	V	19.05	SDSS-QSO(S)
12 51 31.560 +38 12 12.75	3.35	3.39	1.65 - 3.95	3.73	3	1.711e-07	5.07	5.49	2.39	1	$\cdots$	0.03	V	19.44	SDSS-G
12 51 35.475 +37 27 59.93	38.84	37.44	36.59 - 56.08	42.36	3	3.784e-07	5.42	4.97	1.53	7	$\cdots$	0.59	V	21.30	SDSS-G
12 51 37.471 +33 19 46.14	2.28	2.18	<1.84 - 3.70	6.53	3	1.574e-08	4.15	5.41	>1.65	483	$\cdots$	0.75	V	$\cdots$	$\cdots$
12 52 17.120 +32 56 22.42	4.98	4.70	<3.22 - <11.35	4.14	7	2.333e-08	5.25	5.41	>2.11	488	$\cdots$	0.62	V	$\cdots$	$\cdots$
12 52 30.648 +27 11 53.15	15.59	15.43	<10.89 - 19.54	15.31	4	2.135e-08	5.39	6.05	>1.79	4	$\cdots$	0.94	V	$\cdots$	$\cdots$
12 52 50.486 -07 04 29.12	5.08	5.53	2.70 - <7.88	7.66	4	2.003e-11	6.77	6.14	2.21	2	$\cdots$	-5.99	V	$\cdots$	$\cdots$
12 53 02.260 -06 59 44.10	14.66	16.11	9.46 - 21.30	19.27	3	0.000	11.88	8.81	2.25	2	$\cdots$	-4.49	V	$\cdots$	$\cdots$
12 53 20.504 +03 57 59.04	1.22	1.12	0.72 - <3.41	$\cdots$	4	3.090e-07	4.53	5.21	>3.39	984	$\cdots$	-0.65	V	18.72	SDSS-QSO(S)
12 53 23.496 +13 30 53.67	1.62	1.46	<0.96 - <2.37	$\cdots$	3	4.376e-08	5.20	5.26	>1.79	28	$\cdots$	-0.25	V	$\cdots$	$\cdots$
12 53 24.965 -06 41 20.24	1.87	1.97	<1.13 - 2.34	$\cdots$	3	1.429e-07	5.23	5.26	>2.07	8	$\cdots$	-0.66	V	$\cdots$	$\cdots$
12 53 57.385 +30 22 47.27	63.41	62.51	60.55 - 84.24	62.55	6	1.968e-08	4.27	4.00	1.39	6	$\cdots$	0.54	V	$\cdots$	$\cdots$
12 54 30.513 +61 05 10.20	3.49	3.33	1.54 - <11.94	$\cdots$	4	2.182e-07	5.13	4.82	2.71	4	$\cdots$	0.33	V	$\cdots$	$\cdots$
12 55 12.609 +02 21 37.53	6.00	5.64	3.00 - 5.83	$\cdots$	3	4.075e-08	4.12	4.11	>1.27	1	$\cdots$	-0.20	V	$\cdots$	$\cdots$
12 55 44.952 -06 34 38.98	3.78	3.59	<2.03 - 4.04	$\cdots$	2	1.191e-11	6.54	6.56	>1.99	4	$\cdots$	1.50	T	$\cdots$	$\cdots$
12 55 57.938 +01 32 28.37	2.44	2.11	<1.47 - <3.42	$\cdots$	3	6.997e-08	5.28	5.09	>1.56	76	$\cdots$	0.85	V	$\cdots$	$\cdots$
12 56 00.952 +02 02 50.06	9.75	9.52	5.09 - 10.33	11.27	4	1.335e-06	5.31	5.08	2.03	83	$\cdots$	0.71	V	$\cdots$	$\cdots$
12 56 45.703 +00 58 48.20	3.04	2.87	<2.44 - <8.06	4.03	4	7.053e-08	4.00	4.33	>1.32	47	$\cdots$	0.37	V	20.79	SDSS-*
12 57 07.635 +01 57 08.30	1.23	1.08	<0.91 - <1.96	$\cdots$	3	2.630e-07	4.09	4.88	>1.95	83	$\cdots$	-0.20	V	$\cdots$	$\cdots$
12 57 42.404 +02 00 30.17	2.64	2.79	1.09 - <7.47	2.79	4	4.734e-07	5.30	4.85	2.78	82	$\cdots$	-0.55	V	$\cdots$	XMM

Coordinates (J2000)	f (mJy)				N	Measures			Max./Min.	T_{min}	Flags	σ_{nbr}	Type	i	Cross-ID
	Cat.	$\overline{f}$	Range	NVSS		$P(\chi^2,\nu)$	σ_{max}	$\Delta_{max}(\sigma)$		(days)				Mag.	
12 58 02.007 +39 57 35.04	19.03	19.23	8.77 - 22.11	17.82	5	9.619e-08	5.63	5.68	2.52	2	$\cdots$	-1.60	V	23.55	SDSS-G
12 58 29.945 +40 25 31.15	14.83	15.14	6.75 - 16.67	13.55	5	9.992e-16	8.59	6.86	2.26	0	BN	-1.37	V	$\cdots$	$\cdots$
12 58 34.274 +40 21 45.68	13.34	13.74	9.29 - 18.56	11.52	5	1.461e-08	5.57	5.30	1.79	0	BN	-3.06	V	$\cdots$	$\cdots$
12 58 36.185 +37 55 38.94	3.48	3.40	1.54 - <7.89	$\cdots$	5	3.449e-07	5.02	4.81	2.33	460	$\cdots$	0.47	V	19.62	SDSS-G
12 59 45.751 +34 03 27.94	25.00	22.94	15.47 - 35.02	22.56	3	1.860e-12	5.34	6.66	2.26	6	$\cdots$	0.01	V	19.18	SDSS-QSO(P)
13 00 20.713 +16 55 37.33	6.11	6.32	5.05 - 9.50	7.28	3	3.508e-14	5.22	6.56	1.88	30	$\cdots$	0.21	V	$\cdots$	$\cdots$
13 00 31.827 -05 25 31.98	1.57	1.88	<1.21 - 3.09	$\cdots$	2	6.548e-11	5.55	6.08	>2.55	0	$\cdots$	-2.07	T	$\cdots$	$\cdots$
13 00 53.214 +23 41 33.96	1.36	1.23	<0.98 - <4.33	$\cdots$	4	5.313e-07	4.14	4.74	>1.76	7	$\cdots$	0.09	V	$\cdots$	$\cdots$
13 01 19.863 -05 43 22.10	1.95	2.06	<1.45 - <13.63	3.32	4	1.120e-07	4.28	4.87	>1.74	4	$\cdots$	0.70	V	$\cdots$	$\cdots$
13 01 23.591 +33 14 18.42	1.97	2.15	<1.29 - <8.45	$\cdots$	6	7.155e-09	5.04	5.75	>2.14	483	$\cdots$	0.68	V	20.87	SDSS-G
13 01 48.373 +19 43 24.63	3.22	3.34	1.77 - 3.99	$\cdots$	3	1.084e-07	5.26	4.83	2.25	$\cdots$	$\cdots$	-0.42	V	18.63	SDSS-G
13 03 28.260 +54 24 42.47	67.75	68.41	67.00 - 99.73	70.02	6	2.506e-11	4.82	4.39	1.44	1	$\cdots$	0.46	V	$\cdots$	$\cdots$
13 03 40.833 +02 34 05.11	3.51	3.76	2.39 - 4.37	$\cdots$	3	1.886e-07	4.14	4.55	1.75	1	$\cdots$	0.29	V	13.29	SDSS-G
13 03 41.071 +35 37 21.36	1.65	2.00	<1.31 - 4.21	$\cdots$	2	1.958e-11	5.13	6.41	>3.22	5	$\cdots$	0.06	T	19.86	SDSS-G
13 03 51.434 +33 01 35.27	1.62	1.49	<1.12 - <5.29	$\cdots$	5	4.698e-07	4.64	5.06	>1.80	484	$\cdots$	0.14	V	$\cdots$	$\cdots$
13 04 11.063 +14 14 56.42	24.27	23.84	23.36 - 37.65	20.24	3	4.747e-08	5.48	5.14	1.61	18	$\cdots$	-0.50	V	19.95	SDSS-QSO(P)
13 04 49.482 +00 32 00.35	2.13	2.10	<2.06 - 11.00	$\cdots$	4	1.236e-09	5.11	5.65	>5.34	5	$\cdots$	-0.47	V	$\cdots$	$\cdots$
13 05 16.663 +34 58 36.50	1.09	1.19	<0.60 - 5.62	$\cdots$	3	5.884e-15	5.94	6.67	>3.36	1	$\cdots$	1.09	V	$\cdots$	$\cdots$
13 05 29.092 +12 49 35.94	1.53	1.63	1.01 - 2.39	$\cdots$	3	7.008e-08	3.49	4.88	>1.61	4	$\cdots$	-0.09	V	12.16	TYCHO-STAR
13 05 32.736 +30 58 47.75	1.74	1.22	<1.00 - 1.98	$\cdots$	3	5.721e-07	4.00	5.08	>1.97	411	$\cdots$	0.27	T	$\cdots$	$\cdots$
13 05 49.215 +44 27 24.43	18.10	16.94	16.45 - 23.10	18.50	5	1.503e-08	3.75	3.59	1.38	1	$\cdots$	2.41	V	$\cdots$	$\cdots$
13 06 22.368 +37 26 44.59	11.77	11.66	8.97 - 17.56	13.82	4	0.000	5.49	6.94	1.96	6	$\cdots$	-0.03	V	22.24	SDSS-*
13 06 47.446 +01 34 18.56	3.83	3.79	2.34 - <6.33	$\cdots$	4	8.374e-10	5.28	5.22	2.51	77	$\cdots$	0.71	V	$\cdots$	$\cdots$
13 07 09.075 -04 13 06.39	4.71	4.57	<2.79 - <5.80	3.00	4	3.457e-09	6.17	5.98	>1.73	12	$\cdots$	-0.05	V	$\cdots$	$\cdots$
13 07 17.047 +06 34 06.39	3.12	3.41	1.45 - <24.64	$\cdots$	4	6.502e-12	5.86	6.34	4.05	1	$\cdots$	-0.22	V	$\cdots$	$\cdots$
13 07 34.991 -01 52 02.73	4.38	4.93	<3.33 - <12.10	5.40	4	9.571e-09	5.75	5.45	>1.55	11	$\cdots$	0.40	V	$\cdots$	SDSS-UNKNOWN
13 07 37.804 +32 01 53.27	16.50	17.23	11.90 - 18.09	15.34	5	1.251e-05	5.21	4.24	1.48	1	$\cdots$	-0.37	V	19.55	SDSS-G
13 08 11.063 +61 11 38.35	1.45	1.36	<0.93 - 2.03	$\cdots$	3	4.264e-07	4.54	5.33	>2.18	4	$\cdots$	-0.74	V	$\cdots$	$\cdots$
13 08 32.944 -03 10 13.21	3.06	2.81	1.19 - <8.72	$\cdots$	4	3.882e-07	4.51	5.23	3.34	0	$\cdots$	0.05	V	$\cdots$	$\cdots$
13 08 37.419 +61 03 54.02	3.11	3.19	<1.69 - 8.51	2.30	4	4.399e-10	5.73	5.57	>1.97	4	$\cdots$	-0.03	V	$\cdots$	$\cdots$
13 08 42.330 -00 05 44.78	12.41	12.38	<8.63 - 13.31	8.59	4	1.354e-06	5.39	5.14	>1.54	2	$\cdots$	0.64	V	$\cdots$	$\cdots$

Table A.1 – Continued

Coordinates (J2000)	f (mJy)				N	Measures			$\frac{\text{Max.}}{\text{Min.}}$	$T_{\min}$	Flags	σ_{nbr}	Type	i	Cross-ID
	Cat.	$\overline{f}$	Range	NVSS		$P(\chi^2,\nu)$	$\sigma_{\max}$	$\Delta_{\max}(\sigma)$		(days)				Mag.	
13 08 47.238 -00 18 04.33	3.55	3.66	<2.59 - <12.17	$\cdots$	4	5.987e-08	5.61	5.44	>1.55	1	$\cdots$	0.84	V	$\cdots$	$\cdots$
13 08 50.537 -05 36 40.92	13.20	11.61	11.37 - 17.53	12.44	4	3.184e-07	3.70	3.62	1.54	4	$\cdots$	0.63	V	$\cdots$	$\cdots$
13 09 08.632 -04 55 13.97	7.02	7.08	4.13 - <23.64	4.96	4	4.663e-14	7.68	6.38	1.87	13	$\cdots$	0.10	V	$\cdots$	$\cdots$
13 09 23.101 +35 38 19.62	86.13	86.80	81.41 - 148.69	88.31	5	4.142e-09	5.61	5.61	1.83	0	$\cdots$	-0.74	V	21.27	SDSS-G
13 09 55.964 +10 05 19.79	12.57	13.18	<9.37 - 14.09	10.59	4	6.246e-08	5.14	5.17	>1.50	4	$\cdots$	-0.21	V	$\cdots$	$\cdots$
13 10 04.446 +00 22 27.34	2.35	2.32	<1.62 - <11.52	$\cdots$	4	1.592e-08	4.81	5.68	>1.86	6	$\cdots$	0.20	V	$\cdots$	$\cdots$
13 10 15.458 -00 35 41.94	7.74	7.68	3.14 - 7.85	6.25	4	2.509e-06	5.18	4.83	2.49	4	$\cdots$	-0.77	V	19.62	SDSS-G
13 10 23.698 -07 49 59.92	2.33	2.09	1.16 - 3.42	$\cdots$	3	3.174e-07	4.29	4.86	2.32	3	$\cdots$	1.08	V	$\cdots$	$\cdots$
13 10 46.381 +32 22 05.42	18.67	19.76	9.96 - <26.01	10.18	5	5.890e-10	4.98	4.27	2.05	1	BN	-0.32	V	22.23	SDSS-G
13 11 16.439 +39 01 16.46	3.18	3.23	2.16 - 4.31	$\cdots$	3	3.636e-07	4.18	5.34	1.90	1	$\cdots$	-0.60	V	$\cdots$	$\cdots$
13 11 32.706 +31 43 21.96	3.69	4.00	<2.06 - 4.53	3.68	3	9.539e-13	7.30	6.87	>2.07	4	$\cdots$	0.89	V	22.00	SDSS-G
13 12 01.868 +25 47 17.07	2.87	3.31	1.21 - 3.90	3.92	4	9.100e-11	6.25	6.30	3.22	3	$\cdots$	-2.15	V	21.88	SDSS-*
13 12 14.520 +62 00 59.37	16.29	13.68	12.71 - <30.09	15.56	6	8.800e-08	4.58	4.48	1.47	4	$\cdots$	-0.06	V	20.85	SDSS-G
13 12 52.892 -00 16 29.50	2.04	1.93	<1.23 - <6.24	$\cdots$	4	1.721e-09	5.51	5.94	>1.94	1	$\cdots$	-0.51	V	$\cdots$	$\cdots$
13 13 28.147 +03 24 07.07	2.31	2.13	<1.35 - 2.58	$\cdots$	3	4.743e-10	5.67	6.03	>1.91	4	$\cdots$	-0.47	T	$\cdots$	$\cdots$
13 13 40.844 +31 06 54.87	2.93	3.47	1.17 - <10.99	$\cdots$	5	5.551e-16	7.53	7.10	>3.33	411	$\cdots$	0.40	V	$\cdots$	$\cdots$
13 13 41.938 +28 03 00.77	12.68	12.52	<10.28 - 17.70	10.84	5	3.860e-10	4.33	5.69	>1.72	927	$\cdots$	-0.04	V	$\cdots$	$\cdots$
13 13 59.011 +04 52 15.66	1.39	1.44	<1.18 - <4.49	$\cdots$	4	1.411e-07	4.08	4.61	>1.64	1	$\cdots$	0.33	V	$\cdots$	$\cdots$
13 14 43.583 +28 16 31.10	3.51	3.46	1.53 - <9.57	3.11	4	2.667e-09	5.81	5.82	2.54	921	$\cdots$	-0.86	V	$\cdots$	$\cdots$
13 16 54.888 +41 05 08.69	1.93	2.03	<1.40 - <3.56	$\cdots$	3	3.761e-09	5.02	5.88	>1.92	5	$\cdots$	0.21	V	20.15	SDSS-*
13 17 12.748 +34 34 18.38	1.11	0.80	<0.76 - <2.49	$\cdots$	3	9.208e-08	4.25	5.34	>2.53	5	$\cdots$	0.29	V	$\cdots$	$\cdots$
13 17 41.649 +39 48 42.73	1.32	1.27	0.83 - <3.02	$\cdots$	4	1.458e-07	4.53	5.26	2.97	1	$\cdots$	-0.47	V	18.32	SDSS-G
13 18 12.521 -07 05 00.31	3.41	3.35	1.74 - <10.94	$\cdots$	4	2.360e-07	4.26	5.50	3.15	11	BN	0.24	V	$\cdots$	GSC2-FIRST-G
13 18 25.331 +57 45 24.42	1.46	1.35	0.76 - <7.60	$\cdots$	4	9.436e-08	3.34	4.49	3.00	0	$\cdots$	1.57	V	$\cdots$	$\cdots$
13 18 42.220 +32 55 07.39	3.43	3.37	1.31 - 3.66	2.99	4	4.387e-07	5.49	5.31	2.78	484	$\cdots$	0.08	V	16.28	SDSS-G
13 18 42.535 +15 51 10.70	1.52	1.32	<1.09 - <3.96	$\cdots$	4	9.361e-08	4.24	4.51	>1.69	1	$\cdots$	3.03	V	$\cdots$	$\cdots$
13 19 09.316 -06 32 34.88	2.17	2.20	1.40 - 3.80	$\cdots$	3	2.604e-07	3.86	5.11	2.71	4	BN	0.89	V	$\cdots$	GSC2-FIRST-G
13 19 10.701 +00 09 55.61	47.45	43.32	41.69 - 61.81	49.73	4	5.491e-13	4.73	4.54	1.48	1	$\cdots$	0.49	V	$\cdots$	$\cdots$
13 19 17.952 +20 23 26.52	13.73	14.23	8.83 - 14.47	10.58	3	9.611e-11	5.15	4.42	1.64	5	$\cdots$	-0.38	V	$\cdots$	$\cdots$
13 20 04.351 +55 04 52.33	3.12	3.18	1.45 - <8.65	$\cdots$	4	5.936e-08	5.49	5.42	2.45	47	$\cdots$	-0.05	V	$\cdots$	$\cdots$
13 20 08.719 -02 08 13.10	2.39	2.22	1.07 - 2.87	$\cdots$	3	2.857e-07	4.73	5.17	2.67	1	$\cdots$	-0.06	V	17.69	SDSS-G

Coordinates (J2000)	f (mJy)				N	Measures			$\frac{\text{Max.}}{\text{Min.}}$	$T_{\min}$	Flags	σ_{nbr}	Type	i	Cross-ID
	Cat.	$\overline{f}$	Range	NVSS		$P(\chi^2,\nu)$	$\sigma_{\max}$	$\Delta_{\max}(\sigma)$		(days)				Mag.	
13 20 17.758 +03 09 09.49	5.73	5.64	<3.14 - 5.94	5.34	4	4.822e-11	6.99	6.54	>1.89	70	$\cdots$	0.39	V	20.39	SDSS-G
13 20 22.573 +32 47 05.37	4.77	4.63	3.61 - 6.09	5.08	5	3.121e-08	4.09	5.41	>1.69	3	$\cdots$	-0.10	V	17.10	SDSS-G
13 21 04.479 +26 08 05.36	3.65	4.18	<2.83 - <7.70	3.39	5	3.018e-08	5.50	5.23	>1.53	29	$\cdots$	-3.77	V	$\cdots$	$\cdots$
13 21 12.762 +31 36 45.01	39.25	37.92	36.21 - 52.31	37.84	5	1.232e-10	4.19	4.11	1.42	95	$\cdots$	0.49	V	15.24	SDSS-G
13 21 29.528 +38 47 13.69	2.44	2.34	1.63 - <3.46	$\cdots$	3	3.928e-07	4.38	4.66	1.78	5	$\cdots$	0.44	V	$\cdots$	$\cdots$
13 21 40.280 +58 27 28.42	1.41	1.51	1.12 - <3.32	$\cdots$	4	2.252e-07	4.44	5.17	2.25	450	$\cdots$	0.21	V	17.04	SDSS-G
13 22 02.578 +10 57 52.05	3.88	4.12	1.94 - <15.84	2.08	4	2.464e-08	5.47	5.22	2.50	1	BN	-1.04	V	$\cdots$	$\cdots$
13 22 18.461 +37 59 44.48	4.36	4.29	3.67 - 7.73	3.78	4	2.296e-10	4.82	5.42	2.11	5	$\cdots$	0.57	V	18.82	SDSS-G
13 22 19.329 +37 32 34.56	2.08	1.96	<1.38 - 3.27	$\cdots$	4	1.673e-07	5.03	4.93	>1.64	6	$\cdots$	0.25	V	$\cdots$	$\cdots$
13 22 23.126 +19 09 59.63	47.84	47.83	46.58 - 65.60	51.70	6	6.569e-08	3.59	3.47	1.41	$\cdots$	$\cdots$	0.19	V	$\cdots$	$\cdots$
13 22 43.132 -04 06 35.70	8.23	7.42	3.15 - 7.61	11.57	3	2.068e-12	5.48	5.04	2.18	916	$\cdots$	1.21	V	$\cdots$	GSC2-FIRST-G
13 22 45.824 -03 48 56.94	4.82	5.32	2.63 - <10.63	6.62	4	3.031e-10	6.48	5.63	2.15	916	$\cdots$	0.30	V	$\cdots$	GSC2-FIRST-G
13 22 56.312 +32 52 32.86	7.91	8.06	4.51 - 9.82	4.90	4	2.200e-09	5.18	5.72	2.18	488	$\cdots$	-0.00	V	18.22	SDSS-G
13 22 56.462 -05 41 21.84	3.89	4.17	<2.46 - 5.18	4.93	3	7.012e-12	6.41	7.04	>2.11	4	$\cdots$	2.12	V	$\cdots$	$\cdots$
13 23 33.475 +38 59 21.90	6.00	5.73	3.38 - 7.41	3.92	4	4.864e-11	5.39	4.99	1.52	1	$\cdots$	-0.61	V	19.26	SDSS-QSO(P)
13 24 05.808 -03 31 31.80	7.69	7.61	3.92 - 10.04	9.50	4	4.707e-07	4.81	4.80	2.56	0	$\cdots$	0.32	V	$\cdots$	$\cdots$
13 24 07.789 +34 39 58.05	39.36	37.49	36.58 - 58.16	43.16	5	1.198e-12	5.66	5.28	1.59	1	$\cdots$	0.47	V	$\cdots$	$\cdots$
13 24 49.021 +16 40 00.70	1.79	1.72	<1.12 - 2.72	$\cdots$	3	3.412e-10	5.57	5.70	>2.04	6	$\cdots$	-0.18	V	19.00	SDSS-G
13 25 14.315 +57 01 05.68	43.01	39.56	38.35 - 60.71	37.87	4	8.993e-15	5.74	5.38	1.58	0	BN	-0.46	V	21.97	SDSS-*
13 25 16.725 +04 15 33.17	4.18	4.24	2.09 - <15.24	4.70	4	5.990e-11	5.58	5.74	2.29	15	$\cdots$	0.20	V	19.49	SDSS-G
13 25 58.572 +31 43 15.58	16.16	15.09	6.12 - 30.94	$\cdots$	2	0.000	9.35	9.75	5.06	95	BN	-6.42	T	$\cdots$	$\cdots$
13 26 04.318 +02 47 45.16	3.39	3.69	1.82 - 4.15	$\cdots$	3	2.466e-07	3.90	4.22	1.93	3	$\cdots$	0.03	V	19.71	SDSS-G
13 26 13.367 +31 20 53.73	86.34	85.60	47.40 - 112.01	86.30	4	3.334e-09	4.91	6.29	2.36	412	$\cdots$	-2.48	V	$\cdots$	$\cdots$
13 27 25.005 -02 53 58.42	2.77	2.87	2.55 - <10.05	2.95	4	9.709e-10	5.04	6.14	>1.88	0	$\cdots$	-1.05	V	21.35	SDSS-G
13 27 48.406 +31 47 10.95	9.76	9.16	<7.96 - 18.93	6.21	3	0.000	8.24	7.72	>2.38	4	BN	2.67	V	$\cdots$	$\cdots$
13 28 01.080 +34 21 17.48	3.70	4.03	<2.39 - 4.31	3.71	3	1.287e-06	5.08	5.16	>1.80	5	$\cdots$	0.68	V	18.57	SDSS-G
13 28 04.761 +36 46 44.08	11.02	9.48	4.98 - 10.06	9.55	4	2.156e-12	4.58	4.58	2.02	45	$\cdots$	-0.78	V	$\cdots$	$\cdots$
13 28 18.201 -02 58 14.46	8.77	9.06	6.04 - <22.11	9.04	4	8.238e-07	5.25	4.36	1.55	6	$\cdots$	-0.37	V	$\cdots$	$\cdots$
13 28 30.513 +11 31 32.73	65.75	68.63	67.99 - 98.67	73.48	5	5.142e-12	4.45	4.06	1.45	1	$\cdots$	0.91	V	20.44	SDSS-QSO(S)
13 28 31.864 +56 55 00.60	5.32	5.29	4.45 - 8.08	$\cdots$	3	2.252e-09	4.65	5.41	1.82	3	BN	-0.89	V	21.30	SDSS-G
13 28 40.291 +15 20 53.28	1.47	1.52	<0.93 - 2.28	$\cdots$	3	1.155e-10	4.90	6.07	>2.45	3	$\cdots$	0.21	T	$\cdots$	$\cdots$

Coordinates (J2000)	f (mJy)				N	Measures			$\frac{\text{Max.}}{\text{Min.}}$	$T_{\min}$	Flags	σ_{nbr}	Type	i	Cross-ID
	Cat.	$\overline{f}$	Range	NVSS		$P(\chi^2,\nu)$	$\sigma_{\max}$	$\Delta_{\max}(\sigma)$		(days)				Mag.	
13 29 01.099 +24 31 54.17	18.80	16.49	14.99 - 22.86	18.08	3	3.827e-09	4.25	4.69	1.52	1	$\cdots$	0.36	V	$\cdots$	$\cdots$
13 29 05.585 +02 46 15.82	2.75	2.78	1.24 - 3.35	2.29	3	1.147e-10	4.76	5.24	2.69	3	$\cdots$	-0.11	V	$\cdots$	$\cdots$
13 29 26.118 +01 25 13.29	1.36	1.38	<1.06 - <4.30	$\cdots$	4	2.069e-07	4.21	5.19	>1.87	1	$\cdots$	0.07	V	$\cdots$	$\cdots$
13 30 12.092 +38 48 39.31	2.32	2.51	1.17 - 3.25	$\cdots$	4	1.762e-09	5.68	5.85	2.77	5	$\cdots$	0.79	V	$\cdots$	$\cdots$
13 30 38.547 +27 37 57.96	2.80	2.89	2.29 - 3.86	2.28	3	5.277e-07	3.19	4.41	>1.38	43	$\cdots$	0.65	V	15.94	SDSS-G
13 31 29.648 +58 15 06.94	2.76	2.66	<1.88 - 2.99	$\cdots$	3	9.432e-08	5.43	5.13	>1.59	450	$\cdots$	-0.59	V	20.72	SDSS-G
13 31 32.054 +21 59 22.07	1.25	0.95	<0.67 - <3.28	$\cdots$	4	2.095e-07	4.27	5.18	>2.54	1002	$\cdots$	1.09	V	$\cdots$	$\cdots$
13 31 33.431 +17 12 50.56	177.24	168.17	163.96 - 239.74	177.24	6	4.511e-11	3.99	3.84	1.46	0	$\cdots$	0.33	V	19.28	SDSS-QSO(P)
13 32 00.883 -01 19 21.14	2.28	2.28	1.06 - 3.09	2.72	3	1.364e-08	5.17	5.46	2.93	2	$\cdots$	0.26	V	17.97	SDSS-G
13 32 18.933 -07 10 29.79	3.28	3.01	<2.28 - 3.66	4.40	3	1.048e-07	5.03	5.61	>1.60	2	$\cdots$	0.88	V	$\cdots$	$\cdots$
13 32 27.290 +02 24 37.44	3.91	3.88	1.50 - 4.76	3.14	3	1.106e-10	5.99	6.37	3.17	2	BN	1.87	V	20.83	SDSS-G
13 33 19.977 +06 50 43.31	3.67	3.61	1.35 - <8.15	$\cdots$	4	2.305e-09	6.07	5.82	2.95	1	$\cdots$	-0.88	V	$\cdots$	$\cdots$
13 34 14.183 +57 12 01.57	17.59	15.84	14.86 - 25.91	18.72	4	1.719e-12	5.67	5.74	1.74	0	$\cdots$	1.67	V	$\cdots$	$\cdots$
13 34 43.264 +27 08 25.41	12.28	12.51	<7.88 - 15.98	10.57	5	5.201e-11	5.79	6.41	>2.03	5	$\cdots$	-0.21	V	22.11	SDSS-*
13 35 23.789 +41 03 06.09	1.00	0.76	<0.41 - <4.54	$\cdots$	3	1.591e-10	5.49	5.68	>3.60	427	$\cdots$	0.16	V	$\cdots$	$\cdots$
13 36 02.823 +27 27 51.45	61.56	56.62	55.70 - 76.46	73.80	5	1.157e-10	4.14	3.74	1.37	1	$\cdots$	0.09	V	19.16	SDSS-QSO(P)
13 36 06.310 -04 13 23.83	3.93	4.01	2.03 - <18.96	3.43	4	5.695e-08	4.07	4.21	2.13	923	$\cdots$	-0.07	V	$\cdots$	$\cdots$
13 36 19.812 -06 13 12.90	4.04	4.02	<2.88 - <15.57	2.91	4	9.934e-08	5.25	5.36	>1.53	4	BN	1.16	V	$\cdots$	$\cdots$
13 36 55.177 -05 56 07.87	12.57	12.87	5.47 - 13.17	13.07	4	7.624e-06	5.08	4.79	2.41	6	$\cdots$	0.37	V	$\cdots$	$\cdots$
13 37 14.282 -03 17 25.48	5.77	5.68	3.33 - 5.85	$\cdots$	3	1.439e-07	4.33	4.27	>1.32	0	$\cdots$	-0.86	V	$\cdots$	$\cdots$
13 37 15.322 -05 28 37.55	3.04	1.87	<0.72 - 3.74	$\cdots$	3	0.000	8.35	8.11	>5.20	982	$\cdots$	-3.39	T	$\cdots$	$\cdots$
13 37 18.658 +39 17 14.45	8.18	8.40	4.55 - <24.31	8.31	5	2.476e-06	5.22	4.61	1.87	1	$\cdots$	0.21	V	19.58	SDSS-QSO(P)
13 37 21.500 +15 49 34.68	4.76	4.36	3.90 - <10.72	4.07	4	1.261e-07	5.02	5.35	1.74	15	$\cdots$	0.32	V	21.13	SDSS-G
13 37 31.176 -05 29 03.10	3.95	2.24	<1.10 - <9.29	$\cdots$	5	0.000	8.98	7.69	>3.65	982	$\cdots$	-0.69	V	$\cdots$	$\cdots$
13 38 01.121 -06 05 57.72	1.60	1.40	<0.93 - 2.97	$\cdots$	3	6.288e-12	5.08	6.28	>3.18	4	BN	0.99	T	$\cdots$	$\cdots$
13 38 56.653 +31 20 49.85	5.08	5.11	2.51 - <14.34	4.80	6	1.275e-08	3.94	4.07	2.18	97	$\cdots$	-0.20	V	$\cdots$	$\cdots$
13 39 19.149 +15 35 00.23	1.44	1.13	0.68 - <10.58	$\cdots$	4	4.115e-07	4.08	4.96	3.40	16	$\cdots$	0.65	V	18.17	SDSS-G
13 39 31.963 -06 24 38.12	8.11	8.93	5.60 - 9.74	$\cdots$	4	8.474e-09	4.98	4.71	1.74	8	BN	-0.10	V	$\cdots$	$\cdots$
13 41 45.092 +19 05 36.69	11.08	11.53	9.40 - 16.96	10.18	3	3.880e-11	5.42	6.73	1.80	$\cdots$	$\cdots$	-0.41	V	19.39	SDSS-QSO(P)
13 41 49.047 +26 09 01.18	12.65	13.57	6.94 - 15.30	10.86	5	5.343e-08	4.58	4.28	>1.54	2	$\cdots$	0.93	V	20.56	SDSS-QSO(P)
13 42 00.831 -02 55 59.41	61.32	54.15	35.97 - 74.99	67.34	6	1.791e-13	4.70	5.52	2.05	8	$\cdots$	-0.32	V	19.64	SDSS-QSO(S)

Coordinates (J2000)	f (mJy)				N	Measures			$\frac{\text{Max.}}{\text{Min.}}$	$T_{\min}$	Flags	σ_{nbr}	Type	i	Cross-ID
	Cat.	$\overline{f}$	Range	NVSS		$P(\chi^2,\nu)$	$\sigma_{\max}$	$\Delta_{\max}(\sigma)$		(days)				Mag.	
13 42 59.952 +19 11 52.79	3.31	3.44	<2.26 - <6.93	$\cdots$	4	1.568e-07	5.27	5.42	>1.69	$\cdots$	$\cdots$	0.85	V	19.35	SDSS-G
13 43 05.859 +54 13 51.27	5.81	5.89	3.12 - <7.66	2.95	4	2.918e-07	5.26	5.08	2.10	13	$\cdots$	1.05	V	$\cdots$	$\cdots$
13 43 39.979 +01 52 48.47	12.94	12.52	8.33 - 14.42	12.59	4	3.087e-06	5.09	4.20	1.53	4	$\cdots$	-0.55	V	18.74	SDSS-QSO(S)
13 43 43.942 +18 55 49.01	22.20	23.83	9.07 - 27.78	16.84	4	7.213e-08	5.42	5.96	3.06	$\cdots$	$\cdots$	-1.38	V	19.97	SDSS-QSO(P)
13 43 56.309 +19 06 28.24	7.59	8.02	5.03 - 12.53	10.20	3	8.882e-16	7.02	6.85	2.49	$\cdots$	$\cdots$	-0.81	V	$\cdots$	$\cdots$
13 44 22.185 +60 24 15.78	3.34	3.39	2.05 - <17.11	$\cdots$	4	3.131e-07	4.06	4.77	1.98	3	BN	-0.04	V	$\cdots$	$\cdots$
13 44 29.220 +02 47 01.23	2.14	1.94	<1.45 - 2.82	$\cdots$	3	3.426e-08	4.61	5.74	>1.95	6	$\cdots$	0.25	V	$\cdots$	$\cdots$
13 44 36.200 +44 36 55.38	2.83	2.66	1.47 - 3.40	$\cdots$	3	2.864e-11	5.10	5.99	2.31	1	$\cdots$	-1.61	V	16.37	SDSS-G
13 44 41.924 +60 04 44.99	22.44	21.72	<14.43 - 25.84	$\cdots$	4	2.582e-09	5.74	6.13	>1.79	3	BN	-0.09	V	$\cdots$	$\cdots$
13 45 14.641 +22 12 33.46	1.17	0.91	<0.79 - 2.05	$\cdots$	3	1.904e-07	4.05	5.31	>2.60	997	$\cdots$	0.46	T	$\cdots$	$\cdots$
13 45 15.212 -01 02 09.98	5.95	6.22	1.98 - 7.07	8.06	3	4.089e-13	7.24	7.11	3.57	0	$\cdots$	0.33	V	$\cdots$	$\cdots$
13 45 21.467 -04 21 51.37	4.30	4.70	<2.34 - 4.84	3.95	3	1.590e-09	6.34	6.11	>2.07	9	$\cdots$	-0.78	V	$\cdots$	$\cdots$
13 45 30.055 +02 12 53.37	1.98	1.97	<1.45 - <4.28	$\cdots$	4	1.249e-07	4.53	4.88	>1.60	2	$\cdots$	-0.07	V	22.01	SDSS-G
13 45 45.612 +41 11 02.57	1.95	2.00	0.87 - 2.33	$\cdots$	3	4.455e-10	6.33	5.53	2.67	427	$\cdots$	-0.29	V	22.41	SDSS-*
13 45 57.726 -03 46 51.45	10.91	10.81	5.06 - 11.30	8.69	4	8.865e-07	5.27	4.84	2.23	5	$\cdots$	0.16	V	$\cdots$	$\cdots$
13 46 00.688 +20 29 57.88	5.04	4.86	2.83 - 5.44	5.59	4	6.187e-09	5.84	5.71	1.93	5	$\cdots$	-0.65	V	19.51	SDSS-G
13 46 29.729 +16 04 45.33	2.31	2.29	<1.92 - <17.34	$\cdots$	6	8.213e-08	4.44	5.69	>3.17	24	$\cdots$	0.78	V	$\cdots$	$\cdots$
13 46 49.838 +00 35 35.92	11.34	10.68	4.36 - 11.57	9.41	4	3.905e-07	5.63	5.11	2.46	67	$\cdots$	1.18	V	$\cdots$	$\cdots$
13 47 02.955 +23 37 38.18	13.18	12.71	8.40 - 16.48	10.58	3	9.129e-13	6.12	6.97	1.96	9	$\cdots$	-0.24	V	19.96	SDSS-G
13 47 13.575 -01 19 29.93	6.24	6.21	<3.01 - 7.24	6.10	3	0.000	8.21	8.25	>2.41	8	$\cdots$	1.24	V	$\cdots$	SDSS-UNKNOWN
13 47 57.620 +14 21 04.36	61.78	61.60	60.47 - 83.61	60.41	6	4.479e-09	4.21	3.83	1.38	12	$\cdots$	-0.57	V	$\cdots$	$\cdots$
13 48 12.773 +19 02 52.54	2.85	2.96	2.21 - 4.99	3.03	3	5.393e-07	4.15	5.11	2.26	$\cdots$	$\cdots$	0.89	V	20.97	SDSS-G
13 49 03.094 +39 02 16.86	2.71	2.65	1.93 - <4.46	$\cdots$	4	8.944e-09	4.33	5.82	2.05	1	$\cdots$	-0.33	V	20.04	SDSS-G
13 49 20.984 +28 15 25.81	3.22	3.37	<2.09 - <9.72	$\cdots$	6	1.076e-08	5.54	5.65	>1.76	920	$\cdots$	-1.74	V	$\cdots$	SDSS-FIRST-G
13 49 32.095 +15 05 14.73	48.67	47.85	47.43 - 66.84	53.57	5	3.424e-08	4.12	3.74	1.41	5	$\cdots$	0.22	V	$\cdots$	$\cdots$
13 49 34.742 +30 39 49.22	2.46	2.41	<1.60 - <13.32	$\cdots$	5	5.134e-07	5.04	5.01	>2.30	3	$\cdots$	-0.62	V	$\cdots$	$\cdots$
13 50 06.160 +11 38 57.79	2.12	2.34	1.25 - <3.82	$\cdots$	4	2.684e-08	5.38	5.24	2.27	1	$\cdots$	0.09	V	18.77	SDSS-G
13 50 13.198 +12 00 35.02	6.07	6.09	3.52 - 7.08	$\cdots$	3	4.023e-10	5.75	5.95	2.01	2	$\cdots$	1.13	V	$\cdots$	$\cdots$
13 50 13.275 +18 28 28.01	6.02	6.23	<3.83 - 6.90	5.83	4	1.669e-06	5.24	5.16	>1.69	$\cdots$	$\cdots$	-0.12	V	$\cdots$	$\cdots$
13 50 45.392 -07 24 58.62	4.99	4.83	2.67 - 4.99	4.55	3	2.369e-09	5.22	5.17	>1.80	11	$\cdots$	0.51	V	$\cdots$	$\cdots$
13 50 46.315 +38 57 44.57	3.33	3.46	1.94 - 4.35	$\cdots$	4	1.113e-09	6.11	5.50	2.03	1	$\cdots$	0.63	V	$\cdots$	$\cdots$

Coordinates (J2000)	f (mJy)				N	Measures			$\frac{\text{Max.}}{\text{Min.}}$	$T_{\min}$	Flags	σ_{nbr}	Type	i	Cross-ID
	Cat.	$\overline{f}$	Range	NVSS		$P(\chi^2,\nu)$	$\sigma_{\max}$	$\Delta_{\max}(\sigma)$		(days)				Mag.	
13 50 49.655 +38 41 04.18	4.82	5.04	2.30 - <8.95	$\cdots$	5	1.628e-12	6.54	5.74	2.08	5	$\cdots$	0.97	V	16.94	SDSS-G
13 51 48.212 +17 40 32.22	3.99	4.13	1.65 - <6.38	4.10	4	1.782e-07	5.49	5.16	2.66	2	$\cdots$	0.72	V	21.59	SDSS-G
13 52 25.206 -01 04 01.96	12.52	13.03	5.39 - 13.10	10.05	3	8.419e-07	5.25	4.82	2.43	8	$\cdots$	-0.16	V	$\cdots$	$\cdots$
13 53 01.512 +55 24 11.58	3.68	3.76	2.17 - 5.02	3.12	4	1.416e-07	5.45	5.10	1.92	49	$\cdots$	-0.21	V	$\cdots$	$\cdots$
13 53 10.173 -01 14 02.88	1.70	1.65	<1.42 - <6.94	$\cdots$	4	3.486e-07	4.11	5.35	>1.85	8	$\cdots$	1.14	V	$\cdots$	$\cdots$
13 54 40.298 +09 41 07.72	2.09	1.99	1.07 - <3.48	2.18	4	4.926e-08	4.04	5.45	>2.59	0	$\cdots$	0.86	V	$\cdots$	$\cdots$
13 54 48.724 +36 38 21.64	1.77	1.61	<1.16 - 2.20	$\cdots$	3	7.674e-08	4.61	5.53	>1.90	5	$\cdots$	-0.79	T	$\cdots$	$\cdots$
13 55 50.632 +54 56 10.72	2.70	2.70	2.18 - <5.58	3.69	4	4.897e-07	4.38	5.16	2.11	47	$\cdots$	0.02	V	20.02	SDSS-QSO(S)
13 55 52.229 -04 45 49.07	2.30	2.32	1.11 - 3.37	$\cdots$	3	5.093e-11	5.78	5.90	3.04	6	$\cdots$	0.07	V	21.24	SDSS-G
13 56 20.779 +25 53 03.95	1.69	1.80	<1.26 - 2.53	$\cdots$	3	4.808e-09	5.22	6.07	>2.00	1	$\cdots$	-0.49	V	$\cdots$	$\cdots$
13 56 27.861 +28 01 59.87	1.12	1.22	<0.83 - <4.58	$\cdots$	4	2.336e-07	4.72	4.99	>1.94	5	$\cdots$	0.06	V	17.22	SDSS-G
13 57 02.351 +19 08 24.06	4.60	4.84	<3.46 - 7.88	$\cdots$	4	8.741e-13	5.75	7.42	>2.28	$\cdots$	BN	0.00	V	18.82	SDSS-*
13 57 17.919 +19 22 43.15	11.49	12.42	4.80 - 12.84	10.41	4	1.229e-12	5.68	5.27	2.67	$\cdots$	BN	-0.44	V	$\cdots$	$\cdots$
13 57 59.854 +16 03 20.04	12.17	11.71	7.15 - 14.24	8.93	4	1.337e-10	5.88	6.32	1.99	24	$\cdots$	-0.31	V	19.23	SDSS-G
13 58 04.094 +14 10 59.93	6.96	7.26	4.29 - 7.78	$\cdots$	3	2.227e-07	5.46	4.67	1.72	12	$\cdots$	-0.23	V	18.48	SDSS-QSO(P)
13 58 29.370 +22 09 17.02	64.62	60.16	59.19 - 84.13	69.17	5	4.211e-10	4.05	3.65	1.42	2	$\cdots$	0.07	V	$\cdots$	$\cdots$
13 58 36.793 +53 51 12.40	3.86	3.75	1.89 - 5.37	5.51	3	1.172e-13	6.40	6.99	2.84	2426	$\cdots$	-0.12	V	19.28	SDSS-G
13 58 44.850 +01 23 56.76	7.16	7.12	<3.15 - <11.16	6.47	4	0.000	9.25	8.43	>2.41	3	$\cdots$	-0.01	V	$\cdots$	$\cdots$
13 58 49.069 -02 19 35.27	2.71	2.59	<1.70 - <4.06	$\cdots$	4	4.902e-08	5.65	5.31	>1.62	13	$\cdots$	-0.36	V	18.69	SDSS-G
13 59 25.192 +57 15 55.49	1.58	1.74	0.89 - <5.00	$\cdots$	4	2.810e-08	4.19	5.49	3.00	0	$\cdots$	0.58	V	21.02	SDSS-*
13 59 35.098 -07 25 44.04	19.46	18.47	17.87 - 27.67	23.27	3	1.717e-07	5.06	4.83	1.55	11	$\cdots$	1.01	V	19.33	SDSS-*
13 59 52.196 +04 37 09.61	3.41	3.52	<2.14 - 3.81	2.88	3	3.994e-07	5.33	5.18	>1.72	380	$\cdots$	-0.32	V	$\cdots$	$\cdots$
13 59 59.216 +26 54 51.46	4.82	4.92	2.18 - <13.76	4.18	6	3.614e-09	4.88	4.65	2.15	1	$\cdots$	-0.15	V	$\cdots$	$\cdots$
14 00 14.033 +35 49 48.61	3.11	3.08	1.92 - 4.53	$\cdots$	4	2.467e-07	4.25	5.45	2.36	1	$\cdots$	0.06	V	$\cdots$	$\cdots$
14 00 29.077 -06 10 45.36	5.44	5.23	2.17 - <6.10	$\cdots$	4	4.079e-10	4.84	5.24	2.71	8	$\cdots$	0.99	V	$\cdots$	$\cdots$
14 01 08.375 +24 40 11.02	2.37	2.10	<1.45 - 2.61	$\cdots$	3	3.722e-08	5.31	5.65	>1.80	2	BN	-0.92	V	19.02	SDSS-QSO(P)
14 02 26.060 +01 45 59.10	3.52	2.97	1.24 - 3.27	3.32	3	4.122e-07	5.19	5.22	2.63	2	$\cdots$	-1.77	V	$\cdots$	$\cdots$
14 02 44.773 +52 43 36.87	3.41	3.70	2.22 - 4.45	2.24	3	1.596e-07	5.09	4.61	2.00	2	$\cdots$	0.91	V	$\cdots$	$\cdots$
14 03 05.793 +04 43 35.11	5.87	5.98	<2.81 - 7.03	6.71	3	1.058e-09	6.39	6.16	>2.17	380	$\cdots$	0.67	V	$\cdots$	$\cdots$
14 03 06.907 +35 08 32.33	19.80	20.35	12.37 - 20.73	17.29	5	1.126e-08	5.26	4.55	1.68	1	BN	0.43	V	19.70	SDSS-G
14 03 09.990 +09 25 54.21	2.37	2.44	<2.03 - <12.45	2.22	4	8.364e-08	4.11	4.62	>1.42	3	BN	-0.41	V	21.00	SDSS-G

Coordinates (J2000)	f (mJy)				N	Measures			$\frac{\text{Max.}}{\text{Min.}}$	$T_{\min}$	Flags	σ_{nbr}	Type	i	Cross-ID
	Cat.	$\overline{f}$	Range	NVSS		$P(\chi^2,\nu)$	$\sigma_{\max}$	$\Delta_{\max}(\sigma)$		(days)				Mag.	
14 03 15.513 +28 08 57.71	3.99	3.87	2.37 - 5.42	$\cdots$	3	6.567e-10	5.22	6.14	2.28	920	$\cdots$	-0.95	V	16.18	SDSS-G
14 03 16.157 +16 45 34.64	3.26	3.49	1.92 - <13.54	$\cdots$	4	2.474e-07	4.45	4.54	2.01	6	$\cdots$	-0.71	V	$\cdots$	$\cdots$
14 03 29.337 +19 34 23.14	7.06	7.37	3.25 - 8.32	8.44	3	0.000	10.08	8.15	2.56	$\cdots$	$\cdots$	0.67	V	$\cdots$	$\cdots$
14 03 30.011 +08 59 29.36	2.91	2.94	<0.93 - <6.28	$\cdots$	4	0.000	11.18	11.36	>5.28	2	BN	1.21	V	$\cdots$	$\cdots$
14 03 31.187 +31 15 02.60	8.56	7.54	6.67 - 12.06	10.17	3	2.480e-13	5.93	6.43	1.81	97	$\cdots$	0.34	V	$\cdots$	$\cdots$
14 03 52.863 +35 59 25.54	56.95	55.47	51.12 - 76.37	59.35	4	3.399e-07	4.19	4.48	1.49	4	$\cdots$	0.07	V	20.84	SDSS-G
14 03 58.510 -04 38 51.27	2.14	1.99	<1.09 - <3.53	$\cdots$	4	6.402e-10	5.47	5.91	>2.48	7	$\cdots$	-0.31	V	$\cdots$	$\cdots$
14 04 32.142 +34 09 39.87	6.19	6.66	2.97 - 7.42	6.70	4	8.941e-12	7.02	6.20	2.44	1	BN	-0.19	V	$\cdots$	$\cdots$
14 04 33.105 +04 53 02.76	3.54	3.53	<2.08 - <19.93	3.19	4	2.174e-08	5.72	5.75	>1.84	381	$\cdots$	-0.10	V	19.60	SDSS-G
14 04 49.603 +03 04 47.56	2.83	3.18	1.85 - 3.90	$\cdots$	3	1.234e-07	4.41	5.05	2.10	87	$\cdots$	1.73	V	$\cdots$	$\cdots$
14 05 38.848 +08 59 51.58	2.37	2.53	1.34 - <6.66	2.17	4	6.132e-09	4.55	5.26	>1.58	2	BN	-1.41	V	$\cdots$	$\cdots$
14 06 01.472 -06 41 54.63	7.85	7.61	2.80 - 7.99	6.37	4	3.618e-07	5.63	5.35	2.83	0	$\cdots$	-0.31	V	$\cdots$	$\cdots$
14 06 18.116 +35 39 22.32	234.93	215.34	212.41 - 397.53	241.57	5	6.339e-14	6.45	6.13	1.87	1	$\cdots$	0.59	V	20.97	SDSS-QSO(P)
14 06 38.210 +01 02 55.05	8.24	8.44	6.79 - 10.20	13.93	3	2.327e-08	3.87	4.78	1.49	74	$\cdots$	-0.48	V	17.73	SDSS-QSO(S)
14 06 56.334 -06 50 47.98	10.12	9.38	3.96 - 12.34	8.11	4	5.335e-08	4.88	5.71	3.12	6	$\cdots$	-0.64	V	$\cdots$	$\cdots$
14 07 04.948 +20 23 01.34	2.07	2.16	<1.40 - 2.38	$\cdots$	3	2.009e-06	5.03	4.86	>1.68	$\cdots$	$\cdots$	-2.06	V	$\cdots$	$\cdots$
14 07 09.397 -02 46 02.49	3.91	3.75	<2.57 - <5.57	3.65	4	1.040e-07	5.19	5.23	>1.57	2	BN	0.49	V	21.19	SDSS-G
14 07 39.269 -05 15 04.75	1.84	1.70	<1.08 - 2.52	$\cdots$	3	8.923e-09	5.47	5.68	>2.00	9	$\cdots$	0.30	V	$\cdots$	$\cdots$
14 07 40.796 +09 59 32.45	3.75	3.81	2.36 - 4.58	4.95	3	4.355e-07	3.41	4.21	1.59	2	$\cdots$	1.27	V	$\cdots$	$\cdots$
14 08 19.354 +29 49 50.57	21.51	21.32	19.16 - 28.75	20.73	3	2.212e-08	4.49	5.00	1.50	19	$\cdots$	-0.03	V	17.74	SDSS-QSO(P)
14 08 20.537 +01 38 09.55	24.23	21.61	18.35 - 35.49	17.71	4	1.388e-14	6.19	7.04	1.93	2	$\cdots$	0.03	V	20.97	SDSS-G
14 08 46.970 +20 00 39.92	5.10	5.47	3.45 - 5.85	5.57	3	2.352e-07	5.40	4.76	1.70	$\cdots$	$\cdots$	0.02	V	21.68	SDSS-*
14 09 09.492 +20 08 09.53	3.97	4.05	<2.52 - 4.22	3.38	3	2.703e-10	5.81	5.59	>1.67	$\cdots$	$\cdots$	0.46	T	$\cdots$	$\cdots$
14 09 21.899 +35 46 21.11	2.72	2.81	1.55 - 5.00	$\cdots$	4	3.315e-07	4.16	4.42	2.07	4	$\cdots$	0.51	V	$\cdots$	$\cdots$
14 10 01.014 +21 01 11.40	11.65	11.73	8.71 - 13.55	8.52	4	2.851e-09	5.91	5.53	1.56	5	$\cdots$	0.71	V	20.43	SDSS-QSO(P)
14 10 07.844 +03 26 58.38	2.70	2.81	1.39 - 6.55	4.22	3	0.000	7.56	9.34	4.71	20	$\cdots$	0.48	V	21.02	SDSS-G
14 10 17.208 +20 35 57.53	2.51	2.40	1.25 - 3.24	$\cdots$	3	5.134e-11	4.79	5.96	>1.74	5	$\cdots$	-0.21	V	$\cdots$	$\cdots$
14 10 19.398 -00 54 26.38	3.22	3.42	1.80 - 4.99	$\cdots$	3	3.670e-11	6.14	5.40	2.17	4	$\cdots$	1.49	V	$\cdots$	GSC2-FIRST-S
14 10 29.077 +14 02 48.39	9.33	9.50	6.45 - 13.44	9.56	4	5.608e-07	3.81	5.34	2.09	0	$\cdots$	0.60	V	$\cdots$	$\cdots$
14 10 35.706 +19 20 02.88	2.33	2.33	1.65 - 5.70	$\cdots$	4	1.690e-09	4.02	4.72	3.46	$\cdots$	$\cdots$	0.68	V	18.00	SDSS-G
14 11 00.930 +12 18 59.48	3.38	3.44	2.05 - <4.79	$\cdots$	4	3.486e-09	5.77	5.45	1.98	2	$\cdots$	-0.13	V	$\cdots$	$\cdots$

Continued on next page. . .

144

Coordinates (J2000)	f (mJy)				N	Measures			$\frac{\text{Max.}}{\text{Min.}}$	$T_{\min}$	Flags	σ_{nbr}	Type	i	Cross-ID
	Cat.	$\overline{f}$	Range	NVSS		$P(\chi^2,\nu)$	$\sigma_{\max}$	$\Delta_{\max}(\sigma)$		(days)				Mag.	
14 11 05.442 +20 06 09.98	1.92	2.04	1.26 - <7.83	$\cdots$	4	3.208e-08	4.21	5.56	>2.55	$\cdots$	$\cdots$	0.03	V	$\cdots$	$\cdots$
14 11 37.365 +12 22 41.64	2.94	2.71	2.02 - 3.89	2.01	3	4.854e-08	4.08	4.53	1.93	4	$\cdots$	-2.43	V	$\cdots$	$\cdots$
14 12 08.221 +38 35 21.73	3.75	3.89	<2.88 - <9.87	2.50	5	1.072e-08	5.02	4.91	>1.43	497	$\cdots$	0.58	V	19.94	SDSS-QSO(S)
14 12 18.094 -06 35 18.38	2.37	2.26	1.95 - 7.62	$\cdots$	3	1.172e-10	5.80	6.04	3.91	4	$\cdots$	0.02	V	$\cdots$	$\cdots$
14 13 15.568 +12 34 27.61	3.71	4.43	<1.77 - <9.03	$\cdots$	3	2.354e-14	7.50	6.90	>2.84	2	$\cdots$	2.18	V	$\cdots$	$\cdots$
14 13 17.648 +44 28 35.78	10.70	11.09	8.90 - 14.04	9.05	4	1.226e-08	3.89	5.08	1.58	31	$\cdots$	1.10	V	$\cdots$	$\cdots$
14 14 17.318 +49 06 02.71	6.11	5.48	5.20 - <18.02	4.83	6	4.894e-07	5.34	5.40	1.93	0	$\cdots$	-0.10	V	$\cdots$	$\cdots$
14 15 08.573 +36 14 45.13	3.30	3.37	1.46 - <4.09	3.91	4	5.407e-11	5.49	5.81	>2.68	5	$\cdots$	-0.16	V	$\cdots$	$\cdots$
14 15 14.092 +17 00 57.25	4.64	4.83	2.02 - 5.00	4.51	3	1.007e-08	6.02	5.51	2.47	29	$\cdots$	0.52	V	$\cdots$	$\cdots$
14 15 21.339 +49 17 20.02	10.77	9.76	8.82 - 14.31	9.51	3	4.839e-07	4.91	5.29	1.62	1	$\cdots$	0.25	V	$\cdots$	$\cdots$
14 15 31.058 -03 28 54.56	2.42	2.52	<1.78 - 3.11	$\cdots$	3	8.524e-07	5.10	4.88	>1.50	1	$\cdots$	-0.60	V	$\cdots$	$\cdots$
14 15 46.150 -06 29 35.68	2.28	2.35	1.55 - 3.01	$\cdots$	3	3.003e-07	4.06	4.92	>1.50	0	$\cdots$	-1.08	V	$\cdots$	$\cdots$
14 15 58.477 +34 05 06.63	4.68	4.72	1.82 - 5.14	4.35	3	7.504e-08	5.52	5.37	2.83	1	$\cdots$	0.64	V	$\cdots$	$\cdots$
14 16 19.779 +36 40 28.58	19.59	19.47	17.13 - 24.15	19.78	4	5.033e-07	3.29	4.18	1.41	7	$\cdots$	-0.50	V	21.61	SDSS-G
14 16 36.804 +07 12 05.14	12.00	12.61	<7.25 - 12.88	7.04	3	3.331e-16	6.18	5.90	>1.78	3	BN	1.87	T	$\cdots$	$\cdots$
14 16 44.498 -03 46 17.69	6.33	5.39	<4.00 - 7.63	6.07	4	1.601e-10	4.95	5.09	>1.45	3	BN	-0.85	V	$\cdots$	$\cdots$
14 17 07.031 +46 13 11.99	2.61	2.62	<1.76 - <4.32	$\cdots$	4	9.959e-14	5.91	6.87	>2.01	2	BN	-0.73	V	$\cdots$	$\cdots$
14 17 27.374 +46 04 29.11	3.15	2.93	<1.67 - <5.00	$\cdots$	4	2.366e-13	6.74	7.15	>2.16	1	BN	-0.23	V	19.91	SDSS-G
14 17 31.846 -03 22 02.84	7.53	7.53	<4.07 - 7.66	$\cdots$	4	1.373e-08	6.24	5.93	>1.88	1	$\cdots$	1.46	V	$\cdots$	$\cdots$
14 17 35.284 +07 40 16.17	4.90	5.10	2.31 - <13.21	5.76	4	2.979e-08	5.58	5.57	2.44	2	BN	1.14	V	$\cdots$	$\cdots$
14 17 53.544 +31 26 26.38	4.75	4.89	3.40 - 6.71	$\cdots$	4	6.461e-08	4.12	5.02	1.94	95	$\cdots$	0.95	V	$\cdots$	$\cdots$
14 18 06.434 -03 11 53.63	7.25	7.13	2.06 - 8.28	6.60	3	0.000	9.72	8.33	4.02	0	$\cdots$	-0.99	V	20.84	SDSS-*
14 18 21.779 +31 49 36.77	1.14	1.21	<0.75 - <6.73	$\cdots$	4	2.530e-07	4.93	4.74	>2.00	96	$\cdots$	1.23	V	$\cdots$	$\cdots$
14 18 24.250 +60 24 11.82	9.19	9.16	3.61 - 9.31	8.67	4	5.205e-12	7.41	6.43	2.58	4	$\cdots$	1.04	V	$\cdots$	$\cdots$
14 18 52.588 -06 23 00.30	4.24	3.99	<2.40 - <4.76	$\cdots$	4	4.676e-07	5.33	5.20	>1.73	4	$\cdots$	0.75	V	$\cdots$	$\cdots$
14 19 33.402 +44 32 54.00	3.96	4.18	<2.15 - 4.59	2.31	3	2.313e-11	6.80	6.69	>2.14	5	$\cdots$	1.02	V	$\cdots$	SDSS-UNKNOWN
14 19 36.453 +00 25 25.02	5.25	5.35	2.32 - 5.80	3.28	3	4.460e-07	5.25	5.10	2.51	13	$\cdots$	-0.13	V	$\cdots$	$\cdots$
14 19 55.594 +36 32 32.33	5.46	5.55	2.36 - 5.91	5.06	3	2.851e-13	7.50	6.41	2.50	5	$\cdots$	0.02	V	19.53	SDSS-G
14 20 32.366 -02 58 20.51	5.43	5.94	3.28 - 6.33	$\cdots$	4	7.409e-08	3.59	3.75	>1.17	7	$\cdots$	-1.54	V	19.55	SDSS-G
14 21 13.649 -05 40 59.55	5.83	5.66	3.01 - 5.82	$\cdots$	3	8.315e-08	4.38	4.14	>1.93	4	$\cdots$	-0.56	V	$\cdots$	$\cdots$
14 21 22.251 -05 31 40.53	5.63	5.81	2.55 - <9.52	6.03	4	9.437e-15	7.81	7.06	2.50	0	$\cdots$	-2.76	V	$\cdots$	$\cdots$

Coordinates (J2000)	f (mJy)				N	Measures			$\frac{\text{Max.}}{\text{Min.}}$	$T_{\min}$	Flags	σ_{nbr}	Type	i	Cross-ID
	Cat.	$\overline{f}$	Range	NVSS		$P(\chi^2,\nu)$	$\sigma_{\max}$	$\Delta_{\max}(\sigma)$		(days)				Mag.	
14 21 50.442 +25 25 31.60	2.08	2.32	1.06 - 2.82	2.29	3	4.215e-07	4.27	4.81	>2.66	6	$\cdots$	0.55	V	$\cdots$	$\cdots$
14 22 00.344 -05 07 07.14	3.25	3.34	<2.25 - <9.20	$\cdots$	4	1.416e-06	5.04	5.10	>1.62	9	$\cdots$	0.70	V	$\cdots$	$\cdots$
14 22 11.675 +07 59 27.83	4.91	4.56	4.40 - 8.52	3.49	4	2.457e-07	3.89	4.47	>1.66	5	$\cdots$	-0.08	V	16.25	SDSS-G
14 23 06.152 -05 14 52.30	3.94	4.20	2.98 - 6.04	$\cdots$	3	1.430e-08	4.29	5.59	2.03	9	$\cdots$	-0.09	V	$\cdots$	GSC2-FIRST-G
14 23 12.590 +10 58 25.55	1.22	1.14	<1.09 - <5.41	$\cdots$	4	2.992e-07	3.89	5.07	>1.84	1	$\cdots$	-0.52	V	20.19	SDSS-G
14 23 26.067 +60 35 42.32	3.52	3.30	2.28 - 4.66	4.61	3	2.792e-09	4.45	5.73	2.04	4	$\cdots$	0.93	V	$\cdots$	$\cdots$
14 23 46.040 -05 11 34.48	9.97	9.74	3.46 - 11.66	11.19	3	5.187e-10	6.26	5.75	3.37	9	$\cdots$	0.72	V	$\cdots$	$\cdots$
14 23 58.865 +20 38 47.46	8.58	8.62	<5.50 - 11.64	7.76	5	3.945e-08	5.52	5.32	>2.12	5	$\cdots$	0.23	V	14.57	SDSS-G
14 24 21.489 +22 11 16.91	2.85	2.96	1.76 - 4.05	2.67	3	7.258e-09	4.37	5.73	2.30	1002	$\cdots$	0.72	V	20.07	SDSS-*
14 24 34.237 +19 19 13.16	3.46	3.46	<2.16 - 3.83	$\cdots$	3	4.896e-10	6.12	6.11	>1.77	$\cdots$	BN	1.25	V	21.76	SDSS-G
14 24 50.167 +26 46 57.68	3.10	3.11	<2.03 - 3.60	$\cdots$	3	8.247e-09	5.57	5.87	>1.77	2	$\cdots$	-0.65	V	$\cdots$	$\cdots$
14 25 13.594 +14 26 04.92	2.32	2.23	1.80 - 3.40	2.24	3	1.820e-07	3.93	5.14	>1.62	12	BN	-0.58	V	19.15	SDSS-G
14 25 46.300 +27 16 05.72	1.85	2.03	<1.47 - 5.72	$\cdots$	3	2.030e-07	4.14	5.14	>3.89	4	$\cdots$	-1.58	V	$\cdots$	$\cdots$
14 26 08.496 -03 56 48.47	3.17	2.92	<1.91 - 3.51	$\cdots$	3	9.293e-09	5.73	5.67	>1.83	921	$\cdots$	-0.52	V	$\cdots$	$\cdots$
14 26 24.258 +14 17 09.87	1.28	1.03	<1.06 - <5.69	$\cdots$	4	3.739e-07	4.44	5.10	>3.20	15	BN	0.48	V	18.50	SDSS-G
14 26 33.340 -03 56 20.77	4.56	4.17	3.81 - 7.20	5.01	3	9.097e-08	5.29	5.51	1.89	918	$\cdots$	-0.75	V	$\cdots$	$\cdots$
14 26 35.900 +14 40 59.01	1.54	1.49	<1.07 - 2.43	$\cdots$	3	5.387e-07	4.37	5.28	>2.27	3	BN	1.13	V	22.17	SDSS-*
14 26 45.520 +24 15 22.96	9.34	9.23	5.34 - 9.45	5.49	3	9.024e-09	5.42	4.75	1.77	1	BN	-1.94	V	18.85	SDSS-QSO(S)
14 27 13.729 +49 42 52.11	26.85	24.20	23.57 - 32.60	27.95	5	1.032e-09	4.29	3.95	1.38	2	$\cdots$	-0.45	V	$\cdots$	$\cdots$
14 27 46.011 +25 51 43.93	2.33	2.47	1.52 - 3.04	$\cdots$	3	3.250e-08	4.26	4.79	>1.49	2	$\cdots$	-1.18	V	$\cdots$	$\cdots$
14 28 08.064 -06 09 22.78	1.94	1.80	<1.25 - <7.29	$\cdots$	4	1.054e-07	4.78	5.31	>2.34	2	$\cdots$	-0.81	V	$\cdots$	$\cdots$
14 28 31.512 +18 47 36.33	2.39	2.27	1.87 - 4.20	$\cdots$	4	1.670e-07	4.97	5.45	>2.24	$\cdots$	$\cdots$	0.42	V	18.97	SDSS-G
14 28 33.311 -01 24 44.92	3.98	4.09	<3.64 - <18.61	$\cdots$	4	5.074e-08	4.62	5.67	>2.73	8	BN	-0.82	V	$\cdots$	$\cdots$
14 30 13.605 -06 30 20.48	5.22	5.47	2.03 - 5.58	5.00	3	1.235e-07	5.57	5.17	2.75	4	$\cdots$	-1.14	V	$\cdots$	$\cdots$
14 30 51.614 +00 25 14.50	1.77	1.54	<1.19 - 2.69	$\cdots$	3	4.910e-08	4.14	5.77	>2.27	14	$\cdots$	-1.29	V	18.23	SDSS-G
14 31 31.450 +03 54 23.68	4.32	4.46	2.86 - 7.74	5.37	4	4.441e-16	6.85	7.14	2.06	983	$\cdots$	-3.78	V	$\cdots$	$\cdots$
14 31 37.053 +44 45 12.25	35.19	34.75	34.11 - 47.28	33.95	5	2.782e-07	4.10	3.77	1.39	2	$\cdots$	0.25	V	$\cdots$	RASS-FSC
14 32 08.712 +16 32 08.55	1.64	1.88	1.17 - <5.28	$\cdots$	4	1.225e-07	4.19	4.93	2.39	1	$\cdots$	0.06	V	$\cdots$	$\cdots$
14 32 37.375 +08 21 42.28	19.18	17.66	15.18 - 33.54	17.75	4	0.000	8.42	9.02	2.21	0	$\cdots$	-0.23	V	20.43	SDSS-QSO(P)
14 32 45.557 -01 35 51.48	2.28	2.23	<1.82 - <9.50	$\cdots$	4	1.066e-07	4.11	5.56	>2.34	2	$\cdots$	0.21	V	17.02	SDSS-G
14 33 32.878 +03 36 10.57	3.73	3.86	1.86 - 7.43	$\cdots$	4	1.299e-09	4.46	5.04	2.44	76	$\cdots$	-2.27	V	18.94	SDSS-G

Continued on next page. . .

Coordinates (J2000)	f (mJy)				N	Measures			$\frac{\text{Max.}}{\text{Min.}}$	$T_{\min}$	Flags	σ_{nbr}	Type	i	Cross-ID
	Cat.	$\overline{f}$	Range	NVSS		$P(\chi^2,\nu)$	$\sigma_{\max}$	$\Delta_{\max}(\sigma)$		(days)				Mag.	
14 33 39.324 +35 40 13.16	3.21	3.28	1.79 - 3.79	2.49	3	7.292e-09	5.73	5.67	2.12	4	$\cdots$	-0.02	V	20.13	SDSS-G
14 33 40.258 +09 14 21.46	5.41	5.32	2.10 - 10.32	4.10	4	0.000	17.07	13.46	4.91	1	$\cdots$	0.13	V	19.91	SDSS-*
14 34 16.161 +29 43 52.08	3.78	3.74	<2.56 - 5.03	$\cdots$	4	8.932e-08	5.66	5.34	>1.55	2	$\cdots$	0.22	V	$\cdots$	SDSS-UNKNOWN
14 34 27.316 +18 41 30.15	6.91	7.07	3.53 - 9.71	5.84	6	1.034e-11	5.84	5.58	>1.57	$\cdots$	$\cdots$	-0.30	V	$\cdots$	$\cdots$
14 34 49.113 +35 42 46.98	21.57	20.60	18.87 - 28.33	$\cdots$	4	2.895e-08	4.03	4.41	1.50	4	$\cdots$	-2.27	V	16.15	SDSS-G
14 36 25.283 -02 08 55.12	1.80	1.88	1.48 - 5.38	3.03	3	5.249e-13	5.26	5.76	3.19	48	$\cdots$	0.96	V	19.71	SDSS-*
14 37 30.648 +07 36 45.09	12.47	12.35	5.43 - 13.65	16.19	5	1.152e-05	5.16	4.71	2.28	0	$\cdots$	-0.08	V	19.61	SDSS-G
14 37 47.417 +45 46 29.58	8.91	9.02	6.23 - <11.61	4.85	5	3.713e-10	5.38	4.82	1.55	3	$\cdots$	-0.02	V	21.71	SDSS-*
14 39 14.260 +08 04 21.42	2.66	2.52	<1.61 - 3.95	$\cdots$	3	5.077e-12	5.79	6.36	>1.99	5	BN	-2.02	V	$\cdots$	$\cdots$
14 39 27.004 +20 10 53.29	4.54	4.38	1.55 - 4.88	2.88	3	1.228e-10	6.65	6.14	2.98	$\cdots$	$\cdots$	-1.44	V	$\cdots$	$\cdots$
14 39 39.536 +03 11 57.96	2.26	2.26	1.53 - 6.62	$\cdots$	4	2.190e-09	4.34	5.47	>2.26	84	$\cdots$	0.07	V	19.39	SDSS-G
14 39 50.006 +08 00 14.04	9.93	10.15	7.30 - 11.49	10.19	3	9.490e-09	5.67	4.71	1.49	2	BN	0.45	V	20.60	SDSS-QSO(P)
14 40 08.057 +19 44 11.63	2.90	2.90	1.61 - 3.95	3.45	3	7.386e-11	6.02	5.46	2.45	$\cdots$	$\cdots$	-0.06	V	21.04	SDSS-G
14 40 31.545 +35 15 46.87	22.91	19.86	18.74 - 27.83	23.10	5	1.479e-10	4.90	4.84	1.48	68	$\cdots$	-1.22	V	16.73	SDSS-G
14 41 35.193 +22 10 14.28	4.69	4.91	3.43 - 5.85	4.69	3	2.429e-07	4.26	4.92	1.71	1004	$\cdots$	-0.21	V	$\cdots$	$\cdots$
14 41 46.187 +15 12 38.95	4.82	5.01	<3.58 - <5.99	4.28	4	8.412e-07	5.25	5.05	>1.45	4	$\cdots$	-0.48	V	$\cdots$	$\cdots$
14 42 01.978 +44 29 28.25	62.28	58.04	56.53 - 77.06	88.92	5	7.027e-10	3.90	3.61	1.36	4	$\cdots$	1.09	V	$\cdots$	$\cdots$
14 42 13.748 +02 13 12.62	8.34	8.15	3.83 - 11.89	7.69	4	6.459e-13	6.65	6.97	3.10	83	$\cdots$	0.37	V	$\cdots$	$\cdots$
14 42 29.333 +01 30 13.24	1.70	1.51	<1.04 - 2.39	2.97	3	8.730e-09	4.92	5.98	>2.30	1	$\cdots$	0.48	V	17.92	SDSS-G
14 42 42.788 +25 59 39.49	1.16	1.06	<0.76 - <4.64	$\cdots$	4	1.084e-07	4.45	5.19	>2.17	1	$\cdots$	2.02	V	$\cdots$	$\cdots$
14 43 01.897 +36 31 42.32	3.08	3.27	<2.16 - 3.96	$\cdots$	3	1.590e-07	4.97	5.55	>1.83	5	$\cdots$	-0.23	V	20.13	SDSS-G
14 44 44.062 +23 59 31.72	3.90	3.71	2.63 - 4.50	3.50	3	2.437e-07	4.10	4.76	1.71	4	$\cdots$	-0.39	V	$\cdots$	$\cdots$
14 44 47.640 +32 13 12.42	5.88	6.07	2.79 - <10.16	5.59	5	1.803e-06	5.11	4.82	2.24	1	$\cdots$	-0.07	V	19.88	SDSS-*
14 44 55.895 +24 06 09.31	67.47	59.47	33.64 - 81.93	72.16	5	9.548e-14	5.07	6.88	2.44	2	$\cdots$	-0.99	V	21.44	SDSS-G
14 46 14.561 -03 19 27.70	17.39	18.36	10.35 - 19.80	17.31	4	3.989e-06	5.01	4.61	1.91	1	$\cdots$	-0.19	V	$\cdots$	GSC2-FIRST-S
14 46 46.696 +00 37 04.49	6.25	6.20	<4.54 - 6.39	5.49	3	7.793e-07	5.26	5.03	>1.41	1	$\cdots$	0.36	V	$\cdots$	$\cdots$
14 47 53.313 +19 58 19.30	1.25	1.24	<1.34 - <2.97	$\cdots$	4	2.805e-07	4.17	4.78	>1.67	$\cdots$	BN	0.20	V	$\cdots$	$\cdots$
14 47 55.679 +13 09 43.36	53.05	50.80	49.67 - 70.45	56.87	6	8.653e-13	4.36	4.04	1.42	4	$\cdots$	0.26	V	20.80	SDSS-QSO(P)
14 48 13.422 +00 39 21.17	1.59	1.61	<1.33 - 2.43	$\cdots$	3	1.550e-07	4.00	5.30	>1.82	1	BN	0.07	V	18.70	SDSS-QSO(S)
14 49 02.542 +47 19 38.82	4.15	4.30	2.32 - 5.09	2.42	4	9.902e-07	5.00	4.92	2.06	2	$\cdots$	0.71	V	20.31	SDSS-G
14 49 11.268 -00 26 25.68	2.75	2.80	1.15 - 3.15	2.72	3	3.833e-07	5.18	4.74	2.73	1	$\cdots$	0.93	V	18.10	SDSS-G

Coordinates (J2000)	f (mJy)				N	Measures			$\frac{\text{Max.}}{\text{Min.}}$	$T_{\min}$	Flags	σ_{nbr}	Type	i	Cross-ID
	Cat.	$\overline{f}$	Range	NVSS		$P(\chi^2,\nu)$	$\sigma_{\max}$	$\Delta_{\max}(\sigma)$		(days)				Mag.	
14 49 11.682 +00 09 20.38	11.19	12.02	<7.75 - 12.47	9.29	4	1.859e-07	5.81	5.44	>1.56	13	BN	-0.36	V	19.50	SDSS-G
14 49 12.697 +03 30 19.90	2.02	2.08	<1.70 - 2.86	$\cdots$	3	2.138e-09	4.39	5.64	>1.68	95	$\cdots$	0.55	T	$\cdots$	$\cdots$
14 49 27.927 +27 46 50.15	60.55	58.79	45.23 - 80.85	58.75	5	6.468e-08	3.75	5.02	1.68	2	$\cdots$	-1.49	V	13.23	SDSS-G
14 49 52.639 +01 42 49.14	1.24	1.16	<0.91 - 2.35	$\cdots$	3	1.567e-08	4.21	5.87	>2.59	2	$\cdots$	0.76	V	$\cdots$	$\cdots$
14 49 57.473 -01 37 59.35	3.29	3.24	1.20 - <7.83	$\cdots$	4	1.291e-10	6.32	6.48	3.16	2	$\cdots$	1.54	V	$\cdots$	$\cdots$
14 50 06.599 -07 27 40.57	2.26	2.18	1.26 - <7.25	2.41	4	5.612e-08	3.88	5.30	>2.44	2	$\cdots$	2.07	V	$\cdots$	$\cdots$
14 50 12.938 +60 50 52.19	50.02	47.79	41.86 - 64.29	54.30	4	6.059e-08	3.92	4.79	1.45	0	$\cdots$	0.35	V	$\cdots$	$\cdots$
14 50 19.226 +61 00 41.84	10.06	9.13	8.77 - 13.37	11.00	3	5.012e-08	4.20	4.17	1.52	0	$\cdots$	-0.08	V	17.53	SDSS-G
14 50 47.175 -07 17 56.27	22.86	22.64	21.52 - 31.92	15.61	4	2.173e-12	4.87	4.74	1.48	11	$\cdots$	1.05	V	$\cdots$	GSC2-FIRST-G
14 50 54.448 +36 19 28.63	4.04	4.42	2.33 - 5.39	4.14	4	6.682e-08	4.65	5.42	2.31	5	$\cdots$	-0.61	V	$\cdots$	$\cdots$
14 51 26.927 +58 05 01.79	4.77	5.13	<3.70 - 7.86	5.24	5	4.600e-08	4.77	5.41	>2.12	442	$\cdots$	-1.33	V	$\cdots$	$\cdots$
14 51 38.793 +03 39 46.16	2.78	2.84	2.00 - 3.81	$\cdots$	3	4.671e-07	4.14	4.84	1.90	75	$\cdots$	0.60	V	19.35	SDSS-QSO(S)
14 51 41.129 -01 39 12.43	2.95	3.24	<0.80 - 5.35	$\cdots$	4	0.000	12.79	11.45	>6.66	2	$\cdots$	0.42	T	$\cdots$	$\cdots$
14 51 45.970 -03 10 10.76	3.49	3.32	2.32 - 5.06	3.73	4	3.977e-07	4.03	4.38	1.69	0	$\cdots$	-0.49	V	19.03	SDSS-G
14 53 02.802 +19 02 11.49	3.48	3.44	1.48 - 3.92	2.71	3	1.741e-08	5.11	5.39	2.66	$\cdots$	$\cdots$	0.64	V	$\cdots$	$\cdots$
14 53 31.036 -06 49 08.22	3.91	3.87	3.14 - <6.94	5.26	4	7.124e-09	3.95	4.90	1.96	4	$\cdots$	0.47	V	$\cdots$	$\cdots$
14 53 37.017 +16 02 59.60	2.08	2.15	1.67 - <5.83	$\cdots$	4	3.488e-07	3.44	4.45	2.02	19	$\cdots$	0.44	V	$\cdots$	$\cdots$
14 53 59.106 +11 57 55.07	1.65	1.42	0.74 - 4.47	$\cdots$	4	2.223e-09	4.08	4.90	3.08	3	$\cdots$	0.70	V	$\cdots$	$\cdots$
14 54 05.409 -01 58 33.40	6.61	7.14	5.34 - 8.18	8.39	3	2.521e-07	4.96	5.00	1.53	52	$\cdots$	-0.06	V	$\cdots$	$\cdots$
14 54 11.389 +30 28 28.42	1.13	0.93	<0.96 - 2.51	$\cdots$	4	5.047e-07	4.38	5.16	>2.61	10	$\cdots$	0.86	V	$\cdots$	$\cdots$
14 54 37.013 -04 42 37.13	16.21	15.89	7.08 - 19.08	12.82	4	6.800e-11	6.33	6.43	2.69	29	BN	-0.13	V	$\cdots$	$\cdots$
14 55 50.350 +27 45 10.16	16.63	16.01	10.62 - 17.78	13.69	3	7.013e-08	5.50	4.91	1.67	2	$\cdots$	-1.23	V	$\cdots$	$\cdots$
14 56 14.363 -03 42 26.30	2.68	2.75	<1.94 - 3.47	2.55	3	2.910e-08	5.55	4.99	>1.79	1	$\cdots$	-2.10	V	$\cdots$	$\cdots$
14 56 30.571 +20 19 16.34	9.51	10.12	6.52 - 11.62	11.00	4	1.004e-09	6.50	5.25	1.64	1	$\cdots$	-1.44	V	20.99	SDSS-QSO(P)
14 56 30.718 +20 11 10.49	8.20	9.08	5.86 - 9.42	8.44	3	3.136e-08	5.76	4.78	1.61	$\cdots$	$\cdots$	0.58	V	$\cdots$	$\cdots$
14 56 30.765 -03 48 42.92	3.60	3.62	2.02 - 4.10	3.35	4	7.407e-08	5.09	5.10	2.03	0	$\cdots$	-1.37	V	$\cdots$	$\cdots$
14 56 45.853 +36 34 21.15	8.95	8.12	3.44 - <9.23	8.61	5	3.041e-06	5.01	4.76	2.42	5	$\cdots$	-0.99	V	$\cdots$	$\cdots$
14 57 17.721 +37 08 15.90	90.69	88.08	84.67 - 120.90	88.33	5	1.356e-10	4.65	4.37	1.41	1	$\cdots$	0.41	V	$\cdots$	$\cdots$
14 57 29.476 +05 40 25.28	4.24	4.16	2.77 - 4.49	3.94	3	4.651e-07	4.25	4.42	>1.31	0	$\cdots$	1.22	V	$\cdots$	$\cdots$
14 57 40.327 +59 19 16.53	21.87	21.87	13.96 - 23.74	22.12	4	8.304e-14	7.89	5.60	1.60	1	BN	0.13	V	$\cdots$	$\cdots$
14 57 44.407 -05 46 09.25	4.15	4.01	<2.95 - 4.65	3.46	4	1.399e-09	4.82	5.24	>1.58	2	$\cdots$	-1.01	V	$\cdots$	GSC2-FIRST-G

Coordinates (J2000)	f (mJy)				N	Measures			$\frac{\text{Max.}}{\text{Min.}}$	$T_{\min}$	Flags	σ_{nbr}	Type	i	Cross-ID
	Cat.	$\overline{f}$	Range	NVSS		$P(\chi^2, \nu)$	$\sigma_{\max}$	$\Delta_{\max}(\sigma)$		(days)				Mag.	
14 57 49.761 +05 28 24.47	3.72	3.71	<2.22 - 4.19	$\cdots$	3	1.566e-09	5.97	6.12	>1.89	1	$\cdots$	1.07	V	$\cdots$	$\cdots$
14 58 07.731 +02 26 23.22	6.46	7.02	2.67 - 8.74	6.67	4	2.183e-08	5.37	5.08	2.70	4	$\cdots$	0.57	V	19.01	SDSS-G
14 58 27.352 +48 32 46.20	2.57	2.84	1.54 - 4.76	$\cdots$	4	2.337e-10	5.18	6.81	3.09	3	$\cdots$	0.46	V	19.38	SDSS-G
14 58 44.487 -06 31 30.83	3.45	3.49	<2.15 - 4.12	$\cdots$	2	1.103e-12	6.77	6.64	>1.92	0	$\cdots$	0.11	T	$\cdots$	$\cdots$
14 58 45.773 -06 47 26.30	5.09	4.71	2.34 - 4.99	6.02	4	8.161e-11	4.27	4.34	>1.49	0	$\cdots$	0.29	V	$\cdots$	$\cdots$
14 58 55.829 +09 35 21.98	2.43	2.45	<1.71 - 3.21	$\cdots$	3	2.561e-10	5.63	5.78	>1.86	2	$\cdots$	0.37	V	$\cdots$	$\cdots$
14 59 01.395 +42 45 20.32	9.30	9.10	7.65 - 16.98	12.20	4	2.010e-13	6.87	7.63	2.22	429	$\cdots$	0.56	V	21.02	SDSS-*
14 59 20.402 +10 00 13.49	2.20	2.00	<1.24 - 2.84	$\cdots$	3	2.323e-08	5.40	5.39	>1.82	1	$\cdots$	2.68	V	$\cdots$	$\cdots$
15 00 12.184 +08 54 29.35	1.74	1.82	<0.69 - 4.77	$\cdots$	3	0.000	7.96	10.51	>6.96	2	BN	-0.36	T	$\cdots$	$\cdots$
15 00 33.186 -01 48 51.90	1.34	1.42	<1.02 - <3.72	$\cdots$	4	5.275e-07	4.67	4.75	>1.75	4	$\cdots$	0.25	V	20.74	SDSS-*
15 00 44.297 +42 30 20.96	1.82	1.74	<1.38 - 3.59	2.49	3	1.213e-07	4.59	4.54	>2.61	55	$\cdots$	-0.48	V	20.98	SDSS-G
15 01 06.244 +55 27 50.77	11.58	11.65	7.45 - 14.31	10.80	4	4.776e-09	4.52	4.34	1.92	15	$\cdots$	1.80	V	19.66	SDSS-QSO(S)
15 01 24.675 +56 19 49.27	164.92	148.85	147.86 - 202.10	170.30	3	2.154e-07	4.15	3.66	1.37	2	$\cdots$	-2.12	V	18.14	SDSS-QSO(S)
15 02 13.433 +31 14 02.26	2.28	2.34	<1.72 - 2.71	2.37	3	4.632e-07	5.00	5.36	>1.58	96	$\cdots$	-0.24	V	$\cdots$	$\cdots$
15 02 14.227 +57 02 04.97	23.75	26.12	9.87 - 27.26	17.93	4	6.438e-06	5.11	4.90	2.76	3	$\cdots$	0.81	V	$\cdots$	$\cdots$
15 02 41.653 +12 51 27.21	1.48	1.57	0.86 - 2.87	$\cdots$	3	1.563e-07	4.35	5.37	>3.34	4	$\cdots$	-0.31	V	$\cdots$	$\cdots$
15 02 46.490 +29 35 12.07	3.57	3.50	2.16 - 4.65	$\cdots$	4	5.043e-11	5.67	5.82	2.08	32	$\cdots$	-0.61	V	17.98	SDSS-G
15 02 55.594 +39 57 20.71	4.41	4.45	2.52 - 5.34	3.22	4	3.121e-08	5.50	4.92	1.91	1	$\cdots$	0.87	V	$\cdots$	$\cdots$
15 03 08.873 +39 24 10.91	2.08	2.25	1.20 - 3.58	$\cdots$	4	9.632e-08	4.08	5.53	2.99	6	$\cdots$	-1.73	V	$\cdots$	$\cdots$
15 03 11.298 +28 19 02.44	5.28	5.21	2.76 - <17.99	$\cdots$	6	1.419e-09	4.42	4.32	>1.79	920	$\cdots$	-0.40	V	$\cdots$	$\cdots$
15 03 30.249 +28 35 52.33	4.66	4.83	3.51 - 6.21	3.32	3	9.661e-09	4.73	5.01	1.77	5	BN	-1.29	V	$\cdots$	$\cdots$
15 03 48.864 -01 38 26.01	3.45	3.45	2.36 - 4.98	2.56	4	1.393e-08	4.93	5.23	1.92	2	$\cdots$	-0.54	V	$\cdots$	$\cdots$
15 04 21.379 +36 51 34.40	14.66	13.13	10.76 - 23.94	12.93	5	4.535e-08	5.61	6.11	2.22	6	$\cdots$	1.33	V	20.25	SDSS-*
15 04 46.285 +10 26 57.31	8.16	7.75	4.25 - 8.93	3.38	2	1.527e-11	6.38	6.07	2.10	0	BN	0.05	V	$\cdots$	$\cdots$
15 04 56.228 +09 59 19.03	1.38	1.26	<0.96 - 4.12	$\cdots$	3	1.142e-13	5.43	6.68	>4.27	1	$\cdots$	-0.05	T	$\cdots$	$\cdots$
15 05 21.973 +03 37 13.00	1.31	1.23	<0.82 - <5.15	$\cdots$	4	1.678e-09	5.27	5.54	>2.57	75	BN	-0.96	V	22.62	SDSS-G
15 06 04.717 +36 49 30.83	3.48	3.67	<2.05 - 4.67	$\cdots$	4	2.220e-15	7.85	7.78	>2.28	6	$\cdots$	0.22	V	$\cdots$	$\cdots$
15 06 05.109 +37 37 55.67	9.01	9.59	4.81 - 11.73	9.05	5	7.240e-11	6.12	5.67	>1.61	6	BN	-1.26	V	18.93	SDSS-G
15 06 18.779 +19 52 47.12	2.27	2.30	<1.73 - <10.10	$\cdots$	4	4.558e-09	4.85	5.43	>1.62	$\cdots$	$\cdots$	0.58	V	17.54	SDSS-G
15 07 02.069 +09 18 45.88	4.73	4.89	2.46 - 5.21	$\cdots$	2	2.250e-12	6.93	6.06	2.12	1	BN	-0.92	V	$\cdots$	$\cdots$
15 07 57.784 +42 33 43.60	3.86	3.83	1.91 - <12.14	4.16	5	1.126e-07	3.93	4.00	2.15	5	$\cdots$	0.35	V	$\cdots$	$\cdots$

Coordinates (J2000)	f (mJy)				N	Measures			$\frac{\text{Max.}}{\text{Min.}}$	$T_{\min}$	Flags	σ_{nbr}	Type	i	Cross-ID
	Cat.	$\overline{f}$	Range	NVSS		$P(\chi^2,\nu)$	$\sigma_{\max}$	$\Delta_{\max}(\sigma)$		(days)				Mag.	
15 08 35.984 +37 16 50.56	2.90	2.96	<1.95 - 3.78	3.54	4	2.369e-08	4.54	5.36	>1.94	7	$\cdots$	0.99	V	19.04	SDSS-G
15 09 25.675 +55 31 32.90	10.02	10.19	5.04 - 10.72	7.11	3	5.551e-16	8.12	6.74	2.13	15	$\cdots$	-0.13	V	$\cdots$	PSR
15 10 21.149 +01 47 30.63	1.51	1.68	1.39 - 5.03	$\cdots$	2	1.005e-10	6.18	6.46	3.63	0	$\cdots$	0.13	V	20.40	SDSS-*
15 10 21.240 +31 38 56.51	2.49	2.74	<2.05 - <4.39	$\cdots$	4	9.732e-08	4.90	5.37	>1.62	91	BN	1.24	V	$\cdots$	$\cdots$
15 10 56.788 -05 11 00.75	1.56	1.44	<1.01 - 4.28	$\cdots$	3	3.775e-15	5.10	6.55	>4.25	2	$\cdots$	0.71	T	$\cdots$	$\cdots$
15 10 57.572 +30 59 25.98	13.51	12.84	12.30 - 19.46	17.94	3	3.068e-08	5.80	5.45	1.57	411	$\cdots$	-0.92	V	19.89	SDSS-QSO(P)
15 11 09.803 +29 44 52.90	4.12	3.77	1.70 - 3.98	2.74	3	1.807e-06	5.06	4.73	2.34	21	$\cdots$	-0.70	V	$\cdots$	$\cdots$
15 11 34.658 -06 22 29.60	7.18	7.14	3.82 - <10.11	$\cdots$	4	1.392e-11	6.92	6.14	2.02	8	$\cdots$	0.32	V	$\cdots$	$\cdots$
15 11 46.201 +47 14 17.89	26.44	29.70	<17.95 - 33.41	23.80	4	2.062e-13	6.87	6.70	>1.86	7	BN	0.58	V	$\cdots$	$\cdots$
15 11 51.614 +40 11 46.26	5.63	5.97	4.60 - 7.40	4.73	5	1.932e-07	4.62	4.47	>1.32	1	$\cdots$	-0.35	V	$\cdots$	$\cdots$
15 12 14.539 -06 21 10.95	2.49	2.45	<2.01 - <14.88	$\cdots$	4	2.185e-08	4.33	5.14	>1.52	8	$\cdots$	-0.90	V	$\cdots$	$\cdots$
15 13 05.687 +20 02 55.34	3.70	3.63	3.06 - 7.01	4.49	4	1.451e-11	5.33	6.05	2.00	$\cdots$	$\cdots$	-0.03	V	$\cdots$	$\cdots$
15 13 07.042 +02 24 59.13	3.84	4.38	1.55 - 4.63	$\cdots$	3	7.772e-16	8.20	6.95	2.98	83	$\cdots$	-0.28	V	$\cdots$	$\cdots$
15 13 34.098 +36 50 25.80	10.30	11.94	4.99 - 12.27	11.36	5	8.238e-14	6.01	5.53	2.46	1	$\cdots$	-4.01	V	20.99	SDSS-G
15 13 36.442 +63 43 22.36	3.59	3.67	1.71 - 4.04	3.14	3	1.127e-07	5.44	5.34	2.37	7	$\cdots$	0.35	V	$\cdots$	$\cdots$
15 14 12.488 +36 50 42.91	2.61	3.03	1.31 - 3.68	2.72	3	2.298e-10	4.92	5.34	2.82	5	$\cdots$	-3.14	V	18.92	SDSS-G
15 15 52.584 +15 21 44.95	2.31	2.40	<1.67 - 8.49	$\cdots$	4	2.763e-08	4.79	4.92	>1.69	1	$\cdots$	0.10	V	19.68	SDSS-G
15 16 07.115 +41 24 07.98	2.26	2.59	1.15 - <24.62	2.33	5	1.198e-08	5.19	4.52	2.44	1	$\cdots$	0.06	V	$\cdots$	$\cdots$
15 17 02.087 +19 32 50.11	3.78	3.51	<2.31 - 3.90	$\cdots$	3	3.998e-09	5.99	6.03	>1.69	$\cdots$	$\cdots$	-1.77	V	$\cdots$	$\cdots$
15 17 26.334 +20 01 16.72	2.94	3.05	<1.74 - 4.08	2.35	3	1.767e-12	6.39	7.24	>2.34	$\cdots$	$\cdots$	0.25	V	21.86	SDSS-G
15 17 35.325 +21 29 06.39	2.44	2.25	<1.39 - <4.04	$\cdots$	3	3.050e-08	5.35	5.40	>1.81	3	$\cdots$	-0.50	V	$\cdots$	$\cdots$
15 18 12.883 +41 11 34.65	22.38	22.72	12.37 - 28.03	24.20	5	3.082e-08	4.39	5.49	2.27	426	$\cdots$	1.25	V	$\cdots$	$\cdots$
15 18 16.831 +49 04 34.19	5.03	5.10	<3.37 - <12.09	3.55	5	6.686e-06	5.03	4.87	>1.54	1	$\cdots$	0.32	V	$\cdots$	PSR
15 19 51.277 +21 02 34.13	1.90	1.76	1.08 - 2.44	$\cdots$	3	1.167e-07	4.09	5.11	>1.69	6	$\cdots$	0.08	V	18.36	SDSS-G
15 20 54.686 -01 06 07.43	3.78	3.64	2.98 - 7.27	4.32	3	1.227e-08	5.01	5.67	2.44	8	$\cdots$	-0.40	V	22.12	SDSS-*
15 21 23.837 -06 32 49.18	42.74	42.83	41.11 - 61.30	33.21	3	1.625e-07	5.29	4.98	1.49	4	$\cdots$	0.43	V	$\cdots$	$\cdots$
15 21 54.639 -01 04 14.86	4.85	4.70	2.35 - 5.15	$\cdots$	3	1.736e-08	5.85	5.24	2.09	8	$\cdots$	-0.15	V	$\cdots$	$\cdots$
15 22 52.068 +30 20 33.42	1.37	1.36	<1.02 - <2.03	$\cdots$	3	1.214e-07	4.58	5.06	>1.92	3	$\cdots$	-0.20	V	$\cdots$	$\cdots$
15 22 57.620 +54 25 10.92	3.96	3.95	3.32 - 6.75	4.06	4	7.025e-09	5.81	6.34	2.03	0	$\cdots$	0.52	V	$\cdots$	$\cdots$
15 23 38.236 +11 14 26.11	4.86	4.80	4.31 - 7.83	$\cdots$	4	2.547e-07	5.16	5.51	1.82	0	$\cdots$	-1.94	V	$\cdots$	$\cdots$
15 23 41.276 +38 50 48.06	2.91	2.85	<1.91 - 3.49	$\cdots$	4	3.189e-09	5.41	5.70	>1.82	1	$\cdots$	0.17	V	$\cdots$	$\cdots$

Coordinates (J2000)	f (mJy)				N	Measures			$\frac{\text{Max.}}{\text{Min.}}$	$T_{\min}$	Flags	σ_{nbr}	Type	i	Cross-ID
	Cat.	$\overline{f}$	Range	NVSS		$P(\chi^2,\nu)$	$\sigma_{\max}$	$\Delta_{\max}(\sigma)$		(days)				Mag.	
15 23 41.616 +11 10 39.89	3.18	3.14	1.39 - <11.09	$\cdots$	4	7.422e-08	5.47	5.41	2.55	1	$\cdots$	-0.36	V	18.61	SDSS-G
15 23 54.181 +63 15 41.10	2.82	2.86	2.07 - 4.98	2.92	4	1.326e-07	4.17	4.44	2.41	0	$\cdots$	-0.91	V	$\cdots$	$\cdots$
15 25 29.528 +41 11 19.59	6.17	6.11	3.99 - 7.74	6.77	4	3.883e-08	4.64	5.53	1.94	1	$\cdots$	-0.07	V	$\cdots$	$\cdots$
15 26 16.062 +37 38 11.95	4.13	4.04	3.43 - 6.46	5.75	3	2.530e-08	4.64	5.24	1.88	6	BN	-0.21	V	$\cdots$	$\cdots$
15 26 41.913 +16 32 46.02	93.26	86.28	82.51 - 114.75	87.03	4	4.485e-10	4.22	4.07	1.39	43	$\cdots$	-0.77	V	19.26	SDSS-QSO(P)
15 26 44.286 +20 27 19.58	2.83	2.92	2.22 - 4.39	$\cdots$	3	2.181e-07	3.87	5.14	1.98	1	$\cdots$	0.33	V	20.44	SDSS-G
15 27 31.095 -07 52 39.08	2.85	2.63	<2.04 - <3.71	$\cdots$	3	3.420e-07	4.79	5.01	>1.46	383	$\cdots$	1.00	V	$\cdots$	GSC2-FIRST-G
15 27 57.063 -05 14 45.34	2.98	2.91	2.36 - 4.74	2.37	3	2.082e-07	4.87	5.35	2.01	7	$\cdots$	0.12	V	$\cdots$	$\cdots$
15 28 10.437 +04 48 38.92	3.08	3.16	1.29 - 4.07	2.31	3	6.980e-12	6.37	6.80	3.16	381	$\cdots$	0.56	V	$\cdots$	$\cdots$
15 28 26.177 -07 43 51.39	3.10	2.85	2.44 - <13.85	6.31	4	1.012e-12	6.84	7.19	>2.72	386	$\cdots$	1.54	V	$\cdots$	$\cdots$
15 29 15.333 +18 38 00.16	3.69	4.09	1.82 - 4.70	3.66	3	4.511e-11	6.48	6.19	2.54	$\cdots$	BN	2.07	V	$\cdots$	$\cdots$
15 29 26.697 +29 30 47.86	3.35	3.51	1.46 - 3.79	2.85	3	1.184e-06	5.09	4.74	2.59	0	$\cdots$	0.48	V	$\cdots$	$\cdots$
15 29 41.517 +34 54 31.33	11.53	11.70	6.92 - 12.85	11.77	4	7.057e-08	5.71	5.36	1.86	66	$\cdots$	-0.44	V	$\cdots$	$\cdots$
15 29 55.935 +18 41 55.87	5.08	5.37	3.92 - 6.99	5.29	4	2.847e-08	4.68	5.66	>1.69	$\cdots$	BN	0.81	V	18.33	SDSS-G
15 30 41.788 +31 19 06.25	1.12	0.97	<0.82 - <2.59	$\cdots$	3	9.828e-08	3.92	5.00	>1.77	466	$\cdots$	-0.12	V	20.95	SDSS-G
15 30 43.737 +14 09 41.08	1.47	1.40	<0.91 - 2.09	$\cdots$	3	9.180e-09	4.74	5.96	>2.28	3	$\cdots$	-1.39	T	$\cdots$	$\cdots$
15 30 57.118 +10 52 04.76	2.65	2.60	1.46 - 3.75	$\cdots$	3	1.255e-08	4.00	5.63	2.57	3	$\cdots$	-0.27	V	$\cdots$	$\cdots$
15 31 00.743 +03 24 58.23	2.22	1.95	<1.03 - <10.87	$\cdots$	4	3.841e-09	5.69	6.15	>2.44	11	$\cdots$	0.26	V	$\cdots$	$\cdots$
15 31 03.695 +14 59 35.63	2.05	2.03	1.70 - 4.08	$\cdots$	4	1.753e-07	4.98	5.42	>2.40	5	$\cdots$	0.90	V	$\cdots$	$\cdots$
15 31 17.791 +24 48 42.29	4.48	4.68	2.98 - 10.92	3.97	4	1.284e-09	4.75	5.74	2.57	1	$\cdots$	0.31	V	$\cdots$	$\cdots$
15 31 27.528 +26 41 02.90	14.89	14.54	<12.46 - 21.84	15.63	6	2.409e-07	3.78	4.65	>1.45	8	$\cdots$	0.03	V	19.95	SDSS-G
15 31 31.838 +01 36 13.20	8.45	8.23	3.98 - <22.06	6.24	6	1.075e-10	4.71	4.53	2.14	80	$\cdots$	-0.88	V	$\cdots$	$\cdots$
15 32 29.399 +19 52 54.47	6.60	6.96	4.56 - 7.92	6.06	4	8.600e-08	4.18	4.65	1.74	$\cdots$	$\cdots$	-0.43	V	16.28	SDSS-*
15 32 45.699 -00 44 26.28	5.84	4.86	2.84 - <7.99	5.38	3	2.559e-11	4.86	6.49	2.72	1	$\cdots$	-0.42	V	19.63	SDSS-*
15 32 56.733 +29 09 43.41	3.71	3.77	<2.59 - 5.29	3.94	3	6.632e-10	5.44	6.08	>2.04	6	$\cdots$	1.85	V	$\cdots$	GSC2-FIRST-G
15 33 47.106 +61 29 01.43	2.39	2.48	<1.58 - <3.24	4.91	3	1.458e-07	5.05	5.22	>1.74	3	$\cdots$	0.48	V	19.43	SDSS-G
15 33 51.343 +20 04 15.78	1.56	1.45	<0.89 - <5.41	$\cdots$	4	5.190e-11	5.50	6.48	>2.43	$\cdots$	$\cdots$	-0.66	V	$\cdots$	$\cdots$
15 34 18.431 +24 02 13.57	8.42	9.25	4.39 - 9.43	8.50	3	4.026e-09	6.14	5.46	2.15	1	$\cdots$	0.30	V	20.49	SDSS-G
15 34 22.881 +02 17 25.54	3.40	3.55	<2.54 - <7.71	$\cdots$	4	2.263e-07	4.84	5.01	>2.14	2	$\cdots$	0.14	V	$\cdots$	$\cdots$
15 34 28.414 +27 31 47.81	3.26	3.31	<2.17 - 3.80	$\cdots$	4	5.311e-07	5.54	5.15	>1.59	1	$\cdots$	0.01	V	16.99	SDSS-G
15 35 21.075 +13 09 24.77	1.57	1.66	<1.20 - <5.07	$\cdots$	4	2.865e-07	4.84	5.03	>1.68	4	$\cdots$	0.06	V	19.27	SDSS-G

Coordinates (J2000)	f (mJy)				N	Measures			$\frac{\text{Max.}}{\text{Min.}}$	$T_{\min}$	Flags	σ_{nbr}	Type	i	Cross-ID
	Cat.	$\overline{f}$	Range	NVSS		$P(\chi^2, \nu)$	$\sigma_{\max}$	$\Delta_{\max}(\sigma)$		(days)				Mag.	
15 36 00.677 +26 44 27.92	5.36	5.38	3.21 - 6.55	3.63	4	1.743e-10	4.17	5.13	2.04	2	$\cdots$	-0.83	V	$\cdots$	$\cdots$
15 36 39.521 +62 41 48.11	1.27	1.14	<1.16 - <6.10	$\cdots$	4	1.544e-08	4.99	5.75	>2.49	5	$\cdots$	1.05	V	20.34	SDSS-G
15 36 56.378 +33 03 57.46	1.97	1.93	1.02 - <3.04	2.45	4	4.708e-07	4.56	5.16	2.53	487	$\cdots$	-0.63	V	$\cdots$	$\cdots$
15 37 07.555 +22 04 30.64	3.06	2.98	1.67 - <5.81	3.28	4	6.939e-14	6.45	7.18	2.45	410	$\cdots$	0.51	V	20.40	SDSS-G
15 37 40.367 +15 52 58.77	19.42	21.11	12.55 - 22.44	18.44	4	5.039e-08	5.29	4.53	1.79	2	$\cdots$	-3.77	V	20.17	SDSS-G
15 37 54.968 +19 58 52.51	16.80	16.33	12.69 - 49.23	11.85	3	0.000	11.72	12.42	3.88	$\cdots$	$\cdots$	0.50	V	18.33	SDSS-*
15 38 03.278 +15 55 00.42	4.09	4.40	<2.53 - 4.76	4.78	3	4.483e-13	7.16	6.74	>1.88	19	$\cdots$	-2.75	V	$\cdots$	$\cdots$
15 38 59.832 +21 51 00.84	2.69	2.68	<1.90 - <3.85	2.77	4	8.524e-08	5.44	5.13	>1.53	578	$\cdots$	-0.13	V	20.48	SDSS-G
15 39 16.908 +15 52 09.92	3.05	2.94	<2.02 - <11.04	2.29	4	2.859e-08	5.68	5.47	>1.59	4	$\cdots$	-0.50	V	$\cdots$	$\cdots$
15 39 21.636 +03 37 12.71	2.02	2.13	<1.77 - <10.40	$\cdots$	4	1.195e-07	3.99	4.88	>1.54	75	$\cdots$	0.03	V	21.61	SDSS-*
15 39 32.659 +19 43 15.27	1.81	2.03	1.27 - 6.82	$\cdots$	2	0.000	7.63	8.54	5.37	$\cdots$	$\cdots$	0.78	T	$\cdots$	$\cdots$
15 39 33.746 +30 31 38.19	3.77	4.24	2.81 - 4.76	$\cdots$	3	7.352e-09	5.88	4.88	1.69	508	$\cdots$	0.83	V	$\cdots$	$\cdots$
15 39 43.894 -05 28 38.22	6.49	6.28	4.04 - 7.57	$\cdots$	3	2.021e-07	4.67	5.32	1.88	6	BN	-0.56	V	$\cdots$	GSC2-FIRST-G
15 39 46.959 -05 22 51.76	2.14	2.12	0.88 - 2.64	$\cdots$	3	2.079e-07	5.03	5.29	3.00	2	BN	-1.75	V	$\cdots$	$\cdots$
15 40 26.660 -05 11 22.99	4.88	4.93	<2.61 - 5.20	$\cdots$	3	9.685e-10	6.38	5.97	>1.99	2	BN	0.03	V	$\cdots$	$\cdots$
15 40 42.539 +37 33 41.86	2.16	2.15	1.18 - 5.02	$\cdots$	4	1.353e-11	4.77	5.95	4.26	6	$\cdots$	0.94	V	$\cdots$	$\cdots$
15 40 55.942 +62 34 29.69	8.97	8.76	5.81 - 9.26	$\cdots$	3	9.934e-10	6.07	5.08	1.59	5	$\cdots$	0.44	V	$\cdots$	$\cdots$
15 41 35.435 +17 41 28.55	2.51	2.48	<1.86 - 2.94	$\cdots$	3	5.181e-07	4.94	4.95	>1.51	2	$\cdots$	-1.50	V	$\cdots$	$\cdots$
15 41 40.499 +59 13 41.76	3.70	3.44	2.71 - 5.53	$\cdots$	3	6.482e-10	4.38	5.58	1.87	5	$\cdots$	-0.21	V	17.56	SDSS-G
15 41 58.209 +07 28 45.57	38.38	36.70	19.67 - 49.40	39.33	6	4.164e-09	4.22	5.78	2.51	0	$\cdots$	-0.15	V	$\cdots$	$\cdots$
15 42 19.449 +18 29 49.16	3.71	3.63	<2.29 - <5.63	4.57	4	4.937e-11	6.69	6.32	>1.72	$\cdots$	$\cdots$	0.72	V	20.07	SDSS-G
15 42 24.844 +00 22 54.90	3.74	3.53	<2.22 - <4.47	$\cdots$	4	6.000e-11	5.97	6.10	>1.77	1	$\cdots$	0.92	V	19.67	SDSS-QSO(S)
15 42 42.609 +14 59 57.76	5.69	5.85	3.85 - 7.14	4.25	4	1.951e-07	3.59	4.67	1.84	1	BN	-0.44	V	$\cdots$	$\cdots$
15 43 21.460 +60 43 27.98	20.43	20.30	11.55 - 20.90	18.24	4	2.688e-07	5.75	4.82	1.79	0	$\cdots$	0.42	V	20.14	SDSS-G
15 43 40.345 -00 56 55.52	1.29	1.36	0.91 - <12.62	$\cdots$	4	2.124e-12	6.71	7.30	4.65	4	$\cdots$	0.21	V	$\cdots$	$\cdots$
15 43 42.693 +14 02 59.99	25.42	24.61	<17.46 - 30.44	27.29	4	1.521e-10	5.42	6.41	>1.74	21	$\cdots$	-1.79	V	21.82	SDSS-G
15 43 48.582 +61 22 34.23	2.28	2.38	<1.85 - <4.54	2.66	4	1.108e-07	4.79	5.18	>1.57	0	$\cdots$	0.35	V	21.13	SDSS-G
15 44 02.670 +42 22 36.96	7.92	8.13	7.04 - 13.35	8.08	4	8.891e-08	4.90	5.55	1.89	408	$\cdots$	-0.26	V	$\cdots$	$\cdots$
15 44 03.713 +18 26 58.50	2.62	2.70	<1.68 - 3.13	$\cdots$	3	1.961e-11	6.76	6.08	>1.86	$\cdots$	$\cdots$	-0.78	V	$\cdots$	$\cdots$
15 44 13.704 +03 59 36.56	2.21	2.11	1.08 - <3.06	$\cdots$	4	1.019e-08	4.59	5.81	2.80	984	BN	1.81	V	$\cdots$	$\cdots$
15 44 18.959 +61 41 15.82	2.54	2.52	1.51 - 4.19	$\cdots$	3	3.415e-09	4.72	5.53	2.79	3	$\cdots$	0.03	V	19.40	SDSS-G

Coordinates (J2000)	f (mJy)				N	Measures			$\frac{\text{Max.}}{\text{Min.}}$	$T_{\min}$	Flags	σ_{nbr}	Type	i	Cross-ID
	Cat.	$\overline{f}$	Range	NVSS		$P(\chi^2,\nu)$	$\sigma_{\max}$	$\Delta_{\max}(\sigma)$		(days)				Mag.	
15 44 26.825 +60 33 53.54	5.50	5.45	<3.75 - 5.74	5.43	3	1.121e-06	5.21	5.00	>1.49	0	$\cdots$	-1.56	V	18.96	SDSS-G
15 45 01.406 +47 54 25.86	8.67	9.68	3.94 - 9.99	10.63	5	1.602e-10	5.14	4.92	2.54	3	BN	0.88	V	20.36	SDSS-QSO(P)
15 45 39.631 +21 32 42.37	3.99	4.21	2.08 - 4.78	2.19	3	9.938e-08	5.47	5.06	2.15	14	$\cdots$	-0.21	V	20.86	SDSS-G
15 45 59.443 -03 37 00.60	3.34	3.21	1.69 - 3.70	$\cdots$	4	7.397e-09	3.94	4.46	>2.19	1	$\cdots$	-0.77	V	$\cdots$	$\cdots$
15 46 03.669 +29 08 05.75	15.17	14.46	13.42 - 21.23	16.30	3	2.691e-10	5.51	5.57	1.58	11	$\cdots$	-0.93	V	18.71	SDSS-QSO(S)
15 46 04.116 -03 23 54.30	4.55	4.78	2.58 - <11.02	$\cdots$	4	5.832e-08	5.55	5.37	2.03	6	$\cdots$	-0.09	V	$\cdots$	$\cdots$
15 46 11.539 +28 24 26.66	3.94	3.97	2.52 - 5.04	3.72	3	2.465e-11	6.00	5.78	2.00	909	$\cdots$	0.94	V	16.44	SDSS-G
15 46 24.265 -03 46 39.40	7.00	6.77	3.87 - <11.68	$\cdots$	4	3.568e-07	5.13	4.65	1.81	922	$\cdots$	0.03	V	$\cdots$	$\cdots$
15 46 44.249 +31 17 11.47	12.51	13.40	7.40 - 15.68	13.46	4	0.000	10.62	7.78	2.02	507	$\cdots$	0.15	V	$\cdots$	SDSS-QSO(S)
15 47 25.873 +12 03 45.44	1.41	1.31	0.87 - <8.46	$\cdots$	4	4.965e-07	4.01	4.88	>2.55	2	$\cdots$	0.35	V	$\cdots$	$\cdots$
15 47 44.132 +41 24 08.36	4.97	5.43	<4.18 - 8.05	5.30	4	1.524e-09	4.76	5.96	>1.93	1	$\cdots$	0.77	V	14.22	SDSS-G
15 49 04.438 +63 35 00.04	2.10	1.96	<1.33 - <4.46	$\cdots$	4	1.185e-10	5.80	6.12	>1.93	7	$\cdots$	1.16	V	$\cdots$	$\cdots$
15 49 53.049 +62 57 18.25	6.67	6.15	<4.63 - 10.39	7.20	3	0.000	6.73	7.63	>2.20	0	BN	0.84	V	19.77	SDSS-G
15 50 36.281 +12 49 37.82	1.75	1.37	<0.95 - 2.72	$\cdots$	2	6.868e-10	4.65	6.04	>2.84	6	$\cdots$	1.37	T	$\cdots$	$\cdots$
15 52 22.031 +52 41 52.12	73.80	74.08	73.00 - 97.57	73.85	5	1.218e-08	3.61	3.28	1.33	1	$\cdots$	0.06	V	$\cdots$	$\cdots$
15 52 32.834 +20 55 10.84	14.32	14.48	9.63 - 14.70	10.73	5	1.007e-08	4.49	4.32	>1.28	11	$\cdots$	-0.49	V	19.51	SDSS-G
15 52 50.153 +18 16 03.31	24.84	24.66	23.57 - 33.06	24.57	4	8.798e-08	3.59	3.60	1.40	0	$\cdots$	-1.34	V	$\cdots$	$\cdots$
15 53 36.207 +37 07 20.79	18.99	17.38	16.49 - 23.95	17.78	5	1.876e-08	4.44	4.41	1.45	46	$\cdots$	-0.26	V	21.23	SDSS-*
15 55 21.438 +27 40 56.12	4.82	4.72	<3.91 - <9.14	$\cdots$	5	2.516e-08	3.94	3.98	>1.26	1	$\cdots$	0.37	V	$\cdots$	$\cdots$
15 55 25.748 +20 03 24.50	12.45	12.22	8.61 - <24.84	9.70	6	4.461e-08	4.45	4.27	>1.28	$\cdots$	BN	3.40	V	$\cdots$	$\cdots$
15 55 26.788 +19 16 00.32	2.47	2.15	<1.60 - <3.99	2.29	4	8.927e-09	5.15	5.71	>1.71	$\cdots$	$\cdots$	-0.58	V	$\cdots$	$\cdots$
15 55 41.799 +20 41 25.02	2.42	2.16	<1.49 - 3.76	$\cdots$	3	1.300e-09	5.01	6.11	>2.52	0	$\cdots$	-0.72	V	19.35	SDSS-QSO(P)
15 56 12.144 +01 18 03.25	2.60	2.59	<1.73 - 3.12	2.78	3	6.569e-09	5.61	5.74	>1.77	1	$\cdots$	-0.15	V	$\cdots$	$\cdots$
15 56 19.830 +17 11 36.80	4.91	4.68	4.49 - 10.61	7.28	4	4.900e-06	5.19	5.14	2.35	28	$\cdots$	1.33	V	20.03	SDSS-G
15 56 56.345 +07 15 05.35	2.39	2.44	<1.82 - 5.22	$\cdots$	3	7.445e-09	4.68	5.56	>2.87	2	BN	-0.05	V	20.15	SDSS-QSO(P)
15 56 58.524 +15 23 41.75	5.40	5.79	2.70 - <11.73	5.98	6	2.196e-08	6.32	5.59	2.21	2	$\cdots$	-2.47	V	18.27	SDSS-G
15 57 39.803 +13 56 40.68	3.01	3.05	<2.20 - 3.26	$\cdots$	3	8.273e-07	5.18	4.93	>1.49	3	$\cdots$	0.32	V	18.88	SDSS-G
15 58 37.943 +26 58 57.43	7.06	7.40	3.98 - 14.91	$\cdots$	4	0.000	11.08	9.43	3.75	3	$\cdots$	-2.14	V	19.64	SDSS-*
15 59 20.801 +16 47 57.99	4.00	3.95	2.59 - 5.37	2.17	3	1.637e-08	3.87	5.07	1.70	6	BN	0.08	V	19.40	SDSS-G
15 59 42.675 +14 13 03.79	1.66	1.77	1.08 - 2.65	$\cdots$	3	2.355e-07	4.50	3.98	2.25	15	$\cdots$	-0.75	V	17.38	SDSS-G
15 59 42.916 +00 29 14.16	6.86	6.37	<3.73 - 6.49	5.45	4	4.460e-07	5.47	5.33	>1.74	1	$\cdots$	1.04	V	$\cdots$	$\cdots$

Coordinates (J2000)	f (mJy)				N	Measures			$\frac{\text{Max.}}{\text{Min.}}$	$T_{\min}$	Flags	σ_{nbr}	Type	i	Cross-ID
	Cat.	$\overline{f}$	Range	NVSS		$P(\chi^2,\nu)$	$\sigma_{\max}$	$\Delta_{\max}(\sigma)$		(days)				Mag.	
16 00 16.454 +01 47 35.27	6.44	6.31	2.86 - 6.55	6.04	4	2.139e-08	5.79	5.36	2.29	0	$\cdots$	0.26	V	$\cdots$	$\cdots$
16 00 21.544 +01 51 26.15	42.52	41.24	34.16 - 54.36	40.79	4	1.664e-07	3.70	4.70	1.47	2	$\cdots$	-0.39	V	$\cdots$	$\cdots$
16 00 24.276 +01 12 27.07	10.41	10.67	7.76 - 12.05	10.17	4	7.878e-09	4.52	3.89	1.45	1	$\cdots$	0.39	V	$\cdots$	$\cdots$
16 00 28.521 -00 22 59.94	8.36	8.88	3.00 - 10.08	6.89	4	2.127e-12	7.33	6.75	3.36	1	BN	0.63	V	$\cdots$	$\cdots$
16 00 37.416 +02 18 41.63	43.05	40.06	23.38 - 49.52	37.62	4	5.551e-16	7.55	7.30	2.12	2	$\cdots$	1.79	V	20.57	SDSS-G
16 00 44.604 +41 38 53.80	1.25	1.13	<0.71 - <2.95	$\cdots$	3	1.119e-13	6.11	6.35	>3.42	1	$\cdots$	-0.00	V	$\cdots$	$\cdots$
16 01 02.366 +41 47 14.05	5.84	5.78	4.96 - 10.76	6.25	4	4.288e-10	6.09	6.66	2.17	1	$\cdots$	-0.39	V	$\cdots$	$\cdots$
16 01 04.501 +02 01 05.95	6.73	6.90	5.04 - 12.75	$\cdots$	4	1.110e-16	7.28	7.63	2.10	1	$\cdots$	-1.49	V	20.32	SDSS-*
16 01 51.475 +31 01 11.29	1.71	1.60	<0.97 - <1.95	$\cdots$	3	1.667e-07	4.96	5.23	>1.86	562	$\cdots$	0.06	V	$\cdots$	$\cdots$
16 02 06.958 +26 09 50.02	1.45	1.24	<0.81 - <4.44	$\cdots$	4	1.282e-12	5.17	7.03	>3.01	1	$\cdots$	-0.13	V	$\cdots$	$\cdots$
16 02 38.943 +01 55 15.65	5.45	6.45	2.33 - 9.01	$\cdots$	3	0.000	9.56	9.61	3.87	2	$\cdots$	0.47	V	$\cdots$	$\cdots$
16 04 04.237 +31 39 25.09	1.19	1.09	<0.98 - 2.24	$\cdots$	3	5.517e-08	4.49	5.71	>2.28	95	BN	-0.17	T	$\cdots$	$\cdots$
16 04 26.177 +12 23 23.50	37.74	36.48	36.05 - 51.86	38.84	5	7.062e-09	4.37	4.00	1.44	2	$\cdots$	1.22	V	16.63	SDSS-G
16 04 27.968 +02 11 50.74	21.67	19.93	9.56 - 21.65	17.35	3	0.000	9.15	7.07	2.15	0	$\cdots$	-0.04	V	$\cdots$	$\cdots$
16 04 38.134 +03 19 46.19	3.94	3.89	<2.61 - <12.04	4.61	4	2.551e-07	5.29	5.14	>1.55	64	$\cdots$	-0.40	V	24.97	SDSS-G
16 04 53.979 +20 16 48.16	22.68	25.41	11.45 - 27.60	20.69	3	3.553e-15	8.04	6.81	2.41	0	$\cdots$	-0.84	V	$\cdots$	$\cdots$
16 05 15.330 +03 15 03.85	5.17	4.98	3.21 - 5.70	3.47	3	1.235e-07	5.30	4.55	1.65	64	$\cdots$	-2.54	V	$\cdots$	$\cdots$
16 05 42.466 +02 59 06.52	3.94	3.83	1.78 - 4.00	4.62	3	2.516e-07	4.29	4.21	>2.24	3	$\cdots$	1.24	V	20.53	SDSS-G
16 07 05.295 +02 00 49.79	6.96	6.49	<4.60 - 7.06	$\cdots$	4	3.073e-07	5.16	4.93	>1.53	2	$\cdots$	-0.44	V	$\cdots$	$\cdots$
16 07 09.895 +01 59 53.86	4.68	4.38	2.40 - <5.36	$\cdots$	4	1.281e-08	4.63	4.72	>1.58	0	$\cdots$	-0.36	V	$\cdots$	$\cdots$
16 09 11.294 +33 01 49.29	1.69	1.66	1.08 - <7.93	$\cdots$	6	7.126e-10	4.43	5.71	>2.35	484	$\cdots$	0.78	V	$\cdots$	$\cdots$
16 09 14.183 +16 24 11.21	3.08	3.31	2.20 - 4.25	3.44	3	4.793e-08	4.74	5.09	1.94	25	$\cdots$	0.11	V	21.44	SDSS-G
16 09 30.015 +18 25 09.37	3.15	3.07	2.09 - 3.41	$\cdots$	3	1.230e-07	5.15	5.32	>1.57	$\cdots$	$\cdots$	1.23	V	$\cdots$	$\cdots$
16 09 46.553 +32 39 06.10	4.43	4.44	2.96 - 6.33	3.40	4	1.204e-08	4.91	5.35	2.14	2	$\cdots$	0.54	V	19.56	SDSS-*
16 09 50.577 +17 53 52.65	5.96	6.13	3.19 - 7.23	5.64	4	1.624e-07	5.72	5.19	2.05	0	$\cdots$	-1.03	V	19.72	SDSS-G
16 11 36.343 +43 23 00.20	1.76	1.99	<1.27 - <6.46	$\cdots$	5	4.976e-08	4.93	5.02	>1.75	12	$\cdots$	0.04	V	$\cdots$	$\cdots$
16 12 11.602 +31 36 04.20	21.47	22.25	21.22 - 30.85	22.97	5	1.485e-07	4.04	4.01	1.42	95	$\cdots$	-0.15	V	19.70	SDSS-QSO(S)
16 12 11.744 +20 05 01.57	6.62	6.56	3.11 - <12.40	$\cdots$	4	5.551e-14	7.30	6.48	2.24	$\cdots$	$\cdots$	0.17	V	$\cdots$	$\cdots$
16 12 31.055 +22 04 58.79	8.15	8.06	<5.09 - 8.69	5.30	4	1.478e-09	5.98	6.00	>1.71	412	BN	-2.47	V	20.93	SDSS-G
16 12 32.058 +59 41 35.61	5.84	5.73	2.39 - 7.22	5.09	3	1.110e-16	7.53	7.76	3.02	0	BN	-0.68	V	17.85	SDSS-G
16 13 43.092 +13 02 58.54	3.65	3.66	1.60 - 4.06	3.54	3	8.411e-07	5.10	4.69	2.43	6	$\cdots$	0.21	V	$\cdots$	$\cdots$

Coordinates (J2000)	f (mJy)				N	Measures			$\frac{\text{Max.}}{\text{Min.}}$	$T_{\min}$	Flags	σ_{nbr}	Type	i	Cross-ID
	Cat.	$\overline{f}$	Range	NVSS		$P(\chi^2,\nu)$	$\sigma_{\max}$	$\Delta_{\max}(\sigma)$		(days)				Mag.	
16 14 20.013 +21 54 09.53	12.00	11.09	6.38 - 13.56	14.72	4	2.430e-09	6.27	5.16	1.80	988	$\cdots$	-0.23	V	$\cdots$	$\cdots$
16 14 20.208 +02 53 31.56	1.62	1.48	0.90 - 3.88	$\cdots$	4	1.774e-07	3.58	4.83	>2.55	3	$\cdots$	0.45	V	18.09	SDSS-G
16 14 28.682 +15 56 40.92	4.14	4.14	2.44 - 4.97	$\cdots$	3	7.445e-12	6.72	5.79	2.04	1	$\cdots$	0.90	V	21.26	SDSS-G
16 14 29.550 +25 25 57.07	4.69	4.54	3.39 - 5.43	3.98	3	3.135e-07	4.54	4.61	1.55	6	$\cdots$	0.37	V	$\cdots$	$\cdots$
16 16 41.444 +06 58 55.70	2.36	2.18	0.98 - 3.62	$\cdots$	3	2.557e-08	4.96	4.79	2.61	3	$\cdots$	-0.74	V	20.94	SDSS-G
16 17 05.369 +62 41 56.67	2.53	2.40	1.09 - <7.34	6.77	4	6.894e-08	4.56	5.40	2.77	5	$\cdots$	-0.42	V	18.38	SDSS-G
16 17 26.008 +03 47 34.66	8.62	8.73	<4.12 - 11.09	7.20	4	5.104e-13	7.24	7.36	>2.69	908	$\cdots$	0.97	V	$\cdots$	$\cdots$
16 19 02.527 +22 53 55.11	1.71	1.60	<1.14 - 2.41	$\cdots$	3	1.260e-07	4.77	5.37	>2.12	5	$\cdots$	0.77	V	$\cdots$	SDSS-UNKNOWN
16 19 10.166 +59 58 04.07	2.63	2.75	<1.79 - <6.28	2.36	4	2.328e-09	5.96	5.99	>1.79	0	$\cdots$	-0.51	V	19.15	SDSS-G
16 19 19.054 +15 31 17.10	15.34	14.49	14.24 - 22.74	17.41	3	1.119e-07	5.11	4.82	1.60	2	$\cdots$	-0.44	V	$\cdots$	$\cdots$
16 19 37.628 +04 42 42.78	13.58	11.97	10.79 - 17.10	14.43	3	7.837e-09	4.52	5.00	1.59	380	$\cdots$	1.36	V	$\cdots$	$\cdots$
16 20 06.592 +08 16 19.18	5.22	5.33	3.73 - 6.44	5.45	3	1.319e-08	5.15	5.40	1.73	3	$\cdots$	-1.44	V	$\cdots$	$\cdots$
16 20 18.413 +17 18 35.70	2.37	2.13	<1.48 - 2.77	$\cdots$	3	1.910e-08	5.19	5.87	>1.87	1	$\cdots$	0.04	V	15.48	SDSS-G
16 21 03.303 +17 15 57.77	2.51	2.40	1.26 - 4.66	$\cdots$	4	1.158e-07	4.45	4.89	2.34	2	$\cdots$	0.34	V	$\cdots$	$\cdots$
16 21 19.940 +41 38 15.54	5.63	5.59	<3.40 - 6.81	6.14	4	5.788e-08	5.59	5.89	>2.00	0	$\cdots$	-2.21	V	19.82	SDSS-QSO(P)
16 21 45.890 +33 06 46.69	4.08	4.08	3.05 - 5.71	3.10	4	2.449e-10	4.66	5.95	1.87	484	$\cdots$	0.37	V	$\cdots$	$\cdots$
16 22 59.271 +44 01 42.87	7.92	7.63	5.53 - 9.19	7.03	3	1.846e-11	6.26	6.13	1.66	926	$\cdots$	0.55	V	18.51	SDSS-QSO(S)
16 23 04.490 +36 30 48.02	5.53	5.47	<3.62 - 6.13	4.38	3	1.588e-08	5.65	5.83	>1.69	5	$\cdots$	-0.83	V	18.73	SDSS-G
16 23 16.406 +19 44 10.89	1.55	1.59	<0.94 - 2.12	$\cdots$	3	1.365e-08	5.05	5.71	>2.25	$\cdots$	$\cdots$	1.39	T	17.08	SDSS-G
16 23 46.769 +63 08 47.21	8.87	9.30	5.80 - <13.58	8.53	5	9.089e-08	4.35	4.09	1.67	3	$\cdots$	0.04	V	17.46	SDSS-*
16 24 06.552 +23 46 48.93	11.42	11.36	4.79 - 11.68	$\cdots$	5	3.622e-12	4.90	4.62	>2.21	3	BN	0.22	V	20.59	SDSS-*
16 24 27.444 +25 06 04.63	2.67	2.83	<2.17 - <3.64	$\cdots$	3	3.212e-07	4.74	5.08	>1.49	2	$\cdots$	-0.16	V	$\cdots$	$\cdots$
16 24 41.906 +15 42 25.63	4.30	4.44	1.95 - 4.75	6.61	3	1.013e-06	5.14	4.87	2.43	15	BN	-1.19	V	$\cdots$	$\cdots$
16 24 53.445 +15 55 37.71	2.12	2.19	<1.46 - <2.96	$\cdots$	3	8.271e-09	5.34	5.64	>1.81	15	BN	-0.41	V	20.68	SDSS-*
16 25 18.556 +50 02 52.44	65.30	63.79	62.52 - 88.24	70.23	5	8.360e-11	4.33	3.98	1.41	4	$\cdots$	0.74	V	21.83	SDSS-G
16 25 20.881 +15 40 37.18	3.59	3.81	1.32 - <20.72	4.06	4	7.030e-11	6.50	6.54	3.33	17	BN	-1.57	V	21.52	SDSS-G
16 25 53.478 +39 28 55.41	2.42	2.35	<1.42 - <4.91	$\cdots$	4	1.844e-10	6.32	6.43	>1.92	5	$\cdots$	-0.50	V	19.21	SDSS-G
16 25 56.591 +04 46 59.61	4.61	5.01	2.59 - 6.28	4.27	3	4.441e-16	7.46	7.08	2.42	380	$\cdots$	0.60	V	$\cdots$	GSC2-FIRST-G
16 27 07.767 +27 47 26.02	2.97	2.76	1.62 - <12.23	$\cdots$	5	4.077e-07	4.77	5.15	>1.58	1	$\cdots$	-1.07	V	21.10	SDSS-*
16 27 22.819 +18 18 17.92	2.69	2.70	1.15 - <4.55	$\cdots$	4	3.093e-07	4.80	4.99	2.69	$\cdots$	$\cdots$	-0.05	V	19.81	SDSS-G
16 27 58.737 +04 27 16.56	1.49	1.38	<0.91 - <5.15	$\cdots$	3	6.815e-08	5.00	5.20	>1.94	34	$\cdots$	-0.44	V	$\cdots$	$\cdots$

Coordinates (J2000)	f (mJy)				N	Measures			$\frac{\text{Max.}}{\text{Min.}}$	$T_{\min}$	Flags	σ_{nbr}	Type	i	Cross-ID
	Cat.	$\overline{f}$	Range	NVSS		$P(\chi^2,\nu)$	$\sigma_{\max}$	$\Delta_{\max}(\sigma)$		(days)				Mag.	
16 28 15.095 +41 02 34.29	3.48	3.43	1.47 - <19.91	$\cdots$	5	1.238e-08	5.75	5.44	2.53	5	$\cdots$	1.14	V	21.80	SDSS-G
16 28 33.944 +44 12 54.37	4.72	5.46	<4.29 - 6.93	$\cdots$	5	5.042e-07	4.27	4.26	>1.35	4	BN	0.48	V	$\cdots$	$\cdots$
16 29 08.353 +21 01 04.82	1.25	0.96	<0.80 - <4.74	$\cdots$	4	2.727e-08	4.03	5.56	>2.11	3	BN	-0.63	V	17.81	SDSS-G
16 29 38.928 +13 22 50.64	2.81	2.70	1.88 - <13.81	4.13	4	1.987e-12	4.64	5.56	2.25	3	$\cdots$	0.08	V	$\cdots$	$\cdots$
16 29 54.712 +20 43 15.71	5.06	5.26	2.36 - <15.11	4.41	6	2.685e-07	5.37	5.01	2.31	6	$\cdots$	-0.76	V	$\cdots$	$\cdots$
16 29 55.518 +36 35 01.75	7.26	7.11	3.05 - 9.34	9.64	5	1.898e-07	4.41	5.04	3.06	7	$\cdots$	0.24	V	$\cdots$	$\cdots$
16 30 21.969 +42 20 36.37	7.16	7.40	<4.56 - <12.32	7.12	5	2.073e-12	6.57	6.28	>1.71	408	$\cdots$	0.46	V	$\cdots$	$\cdots$
16 30 31.018 +17 05 27.34	4.92	5.15	3.13 - 5.47	6.48	3	1.270e-07	5.29	4.83	1.75	1	$\cdots$	-0.11	V	$\cdots$	$\cdots$
16 31 56.825 +16 47 22.79	4.72	3.88	2.11 - 6.13	5.98	4	1.942e-08	4.50	4.55	>1.97	$\cdots$	$\cdots$	0.06	V	19.06	SDSS-*
16 33 23.273 +13 36 22.40	4.48	4.19	2.33 - <5.30	2.54	4	1.177e-06	5.09	4.85	1.92	10	$\cdots$	-1.45	V	$\cdots$	$\cdots$
16 35 28.718 +07 05 06.97	3.50	3.95	2.64 - 4.61	$\cdots$	4	4.097e-07	4.54	4.64	>1.75	2	$\cdots$	-0.00	V	$\cdots$	$\cdots$
16 37 22.698 +22 03 25.02	3.45	3.54	2.94 - <18.04	$\cdots$	5	3.854e-10	4.73	5.46	2.12	410	$\cdots$	0.37	V	$\cdots$	SDSS-UNKNOWN
16 37 31.472 +11 26 40.23	7.64	6.92	5.18 - <27.72	8.93	6	6.247e-08	4.20	4.73	1.94	0	$\cdots$	-0.22	V	21.25	SDSS-G
16 38 01.366 +16 44 12.24	1.11	0.88	<0.93 - <4.62	$\cdots$	4	2.057e-07	4.59	5.34	>2.34	$\cdots$	$\cdots$	-0.61	V	21.48	SDSS-G
16 39 18.772 +41 23 28.63	1.60	1.60	<1.35 - <3.15	2.10	4	2.171e-07	3.87	5.15	>1.71	1	$\cdots$	0.40	V	16.77	SDSS-G
16 39 22.419 +63 32 32.75	2.99	2.95	<2.07 - <3.68	3.08	4	1.333e-07	5.17	5.56	>1.69	7	$\cdots$	0.17	V	$\cdots$	$\cdots$
16 39 41.847 +40 21 14.15	3.39	3.45	1.59 - 4.59	$\cdots$	3	1.816e-11	6.42	6.00	2.89	5	$\cdots$	1.22	V	$\cdots$	$\cdots$
16 40 42.063 +39 48 25.71	17.07	18.43	<11.62 - <37.60	10.05	5	1.534e-11	5.89	6.32	>1.80	1	BN	-0.58	V	15.34	SDSS-G
16 41 04.340 +29 59 34.52	2.87	2.72	<1.87 - 3.34	2.86	3	2.281e-08	5.43	5.79	>1.71	64	BN	0.19	V	23.16	SDSS-*
16 41 13.737 +16 23 13.08	3.27	3.26	1.34 - 3.58	$\cdots$	3	9.425e-09	5.88	5.63	2.67	$\cdots$	$\cdots$	-0.83	V	$\cdots$	$\cdots$
16 41 48.853 +37 31 40.68	9.29	9.31	4.63 - <13.18	$\cdots$	5	4.773e-08	5.23	5.38	2.35	0	$\cdots$	0.21	V	$\cdots$	$\cdots$
16 42 23.785 +63 22 29.95	19.07	18.45	10.53 - 23.71	23.26	4	2.505e-09	4.87	6.17	2.25	7	$\cdots$	-0.58	V	19.63	SDSS-*
16 43 04.347 +39 48 36.76	10.85	12.64	<4.98 - <28.12	$\cdots$	5	0.000	7.61	7.55	>3.43	1	BN	NA	V	$\cdots$	$\cdots$
16 44 23.309 +49 52 11.67	1.66	1.65	<1.34 - 4.10	$\cdots$	3	1.038e-07	4.37	4.64	>1.56	4	$\cdots$	0.09	V	$\cdots$	GSC2-FIRST-G
16 44 45.875 +33 13 14.34	6.30	6.22	3.85 - <14.39	6.18	6	7.536e-09	4.00	3.93	1.50	484	$\cdots$	0.75	V	$\cdots$	$\cdots$
16 44 54.661 +21 46 57.14	3.58	3.45	2.38 - 4.96	$\cdots$	4	8.175e-11	5.18	5.77	1.95	517	$\cdots$	0.12	V	$\cdots$	$\cdots$
16 45 28.217 +17 00 02.22	21.34	21.13	11.93 - 22.98	16.94	4	3.508e-06	5.04	4.94	1.93	$\cdots$	BN	2.07	V	19.30	SDSS-G
16 46 02.271 +43 21 56.63	6.21	6.03	4.32 - 8.68	3.54	4	3.970e-09	4.72	6.35	2.01	20	$\cdots$	0.49	V	20.24	SDSS-QSO(S)
16 47 11.455 +14 10 47.95	2.77	2.45	1.12 - 3.28	$\cdots$	3	3.955e-07	4.88	4.64	2.37	3	$\cdots$	0.77	V	20.30	SDSS-*
16 47 25.605 +19 32 59.29	4.39	4.40	3.48 - 6.77	4.02	3	2.339e-08	4.76	5.82	1.95	$\cdots$	$\cdots$	-0.75	V	$\cdots$	$\cdots$
16 48 02.886 +62 57 43.98	101.22	102.93	101.66 - 141.28	103.06	5	4.654e-07	4.10	3.72	1.39	3	$\cdots$	1.77	V	21.09	SDSS-*

Coordinates (J2000)	f (mJy)				N	Measures			$\frac{\text{Max.}}{\text{Min.}}$	$T_{\min}$	Flags	σ_{nbr}	Type	i	Cross-ID
	Cat.	$\overline{f}$	Range	NVSS		$P(\chi^2,\nu)$	$\sigma_{\max}$	$\Delta_{\max}(\sigma)$		(days)				Mag.	
16 48 05.314 +40 01 44.27	2.83	3.07	<2.17 - 3.49	$\cdots$	4	2.702e-07	4.99	5.28	>1.61	1	$\cdots$	-0.07	V	21.44	SDSS-G
16 48 59.879 +21 32 04.16	8.65	8.38	5.13 - 10.29	6.22	3	0.000	9.50	7.66	2.01	62	$\cdots$	0.36	V	18.73	SDSS-G
16 49 06.760 +38 39 51.89	1.38	1.22	<1.05 - <2.22	$\cdots$	4	3.827e-07	3.75	5.06	>1.92	5	$\cdots$	-0.48	V	17.52	SDSS-G
16 49 52.932 +32 58 15.25	43.58	44.56	29.65 - 54.51	32.68	4	0.000	8.97	6.73	1.84	488	$\cdots$	-0.05	V	18.73	SDSS-QSO(S)
16 50 44.667 +21 40 51.21	2.94	2.78	<1.83 - <7.21	$\cdots$	4	1.609e-07	5.25	5.21	>1.66	517	$\cdots$	-0.13	V	$\cdots$	$\cdots$
16 51 00.278 +24 15 39.99	8.90	8.78	3.83 - 8.95	4.36	5	2.724e-09	4.40	4.22	2.34	1	$\cdots$	1.02	V	20.09	SDSS-G
16 51 11.887 +64 17 31.75	11.21	10.97	9.40 - <19.49	14.01	6	1.925e-08	4.86	5.73	1.77	499	$\cdots$	0.60	V	16.32	SDSS-G
16 51 37.302 +46 45 22.63	5.57	5.36	4.90 - <17.67	7.53	5	2.453e-07	4.35	4.66	1.60	30	$\cdots$	0.37	V	20.94	SDSS-G
16 51 50.328 +61 36 31.72	3.20	3.33	1.88 - <12.82	5.60	5	2.389e-08	4.42	6.05	2.84	436	$\cdots$	0.03	V	$\cdots$	GSC2-FIRST-G
16 52 03.080 +26 51 39.85	6.27	6.99	1.46 - 8.63	$\cdots$	4	0.000	16.58	12.70	>5.92	2	$\cdots$	0.14	V	$\cdots$	PSR
16 53 12.711 +19 54 56.13	3.42	3.32	<1.75 - 3.65	2.77	3	5.596e-10	6.38	6.26	>2.09	$\cdots$	$\cdots$	0.59	V	20.33	SDSS-*
16 55 01.377 +14 57 06.25	36.66	34.65	30.24 - 54.76	41.37	4	2.885e-13	5.41	6.10	1.81	22	$\cdots$	-0.43	V	$\cdots$	$\cdots$
16 55 48.098 +41 52 27.18	4.10	4.13	3.49 - 6.84	3.05	3	9.387e-09	4.06	4.76	1.96	469	$\cdots$	0.42	V	20.57	SDSS-G
16 56 08.123 +42 45 46.17	6.75	7.17	3.42 - 8.94	6.06	3	7.774e-10	5.34	6.27	2.61	468	$\cdots$	0.83	V	20.68	SDSS-*
16 56 29.125 +22 14 06.32	1.15	0.97	<0.79 - 2.98	$\cdots$	3	7.071e-13	6.27	7.36	>3.77	412	$\cdots$	0.77	T	22.55	SDSS-*
16 56 38.621 +19 04 33.50	1.76	1.62	<1.42 - 2.23	$\cdots$	3	4.215e-07	3.80	5.11	>1.58	$\cdots$	$\cdots$	0.09	V	20.79	SDSS-G
16 57 20.339 +44 02 39.43	16.06	15.81	13.60 - 23.97	17.62	3	2.363e-13	5.36	6.19	1.76	925	$\cdots$	0.24	V	19.47	SDSS-*
16 57 34.457 +16 19 11.69	2.69	2.66	1.39 - <4.24	2.08	4	1.678e-09	4.72	6.08	2.59	$\cdots$	$\cdots$	1.05	V	19.17	SDSS-G
16 58 02.684 +61 26 21.33	8.01	7.79	7.16 - 11.00	8.20	3	4.897e-08	4.19	4.49	1.54	3	$\cdots$	-0.56	V	$\cdots$	$\cdots$
16 58 28.400 +31 36 49.91	12.76	12.55	9.01 - <31.30	9.07	6	4.233e-06	5.07	4.16	1.45	95	$\cdots$	0.61	V	$\cdots$	$\cdots$
16 58 39.617 +30 02 37.33	3.44	3.77	2.02 - <8.70	3.75	5	2.532e-07	4.57	4.58	>1.53	1	$\cdots$	-0.41	V	$\cdots$	$\cdots$
16 58 55.741 +22 54 19.68	2.23	2.50	1.38 - 3.23	$\cdots$	3	1.004e-07	4.65	4.81	2.33	4	$\cdots$	0.41	V	19.47	SDSS-QSO(S)
17 00 27.415 +21 48 22.42	13.82	14.21	11.39 - 17.27	19.69	3	8.284e-09	4.58	5.25	1.52	516	$\cdots$	0.06	V	$\cdots$	$\cdots$
17 01 55.781 +43 51 45.94	4.14	4.10	<2.63 - 5.26	5.22	4	1.777e-07	5.24	5.33	>1.70	5	$\cdots$	0.85	V	17.34	SDSS-G
17 02 11.744 +28 02 35.52	11.70	11.43	4.71 - 16.19	8.11	4	0.000	11.57	10.02	2.37	5	$\cdots$	-0.05	V	21.69	SDSS-*
17 02 26.375 +37 15 02.71	2.20	2.08	1.43 - 3.15	$\cdots$	3	8.221e-10	4.51	5.83	2.20	44	$\cdots$	-0.01	V	$\cdots$	$\cdots$
17 02 36.361 +30 26 24.74	1.40	1.23	<0.83 - 1.70	$\cdots$	3	4.984e-07	4.61	5.22	>2.06	1	$\cdots$	-0.16	V	$\cdots$	$\cdots$
17 05 39.639 +45 22 22.35	1.31	1.26	<1.05 - <2.53	$\cdots$	4	4.912e-07	4.01	5.24	>1.91	18	BN	-0.31	V	$\cdots$	$\cdots$
17 07 07.485 +63 35 11.13	2.88	3.12	2.48 - 7.11	3.41	4	3.940e-07	3.52	4.42	1.67	7	$\cdots$	0.85	V	$\cdots$	$\cdots$
17 07 25.444 +23 12 21.73	60.37	59.93	58.54 - 95.76	65.41	6	6.682e-12	5.17	4.95	1.64	4	$\cdots$	0.83	V	20.99	SDSS-G
17 08 00.337 +36 20 39.97	7.70	8.14	5.43 - 9.32	7.38	3	1.844e-08	5.69	4.63	1.72	7	$\cdots$	-0.07	V	13.54	SDSS-G

Coordinates (J2000)	f (mJy)				N	Measures			$\frac{\text{Max.}}{\text{Min.}}$	$T_{\min}$	Flags	σ_{nbr}	Type	i	Cross-ID
	Cat.	$\overline{f}$	Range	NVSS		$P(\chi^2,\nu)$	$\sigma_{\max}$	$\Delta_{\max}(\sigma)$		(days)				Mag.	
17 08 12.253 +41 16 58.87	2.02	1.87	<1.39 - 2.48	$\cdots$	3	1.322e-07	4.65	5.55	>1.76	1	$\cdots$	0.29	V	20.71	SDSS-G
17 08 34.812 +41 51 23.09	101.31	93.48	82.56 - 131.73	99.89	4	3.664e-15	4.70	5.37	1.51	469	$\cdots$	1.37	V	19.11	SDSS-*
17 09 18.149 +42 07 40.93	1.75	1.64	0.92 - <4.39	$\cdots$	4	2.463e-11	4.49	6.14	3.11	55	$\cdots$	0.08	V	$\cdots$	$\cdots$
17 10 40.320 +36 55 10.08	4.51	4.76	2.58 - 6.80	6.65	5	1.004e-12	4.83	4.67	>1.97	46	$\cdots$	-0.84	V	16.42	SDSS-G
17 10 59.407 +28 29 10.54	1.10	1.00	<0.77 - <5.54	$\cdots$	4	1.334e-09	4.49	5.96	>3.32	28	$\cdots$	0.93	V	$\cdots$	$\cdots$
17 11 18.384 +34 23 33.95	3.19	2.92	1.96 - 4.56	$\cdots$	3	1.395e-07	4.79	5.13	2.32	6	$\cdots$	1.29	V	18.83	SDSS-*
17 11 26.045 +41 39 35.13	2.67	2.73	<1.92 - <5.21	4.12	3	3.764e-10	5.46	6.25	>1.76	1	$\cdots$	-0.11	V	18.32	SDSS-G
17 11 38.005 +36 22 03.72	9.08	8.76	7.21 - 12.46	8.55	4	9.345e-10	5.24	6.39	1.73	5	$\cdots$	0.06	V	$\cdots$	$\cdots$
17 12 01.106 +38 45 23.39	11.01	10.27	9.49 - <18.32	7.75	6	1.011e-07	4.17	4.42	1.46	5	$\cdots$	0.75	V	$\cdots$	SDSS-UNKNOWN
17 15 16.040 +27 04 54.92	3.79	3.67	1.65 - <5.45	$\cdots$	3	5.927e-08	5.32	5.06	2.37	40	$\cdots$	-1.86	V	$\cdots$	$\cdots$
17 15 58.191 +27 01 25.65	8.91	8.76	5.30 - 12.05	6.53	3	0.000	9.25	8.90	2.27	4	$\cdots$	-0.00	V	$\cdots$	$\cdots$
17 16 34.189 +31 49 01.24	2.49	2.47	<2.18 - <11.75	$\cdots$	5	3.733e-09	5.02	5.93	>2.49	95	$\cdots$	0.65	V	$\cdots$	$\cdots$
17 18 13.762 +30 55 25.82	1.94	1.95	1.41 - 3.97	$\cdots$	3	5.422e-09	5.55	6.11	>2.83	70	$\cdots$	-0.86	V	$\cdots$	$\cdots$
17 18 47.402 +31 32 16.73	4.60	4.59	<3.33 - 5.86	5.61	2	1.145e-10	5.24	6.43	>1.76	95	$\cdots$	-1.08	T	19.42	SDSS-G
17 18 52.610 +31 33 32.53	7.90	7.79	3.57 - 9.55	8.12	2	0.000	8.35	8.38	2.67	95	$\cdots$	0.47	V	$\cdots$	$\cdots$
17 21 30.425 +41 12 50.75	4.87	4.90	<2.62 - <11.12	$\cdots$	5	2.651e-13	7.66	7.16	>1.99	1	$\cdots$	0.63	V	$\cdots$	$\cdots$
17 23 32.783 +39 55 21.68	2.08	2.36	1.25 - 3.38	$\cdots$	4	4.042e-11	4.50	5.90	2.58	1	$\cdots$	-1.02	V	19.32	SDSS-G
17 23 42.766 +44 56 02.48	29.75	26.28	24.30 - 44.46	31.59	5	0.000	5.86	6.05	1.83	6	$\cdots$	-1.42	V	21.14	SDSS-*
17 24 10.986 +42 33 20.83	2.91	2.94	1.69 - 4.03	3.18	4	1.204e-08	4.61	5.91	2.39	478	$\cdots$	0.41	V	$\cdots$	GSC2-FIRST-G
17 25 01.187 +40 27 14.37	15.58	16.04	8.31 - 16.89	13.84	5	2.655e-07	4.78	4.69	>1.39	6	BN	-1.26	V	$\cdots$	GSC2-FIRST-G
17 25 04.109 +45 11 57.06	4.06	3.56	2.27 - 3.96	$\cdots$	3	2.015e-07	5.29	4.93	1.74	6	$\cdots$	0.53	V	19.05	SDSS-G
17 25 12.166 +36 31 50.14	3.99	4.08	2.77 - 4.72	4.43	4	6.593e-09	5.56	5.86	>1.64	7	$\cdots$	-0.15	V	21.80	SDSS-*
17 25 41.667 +42 50 44.65	4.92	4.86	2.69 - 6.34	2.62	4	2.067e-11	5.33	6.06	2.26	478	$\cdots$	0.09	V	$\cdots$	GSC2-FIRST-G
17 26 45.776 +40 35 58.53	34.12	34.41	16.24 - 39.23	30.38	5	8.542e-07	5.05	5.32	2.42	2	BN	-0.14	V	$\cdots$	$\cdots$
17 26 59.319 +59 40 17.68	25.85	25.21	8.65 - 25.63	$\cdots$	5	0.000	10.50	8.37	2.96	423	$\cdots$	-0.06	V	19.07	SDSS-QSO(S)
17 28 00.938 +42 34 07.25	3.88	3.97	1.61 - <8.60	$\cdots$	5	1.864e-09	6.22	5.81	2.64	470	$\cdots$	1.12	V	$\cdots$	$\cdots$
17 29 02.073 +41 40 05.18	5.38	5.23	3.87 - 7.11	$\cdots$	4	1.708e-07	4.43	5.13	1.62	470	$\cdots$	0.58	V	$\cdots$	$\cdots$
17 29 17.600 +44 46 46.13	6.09	6.48	4.27 - 7.11	$\cdots$	3	9.859e-11	6.57	5.54	1.67	2	$\cdots$	-0.64	V	$\cdots$	$\cdots$
17 30 44.788 +38 04 55.22	7.30	7.25	3.85 - 7.76	5.98	3	6.004e-08	5.65	4.99	1.94	1	BN	0.16	V	$\cdots$	GSC2-FIRST-G
17 31 40.752 +39 12 36.94	3.36	3.36	1.86 - 4.81	3.11	4	4.021e-07	4.27	4.95	2.60	1	$\cdots$	0.74	V	$\cdots$	$\cdots$
17 32 07.061 +43 25 36.51	3.95	3.97	2.75 - 5.97	$\cdots$	3	3.765e-08	4.64	4.63	2.17	23	$\cdots$	0.70	V	19.28	SDSS-G

Coordinates (J2000)	f (mJy)				N	Measures			$\frac{\text{Max.}}{\text{Min.}}$	$T_{\min}$	Flags	σ_{nbr}	Type	i	Cross-ID
	Cat.	$\overline{f}$	Range	NVSS		$P(\chi^2, \nu)$	$\sigma_{\max}$	$\Delta_{\max}(\sigma)$		(days)				Mag.	
17 35 19.841 +52 55 55.36	79.84	71.98	67.86 - 102.31	83.32	4	1.997e-10	4.60	4.64	1.51	0	$\cdots$	0.09	V	21.69	SDSS-G
17 39 56.689 +47 44 56.59	4.55	4.75	3.31 - 5.58	7.51	2	1.592e-08	5.17	4.97	1.69	3	BN	0.30	V	$\cdots$	$\cdots$
17 40 48.091 +49 56 47.90	5.16	5.12	4.56 - 7.70	3.50	3	1.859e-08	4.47	4.95	1.66	10	$\cdots$	0.19	V	19.51	SDSS-G
17 43 30.469 +62 04 29.54	3.80	3.72	1.63 - 4.03	$\cdots$	3	8.282e-07	5.15	4.98	2.47	0	$\cdots$	-0.18	V	$\cdots$	$\cdots$
17 43 36.387 +59 13 07.16	3.48	3.76	2.33 - 6.61	$\cdots$	4	9.326e-09	4.62	4.72	1.78	4	$\cdots$	-0.15	V	$\cdots$	$\cdots$

Appendix B

Catalog of FR II Quasars

The complete catalogs of spectroscopic and photometric FR II quasars are provided in tables B.1 and B.2, respectively. Column 1 provides the optical QSO position (J2000). Column 2 gives the sum of the angular distances of the "hot spots" in the lobes from the optical QSO position. Column 3 gives the redshift of the QSO derived from the spectroscopic or photometric QSO catalogs from the SDSS as the case may be.

Table B.1: $\theta - z$ Data of FR II Quasars (Spectroscopic Sample)

Coordinates (J2000)	θ ($''$)	z
00 03 45.226 -11 08 18.72	18.4	1.570
00 06 08.049 -01 07 00.83	83.3	0.948
00 06 57.640 -01 03 58.82	17.6	1.436
00 11 38.437 -10 44 58.21	36.6	1.274
00 14 28.737 +00 39 04.67	67.2	1.167
00 16 28.836 +00 45 50.89	28.9	1.062
00 19 14.732 +00 34 31.50	90.3	0.194
00 24 23.415 +00 57 58.53	99.6	0.151
00 29 48.553 +00 44 47.48	29.2	1.008
00 32 59.279 -00 13 17.91	24.7	1.536
00 34 38.462 -00 29 13.61	24.3	1.997
00 43 23.431 -00 15 52.63	22.7	2.813
00 51 15.124 -09 02 08.47	90.0	1.265
00 54 25.662 -00 28 46.70	79.3	0.167
00 55 08.551 -10 52 06.18	60.0	1.381
00 55 50.750 -10 19 05.69	130.7	0.309
00 59 29.116 -10 17 34.98	14.3	1.420
01 03 29.433 +00 40 55.08	35.1	1.432
01 06 18.916 -01 06 08.16	61.7	1.488
01 06 41.051 -00 51 48.79	39.4	0.869
01 09 53.497 +00 51 36.93	55.5	0.044

Continued on next page. . .

Table B.1 – Continued

Coordinates (J2000)	θ ($''$)	z
01 15 46.536 +00 52 08.62	18.8	1.343
01 17 49.912 -09 05 54.64	59.1	0.828
01 18 26.376 -00 29 12.72	43.2	1.162
01 21 36.837 -00 18 10.81	19.6	0.764
01 29 56.707 +00 23 38.31	51.6	1.079
01 29 59.895 -09 39 29.23	66.5	0.358
01 33 52.654 +01 13 45.36	111.3	0.308
01 35 03.698 +01 13 24.30	40.3	0.358
01 40 00.244 -01 12 00.16	77.1	3.086
01 40 57.462 +00 10 52.75	131.0	0.523
01 42 27.999 +00 11 38.30	23.7	0.325
01 48 47.614 -08 19 36.26	47.3	1.679
02 02 34.326 +00 03 01.76	45.6	0.366
02 09 26.410 -08 08 01.17	72.6	1.335
02 20 21.502 +00 44 15.45	34.9	0.213
02 21 15.969 -00 15 54.94	45.2	0.540
02 23 44.810 +00 40 49.63	19.8	2.987
02 25 07.926 -00 35 32.90	19.3	0.685
02 26 50.734 +00 06 03.41	53.5	1.120
02 33 13.820 -00 12 15.43	54.3	0.807
02 45 34.058 +01 08 13.79	60.1	1.537
02 46 07.519 -00 40 12.57	33.6	0.362
02 48 02.561 -07 19 15.80	35.4	0.895

Table B.1 – Continued

Coordinates (J2000)	θ ($''$)	z
02 51 43.260 -00 24 35.98	60.2	0.394
02 55 12.170 -00 52 24.48	23.2	0.801
03 04 43.846 -00 15 11.23	83.3	0.264
03 12 26.119 -00 37 08.95	29.3	0.621
03 13 18.663 +00 36 23.84	63.3	1.259
03 16 56.916 +00 22 15.91	38.3	0.462
07 28 10.301 +39 30 28.01	30.0	2.753
07 28 24.794 +41 35 58.44	59.9	2.212
07 31 33.742 +41 00 18.88	27.4	1.312
07 34 22.202 +47 29 18.80	80.5	0.382
07 34 28.882 +32 50 58.43	56.5	1.807
07 36 31.152 +45 41 28.60	55.3	0.957
07 37 57.178 +29 42 11.93	68.3	0.000
07 41 25.217 +33 33 20.07	130.6	0.364
07 42 18.218 +19 47 19.48	80.0	0.657
07 44 35.962 +47 52 45.24	44.7	1.384
07 44 51.374 +29 20 05.99	26.7	1.184
07 45 41.671 +31 42 56.65	130.0	0.461
07 46 03.907 +50 14 56.91	26.3	1.010
07 46 52.030 +33 39 46.66	33.9	0.480
07 48 41.779 +17 34 56.69	38.1	1.087
07 49 37.687 +38 04 43.38	49.3	1.120
07 52 05.906 +28 02 10.75	25.3	0.942

Continued on next page. . .

Table B.1 – Continued

Coordinates (J2000)	θ ($''$)	z
07 52 06.742 +24 51 18.81	78.5	0.819
07 52 28.565 +37 50 53.60	36.0	1.208
07 53 28.099 +33 50 51.00	33.9	2.070
07 54 04.241 +42 58 04.30	30.2	1.729
07 55 37.034 +25 42 38.98	18.0	0.444
07 56 43.099 +31 02 48.80	31.5	0.271
07 58 39.744 +51 49 13.73	57.7	0.686
08 00 52.642 +41 57 38.84	30.4	1.522
08 01 12.648 +19 15 44.82	101.0	0.408
08 01 29.575 +46 26 22.84	35.5	0.316
08 02 20.518 +30 35 43.05	59.0	1.644
08 04 59.959 +27 22 48.66	148.6	0.578
08 05 55.673 +34 41 32.32	23.5	1.743
08 06 42.338 +19 58 11.96	28.3	1.200
08 06 44.414 +48 41 49.25	107.6	0.370
08 07 54.506 +49 46 27.62	63.4	0.575
08 08 33.372 +42 48 36.39	51.0	0.543
08 09 06.218 +29 12 35.53	137.3	1.481
08 09 20.810 +20 15 38.56	65.5	1.129
08 11 36.902 +28 45 03.56	37.3	1.890
08 12 12.475 +22 00 24.36	26.4	1.105
08 12 13.558 +22 58 46.98	55.6	2.546
08 13 18.850 +50 12 39.82	51.8	0.571

Continued on next page. . .

Table B.1 – Continued

Coordinates (J2000)	θ ($''$)	z
08 14 04.550 +06 02 38.35	40.6	0.561
08 14 09.221 +32 37 31.98	30.6	0.844
08 15 40.841 +39 54 37.83	30.0	0.463
08 17 35.076 +22 37 17.76	29.6	0.982
08 18 19.126 +24 35 42.48	72.1	1.208
08 18 38.882 +43 17 55.66	33.4	0.544
08 19 41.124 +05 49 42.67	121.3	1.701
08 20 37.349 +41 33 08.11	310.7	1.903
08 21 17.150 +48 45 46.29	38.6	1.572
08 21 25.966 +51 37 15.64	64.7	1.437
08 21 30.014 +21 17 20.34	34.0	0.000
08 22 14.182 +30 54 37.77	47.5	1.714
08 25 17.604 +44 36 26.91	31.3	0.902
08 28 06.840 +39 35 40.26	72.5	0.761
08 30 31.934 +05 20 06.74	35.6	2.217
08 30 36.252 +28 36 39.02	56.5	0.746
08 31 36.994 +30 48 26.82	34.5	1.001
08 32 36.338 +33 31 54.74	35.5	1.105
08 32 36.574 +05 03 40.29	40.2	0.000
08 33 13.058 +48 46 39.92	66.3	2.274
08 34 31.618 +24 01 46.25	48.8	1.421
08 38 40.577 +47 34 10.65	48.3	0.695
08 39 23.237 +06 09 58.95	53.1	1.013

Table B.1 – Continued

Coordinates (J2000)	θ ($''$)	z
08 42 52.402 +44 34 10.60	55.9	1.779
08 43 09.862 +29 44 04.70	89.6	0.398
08 43 52.870 +37 42 28.28	40.4	1.741
08 44 41.510 +08 30 59.96	150.3	0.704
08 44 42.696 +49 23 53.63	15.1	2.132
08 46 59.326 +34 48 25.14	36.5	1.582
08 47 02.794 +01 30 01.42	28.9	0.417
08 48 41.297 +45 42 20.64	39.7	1.537
08 48 56.774 +08 01 27.29	29.5	0.958
08 49 40.015 +09 49 21.15	69.0	0.366
08 50 39.950 +54 37 53.39	134.1	0.367
08 51 14.935 +01 59 53.15	52.4	1.074
08 52 00.439 +02 29 34.54	23.7	1.177
08 52 32.827 +38 36 56.04	31.9	1.502
08 53 41.189 +40 52 21.79	71.5	0.573
08 54 17.345 +29 23 14.49	117.2	0.671
08 54 59.981 -00 11 00.23	135.2	0.768
08 56 40.138 +25 31 05.09	56.5	1.218
08 57 48.566 +09 06 48.11	65.0	1.688
08 58 30.612 +08 04 22.85	94.6	0.455
08 59 40.291 +35 06 47.37	89.6	1.389
09 02 29.227 +48 39 06.24	43.0	1.373
09 03 33.017 +27 19 27.81	18.9	1.722

Table B.1 – Continued

Coordinates (J2000)	θ ($''$)	z
09 04 14.100 -00 21 44.94	92.5	0.353
09 04 29.626 +28 19 32.77	28.8	1.121
09 04 34.176 +34 32 05.45	22.7	1.675
09 04 36.360 +51 07 28.20	41.4	1.409
09 05 01.560 +53 39 07.49	39.0	0.594
09 05 13.166 +42 24 51.89	51.4	1.161
09 06 00.089 +57 47 30.11	43.0	4.370
09 06 49.987 +08 32 55.77	85.2	1.617
09 08 08.801 +00 35 00.51	23.9	1.649
09 08 12.173 +51 47 00.81	39.7	1.002
09 08 21.017 +04 50 59.47	42.9	0.524
09 09 47.268 +30 24 03.55	34.2	0.783
09 10 03.974 +27 50 28.92	20.9	1.692
09 10 17.326 +37 42 52.09	34.2	1.431
09 12 07.032 +33 48 29.03	18.9	1.872
09 13 16.421 +03 37 19.99	113.7	2.009
09 13 33.658 -00 42 50.98	111.7	0.426
09 15 19.567 +56 38 37.83	114.9	0.263
09 15 28.774 +44 16 32.89	60.3	1.489
09 17 18.684 +59 03 40.41	36.1	0.927
09 17 57.432 +02 37 34.02	27.1	1.767
09 18 43.087 +40 17 09.71	42.3	0.829
09 19 21.559 +50 48 55.42	56.9	0.921

Continued on next page. . .

Table B.1 – Continued

Coordinates (J2000)	θ ($''$)	z
09 20 23.316 +11 04 19.52	32.5	1.053
09 20 42.516 +29 16 18.22	16.8	1.916
09 21 08.623 +45 38 57.40	153.2	0.174
09 22 25.140 +43 07 49.45	37.7	0.236
09 23 07.397 +30 59 26.47	12.5	0.629
09 23 08.167 +56 14 55.38	54.4	0.249
09 23 13.536 +04 34 44.97	81.4	0.657
09 23 51.526 +28 15 25.16	29.6	0.744
09 24 14.710 +03 09 00.79	200.0	0.128
09 24 25.027 +35 47 12.67	86.4	1.342
09 24 54.559 +49 18 04.23	27.7	1.945
09 25 24.569 +42 17 29.67	17.7	1.884
09 26 11.026 +27 38 28.28	44.1	1.905
09 26 56.714 +04 16 13.22	59.1	1.036
09 27 38.098 +01 44 31.20	97.9	0.419
09 28 37.980 +60 25 21.01	35.0	0.295
09 28 56.830 +07 36 19.01	56.6	0.729
09 31 12.912 +36 47 49.26	40.6	1.398
09 31 38.287 +03 15 10.13	51.3	1.158
09 31 42.542 -00 03 06.02	67.2	0.645
09 32 00.082 +55 33 47.40	125.7	0.266
09 32 42.686 +28 54 52.41	50.1	1.985
09 33 01.594 +49 50 29.61	106.6	0.616

Table B.1 – Continued

Coordinates (J2000)	θ $('')$	z
09 35 53.818 +05 03 53.21	39.1	1.403
09 36 28.678 +01 23 29.25	72.7	1.664
09 40 18.852 +30 15 10.00	38.9	1.594
09 41 04.006 +38 53 51.01	58.1	0.616
09 41 05.791 +11 52 17.69	36.9	2.400
09 41 32.542 +02 04 32.54	21.0	1.375
09 41 44.825 +57 51 23.68	37.7	0.159
09 42 03.048 +54 05 18.92	40.4	2.347
09 43 18.490 +01 03 04.49	109.2	1.058
09 43 58.219 +02 26 30.61	29.5	2.030
09 44 38.794 +08 51 56.98	51.7	0.802
09 45 49.901 +12 05 31.79	16.8	0.967
09 47 40.013 +51 54 56.79	67.5	1.063
09 47 45.146 +07 25 20.58	230.3	0.086
09 48 31.548 +02 34 57.82	89.1	1.296
09 48 56.782 +07 27 48.71	74.8	1.169
09 50 26.371 +05 51 58.09	37.4	0.980
09 51 26.484 +01 46 51.80	32.5	0.495
09 52 28.459 +06 28 10.50	72.1	1.362
09 52 32.021 +35 12 52.53	31.5	1.876
09 52 45.571 +00 00 15.51	39.3	1.063
09 54 55.433 +40 59 14.12	159.3	0.478
09 54 55.562 +57 19 52.80	40.8	0.981

Table B.1 – Continued

Coordinates (J2000)	θ ($''$)	z
09 54 56.899 +09 29 55.81	17.9	0.298
09 55 48.048 +35 33 23.10	24.2	1.244
09 55 56.378 +06 16 42.46	52.0	1.278
09 58 02.822 +44 06 03.68	21.7	2.188
09 58 52.486 +06 20 08.53	45.0	2.061
09 58 55.099 +42 37 04.10	12.7	0.664
10 00 17.669 +00 05 23.71	38.1	0.905
10 00 54.682 +53 32 06.00	31.4	1.347
10 03 02.604 +40 48 13.15	30.1	2.368
10 03 11.561 +50 57 05.19	52.0	1.838
10 03 50.705 +52 53 52.23	43.8	1.335
10 04 03.682 +29 18 35.38	73.9	0.904
10 06 07.709 +32 36 26.18	21.5	1.026
10 06 27.883 +32 02 19.27	78.4	1.268
10 06 33.643 +44 35 00.70	42.5	1.499
10 07 09.821 +13 35 53.43	46.2	0.928
10 07 18.842 +04 08 08.05	71.0	1.024
10 07 26.102 +12 48 56.22	102.9	0.241
10 08 59.786 +35 53 54.36	89.1	1.474
10 09 02.066 +07 13 43.88	63.4	0.456
10 09 43.558 +05 29 53.86	90.0	0.942
10 10 27.526 +41 32 39.08	37.6	0.612
10 10 57.425 +38 17 35.39	46.7	0.826

Table B.1 – Continued

Coordinates (J2000)	θ ($''$)	z
10 12 20.371 +12 43 50.30	48.5	1.149
10 12 54.250 +61 36 34.63	19.6	2.053
10 13 28.774 +07 56 53.78	40.7	0.589
10 14 46.510 +31 34 24.68	34.3	1.360
10 14 47.777 +44 21 33.39	38.2	0.796
10 14 53.640 +30 54 12.38	38.5	2.113
10 15 41.143 +59 44 45.37	37.3	0.527
10 15 57.617 +48 37 59.68	116.0	0.385
10 16 51.739 -00 33 47.01	34.4	1.827
10 17 09.250 -01 18 23.69	25.5	2.200
10 17 18.672 +39 31 21.06	140.4	0.530
10 18 25.454 +38 05 32.75	60.7	0.387
10 20 26.868 +04 47 52.11	95.4	1.131
10 21 06.043 +45 23 31.87	42.9	0.364
10 22 35.570 +45 41 05.50	49.9	0.743
10 22 58.414 +12 34 29.77	20.7	1.729
10 23 13.606 +63 57 09.26	83.8	1.194
10 24 29.016 +05 29 52.52	83.1	1.482
10 25 46.116 +43 17 35.79	44.4	0.959
10 26 31.966 +06 27 33.00	18.3	1.709
10 26 59.316 +41 39 25.11	52.6	0.601
10 27 25.963 +52 26 36.95	41.3	1.339
10 30 24.950 +55 16 22.75	27.3	0.435

Table B.1 – Continued

Coordinates (J2000)	θ ($''$)	z
10 30 50.906 +53 10 28.65	109.6	1.197
10 30 59.095 +31 02 55.81	30.5	0.178
10 31 43.512 +52 25 35.17	55.3	0.166
10 31 44.539 +41 54 20.88	45.0	0.680
10 32 09.276 +31 35 27.06	26.7	1.027
10 34 18.010 +08 36 26.70	37.0	0.633
10 38 38.822 +49 47 36.84	28.3	1.477
10 38 42.026 +04 33 08.58	87.5	0.423
10 38 48.132 +37 29 24.57	73.7	0.730
10 39 02.174 +49 31 39.12	42.8	0.023
10 39 36.672 +07 14 27.40	64.5	1.536
10 40 50.186 +33 07 12.74	86.9	0.000
10 41 10.702 +35 19 16.82	30.2	1.014
10 41 46.774 +52 33 28.23	45.9	0.678
10 42 07.562 +50 13 21.98	72.7	1.265
10 42 31.238 +29 50 56.82	26.5	1.511
10 45 05.482 +45 34 01.18	23.4	1.606
10 45 10.214 +36 46 43.75	25.1	0.642
10 45 37.750 +61 26 05.76	14.7	1.132
10 45 42.185 +52 51 12.64	26.9	1.058
10 45 48.996 +53 47 59.82	43.6	0.662
10 47 05.225 +38 38 09.44	56.2	0.233
10 47 11.102 +35 44 37.33	55.8	0.380

Table B.1 – Continued

Coordinates (J2000)	θ ($''$)	z
10 47 40.474 +02 07 57.29	57.5	1.759
10 48 07.481 +38 37 35.67	21.3	0.606
10 49 27.110 +45 55 49.92	31.4	1.521
10 49 32.222 +05 05 31.74	14.7	1.114
10 51 35.330 +00 51 33.52	39.3	2.007
10 51 41.172 +59 13 05.22	22.1	0.435
10 51 58.685 +36 43 26.12	73.5	0.950
10 52 39.257 +31 34 17.58	33.0	1.686
10 52 45.809 +13 40 57.49	38.4	1.356
10 52 50.062 +33 55 04.95	38.1	1.407
10 53 10.162 +58 55 32.76	26.6	1.174
10 54 43.135 -01 07 01.79	134.9	0.522
10 54 54.972 +06 14 53.09	43.5	0.419
10 54 57.038 -00 45 53.04	70.2	0.917
10 55 00.336 +52 02 00.93	55.2	0.187
10 55 17.268 +02 05 45.10	38.5	0.876
10 55 21.240 +37 26 52.61	80.2	0.589
10 56 32.014 +43 00 55.96	40.5	0.318
10 56 54.158 +05 17 13.26	36.8	0.456
10 59 51.910 +40 51 14.19	30.9	1.750
11 00 47.854 +10 46 13.22	39.2	0.422
11 03 13.306 +30 14 42.74	83.0	0.384
11 03 29.076 +46 14 01.66	38.6	1.179

Table B.1 – Continued

Coordinates (J2000)	θ ($''$)	z
11 04 20.657 +34 31 43.87	18.3	1.589
11 04 50.230 +30 17 04.14	25.9	1.519
11 05 14.278 +01 09 08.19	34.7	1.451
11 07 09.511 +05 47 44.77	85.7	1.799
11 07 15.886 +05 33 06.69	19.3	0.884
11 07 18.881 +10 04 17.72	58.7	0.633
11 07 26.930 +36 16 12.22	27.6	0.392
11 07 45.780 +60 09 13.85	18.4	0.397
11 09 40.841 +40 14 29.65	46.9	0.655
11 10 40.202 +30 19 09.86	50.0	1.521
11 12 14.455 +01 20 48.49	57.0	1.304
11 12 15.451 +11 29 19.29	118.7	1.132
11 12 39.396 +43 25 46.77	62.5	1.682
11 14 40.663 +59 27 43.48	243.3	1.416
11 17 16.596 +57 58 11.77	59.1	1.670
11 17 40.841 +05 28 58.67	23.7	1.289
11 18 58.627 +38 28 52.20	90.8	0.747
11 19 03.281 +38 58 52.60	106.7	0.734
11 19 28.382 +13 02 51.09	78.2	2.401
11 20 04.946 +46 07 46.77	53.5	1.006
11 20 48.504 +03 32 47.06	58.4	0.868
11 22 24.588 +41 00 38.93	64.4	0.751
11 24 11.659 -03 37 04.66	46.2	0.753

Table B.1 – Continued

Coordinates (J2000)	θ ($''$)	z
11 25 06.962 -00 16 47.64	24.8	1.770
11 27 13.990 -01 11 53.29	26.4	1.804
11 29 29.162 +45 20 26.50	19.0	1.120
11 29 46.025 -01 21 40.54	92.6	0.726
11 30 26.177 +36 28 37.00	55.3	1.072
11 31 48.650 +32 59 02.24	75.2	1.268
11 32 35.858 -01 28 48.70	56.4	0.442
11 33 25.152 +55 11 24.45	23.9	1.736
11 33 28.066 +43 33 25.07	36.0	0.438
11 34 40.956 +40 21 15.68	36.5	0.746
11 34 42.062 +41 13 29.85	37.2	1.684
11 35 13.327 +43 40 03.70	23.4	1.234
11 36 04.918 +52 25 58.90	57.3	1.611
11 37 03.091 +01 40 06.30	23.1	1.699
11 37 14.256 -01 53 34.19	43.1	1.295
11 40 01.495 +01 03 41.76	29.3	1.054
11 41 08.664 +14 58 13.43	58.9	1.430
11 41 11.621 -01 43 06.66	27.5	1.266
11 44 33.672 +60 15 38.87	27.6	0.756
11 45 10.385 +01 10 56.29	65.2	0.626
11 45 33.766 +38 56 47.20	22.6	2.284
11 45 34.241 +36 52 29.83	63.5	1.216
11 45 59.455 +44 23 50.67	91.2	1.270

Table B.1 – Continued

Coordinates (J2000)	θ $('')$	z
11 47 25.507 +31 57 05.39	21.2	0.825
11 47 34.296 +04 30 47.27	23.8	1.210
11 48 18.881 +31 54 10.13	28.4	0.550
11 48 47.832 +10 54 58.41	22.8	0.861
11 49 18.967 +02 39 26.17	30.1	1.542
11 49 40.620 +42 50 53.66	47.3	1.172
11 49 58.706 +41 12 09.44	65.9	0.250
11 50 52.752 +34 27 08.49	40.6	0.844
11 51 40.690 +06 43 35.37	46.1	1.517
11 51 44.393 +52 44 12.62	41.7	1.147
11 51 59.942 +49 50 56.16	75.8	3.354
11 54 05.376 +56 20 40.87	54.5	0.514
11 54 36.804 +14 28 17.77	60.9	0.969
11 58 39.924 +62 54 27.86	64.0	0.592
11 58 48.595 +13 49 08.68	48.2	1.942
11 59 53.438 +48 19 02.34	50.0	1.550
12 00 03.893 +41 08 42.41	24.7	1.858
12 00 55.994 +11 57 18.46	38.3	2.016
12 04 48.518 +38 01 40.14	52.4	1.277
12 05 42.422 +15 14 57.90	88.2	0.894
12 06 17.359 +38 12 34.98	41.3	0.838
12 06 29.030 +07 24 14.51	56.3	0.976
12 07 08.021 -02 44 44.11	61.8	1.103

Continued on next page. . .

Table B.1 – Continued

Coordinates (J2000)	θ $('')$	z
12 08 37.111 +61 21 06.42	126.8	0.275
12 09 13.620 +43 39 20.96	15.5	1.398
12 09 21.775 +48 41 39.12	31.8	0.479
12 09 42.792 +48 34 23.33	55.1	0.711
12 09 49.985 +54 26 31.60	38.5	0.864
12 11 28.872 +50 52 54.24	39.6	1.364
12 11 54.866 +60 44 26.05	66.0	0.637
12 12 20.381 +48 31 23.88	39.0	1.120
12 12 44.904 +37 31 43.77	49.0	0.217
12 13 14.825 +14 44 00.63	56.6	0.716
12 13 40.370 +57 07 11.49	57.7	1.580
12 13 47.530 +00 01 29.99	79.5	0.962
12 15 09.950 +46 27 15.08	37.0	0.720
12 15 29.556 +53 35 55.87	38.8	1.069
12 15 41.964 +05 19 32.64	49.4	0.810
12 15 44.371 +45 29 12.80	23.6	1.134
12 15 49.205 +46 03 51.63	28.5	1.541
12 17 01.373 +10 19 52.94	33.9	1.883
12 20 02.940 +40 26 20.53	64.9	1.616
12 20 27.982 +09 28 27.32	26.6	1.082
12 20 45.948 -01 21 15.52	61.7	1.425
12 20 49.145 +58 59 21.57	47.2	0.780
12 21 06.874 +45 48 52.10	44.9	0.525

Table B.1 – Continued

Coordinates (J2000)	θ ($''$)	z
12 23 11.143 +37 07 01.52	42.7	0.491
12 25 06.504 +48 34 35.18	26.8	0.647
12 25 12.938 +12 18 35.70	75.6	0.412
12 26 07.925 +47 37 00.57	27.5	1.056
12 26 38.453 +42 32 40.11	46.4	0.905
12 28 00.391 +07 25 42.12	16.9	0.673
12 28 26.419 +39 47 54.12	61.9	1.245
12 29 25.536 +35 55 32.17	109.8	0.828
12 29 40.886 +62 42 54.67	108.6	0.967
12 30 35.834 +09 45 18.92	100.6	0.638
12 30 36.156 +06 54 24.17	20.8	1.769
12 30 52.565 +39 30 00.77	58.3	2.228
12 31 06.816 +47 59 07.84	31.0	1.834
12 33 16.565 +48 42 00.92	26.1	0.917
12 33 54.458 +48 20 50.00	21.3	1.000
12 34 03.958 +14 18 51.36	31.0	1.779
12 34 29.016 +08 29 35.44	68.1	1.091
12 36 04.512 +10 34 49.27	112.2	0.667
12 36 23.796 +06 02 08.20	63.5	1.050
12 36 33.125 +10 09 28.69	60.1	0.589
12 37 40.565 +36 14 01.62	34.7	1.779
12 38 07.771 +53 25 55.99	146.9	0.348
12 38 18.958 +08 13 07.29	67.7	1.819

Table B.1 – Continued

Coordinates (J2000)	θ ($''$)	z
12 38 59.806 +01 15 07.37	109.4	0.046
12 39 15.398 +53 14 14.64	79.9	0.201
12 39 54.156 +37 39 54.51	52.4	1.841
12 40 00.931 +03 40 51.61	63.5	1.882
12 40 21.144 +35 02 58.79	22.8	1.199
12 41 16.488 +51 41 30.00	68.9	0.823
12 41 39.727 +49 34 05.53	60.0	0.474
12 41 57.547 +63 32 41.62	40.4	2.624
12 42 19.253 +43 56 08.26	56.3	0.612
12 45 38.354 +55 11 32.68	27.2	1.555
12 47 10.291 +55 55 57.34	52.8	0.498
12 47 16.718 +12 36 58.68	16.7	1.327
12 47 58.524 +62 50 49.34	25.3	1.712
12 48 04.102 -03 01 14.43	30.7	1.026
12 48 26.645 +46 42 09.04	16.0	1.233
12 49 23.510 +44 44 50.44	29.8	0.803
12 51 51.029 +49 18 55.05	43.6	1.463
12 52 09.660 -00 15 53.43	29.2	0.813
12 52 48.281 +47 40 43.70	25.9	0.921
12 53 20.412 +46 33 50.09	14.7	2.452
12 54 02.165 -00 49 31.13	52.4	1.374
12 54 10.411 +39 33 23.18	38.6	2.104
12 54 28.831 +45 36 04.31	26.8	1.645

Continued on next page. . .

Table B.1 – Continued

Coordinates (J2000)	θ ($''$)	z
12 55 03.888 +48 09 52.95	32.9	1.718
12 55 08.100 +62 20 50.45	43.1	1.978
12 55 28.301 -00 54 41.99	20.2	1.012
12 57 03.120 +00 24 35.95	24.7	1.258
12 57 10.807 +40 54 29.15	126.7	1.068
12 57 29.796 -01 32 39.59	35.3	1.461
12 57 37.068 -00 32 20.18	33.6	1.027
12 58 24.706 +02 08 46.77	25.7	0.892
12 59 02.050 +39 00 13.67	25.4	0.979
12 59 45.180 +03 17 26.18	44.1	1.528
12 59 49.478 +14 05 47.07	17.6	1.510
13 00 33.302 +40 09 07.72	26.8	1.671
13 01 23.470 +50 18 30.10	24.1	0.386
13 05 08.364 +14 04 18.65	48.5	2.387
13 05 21.329 +49 51 42.32	47.6	1.249
13 07 40.594 +47 33 55.37	15.3	0.260
13 08 28.733 +50 26 23.20	26.5	1.729
13 08 42.881 +02 43 26.74	40.2	0.504
13 09 07.990 +52 24 37.30	23.4	1.587
13 10 40.562 -03 34 11.97	48.1	1.338
13 10 40.740 +02 01 27.08	44.0	1.827
13 11 33.017 +39 42 57.67	82.6	0.629
13 12 11.143 +48 09 25.37	96.2	0.715

Table B.1 – Continued

Coordinates (J2000)	θ ($''$)	z
13 12 54.936 +15 15 28.76	26.3	1.421
13 13 50.558 +15 04 43.44	45.9	0.970
13 14 58.404 +56 03 42.53	30.3	1.751
13 15 06.079 +47 54 24.08	34.0	1.433
13 15 38.719 -01 58 46.18	14.2	1.503
13 16 11.753 +57 51 12.33	72.4	1.055
13 16 14.498 +02 39 38.85	30.0	0.852
13 17 26.129 -02 31 50.47	32.8	1.090
13 18 27.000 +62 00 36.26	54.4	0.307
13 19 46.190 +51 48 05.76	35.7	1.061
13 20 26.590 +40 32 44.66	41.0	1.028
13 20 53.510 +51 06 40.07	29.5	1.398
13 21 03.418 +12 37 48.26	53.6	0.687
13 24 04.200 +43 34 07.14	160.9	0.338
13 26 31.447 +47 37 55.89	60.4	0.682
13 26 55.716 +02 07 27.40	43.6	1.393
13 27 31.694 +45 52 28.70	26.1	0.791
13 27 46.164 +48 42 02.97	51.7	1.030
13 28 34.150 -01 29 17.64	332.5	0.151
13 31 39.907 +31 27 57.73	50.3	3.022
13 32 53.273 +02 00 45.68	119.9	0.216
13 32 58.879 +45 42 01.83	18.3	1.010
13 32 59.170 +49 09 46.84	34.5	1.939

Table B.1 – Continued

Coordinates (J2000)	θ ($''$)	z
13 33 07.013 +04 50 48.53	136.6	1.402
13 33 50.450 +31 20 22.33	21.9	2.666
13 34 11.705 +55 01 24.98	82.5	1.245
13 34 18.641 +48 13 17.16	81.6	2.209
13 34 33.526 +45 11 41.97	70.4	0.739
13 34 37.488 +56 31 47.93	32.6	0.343
13 34 49.730 +31 28 24.06	56.5	1.309
13 38 02.808 +42 39 56.98	33.4	2.237
13 39 48.449 +47 41 17.10	26.0	1.498
13 40 42.883 +02 03 07.53	24.5	1.008
13 40 48.372 +43 33 59.86	32.8	1.499
13 42 54.386 +28 28 05.89	39.0	1.036
13 44 15.754 +33 17 19.14	154.5	0.686
13 44 25.531 +38 41 30.17	24.5	1.538
13 45 23.825 +41 25 41.60	59.3	0.916
13 45 45.360 +53 32 52.31	55.8	0.135
13 46 17.544 +62 20 45.48	50.0	0.116
13 47 39.838 +62 21 49.60	93.1	0.804
13 50 54.590 +05 22 06.50	75.8	0.442
13 51 55.747 +41 06 31.72	53.4	0.764
13 53 05.544 +04 43 38.75	30.9	0.523
13 57 03.835 +02 30 07.09	23.8	2.200
13 58 17.606 +57 52 04.55	50.1	1.373

Table B.1 – Continued

Coordinates (J2000)	θ ($''$)	z
13 58 23.522 +60 25 07.27	19.7	2.341
13 59 39.290 +50 51 46.62	24.8	1.452
13 59 53.801 +59 11 02.97	16.9	0.689
14 00 03.084 +39 10 55.20	30.0	0.803
14 01 03.929 +48 35 54.14	26.1	1.006
14 01 30.689 +41 55 15.28	26.2	1.941
14 01 48.650 +07 13 52.54	42.7	1.704
14 02 14.803 +58 17 46.78	50.6	1.267
14 04 16.826 +34 13 17.29	30.2	0.932
14 05 18.482 +04 34 06.92	28.6	0.352
14 06 56.491 +46 17 12.52	28.1	1.314
14 08 32.647 +00 31 38.53	58.7	1.671
14 09 50.534 +35 04 25.53	37.0	0.718
14 10 54.065 +58 46 55.43	34.6	0.482
14 11 23.510 +00 42 53.00	38.6	2.267
14 11 51.972 +55 09 48.80	61.0	1.889
14 11 55.265 +34 15 10.11	27.6	1.818
14 12 31.178 +54 55 11.51	33.0	1.523
14 13 06.739 +47 42 04.62	17.6	1.741
14 15 32.189 +40 49 51.59	47.0	1.944
14 15 41.839 +12 12 30.57	69.4	0.272
14 16 13.366 +02 19 07.83	16.0	0.158
14 16 58.313 +34 28 52.52	21.0	0.744

Table B.1 – Continued

Coordinates (J2000)	θ ($''$)	z
14 17 08.162 +46 07 05.42	38.2	1.559
14 18 58.860 +39 46 38.79	32.3	0.474
14 20 33.257 -00 32 33.33	22.6	2.676
14 21 27.773 +58 47 57.63	41.9	1.534
14 22 35.892 -01 52 11.26	44.3	0.666
14 24 14.088 +42 14 00.07	20.4	1.608
14 24 34.330 +52 47 30.58	27.9	0.636
14 25 50.717 +24 04 03.40	26.5	0.653
14 27 46.795 +00 28 44.71	34.2	1.260
14 27 58.733 +32 47 41.45	95.3	0.570
14 28 29.935 +44 39 49.76	36.0	1.050
14 28 53.083 +10 01 17.81	44.1	1.499
14 32 44.441 -00 59 15.12	47.7	1.027
14 33 34.313 +32 09 09.27	44.2	0.935
14 34 10.771 -01 23 41.71	64.9	1.020
14 35 13.495 +61 01 23.14	22.8	2.477
14 36 23.664 +06 18 48.67	47.0	0.966
14 36 27.370 +52 14 00.03	19.7	1.328
14 37 56.935 +01 56 38.90	22.0	1.183
14 38 20.928 -02 39 53.15	17.7	1.551
14 39 39.953 +44 28 50.97	65.1	1.695
14 43 02.762 +52 01 37.21	41.1	0.141
14 43 17.590 +31 54 56.76	35.3	0.971

Table B.1 – Continued

Coordinates (J2000)	θ ($''$)	z
14 43 23.215 +42 44 11.47	33.5	0.775
14 43 34.574 -02 19 26.55	25.8	0.933
14 44 14.206 +43 36 55.46	31.9	1.346
14 45 20.698 +47 22 24.86	39.7	1.323
14 45 57.811 +32 15 00.48	40.6	1.247
14 46 00.034 +12 22 40.52	94.5	0.513
14 46 36.902 +00 46 56.52	55.6	0.721
14 47 07.411 +52 03 40.10	44.5	2.064
14 47 32.947 +35 07 53.36	35.2	0.675
14 48 14.942 +57 41 45.69	20.4	1.171
14 49 27.418 -01 31 06.40	133.7	0.559
14 49 45.043 +45 19 41.28	71.8	1.635
14 50 38.839 +45 49 54.63	100.0	1.621
14 50 51.377 +12 12 36.84	37.1	1.779
14 51 34.610 +01 59 36.99	69.6	1.274
14 52 24.682 +45 22 23.68	92.2	0.467
14 52 47.374 +47 35 29.14	65.0	1.158
14 55 46.642 +36 14 14.76	67.4	0.520
15 00 07.265 +56 36 00.81	18.5	0.885
15 00 27.209 +45 08 59.07	57.5	1.203
15 00 31.805 +48 36 46.84	31.0	1.028
15 01 21.965 +01 44 01.25	35.3	0.608
15 03 06.516 +34 24 53.62	34.0	0.000

Continued on next page...

Table B.1 – Continued

Coordinates (J2000)	θ ($''$)	z
15 04 05.110 +46 28 51.34	43.0	0.632
15 04 31.303 +47 41 51.24	18.6	0.824
15 05 45.050 +41 17 26.75	28.0	1.526
15 08 24.737 +56 04 23.28	41.8	0.978
15 08 35.945 +60 32 58.62	51.9	1.214
15 09 40.594 +60 38 21.33	54.1	1.015
15 11 09.226 +56 50 51.77	54.2	0.631
15 11 42.758 +44 30 43.59	32.3	0.965
15 12 15.744 +02 03 16.98	48.3	0.219
15 12 23.796 +39 00 42.05	131.1	0.373
15 13 56.158 +04 20 55.81	16.5	0.720
15 14 15.962 +57 49 03.96	37.1	1.620
15 14 43.070 +36 50 50.41	63.6	0.371
15 15 03.226 +61 35 20.12	22.5	2.404
15 16 09.998 +01 06 37.23	58.5	2.225
15 16 40.222 +00 15 01.83	245.7	0.052
15 17 45.768 +43 51 04.83	71.2	1.910
15 18 30.938 +48 32 14.45	137.2	0.576
15 19 12.818 +37 49 18.47	54.1	2.169
15 19 32.081 +38 44 52.53	41.4	1.520
15 19 36.725 +53 42 55.51	39.1	0.478
15 20 21.038 +02 53 12.09	49.0	1.194
15 20 25.639 +59 39 55.44	13.8	1.279

Table B.1 – Continued

Coordinates (J2000)	θ ($''$)	z
15 21 13.378 +44 08 33.85	91.0	1.062
15 23 46.790 -02 22 39.54	22.7	1.024
15 24 57.348 +33 35 00.92	154.7	0.903
15 25 05.364 +53 06 22.89	27.3	1.726
15 25 56.239 +59 16 59.50	117.5	0.955
15 28 38.400 +48 47 40.66	79.6	1.027
15 31 07.411 +58 44 09.93	83.1	1.724
15 31 28.692 +03 38 02.31	83.0	0.753
15 35 44.443 +57 14 23.68	98.7	0.635
15 41 12.871 +00 50 32.01	57.7	1.137
15 44 30.480 +41 20 13.99	43.0	1.292
15 44 39.713 +44 40 50.98	44.8	1.555
15 46 38.309 +36 44 20.24	59.8	0.938
15 50 02.011 +36 52 16.77	86.1	2.061
15 50 36.708 +01 11 54.17	38.2	1.109
15 52 27.708 +09 39 02.95	32.6	1.541
15 54 38.678 +00 48 46.19	57.1	0.736
15 57 18.998 +45 22 21.57	40.4	0.495
15 57 25.488 +36 01 33.71	23.4	1.499
15 57 29.942 +33 04 46.93	39.8	0.953
15 58 35.398 +27 31 02.29	115.7	0.924
16 02 12.192 +06 15 03.34	52.9	0.875
16 03 17.911 +09 00 37.93	27.3	0.488

Continued on next page. . .

Table B.1 – Continued

Coordinates (J2000)	θ ($''$)	z
16 03 26.338 +49 30 44.30	25.5	1.268
16 04 56.143 -00 19 07.00	31.8	1.629
16 05 15.799 +25 01 47.90	23.2	0.369
16 08 13.795 +29 21 26.31	25.8	1.200
16 08 46.762 +37 48 50.64	36.7	1.431
16 09 53.424 +43 34 11.52	150.4	0.760
16 10 22.339 +32 38 24.16	19.3	1.517
16 13 28.512 +29 37 37.93	36.5	0.977
16 13 42.979 +39 07 32.84	55.5	0.976
16 13 51.338 +37 42 58.71	24.1	0.808
16 16 07.063 +24 32 35.52	22.4	1.455
16 17 42.540 +32 22 34.31	89.5	0.151
16 19 46.301 +43 59 15.46	97.2	0.853
16 20 42.199 +29 39 07.13	60.7	1.345
16 22 29.930 +35 31 25.38	27.9	1.475
16 22 46.274 +29 00 54.12	64.1	2.149
16 24 21.994 +39 24 40.90	27.8	1.116
16 24 39.086 +23 45 12.20	27.8	0.927
16 25 13.800 +40 58 50.99	25.5	1.179
16 28 51.274 +45 52 18.53	54.2	0.675
16 29 17.791 +44 34 52.39	65.3	1.033
16 29 57.802 +42 30 51.42	43.0	1.187
16 30 46.212 +36 13 06.03	21.5	1.258

Table B.1 – Continued

Coordinates (J2000)	θ ($''$)	z
16 31 37.534 +30 23 41.27	82.6	1.262
16 32 34.654 +24 50 48.88	17.3	3.015
16 33 08.347 +57 02 53.38	20.0	2.802
16 33 54.706 +21 44 57.73	23.2	1.190
16 35 24.180 +31 10 00.45	59.7	1.130
16 36 09.242 +26 23 09.12	26.7	1.146
16 36 54.413 +32 20 06.55	45.8	0.758
16 37 02.208 +41 30 22.26	66.1	1.179
16 38 56.537 +43 35 12.57	61.3	0.339
16 39 55.006 +31 00 48.70	68.1	1.719
16 39 55.994 +47 05 23.58	27.1	0.860
16 40 54.163 +31 43 29.88	60.0	0.958
16 44 19.970 +45 46 44.39	37.4	0.225
16 44 52.582 +37 30 09.26	83.7	0.758
16 45 44.693 +37 55 26.12	52.3	0.598
16 49 28.879 +30 46 52.49	118.0	1.123
16 49 31.843 +26 23 23.66	39.4	1.341
16 50 27.672 +36 22 56.46	29.7	1.525
16 51 34.910 +18 50 02.86	22.0	0.964
16 54 38.438 +18 47 45.25	48.1	1.360
16 58 19.548 +62 38 23.20	73.9	0.703
16 58 20.350 +37 33 15.54	42.4	1.710
16 58 44.038 +26 17 08.99	30.4	1.016

Table B.1 – Continued

Coordinates (J2000)	θ ($''$)	z
16 59 43.080 +37 54 22.72	61.1	1.038
17 02 20.064 +59 15 38.65	52.9	1.798
17 03 08.126 +22 11 36.10	28.0	1.189
17 03 35.938 +60 38 51.29	17.2	3.230
17 04 04.498 +38 54 30.74	37.4	0.882
17 04 25.114 +33 31 45.98	52.3	0.290
17 04 41.374 +60 44 30.53	64.9	0.372
17 05 18.523 +35 33 52.26	19.6	1.563
17 06 48.062 +32 14 22.89	61.1	1.070
17 08 01.253 +33 46 46.35	38.7	1.344
17 08 46.128 +24 35 28.87	50.2	1.358
17 13 28.807 +30 59 07.82	33.0	1.212
17 14 30.096 +61 57 46.57	20.8	0.904
17 14 48.194 +27 59 19.04	105.1	0.965
17 15 54.631 +28 44 49.85	45.7	1.459
17 20 51.151 +62 09 44.33	44.5	1.010
17 21 58.608 +55 47 07.48	31.9	1.723
21 07 54.974 -06 25 19.13	21.1	0.609
21 08 18.456 -06 17 40.48	60.0	1.491
21 27 15.336 -06 20 41.67	43.6	0.704
21 28 00.103 -00 46 12.31	23.4	2.668
21 30 04.762 -01 02 44.44	36.7	0.704
21 31 53.676 -07 49 53.00	39.3	2.090

Table B.1 – Continued

Coordinates (J2000)	θ ($''$)	z
21 35 13.104 -00 52 43.86	64.8	1.655
21 41 11.894 -06 39 30.34	80.3	0.552
21 44 32.753 -07 54 42.78	32.9	1.811
21 52 13.512 -07 42 24.90	100.6	0.949
21 54 41.952 +00 10 08.10	54.9	1.147
21 59 34.462 -09 10 22.16	34.2	1.207
22 02 07.054 -00 21 32.69	80.9	0.520
22 07 52.529 -00 17 35.85	20.8	1.632
22 13 56.016 -00 24 55.65	19.5	1.061
22 14 09.967 +00 52 27.03	46.9	0.907
22 14 26.038 -08 16 37.68	52.6	0.706
22 20 30.089 -00 22 16.26	101.6	0.602
22 27 20.558 -00 01 59.27	36.3	0.964
22 27 29.062 +00 05 21.99	28.0	1.518
22 29 12.254 -09 42 18.85	46.1	0.586
22 45 32.527 +00 58 57.93	37.0	0.649
22 55 10.378 -09 07 55.14	22.9	0.412
23 12 12.158 -09 19 28.66	49.7	0.830
23 21 33.773 -01 06 46.03	23.1	1.978
23 35 15.410 -00 52 21.74	37.8	1.277
23 36 24.046 +00 02 46.01	66.6	1.095
23 41 42.319 +00 33 12.55	27.8	0.986
23 45 40.452 -09 36 10.28	68.5	1.275

Table B.1 – Continued

Coordinates (J2000)	θ ($''$)	z
23 47 24.713 +00 52 47.00	26.2	1.323
23 49 21.895 -11 13 52.28	40.4	2.230
23 50 26.405 -10 19 58.08	29.7	1.187
23 51 56.126 -01 09 13.35	26.1	0.174
23 53 21.036 -08 59 30.62	25.4	1.647
23 57 37.961 +00 32 27.81	46.4	3.478

Table B.2: $\theta - z$ Data of FR II Quasars (Photometric Sample)

Coordinates (J2000)	θ ($''$)	z
00 17 23.944 -10 35 38.87	12.8	0.275
00 20 36.832 -00 37 39.74	11.0	0.445
00 28 32.902 -09 40 32.18	30.8	3.435
00 37 04.759 -09 10 53.98	25.2	2.505
00 49 05.728 -00 30 51.26	20.3	3.045
01 21 32.834 +00 06 28.73	10.4	0.505
01 33 04.920 -10 03 41.00	23.1	1.155
01 50 37.647 -09 20 10.31	14.6	1.935
02 27 40.324 -09 22 16.72	30.5	1.035
02 45 00.706 -07 47 36.43	19.2	2.215
07 36 18.727 +27 03 52.61	7.6	1.545
07 39 54.562 +17 52 28.00	53.8	0.335
07 48 01.031 +18 38 06.09	7.9	2.235
07 49 57.804 +17 35 58.17	27.3	0.965
07 50 44.366 +18 43 37.02	23.3	0.215
07 51 51.553 +11 52 55.91	48.3	2.175
07 53 28.184 +33 50 51.40	27.2	2.475
07 54 20.124 +42 49 01.77	32.6	0.505
07 55 54.376 +48 11 31.22	32.8	1.285
07 56 27.364 +39 01 26.00	91.8	0.445
07 56 51.576 +12 35 50.30	10.1	1.015

Continued on next page. . .

Table B.2 – Continued

Coordinates (J2000)	θ ($''$)	z
08 00 15.368 +53 26 02.59	8.9	0.395
08 00 33.743 +13 53 55.65	9.8	0.885
08 04 16.243 +12 41 59.15	10.7	1.935
08 06 22.648 +06 26 16.93	9.7	1.915
08 06 45.944 +06 28 38.20	12.7	1.285
08 07 24.911 +14 30 29.40	33.7	1.285
08 08 38.617 +52 11 47.54	13.2	1.905
08 09 57.657 +07 03 53.95	35.7	1.265
08 11 45.866 +16 52 56.43	80.0	2.175
08 15 02.152 +19 37 38.52	17.1	0.195
08 15 22.846 +13 48 34.12	31.3	1.035
08 15 58.461 +14 20 30.45	42.0	4.565
08 16 05.180 +16 03 45.40	75.5	1.405
08 17 03.108 +16 22 59.80	28.7	2.425
08 18 05.049 +05 42 25.87	45.5	0.805
08 19 00.186 +08 00 20.59	9.9	1.695
08 19 47.824 +16 50 55.47	50.2	1.155
08 20 14.211 +15 45 19.34	24.6	0.965
08 21 28.885 +02 31 13.78	62.2	1.245
08 21 34.253 +02 05 38.93	10.7	1.155
08 22 33.497 +07 21 25.97	44.1	0.735
08 23 51.641 +12 40 35.62	10.2	1.845
08 24 29.940 +31 43 34.66	9.9	0.155

Table B.2 – Continued

Coordinates (J2000)	θ $('')$	z
08 24 43.724 +03 00 20.84	52.6	2.215
08 25 46.768 +49 11 59.60	21.3	2.055
08 26 05.375 +23 24 38.71	51.0	0.305
08 26 43.461 +14 34 27.63	19.8	2.285
08 27 43.064 +29 00 55.20	27.5	1.845
08 28 34.436 +20 40 13.01	9.2	0.345
08 29 09.110 +24 09 07.98	10.7	1.155
08 29 35.309 +24 03 29.75	32.6	0.555
08 30 03.343 +19 10 41.94	22.0	0.675
08 30 04.492 +07 45 44.12	18.1	0.335
08 31 10.010 +49 36 20.65	11.6	0.155
08 32 00.156 +19 53 12.11	71.6	1.105
08 32 28.071 +18 37 51.60	27.4	0.225
08 32 40.482 +17 11 16.86	33.9	1.285
08 32 53.927 +33 55 06.41	10.4	1.285
08 37 25.885 +25 01 39.84	16.6	0.325
08 37 43.638 +37 25 13.25	27.9	1.855
08 37 55.973 +41 55 00.72	34.4	0.925
08 38 13.135 +13 58 10.74	137.9	1.685
08 38 22.915 +12 29 53.72	18.8	0.185
08 38 46.366 +56 12 18.49	10.4	1.285
08 39 06.943 +19 21 48.74	30.9	1.845
08 40 11.668 +05 13 33.22	10.6	2.255

Continued on next page...

Table B.2 – Continued

Coordinates (J2000)	θ ($''$)	z
08 40 45.667 +50 28 45.42	51.6	0.315
08 42 33.203 +35 23 19.77	14.7	0.115
08 43 00.738 +05 13 27.02	160.0	2.165
08 43 54.170 +51 05 00.50	37.6	2.455
08 44 24.659 +52 22 55.72	55.9	1.845
08 44 38.610 +41 43 16.30	11.1	1.765
08 44 42.671 +49 23 53.78	7.7	2.155
08 45 53.929 +35 43 33.35	17.6	1.325
08 46 43.543 +31 26 57.74	107.7	0.185
08 46 58.642 +15 07 50.33	34.4	1.765
08 47 13.948 +21 15 47.49	33.1	1.775
08 48 08.337 +40 19 50.37	16.1	2.475
08 48 47.743 +14 20 57.72	44.3	1.695
08 50 32.545 +48 55 47.74	36.4	1.285
08 51 01.049 +25 52 25.40	13.8	1.795
08 51 02.840 +28 39 56.35	22.3	0.315
08 51 30.366 +27 54 59.85	20.1	0.665
08 51 35.579 +45 15 48.74	23.3	1.285
08 51 35.704 +17 56 22.52	15.0	2.475
08 52 01.165 +24 18 15.06	7.1	1.955
08 52 13.024 +26 21 01.50	24.3	1.575
08 52 24.371 +49 05 42.89	18.6	1.725
08 52 28.510 +50 13 20.29	22.7	2.385

Table B.2 – Continued

Coordinates (J2000)	θ ($''$)	z
08 52 34.224 +42 15 27.17	19.2	0.775
08 53 08.608 +13 52 54.85	10.9	1.245
08 54 22.406 +21 23 44.77	39.6	2.085
08 54 43.921 +18 11 56.04	28.6	0.825
08 55 56.184 +37 13 42.48	46.2	0.675
08 56 24.648 +17 54 00.40	36.7	0.945
08 56 55.180 +00 47 09.79	22.7	1.155
08 57 17.149 +09 48 27.80	80.8	0.115
08 57 42.468 +28 04 28.58	14.5	2.115
08 58 20.335 +46 17 22.28	68.4	0.925
08 59 21.106 +30 31 20.05	96.7	2.475
08 59 56.810 +50 52 35.74	12.3	0.185
09 00 42.465 +17 58 36.35	21.8	0.225
09 00 46.517 +29 42 17.02	22.5	1.285
09 01 05.731 +41 22 30.92	20.8	0.455
09 01 16.998 +05 15 15.80	9.8	0.235
09 01 34.832 +20 24 23.37	48.8	0.345
09 04 46.003 +02 08 42.97	34.8	2.285
09 04 49.716 +22 19 34.98	10.9	1.305
09 04 53.483 +20 30 01.97	19.3	1.115
09 05 59.795 +25 13 56.12	8.9	1.285
09 06 03.000 +47 08 15.41	9.0	0.405
09 06 19.875 +60 09 45.53	87.0	1.325

Table B.2 – Continued

Coordinates (J2000)	θ ($''$)	z
09 06 31.876 +16 46 11.86	28.1	0.425
09 06 55.429 +27 49 28.27	42.4	0.735
09 07 44.891 +37 23 59.67	11.5	3.035
09 08 42.762 +57 03 25.11	47.8	0.235
09 09 11.019 +21 31 05.36	27.5	1.325
09 10 50.024 +02 24 52.06	47.9	1.535
09 11 01.066 +45 24 08.61	21.3	1.845
09 13 16.048 +25 48 39.06	27.8	1.395
09 13 35.407 +39 47 13.75	17.6	1.485
09 13 35.880 +25 12 30.38	12.3	2.205
09 13 52.419 +39 02 12.11	43.9	2.315
09 13 58.280 +06 18 59.47	21.0	1.425
09 14 10.879 +26 34 42.79	20.7	0.215
09 14 19.809 +17 26 08.87	22.5	4.285
09 15 05.065 +58 22 07.89	10.3	1.775
09 15 23.303 +34 01 36.44	69.1	2.225
09 15 55.238 +10 59 32.72	13.0	1.275
09 16 23.283 +19 24 16.69	13.6	1.325
09 16 34.674 +19 59 52.76	8.5	0.945
09 17 11.524 +25 32 17.22	43.8	1.275
09 17 47.554 +03 37 13.34	12.4	0.765
09 18 23.698 +28 01 59.09	8.9	0.155
09 18 58.795 +24 52 45.94	12.4	2.175

Table B.2 – Continued

Coordinates (J2000)	θ ($''$)	z
09 20 04.253 +42 30 29.52	10.7	1.845
09 20 15.321 +23 59 58.49	9.3	1.325
09 20 45.616 +23 39 00.98	46.7	1.545
09 20 47.184 +21 50 46.80	19.5	1.555
09 22 24.228 +33 30 40.28	12.2	1.315
09 25 05.560 +49 48 47.38	33.5	1.005
09 25 25.204 +30 26 32.15	10.7	1.395
09 26 28.901 +47 22 36.07	115.7	1.775
09 29 47.090 +51 56 55.29	58.9	2.235
09 30 07.789 +36 56 16.19	16.1	2.285
09 30 34.565 +57 19 12.29	14.9	0.675
09 30 40.060 +19 36 53.76	23.4	1.285
09 30 41.189 +18 59 58.91	12.2	2.585
09 30 44.090 +21 21 08.05	10.0	1.905
09 31 08.597 +34 43 32.48	15.3	0.985
09 32 33.733 +21 58 24.83	41.7	0.195
09 33 41.812 +39 21 52.77	20.1	1.265
09 33 48.083 +51 14 05.36	53.2	0.655
09 33 55.906 +63 35 52.97	20.2	0.335
09 34 47.909 +37 02 17.22	9.3	0.885
09 35 04.648 +22 14 54.36	104.2	0.805
09 36 36.223 +27 25 44.86	24.0	1.275
09 37 01.721 +23 24 35.64	14.2	1.155

Table B.2 – Continued

Coordinates (J2000)	θ ($''$)	z
09 37 45.094 +11 07 54.65	49.2	2.255
09 38 05.978 +26 18 40.88	12.3	1.685
09 39 11.768 +03 43 58.21	16.6	1.325
09 39 18.002 +50 45 54.36	17.2	2.205
09 40 20.857 +21 18 42.71	19.6	1.395
09 42 20.046 +27 10 31.77	54.6	1.285
09 43 37.188 +24 34 52.95	17.2	0.335
09 44 18.848 +23 31 19.86	111.7	1.055
09 45 04.703 +25 06 05.15	109.9	1.085
09 45 12.517 +04 51 31.47	30.1	1.215
09 45 56.903 +06 56 25.07	105.7	1.465
09 48 07.854 +19 12 34.86	26.3	0.135
09 48 36.891 +22 00 53.17	36.6	0.755
09 50 32.536 +48 35 34.19	9.5	1.755
09 50 35.728 +21 22 36.64	15.3	2.755
09 51 13.523 +22 34 04.89	85.2	0.315
09 51 52.459 +07 20 47.56	10.1	1.305
09 52 04.180 +53 02 15.14	24.7	0.245
09 52 27.189 +22 40 06.17	57.2	1.245
09 52 35.209 +06 50 32.85	27.8	0.075
09 52 46.071 +53 04 18.63	8.7	1.685
09 54 07.032 +21 22 35.94	100.6	0.315
09 54 43.087 +40 36 44.53	21.2	0.805

Continued on next page. . .

Table B.2 – Continued

Coordinates (J2000)	θ ($''$)	z
09 58 02.788 +38 29 59.26	18.4	1.395
09 58 10.137 +26 49 29.42	8.6	1.485
09 58 40.761 +20 53 56.82	16.3	0.925
09 58 49.183 +58 24 57.18	20.1	0.215
10 00 21.804 +22 33 18.70	32.5	0.415
10 01 30.797 +29 16 02.46	35.5	1.255
10 01 34.380 +41 06 51.14	11.1	0.275
10 02 04.947 +45 08 39.91	21.3	1.325
10 02 12.299 +28 04 02.73	14.1	0.315
10 02 33.244 +46 44 47.67	8.3	1.875
10 03 44.664 +10 28 07.34	67.4	2.195
10 04 38.506 +23 47 44.66	34.1	1.285
10 04 45.747 +22 25 19.29	64.7	1.135
10 05 21.162 +07 20 03.91	28.0	1.625
10 05 39.353 +23 28 32.59	26.0	1.765
10 06 40.543 +48 13 09.14	9.3	0.165
10 06 53.879 +59 55 19.63	28.2	3.045
10 07 15.176 +21 00 07.68	44.3	1.395
10 07 42.252 +59 08 09.19	14.3	2.235
10 08 15.681 +08 59 05.70	14.9	2.365
10 08 35.557 +62 52 34.66	15.7	0.285
10 08 45.108 +04 56 59.66	56.1	1.865
10 09 33.685 +44 42 33.54	56.8	0.305

Table B.2 – Continued

Coordinates (J2000)	θ ($''$)	z
10 09 55.817 +30 47 52.88	49.2	0.335
10 10 25.813 +18 51 55.50	8.7	0.605
10 10 51.245 +08 54 36.35	70.2	1.605
10 11 00.805 +00 35 19.68	16.9	2.715
10 12 58.770 +22 29 51.81	17.5	1.405
10 13 47.303 +41 49 09.47	14.5	0.225
10 14 16.950 +23 04 16.56	20.5	1.315
10 14 47.064 +23 01 16.63	49.4	0.645
10 15 02.990 +31 42 20.00	30.7	2.745
10 15 28.798 +19 44 51.78	28.8	1.905
10 16 25.411 +12 30 47.24	11.6	1.455
10 17 03.353 +22 33 22.06	13.4	1.215
10 17 49.381 +27 32 04.12	20.3	0.505
10 18 56.665 +36 56 30.89	29.4	2.225
10 19 36.490 +30 00 11.25	27.8	1.285
10 21 02.207 +24 42 53.16	21.9	1.285
10 21 34.441 +30 39 59.06	12.8	0.455
10 21 38.983 +40 31 47.19	9.5	0.975
10 22 48.651 +33 50 57.86	32.8	1.285
10 23 29.794 +48 24 37.19	38.0	1.285
10 24 00.147 +49 45 28.66	14.3	2.195
10 24 59.806 +06 24 53.81	9.2	0.415
10 25 56.312 +08 42 02.14	14.1	0.415

Continued on next page. . .

Table B.2 – Continued

Coordinates (J2000)	θ ($''$)	z
10 27 17.865 +08 01 44.47	25.8	1.585
10 27 34.022 +13 51 08.17	33.2	0.605
10 27 47.132 +35 57 32.44	59.2	0.915
10 28 22.956 +05 51 31.07	15.1	0.125
10 28 33.110 +43 06 26.95	36.5	1.155
10 29 18.436 +27 12 36.61	25.6	1.805
10 30 39.889 +28 53 28.14	33.2	2.985
10 30 57.526 +27 56 02.34	20.9	1.405
10 32 15.861 +23 39 22.55	17.9	1.265
10 32 33.068 +44 34 52.18	8.6	1.275
10 32 48.617 +09 25 49.10	7.2	0.255
10 33 54.433 +56 38 35.98	14.6	2.285
10 33 56.652 +39 17 43.83	20.8	0.935
10 34 29.927 +37 59 30.81	10.7	1.205
10 34 33.843 +31 06 30.59	29.1	1.035
10 34 56.063 +39 10 42.92	38.5	0.535
10 35 05.190 +04 54 22.58	26.5	1.935
10 35 11.658 +34 06 25.29	43.2	0.565
10 36 42.979 +12 11 23.52	44.6	0.215
10 38 18.041 +48 25 47.96	17.5	1.285
10 38 19.310 +34 03 56.93	38.6	1.675
10 39 16.845 +10 25 43.23	29.1	1.015
10 39 32.154 +26 32 44.57	50.7	2.425

Table B.2 – Continued

Coordinates (J2000)	θ ($''$)	z
10 39 56.789 +42 25 38.18	17.6	0.885
10 40 41.936 +10 28 35.90	9.0	1.625
10 40 58.998 +26 55 02.59	15.9	1.285
10 41 02.145 +31 49 57.52	19.5	1.805
10 41 04.605 +42 57 24.30	8.7	1.805
10 43 12.835 -00 13 49.14	9.1	2.475
10 44 15.860 +28 58 52.01	42.0	3.205
10 44 34.166 +07 03 02.63	10.6	1.865
10 44 43.323 +10 38 24.04	13.6	0.275
10 45 34.963 -00 55 29.54	54.2	0.975
10 45 46.527 +26 18 05.56	9.4	1.285
10 45 56.868 +27 17 59.59	57.6	1.125
10 47 10.975 +49 19 26.24	32.1	1.885
10 47 26.666 +01 11 47.52	25.8	3.675
10 48 01.185 +19 36 24.73	26.1	2.215
10 48 08.670 +10 52 06.59	25.4	2.595
10 48 51.815 +32 09 03.14	124.9	2.475
10 49 51.944 +17 47 28.42	83.8	0.485
10 49 53.289 +49 53 22.12	58.4	0.255
10 50 13.161 +21 44 29.26	15.2	0.345
10 50 42.583 +02 18 56.75	50.3	2.015
10 51 29.363 +23 48 01.30	14.9	1.285
10 52 29.504 +47 21 20.15	19.0	0.495

Continued on next page. . .

Table B.2 – Continued

Coordinates (J2000)	θ ($''$)	z
10 53 29.401 +22 27 05.40	10.3	1.755
10 53 46.085 +52 24 07.32	16.8	0.315
10 54 26.032 +42 32 30.99	28.1	0.415
10 54 26.605 +27 03 17.44	39.6	1.305
10 54 48.728 +04 47 06.65	33.2	1.245
10 54 49.537 +25 26 50.77	35.7	2.285
10 55 15.927 +16 42 10.34	16.1	0.885
10 55 47.805 +26 23 35.83	14.7	0.885
10 55 50.603 +16 30 51.16	42.5	0.855
10 58 04.782 +20 48 12.44	7.0	1.625
10 59 45.169 +05 27 39.94	16.1	1.815
10 59 54.830 +21 08 37.88	11.7	2.405
11 00 01.143 +23 14 13.14	61.8	0.555
11 00 15.584 +42 59 35.81	21.3	1.605
11 01 20.362 +41 53 08.19	16.6	1.325
11 01 26.185 +48 50 30.83	8.6	1.435
11 05 11.213 +23 07 18.09	14.0	1.685
11 05 20.943 +27 11 24.63	13.5	1.745
11 05 33.487 +30 16 28.05	25.1	0.675
11 05 43.276 +08 47 21.21	15.0	1.135
11 06 31.770 -00 52 52.37	19.2	0.415
11 06 35.264 +15 04 47.24	28.4	1.605
11 06 49.654 +61 19 20.43	15.8	0.315

Continued on next page. . .

Table B.2 – Continued

Coordinates (J2000)	θ ($''$)	z
11 06 52.627 +34 38 25.36	26.3	0.215
11 07 15.046 +16 28 02.31	37.4	0.655
11 07 32.138 +33 33 04.36	11.0	1.055
11 07 56.235 +12 21 51.34	17.4	0.415
11 08 25.531 +46 59 14.26	9.8	1.795
11 08 27.375 +23 09 50.30	12.5	1.545
11 10 19.184 +25 05 56.44	22.0	0.995
11 12 07.108 +38 04 15.91	25.2	1.795
11 13 21.340 +30 10 15.03	10.8	1.745
11 13 37.185 +19 13 48.00	49.6	0.745
11 13 41.083 +25 04 15.48	12.2	1.275
11 14 03.429 +30 43 51.49	73.5	1.285
11 14 26.436 +22 57 56.89	24.1	1.005
11 15 16.405 +46 35 52.81	21.1	0.645
11 15 29.258 +62 47 51.37	25.6	1.755
11 16 19.039 +01 29 32.07	53.5	0.235
11 17 04.766 +27 00 36.73	10.2	0.855
11 17 08.860 +00 43 10.75	30.6	1.315
11 18 33.785 +34 57 40.74	23.3	1.535
11 18 34.179 +36 55 32.73	6.0	0.215
11 19 02.248 +24 10 26.63	43.8	0.855
11 19 31.692 +17 03 27.69	15.4	2.695
11 19 48.480 +33 35 35.50	18.8	1.965

Table B.2 – Continued

Coordinates (J2000)	θ $('')$	z
11 19 56.753 +55 12 15.12	14.8	1.325
11 20 37.001 +26 17 41.12	17.0	2.245
11 20 41.009 +22 39 02.48	56.1	1.115
11 21 13.019 +38 44 28.80	96.4	1.405
11 23 10.301 +51 23 56.91	13.1	1.735
11 23 23.155 +60 06 52.82	50.7	3.675
11 23 54.640 +17 28 58.49	38.8	1.135
11 24 12.229 +43 25 49.99	11.9	2.225
11 26 27.124 +12 20 34.80	22.4	1.425
11 26 46.470 +16 28 04.14	21.9	1.265
11 27 05.676 +31 53 52.13	52.4	0.275
11 28 16.505 +25 53 55.38	18.0	1.135
11 28 26.332 +20 24 13.70	29.0	0.885
11 28 29.385 +28 01 27.11	68.9	1.155
11 28 39.555 +16 29 31.78	54.5	2.255
11 29 39.491 +35 40 20.89	66.5	2.255
11 30 02.719 +35 40 45.67	40.3	1.455
11 30 44.312 +01 37 24.85	43.7	0.735
11 32 09.656 +05 17 49.96	19.2	1.675
11 32 16.999 +09 11 56.18	34.9	0.275
11 32 29.493 +52 27 32.44	8.6	1.805
11 32 41.935 +12 13 10.05	15.1	4.135
11 33 54.152 +35 47 43.19	40.7	1.855

Continued on next page. . .

Table B.2 – Continued

Coordinates (J2000)	θ ($''$)	z
11 35 26.944 +29 26 48.72	8.1	1.875
11 35 45.056 +54 33 18.38	12.7	1.015
11 35 59.631 +35 55 27.19	22.9	2.045
11 37 01.189 +29 36 15.86	30.3	1.805
11 37 16.690 +12 46 45.43	9.3	1.425
11 37 16.897 +23 48 40.35	76.6	0.215
11 38 23.712 +25 22 32.91	33.1	2.455
11 39 20.986 +05 14 42.37	10.2	1.755
11 40 09.437 +21 20 12.85	9.7	1.395
11 40 19.406 +23 13 56.46	74.5	1.935
11 40 37.352 +05 40 28.38	35.3	1.305
11 42 11.535 +03 15 42.54	25.8	1.515
11 42 13.006 +41 36 41.87	9.2	2.195
11 42 19.215 +22 32 45.87	20.7	0.485
11 42 54.636 +20 01 19.87	71.6	1.215
11 42 57.217 +21 29 11.29	22.5	1.275
11 43 05.554 +52 27 26.89	40.4	0.125
11 43 06.031 +18 43 42.93	21.3	0.395
11 43 26.687 +20 19 57.21	22.0	0.165
11 43 27.560 +30 05 48.17	18.3	2.285
11 43 44.287 +13 42 01.26	47.8	0.215
11 43 47.043 +27 30 27.61	14.5	1.285
11 44 45.428 +35 02 28.55	11.6	1.325

Table B.2 – Continued

Coordinates (J2000)	θ ($''$)	z
11 44 54.964 +20 41 41.34	18.4	2.395
11 45 22.416 +27 51 05.30	88.8	0.675
11 45 33.384 +40 26 05.90	62.1	1.155
11 46 27.442 +17 44 37.33	10.2	1.145
11 46 36.130 +21 01 20.53	23.5	1.295
11 48 24.961 +61 12 36.43	8.0	0.075
11 48 51.846 +13 52 17.97	22.9	0.235
11 48 53.816 +21 11 09.83	48.8	1.045
11 49 00.271 +09 54 18.79	30.6	1.605
11 49 35.655 +35 48 12.39	29.0	1.955
11 50 16.536 +16 32 09.08	11.5	0.675
11 50 22.999 +17 14 19.60	24.3	1.685
11 51 03.582 +40 44 14.73	28.0	0.645
11 51 05.089 +63 14 35.37	42.6	3.535
11 51 48.901 +00 34 31.12	22.6	1.325
11 52 33.328 +07 53 11.25	53.1	1.395
11 52 48.973 +26 14 09.91	46.1	0.275
11 53 21.557 +34 15 12.55	31.3	1.935
11 53 39.941 +45 01 25.82	14.1	1.425
11 55 38.593 -01 35 59.20	37.9	0.765
11 56 13.584 +30 19 06.58	16.8	0.415
11 56 41.652 +04 30 02.26	13.4	0.285
11 56 42.995 +42 13 39.27	8.8	1.325

Table B.2 – Continued

Coordinates (J2000)	θ ($''$)	z
11 58 23.901 +27 02 46.77	55.0	1.315
11 59 05.163 +01 40 58.57	33.3	0.215
11 59 26.208 +21 06 55.95	175.5	0.325
11 59 36.622 +39 55 38.53	34.3	0.225
11 59 46.448 +11 33 48.52	22.3	2.505
12 00 39.844 +27 36 23.55	23.8	1.095
12 01 13.852 +50 52 00.96	47.3	1.725
12 01 15.497 +18 09 48.01	61.3	1.155
12 01 38.892 +60 36 32.56	28.0	1.735
12 02 20.549 +53 29 05.65	17.9	1.075
12 02 26.093 +13 13 10.91	42.5	2.195
12 03 07.306 +31 25 52.33	47.0	2.695
12 03 31.801 +24 26 55.98	35.0	2.475
12 04 56.788 +17 10 01.46	19.2	1.745
12 05 05.820 +23 20 51.50	37.0	1.475
12 05 21.475 +49 54 10.60	14.5	0.265
12 05 53.707 +21 20 03.31	12.6	0.405
12 06 02.630 +32 31 27.04	49.2	0.165
12 06 15.131 +45 34 30.64	10.4	1.215
12 06 22.406 +50 17 44.29	26.4	1.395
12 06 24.732 +09 55 12.44	14.1	1.265
12 06 50.072 +11 51 31.77	20.5	1.325
12 06 56.815 +48 15 12.58	32.9	0.885

Continued on next page. . .

Table B.2 – Continued

Coordinates (J2000)	θ ($''$)	z
12 07 46.064 +11 27 50.65	6.6	1.795
12 07 51.896 +25 34 56.57	59.2	0.065
12 08 04.146 +38 00 02.92	15.9	2.245
12 08 19.377 -03 03 25.61	12.2	0.995
12 08 22.000 +22 19 58.18	109.5	2.455
12 08 38.035 +47 11 19.04	21.4	1.725
12 10 37.569 +31 57 06.03	79.8	0.375
12 10 50.819 +31 55 14.28	17.3	1.605
12 11 06.691 +18 20 34.29	31.6	1.505
12 11 10.823 +25 08 30.12	15.1	1.285
12 11 13.771 +36 28 01.03	72.2	0.315
12 11 48.523 +05 11 19.34	26.3	1.475
12 12 13.838 +05 40 01.11	9.9	1.745
12 12 32.021 +11 02 24.10	22.3	2.165
12 12 56.100 +19 25 47.03	24.8	1.155
12 13 03.371 +03 10 01.78	22.0	0.225
12 13 04.092 -01 25 45.43	49.2	0.265
12 13 40.599 +48 23 25.15	30.9	2.085
12 14 13.693 +21 10 47.09	9.8	1.795
12 14 25.061 +11 38 03.70	15.0	2.265
12 15 18.873 +20 16 05.32	27.1	0.335
12 15 50.424 +16 26 49.16	23.5	2.475
12 15 57.583 -00 07 19.54	10.6	1.055

Continued on next page. . .

Table B.2 – Continued

Coordinates (J2000)	θ ($''$)	z
12 16 29.311 +25 15 28.28	14.3	1.805
12 16 34.882 +37 23 28.39	27.6	0.765
12 16 46.040 +41 39 58.13	31.4	0.415
12 17 44.589 +17 54 45.90	11.7	1.085
12 17 48.454 +27 40 09.16	34.6	0.455
12 18 53.569 +24 55 09.77	13.0	2.025
12 19 05.955 +13 20 43.63	56.6	2.205
12 20 07.696 +06 04 15.14	13.8	1.545
12 20 22.624 +23 05 04.97	15.6	0.215
12 20 28.878 +14 57 18.90	39.2	2.255
12 20 59.240 +26 42 18.53	14.5	1.955
12 21 23.598 +50 35 25.92	11.6	0.945
12 21 37.187 +57 28 58.57	27.3	1.155
12 21 53.407 +31 30 56.96	39.5	0.375
12 22 44.360 +27 58 39.49	9.4	0.995
12 22 53.732 +31 51 23.80	14.0	1.875
12 23 46.187 +18 21 06.64	23.0	1.325
12 23 51.905 +16 08 12.33	11.9	0.185
12 24 54.930 +40 54 28.74	18.8	1.155
12 24 57.876 +53 15 51.81	16.0	1.385
12 25 12.284 +19 27 20.99	20.5	2.475
12 25 16.977 +31 45 35.40	40.6	1.365
12 25 21.371 +03 39 45.26	11.6	0.115

Table B.2 – Continued

Coordinates (J2000)	θ (″)	z
12 25 31.237 +07 15 53.30	27.2	1.085
12 25 39.557 +24 58 36.39	66.8	0.345
12 26 00.034 +20 20 54.28	65.0	1.475
12 27 12.807 +64 03 01.20	13.1	0.235
12 27 23.017 +42 59 22.02	66.4	0.315
12 28 11.737 +20 23 52.53	81.4	0.885
12 29 52.752 +11 08 29.70	26.9	1.795
12 31 01.713 +47 56 53.51	9.3	3.245
12 31 03.158 +18 58 55.83	17.2	1.265
12 31 03.384 +58 06 35.23	30.5	0.165
12 31 09.909 +35 00 59.05	37.8	1.525
12 31 22.569 +20 27 23.70	16.0	1.255
12 31 29.218 +14 58 17.30	22.9	1.265
12 31 55.996 +33 47 32.28	32.6	1.685
12 32 07.678 -02 57 04.68	12.6	2.115
12 32 47.425 +20 37 45.33	157.6	0.665
12 32 48.120 +12 25 23.66	7.9	1.275
12 33 57.881 +52 06 54.48	13.0	1.425
12 34 18.981 +38 50 23.06	16.7	2.085
12 34 48.873 +04 00 42.80	15.9	1.685
12 35 18.414 +23 50 13.18	38.3	1.685
12 36 03.123 +35 15 49.81	36.6	0.205
12 36 08.736 +06 28 35.76	89.8	0.315

Table B.2 – Continued

Coordinates (J2000)	θ ($''$)	z
12 36 31.319 +26 35 08.70	21.0	1.355
12 36 43.187 +30 18 57.95	8.4	0.415
12 36 44.350 +38 20 46.19	18.1	1.365
12 36 51.574 +25 07 50.67	78.1	0.555
12 37 09.675 +04 21 42.67	8.6	0.245
12 37 14.037 +24 58 05.03	20.7	1.285
12 37 53.847 +00 16 37.98	38.6	0.395
12 39 58.538 +18 58 19.79	11.8	0.475
12 39 59.784 +18 00 57.72	57.1	1.085
12 40 44.688 +33 03 49.83	35.4	0.855
12 40 52.876 +12 37 35.81	9.1	2.695
12 40 53.171 +24 04 56.66	15.3	1.285
12 41 21.926 +14 50 27.98	11.8	1.765
12 41 31.377 +43 40 15.42	10.5	1.465
12 42 12.038 +26 36 33.86	57.3	0.915
12 42 16.389 +00 47 43.96	42.1	1.305
12 42 48.294 +25 44 06.14	17.4	0.275
12 42 53.746 +43 29 01.90	12.4	1.965
12 43 57.652 +16 22 53.44	14.8	0.595
12 43 57.863 +19 33 50.90	27.9	1.515
12 44 15.993 +16 06 27.44	11.1	1.605
12 44 52.011 +28 07 29.21	22.4	1.285
12 46 35.498 +25 22 45.03	28.0	0.995

Table B.2 – Continued

Coordinates (J2000)	θ ($''$)	z
12 46 38.312 +58 39 44.59	16.6	0.485
12 46 41.899 +34 52 51.28	51.0	1.065
12 47 20.772 +32 09 00.74	22.4	1.035
12 48 06.979 +18 38 12.57	27.0	0.735
12 49 22.162 +57 59 48.43	40.5	0.235
12 50 13.315 +11 33 08.04	24.7	3.675
12 50 25.552 +30 16 39.76	28.3	1.085
12 50 47.141 +02 15 48.99	34.2	1.275
12 51 22.715 +32 15 00.02	67.3	0.765
12 51 29.174 +04 46 35.62	23.8	3.085
12 51 56.294 +07 09 29.28	22.6	2.215
12 52 11.070 +08 11 58.76	25.0	0.465
12 52 45.267 +05 17 00.58	18.8	0.195
12 52 50.064 +17 40 00.81	19.0	1.325
12 53 02.247 +26 27 22.55	51.4	1.215
12 54 10.456 +39 33 23.24	32.4	0.425
12 54 10.808 +09 14 46.08	28.2	1.325
12 55 18.487 +28 55 44.46	13.2	1.325
12 55 21.416 +21 38 00.76	10.5	1.375
12 55 29.473 +51 31 15.75	16.5	1.395
12 55 43.167 +08 41 45.34	99.5	2.475
12 55 56.810 +10 20 47.12	9.8	2.205
12 56 07.668 +10 08 53.55	23.3	2.485

Table B.2 – Continued

Coordinates (J2000)	θ ($''$)	z
12 56 37.674 +28 16 41.33	46.4	1.285
12 56 40.872 +12 22 02.34	13.5	2.065
12 58 01.552 +52 51 44.45	27.2	1.285
12 58 21.158 +31 31 32.63	24.0	1.285
12 58 44.341 +54 43 29.67	15.2	1.795
12 59 09.868 +59 03 58.37	8.2	0.505
12 59 13.274 +03 34 29.42	29.2	2.155
13 00 07.778 +46 33 44.78	25.3	0.595
13 00 27.867 +10 56 27.70	34.6	0.965
13 00 44.661 +15 26 20.47	36.3	1.465
13 01 38.957 +14 46 16.03	30.0	1.285
13 02 43.364 +19 13 18.13	14.9	2.385
13 03 02.782 +06 01 18.24	10.7	2.145
13 03 14.275 +27 30 12.58	21.8	1.805
13 03 15.476 +49 16 06.03	13.6	1.615
13 03 30.110 +47 54 28.82	76.9	0.315
13 03 36.542 +20 23 02.83	10.6	0.765
13 03 43.105 +20 55 32.73	50.3	0.225
13 04 14.358 +59 02 42.57	53.3	1.685
13 04 15.135 +07 58 52.32	65.8	1.545
13 04 20.378 +08 38 47.05	6.6	0.125
13 04 30.799 +50 41 08.02	103.9	2.715
13 05 02.499 +27 52 21.81	19.6	0.825

Continued on next page. . .

Table B.2 – Continued

Coordinates (J2000)	θ ($''$)	z
13 05 47.235 +19 01 40.71	11.3	0.185
13 06 19.223 +36 31 50.51	10.1	0.545
13 06 37.169 +17 25 53.17	63.7	1.675
13 06 44.917 +22 13 30.99	22.8	0.425
13 06 45.757 +10 59 46.82	27.8	1.625
13 06 50.401 +26 49 17.06	31.6	1.365
13 07 00.795 +25 24 55.02	18.4	1.135
13 07 09.804 +09 33 10.62	48.0	0.595
13 07 24.323 +21 30 30.08	14.7	1.005
13 07 29.246 +27 46 59.43	67.2	1.085
13 07 33.183 +32 33 08.30	25.2	1.265
13 07 42.792 +03 00 29.31	16.4	2.315
13 07 53.929 +06 42 13.89	41.9	0.665
13 07 58.571 +24 41 17.96	19.4	1.285
13 08 12.019 -01 28 59.91	42.5	0.215
13 08 41.288 +33 44 01.26	41.5	1.395
13 09 13.316 +16 25 55.76	35.9	1.475
13 09 17.602 +11 17 12.91	28.3	0.215
13 10 12.489 +07 01 56.50	19.2	1.285
13 10 15.161 +15 03 42.77	35.3	1.845
13 10 25.218 +55 31 53.01	12.5	1.885
13 10 32.610 +20 37 02.88	32.2	1.425
13 10 36.717 +35 26 11.87	22.0	0.875

Continued on next page...

Table B.2 – Continued

Coordinates (J2000)	θ ($''$)	z
13 10 53.256 +17 03 30.85	38.4	1.685
13 10 56.773 +17 59 37.79	9.9	1.725
13 11 21.158 +00 53 19.55	24.5	1.105
13 11 26.437 +24 43 33.71	16.2	1.475
13 11 30.184 +31 16 07.00	33.5	1.635
13 11 39.045 +32 52 38.99	11.0	2.365
13 11 54.520 +20 08 54.15	40.0	1.285
13 12 13.962 +24 47 58.12	22.0	1.305
13 12 14.746 +08 54 53.00	28.5	1.465
13 12 34.732 +11 10 03.40	43.4	2.285
13 13 15.275 +03 34 40.70	12.3	1.625
13 13 20.021 +29 19 00.19	10.5	0.995
13 13 22.603 +32 21 06.11	12.6	1.805
13 13 41.437 +30 03 12.04	24.4	1.395
13 13 44.322 +16 08 01.27	34.6	0.935
13 13 46.999 +07 39 32.34	12.4	1.845
13 14 41.503 +14 26 05.49	11.3	0.915
13 15 36.761 +19 14 59.90	55.2	0.495
13 18 32.406 +37 16 10.02	43.5	1.685
13 18 42.343 +30 08 01.15	18.1	1.295
13 19 07.872 +06 48 05.01	23.3	0.275
13 19 22.433 +09 25 35.88	10.7	1.525
13 19 38.673 +36 23 32.18	36.3	0.275

Table B.2 – Continued

Coordinates (J2000)	θ ($''$)	z
13 19 45.550 +46 08 27.23	32.4	1.395
13 19 52.420 +37 47 25.19	10.1	0.785
13 19 54.083 +31 35 54.66	16.0	1.925
13 19 56.843 +44 30 59.44	45.6	0.435
13 20 53.633 +10 37 51.50	23.1	3.395
13 21 06.654 +37 41 53.51	90.4	1.155
13 21 19.985 +22 33 43.74	30.3	1.535
13 21 20.323 +28 58 05.33	8.0	1.395
13 22 03.291 +08 25 54.27	49.1	1.775
13 22 20.150 +18 48 26.45	65.8	1.505
13 23 09.603 +25 32 26.58	16.7	0.595
13 23 49.638 +06 53 02.92	12.4	2.385
13 24 42.564 +44 08 29.64	19.4	2.165
13 25 09.707 +00 49 33.99	11.9	2.395
13 25 12.199 +51 19 33.36	23.8	2.395
13 26 54.711 +21 31 26.11	71.1	1.195
13 27 49.198 +22 05 04.71	20.6	1.275
13 28 09.855 +25 15 37.13	18.0	0.985
13 28 16.099 +23 09 16.74	120.6	2.195
13 28 51.684 +37 10 24.28	9.3	2.165
13 29 19.416 +48 03 00.69	131.8	0.305
13 29 42.493 +45 40 00.17	22.5	0.745
13 30 10.429 +05 00 38.08	26.8	2.745

Table B.2 – Continued

Coordinates (J2000)	θ ($''$)	z
13 30 28.071 +53 20 58.46	9.6	1.855
13 30 57.593 +62 37 22.50	77.8	0.265
13 31 27.824 +25 00 50.11	99.5	2.475
13 31 56.723 -02 59 24.35	13.1	1.875
13 33 05.952 +43 24 24.88	15.9	1.075
13 33 38.657 +22 22 12.96	55.8	1.765
13 34 23.850 +15 21 59.97	36.8	1.195
13 34 25.830 +21 28 26.74	59.0	0.195
13 34 35.656 +36 32 19.43	11.9	0.855
13 35 41.901 +23 41 39.04	29.9	1.425
13 35 43.283 +42 41 35.28	27.9	1.435
13 36 32.184 +16 11 07.01	22.1	1.395
13 36 37.923 +55 40 33.35	84.2	2.715
13 36 54.444 +17 10 40.39	19.7	1.155
13 37 31.893 -01 15 43.53	8.1	2.475
13 38 58.299 +07 50 44.83	53.1	0.215
13 39 04.295 +28 12 41.23	30.2	0.275
13 39 20.231 +52 06 17.39	27.5	2.425
13 39 28.764 +22 08 23.86	14.3	2.715
13 39 33.922 -00 16 12.40	43.9	1.815
13 40 23.030 +40 13 07.91	26.0	1.495
13 40 57.745 +26 37 00.31	9.4	1.365
13 41 11.298 +18 48 41.76	46.5	0.105

Table B.2 – Continued

Coordinates (J2000)	θ ($''$)	z
13 41 14.379 +15 56 35.23	38.8	1.705
13 42 08.157 +31 19 36.99	24.1	1.205
13 42 13.138 +09 05 40.79	44.3	1.155
13 43 10.335 +07 16 28.79	11.9	1.685
13 44 09.623 +52 54 00.60	18.8	1.155
13 44 30.919 +19 48 34.52	20.6	1.625
13 44 40.868 +60 04 58.74	19.3	1.405
13 45 08.848 +22 24 38.43	39.7	0.185
13 45 19.744 +57 33 20.52	10.2	2.395
13 47 23.443 +52 48 37.11	13.7	1.475
13 47 42.483 +55 10 18.08	44.0	4.165
13 48 31.383 +16 53 42.71	20.2	1.885
13 49 18.522 +35 24 15.79	38.6	1.285
13 50 30.687 +12 21 59.97	14.4	2.165
13 50 31.513 +16 45 24.14	66.8	1.925
13 50 34.241 +17 40 27.78	10.4	2.255
13 50 48.400 +33 12 18.58	38.1	1.325
13 51 38.689 -03 20 40.94	19.6	1.575
13 53 35.923 +26 31 47.53	168.9	0.325
13 54 22.168 +54 51 55.67	36.1	1.325
13 54 29.784 +17 19 05.10	12.3	1.285
13 55 38.047 +06 11 19.11	13.5	2.315
13 55 41.438 +01 55 53.35	10.1	1.285

Table B.2 – Continued

Coordinates (J2000)	θ ($''$)	z
13 56 00.047 +19 04 20.84	90.8	2.215
13 56 35.831 +11 22 08.43	23.6	0.115
13 57 07.194 +20 47 42.01	99.8	0.595
13 58 33.563 +04 32 04.04	44.8	0.215
13 59 01.728 +51 13 13.55	11.5	1.395
13 59 28.570 +54 55 13.78	14.9	0.075
13 59 35.565 +27 47 25.60	7.1	0.965
13 59 48.190 +09 45 18.82	25.8	1.385
14 01 03.389 +11 25 34.65	11.5	1.515
14 01 08.629 +24 12 54.52	16.3	0.315
14 01 59.634 +23 40 24.06	53.3	0.285
14 02 27.280 +52 04 32.17	34.0	0.945
14 02 41.651 +51 50 43.19	14.7	1.085
14 02 43.272 +12 04 41.71	15.8	0.255
14 03 26.326 +25 26 35.52	9.4	2.795
14 04 05.661 +24 52 31.50	23.7	2.455
14 05 00.816 +29 25 14.07	65.3	2.585
14 07 31.424 +15 51 42.35	13.8	1.405
14 07 43.028 +15 52 14.05	8.7	0.375
14 07 53.984 +23 36 32.30	9.2	0.915
14 08 15.393 +52 29 46.23	28.3	0.415
14 08 41.588 +19 06 51.29	24.9	1.775
14 09 04.113 +10 03 43.05	19.0	2.585

Table B.2 – Continued

Coordinates (J2000)	θ ($''$)	z
14 09 30.487 +04 06 34.85	9.9	1.325
14 09 31.757 +34 10 53.61	13.9	1.625
14 09 41.843 +22 10 29.77	12.0	0.215
14 10 22.279 +26 49 25.36	57.3	1.795
14 10 43.810 +14 08 01.72	24.6	1.155
14 10 52.653 +15 15 15.23	29.8	0.335
14 11 08.038 +19 53 03.24	29.2	0.515
14 12 14.221 +11 19 21.23	13.2	1.275
14 12 44.098 +42 12 57.69	92.5	2.315
14 12 59.327 +30 02 27.94	10.4	1.605
14 13 59.966 +29 44 59.08	40.9	1.815
14 14 50.829 +56 33 42.34	50.5	0.985
14 14 59.199 +23 30 46.32	8.6	1.875
14 16 59.415 +49 28 38.79	10.6	0.415
14 17 17.896 +23 17 20.19	32.6	0.925
14 17 18.021 +06 08 04.57	70.8	2.855
14 17 33.945 +41 11 22.89	27.1	1.985
14 18 23.277 +19 21 57.14	52.2	0.885
14 18 50.722 +15 41 06.39	18.6	1.485
14 18 59.386 +11 07 17.28	101.9	0.535
14 19 07.669 +35 09 00.19	13.4	0.225
14 19 32.595 +00 31 20.39	12.9	2.325
14 19 46.187 +42 02 33.30	45.2	0.225

Table B.2 – Continued

Coordinates (J2000)	θ ($''$)	z
14 20 38.202 +11 31 16.04	40.4	0.235
14 21 08.555 +11 18 19.22	31.3	1.935
14 21 29.390 +57 39 34.45	23.4	1.105
14 21 56.853 +22 19 40.05	13.8	2.365
14 22 13.581 +11 05 10.74	10.8	1.905
14 22 24.508 +28 33 10.42	14.5	0.365
14 22 44.514 +10 47 54.24	71.5	1.325
14 23 01.099 +42 44 29.83	24.8	2.475
14 23 19.803 +32 55 57.39	10.0	1.795
14 23 37.990 +08 46 22.93	19.2	1.015
14 24 56.925 +20 00 26.34	10.2	0.875
14 24 57.803 +12 47 49.53	23.9	0.785
14 25 01.058 +30 27 15.58	19.1	0.225
14 25 09.215 -01 15 59.36	21.8	0.455
14 27 02.530 +21 38 35.95	10.2	1.325
14 27 02.684 +16 43 08.69	31.1	1.275
14 27 31.584 +31 35 21.04	34.7	1.545
14 27 35.608 +26 32 14.54	237.6	0.355
14 28 10.878 +15 42 22.30	19.0	1.755
14 30 07.739 +23 35 24.96	19.8	1.325
14 30 52.385 +45 06 36.61	42.7	1.065
14 30 59.003 +08 23 41.97	50.6	0.605
14 31 45.047 +06 38 09.23	40.8	2.315

Table B.2 – Continued

Coordinates (J2000)	θ ($''$)	z
14 32 02.593 -01 59 00.37	45.0	1.045
14 32 08.876 +07 26 42.59	14.8	1.155
14 32 12.740 +15 48 46.91	70.9	1.595
14 33 31.881 +19 07 11.67	23.4	2.395
14 34 21.289 +18 59 18.37	22.0	1.015
14 34 21.565 +04 41 37.21	44.1	0.395
14 35 45.346 +15 41 10.35	21.1	0.415
14 35 48.561 +20 13 21.23	177.6	0.255
14 36 01.870 +21 31 34.45	14.9	1.935
14 36 27.675 +56 05 59.13	51.4	1.795
14 36 33.780 +13 45 05.16	26.6	1.285
14 36 43.830 +01 54 35.64	30.0	1.845
14 37 47.740 +07 48 56.20	92.4	1.425
14 38 01.577 +05 47 59.10	40.3	0.185
14 39 13.313 +15 08 41.00	38.9	2.195
14 39 17.917 +09 55 23.54	18.3	1.065
14 41 37.783 +18 19 38.17	10.8	1.625
14 42 35.773 +49 34 04.55	7.3	0.275
14 44 07.101 +39 41 09.80	34.1	0.185
14 44 33.994 +56 35 51.63	15.4	1.445
14 44 57.102 +07 37 57.74	97.4	1.045
14 45 31.482 +00 04 35.40	32.5	1.325
14 45 32.223 +26 23 49.69	10.5	1.475

Table B.2 – Continued

Coordinates (J2000)	θ ($''$)	z
14 47 36.258 +20 31 49.39	22.8	1.285
14 48 09.011 +44 12 25.32	24.9	0.885
14 49 16.545 +34 05 02.76	14.0	1.735
14 49 19.981 +00 58 08.28	11.2	1.795
14 50 19.903 +37 47 14.33	10.5	1.425
14 52 16.025 +09 43 30.16	11.0	1.935
14 53 07.999 +22 17 07.74	116.1	0.315
14 53 35.865 +42 14 33.61	16.6	0.425
14 54 03.381 +34 18 09.93	73.3	0.125
14 54 06.332 +29 04 24.70	55.0	1.345
14 56 16.235 +41 34 33.84	16.4	1.285
14 56 20.105 +55 52 57.37	19.0	1.325
14 56 40.962 +42 53 13.47	26.7	1.445
14 57 23.093 +24 59 15.43	49.9	0.885
14 58 10.979 +13 08 42.81	15.5	1.285
14 58 46.591 +07 58 02.39	28.8	1.205
14 59 18.877 +49 44 48.35	10.3	0.185
15 00 58.506 +52 27 10.22	37.8	2.265
15 01 39.543 +33 12 18.37	148.5	0.395
15 03 07.728 +32 25 13.58	23.7	1.285
15 03 24.542 +16 28 03.98	28.1	1.155
15 03 59.330 +09 13 03.81	9.6	2.205
15 04 31.895 +38 49 33.78	30.4	1.005

Table B.2 – Continued

Coordinates (J2000)	θ (″)	z
15 04 39.427 +05 13 53.58	30.6	1.155
15 05 43.569 +14 02 19.93	8.0	0.405
15 06 58.635 +41 07 05.57	9.2	1.715
15 07 08.952 +16 07 15.13	10.0	0.315
15 07 39.499 +11 04 03.71	141.0	0.485
15 07 49.260 +20 32 12.12	11.3	0.275
15 07 59.057 +43 56 17.88	9.9	1.955
15 08 15.666 +38 36 43.66	61.7	0.155
15 08 21.100 +37 59 51.85	25.9	2.045
15 09 15.949 +09 48 49.26	155.3	2.715
15 11 20.325 +08 20 01.42	10.7	1.245
15 12 12.182 +54 17 47.55	10.8	2.255
15 12 40.943 +49 44 36.16	17.8	1.805
15 13 29.293 +10 11 05.54	34.7	1.405
15 14 05.093 +35 10 01.51	10.6	2.475
15 15 09.648 +41 18 36.73	165.3	0.985
15 16 39.807 +14 05 57.42	57.9	2.485
15 16 59.608 +41 59 38.18	10.7	2.765
15 17 50.694 +11 39 48.84	57.7	1.055
15 18 09.759 +07 50 34.87	11.0	1.205
15 19 28.979 +32 20 10.11	15.1	1.425
15 19 31.415 +12 40 01.38	42.6	1.385
15 19 56.070 +06 49 25.04	13.3	1.285

Table B.2 – Continued

Coordinates (J2000)	θ ($''$)	z
15 20 07.651 +06 25 15.38	17.5	1.325
15 20 15.340 +17 25 53.61	15.2	1.305
15 20 47.565 +07 57 33.28	14.1	1.685
15 21 33.097 +22 27 23.68	16.3	0.165
15 21 43.536 +05 17 05.18	51.2	2.365
15 21 45.617 +14 36 48.57	25.3	1.725
15 22 20.775 +17 28 07.08	11.3	0.515
15 23 04.197 +09 39 29.82	16.4	2.235
15 23 07.556 +10 31 54.75	26.7	1.325
15 23 25.203 +27 04 57.40	10.3	0.445
15 25 42.906 +06 52 45.74	79.6	0.405
15 25 43.790 +06 49 42.34	22.2	1.975
15 25 50.808 +05 36 34.24	7.7	1.275
15 27 01.889 +42 30 45.92	11.3	1.195
15 27 30.628 +08 06 15.91	11.8	1.795
15 27 50.026 +11 16 33.18	42.7	1.595
15 28 06.636 +13 23 45.85	41.1	2.475
15 28 08.547 +02 53 26.54	39.0	0.485
15 29 09.601 +17 13 28.00	16.9	1.425
15 31 05.719 +04 53 50.06	11.7	1.035
15 31 43.280 +24 04 21.07	13.7	0.115
15 31 49.919 +11 34 25.11	30.6	0.715
15 32 24.641 +11 10 18.79	112.1	1.285

Continued on next page. . .

Table B.2 – Continued

Coordinates (J2000)	θ ($''$)	z
15 32 56.286 +10 22 39.27	57.0	0.635
15 32 57.925 +12 00 06.65	17.5	1.795
15 33 08.889 +07 44 29.64	54.9	0.405
15 33 15.074 +13 32 25.14	10.2	0.365
15 33 41.727 +22 07 51.71	74.9	1.775
15 34 09.803 +50 45 12.84	65.8	2.475
15 35 46.332 +26 39 14.53	43.6	1.035
15 37 38.942 +10 11 07.08	12.5	1.425
15 37 52.331 +27 21 20.89	26.2	0.145
15 37 53.740 +64 03 38.70	8.5	0.115
15 38 00.009 +44 41 33.31	22.0	0.285
15 38 24.821 +35 50 04.65	48.6	0.235
15 38 42.935 +47 35 30.61	34.7	0.055
15 38 50.821 +13 25 23.12	51.9	2.105
15 40 09.198 +14 21 14.46	11.9	0.315
15 41 04.762 +18 05 50.05	11.7	0.955
15 41 07.448 +45 25 24.55	16.7	1.285
15 41 46.738 +17 14 25.21	19.8	1.285
15 42 51.182 +57 32 28.26	13.9	1.215
15 42 56.123 +10 54 36.59	35.5	1.045
15 46 53.285 +47 53 40.76	11.1	2.145
15 47 20.990 +27 48 21.28	19.5	1.395
15 47 42.229 +54 14 43.87	14.3	1.215

Continued on next page. . .

Table B.2 – Continued

Coordinates (J2000)	θ ($''$)	z
15 47 43.539 +20 52 16.66	84.7	0.385
15 47 46.407 +32 30 50.40	15.4	0.405
15 47 56.785 +30 14 10.53	9.7	0.935
15 48 04.956 +16 44 13.49	19.2	2.545
15 48 58.281 +18 49 17.90	58.8	2.435
15 49 48.134 +07 38 44.06	29.7	1.255
15 50 22.300 +07 44 53.66	60.3	1.055
15 51 27.321 +48 10 50.84	49.6	0.735
15 52 28.793 +15 56 52.89	14.8	0.495
15 52 55.451 +19 34 05.43	113.6	2.205
15 56 27.849 +17 06 31.72	44.2	1.285
15 57 10.119 +35 59 44.24	10.8	0.395
15 57 17.322 +36 23 19.44	24.4	1.425
15 57 24.399 +30 13 56.07	15.4	1.385
15 57 46.519 +07 09 14.59	8.8	0.375
16 01 26.431 +30 26 58.74	32.0	0.775
16 01 31.186 +32 45 37.30	39.4	1.305
16 01 51.568 +17 54 10.18	104.9	0.665
16 02 07.429 +39 29 57.10	17.4	0.155
16 02 13.085 +35 55 49.13	27.0	2.475
16 02 16.261 +29 11 18.44	38.3	1.475
16 03 13.853 +15 04 39.32	26.6	1.045
16 05 06.142 +42 24 01.09	30.7	1.275

Table B.2 – Continued

Coordinates (J2000)	θ ($''$)	z
16 05 27.475 +30 59 45.61	44.2	0.215
16 06 01.283 +17 47 41.23	20.2	1.795
16 08 11.281 +28 49 02.22	30.3	0.415
16 08 13.588 +35 13 34.39	46.7	2.425
16 08 41.944 +41 08 33.50	9.9	3.315
16 09 02.418 +61 09 44.77	71.5	2.485
16 11 03.522 +09 22 14.05	82.2	1.285
16 11 38.189 +39 05 26.87	71.6	1.025
16 12 01.540 +28 29 05.88	75.7	2.965
16 12 46.559 +51 36 52.17	14.5	1.445
16 13 21.100 +52 03 11.26	26.8	1.855
16 13 49.510 +57 10 56.83	29.1	1.475
16 15 10.290 +32 09 04.80	81.4	1.215
16 15 32.257 +15 34 37.52	48.4	1.285
16 15 40.630 +58 14 54.80	13.7	0.405
16 16 33.186 +45 07 10.83	21.1	2.475
16 18 58.474 +15 59 25.59	26.6	0.835
16 19 45.001 +36 56 36.38	25.8	0.445
16 20 43.402 +42 17 18.90	39.0	1.085
16 20 56.628 +49 00 03.60	47.6	1.395
16 21 48.277 +18 28 55.42	51.2	2.425
16 23 37.840 +45 45 00.20	93.9	1.285
16 25 12.609 +29 33 19.78	16.2	1.515

Continued on next page...

Table B.2 – Continued

Coordinates (J2000)	θ ($''$)	z
16 26 02.330 +55 38 56.59	11.0	1.295
16 26 32.596 +13 22 40.16	27.0	0.955
16 26 37.243 +58 09 17.62	33.2	0.755
16 26 52.038 +56 49 51.25	22.5	1.545
16 29 06.673 +44 35 42.25	33.4	2.395
16 30 39.236 +27 09 01.01	17.1	1.545
16 31 27.064 +55 18 06.65	60.8	1.065
16 32 19.866 +32 43 44.34	10.4	1.505
16 33 08.097 +55 13 32.62	15.6	1.025
16 35 27.860 +31 16 31.13	17.9	1.915
16 36 53.283 +28 44 32.09	38.3	4.305
16 37 42.392 +36 14 33.34	8.5	1.545
16 38 09.600 +45 33 08.67	136.9	2.745
16 39 18.362 +12 55 06.98	12.1	1.685
16 39 30.522 +12 47 43.00	13.8	1.285
16 39 59.173 +51 19 31.00	41.3	1.155
16 42 42.903 +37 53 45.57	46.8	1.285
16 47 49.157 +34 32 52.98	101.7	2.195
16 48 16.829 +32 56 55.90	52.2	1.325
16 48 41.405 +51 11 21.31	17.8	1.695
16 49 32.465 +29 32 45.77	23.7	1.285
16 50 32.604 +34 58 45.99	14.8	0.185
16 51 05.183 +50 31 40.30	40.0	0.765

Table B.2 – Continued

Coordinates (J2000)	θ ($''$)	z
16 52 09.564 +32 46 00.27	21.1	0.405
16 57 38.203 +41 42 30.83	13.1	1.285
17 00 17.358 +45 58 40.31	30.0	0.855
17 03 07.724 +37 51 26.35	18.6	2.425
17 06 02.547 +39 03 39.04	10.9	1.285
17 07 26.316 +33 45 13.51	30.3	0.655
17 11 23.897 +43 48 37.87	33.5	0.495
17 17 10.893 +41 22 47.91	15.2	2.145
17 19 38.814 +29 18 54.42	61.4	1.285
17 20 43.258 +64 10 24.95	13.6	3.375
17 20 52.303 +57 55 13.25	28.7	0.945
17 25 45.317 +36 54 16.24	22.8	0.815
17 26 38.844 +53 06 27.49	15.2	0.455
17 30 16.042 +35 12 37.65	34.6	0.595
21 29 39.406 -00 07 19.78	21.5	2.745
21 31 53.669 -07 49 52.97	31.6	2.085
21 37 19.369 -08 28 04.31	24.7	1.325
21 45 44.500 -07 49 17.71	19.0	0.215
21 54 35.653 -07 58 44.86	26.1	1.605
22 46 23.984 -09 14 11.37	11.9	0.635
22 47 15.794 -09 06 07.56	18.6	1.475
22 47 20.890 -08 04 14.05	18.3	1.155
23 23 29.172 -09 17 26.71	38.2	0.885

Table B.2 – Continued

Coordinates (J2000)	θ ($''$)	z
23 34 06.817 +00 59 01.40	24.3	1.285
23 36 25.034 -09 45 26.20	36.1	2.475
23 37 21.668 -09 58 37.15	20.5	0.225
23 54 04.812 -09 40 02.83	59.1	0.895